MUSÉUM NATIONAL D'HISTOIRE NATURELLE
Ecole Doctorale DIVONA (Diversités, Origines, Natures) – ED 227

Année 2026

N° attribué par la bibliothèque
|_|_|_|_|_|_|_|_|_|_|_|_|_|

THÈSE

Pour obtenir le grade de

Docteur du Muséum National d'Histoire Naturelle

Spécialité: Sciences écologiques et agronomiques

Josquin GUERBER

Soutenue publiquement le 13 octobre 2026

What are the links between community stability and long-term population trends ?

Quels sont les liens entre stabilité des communautés et tendances de populations ?

Sous la direction de : **Colin Fontaine et Elisa Thébault (HDR)**

Présidente du jury : **Ana Rodrigues**

Jury composé de :

Vasilis Dakos	Chargé de recherche, CNRS (ISEM, Montpellier)	**Rapporteur**
Ian Donohue	Professor, Trinity College Dublin	**Rapporteur**
Sandrine Pavoine	Professeure, MNHN (CESCO, Paris)	**Examinatrice**
Ana Rodrigues	Directrice de recherche, CNRS (CEFE, Montpellier)	**Examinatrice**
Colin Fontaine	Chargé de recherche, CNRS (CESCO, Paris)	**Encadrant de thèse**
Elisa Thébault	Directrice de recherche, CNRS (iEES, Paris)	**Directrice de thèse**

Rac va lestr a zo bihan hac ar mor a zo bras

Remerciements

First I would like to thank all members of the jury who kindly accepted to assess my work, Vasilis Dakos, Ian Donohue, Sandrine Pavoine and Ana Rodrigues. I hope that you will enjoy reading this thesis and I look forward to discussing with you about all of this.

Merci Colin et Elisa pour votre encadrement tout au long de ces trois ans. Merci de m'avoir confiance lors de la construction du projet de thèse, merci pour toutes ces fois où je suis arrivé en réunion avec l'impression de m'être perdu dans des analyses, et où je repartais avec une meilleure idée de comment continuer. Merci pour vos relectures qui auront bien aidé à remanier mes drafts, et plus généralement un grand merci pour vos conseils, votre soutien et votre bienveillance.

Un grand merci aussi à toutes les autres personnes qui ont rendu ces travaux possibles, en premier lieu les observatrices et observateurs du STOC, dont l'inlassable travail bénévole permet d'assembler un jeu de données de qualité, que l'on n'aura jamais fini d'analyser. Merci Grégoire et Tanguy de m'avoir accueilli sur vos carrés, et merci Benoît et Romain pour les exports de données. Merci aux membres du GT Oiseaux pour nos échanges méthodo, et merci à Jean-François et Stéphane pour leurs précieux conseils. Merci aux stagiaires dont j'ai eu le plaisir d'encadrer le travail, Melaine, Zélie, et Damien pour tes dizaines de pages de calcul qui nous auront bien aidé dans ces histoires de bosses. Merci à l'équipe SACADO MeSU pour leur support technique et merci aux équipes de gestion et de direction du CESCO, de l'iEES et de l'ED227. Enfin, merci à mon comité de suivi de thèse, Alain, Claire et Maud, pour vos conseils et votre écoute.

Le moment de conclure ma formation universitaire étant venu, j'aimerais adresser de chaleureux remerciements aux encadrant.e.s de mes stages passés. Les mesures de transparence d'ailes de papillons avec Marianne et Charline, the cold waters of Norwegian fjords with Èric, ma rencontre avec la stabilité écologique avec Sonia, avec l'écologie théorique avec Nicolas et Isabelle, et ma découverte du CESCO

et des indicateurs de biodiversité avec Benoît, Charles et Mathilde, toutes ces opportunités ont contribué à orienter mon parcours en écologie et à nourrir mes réflexions, et je vous remercie de me les avoir offertes.

Merci à mes collègues d'enseignement et diffusion au Muséum, Angélique, Antoine, Coralie, Lara, Robin, Sami, Sophie, Thomas ainsi qu'à Emilie et Séverine, c'était un plaisir d'avoir l'occasion de diversifier mes activités en thèse à vos côtés, une parenthèse souvent bienvenue pour passer quelques journées loin d'un écran d'ordinateur.

Un double encadrement est aussi une double vie de laboratoire, des deux côtés du jardin des Plantes, où j'ai eu la chance de rencontrer des cadres bienveillants et accueillants. A l'iEES, merci aux membres de l'équipe DYNECO et aux jeunes chercheur.se.s pour votre accueil, Alban, Amandine, Antoine, Laurence, Madeleine, Maya, Marwa, Mattéo, les deux Nicolas, Noé, Quentin, Romain, Shanèze, Sarah, Théo, Vincent. Au CESCO, merci à l'équipe du cambouis pour avoir apporté vos lumières à mes tunnels, Clément, les deux Jean, Lisa, Lise, Lorenzo, Mathis, Maud, Milena, Pauline, Simon, Zoé, et un grand merci en vrac à tout Vigie-Nature, le 61 et le 135 !

En particulier, merci à toute l'équipe du tarot du midi, étendue aux doctorant.e.s du 61 qui ne sont pas tombés dedans. Merci Marie et Thibault pour l'achat de la nouvelle cafetière, Léa et Juliette les queens, Solène pour les sorties Vigie-Flore, Aurélien pour les pauses footing, merci Adèle, Emilie, Gauthier, Laura, Ludo, Marceline, Nelly, Olivier, Sandra. Merci à vous pour les excursions "télétravail", les sorties, les soirées déguisement de Rocheton et surtout pour ce sens du soutien collectif qui facilite le quotidien.

Merci aussi à toute la team course à pied de l'ASMu et merci à l'organisation du cross ! Merci à la horde lagomorphe, Avrile, Claire-Hélène, Jeanne(s), Lilas, Nicolas et Xavier, entre séances de Richard et expéditions trail. Merci à mes ami.e.s pour leur soutien depuis bien avant ces trois ans de thèse, Agathe, Chloé, Eloi, Jojo, Juliette, Leslie, Luc, Lucas, Marco, Max, Noé, Paul, Rachel, Romain, Thibault.

Merci à ma famille pour leurs encouragements, merci Alix et Anaëlle pour toujours être là quand on en a besoin, et meilleures pensées à mes parents. Enfin, merci à Elsa pour ton soutien si réconfortant et motivant.

Table of contents

Remerciements **i**

Summaries and communications **v**

I Introduction **1**
I.1 From single perturbations to dimensions of ecological stability . . . 5
I.2 Temporal variability around an equilibrium . . . 12
I.3 Long-term population trends across ecological scales . . . 18
I.4 Main research questions . . . 27

II General methods **29**
II.1 The French Breeding Bird Survey . . . 31
II.2 Disentangling trends and variability . . . 34
II.3 Notes on implementation . . . 37

III Chapter 1: Populations trends and variability are amplified by intense land use **41**
III.1 Context and aim of the study . . . 43
III.2 Article: “Population trends and variability within bird communities are amplified by intense land use” . . . 44
III.3 Supplementary Information for Chapter 1 . . . 61

IV Chapter 2: Press perturbations induce transient changes in temporal variability **77**
IV.1 Context and aim of the study . . . 79
IV.2 Article: “Population and community variability deviate from stationary expectations during transient dynamics” . . . 80
IV.3 Supplementary Information for Chapter 2 . . . 102

V Chapter 3: Temporal changes in integrative stability dimensions **115**
V.1 Context and aim of the study . . . 117
V.2 Article: “Temporal changes of trends and variability of bird communities over 25 years in France” . . . 118
V.3 Supplementary Information for Chapter 3 . . . 144

VI Discussion **155**
VI.1 Conjointly measuring trends and variability to better understand biodiversity dynamics . . . 157
VI.2 Ecological stability out of equilibrium . . . 165
VI.3 Ecological theory, biodiversity conservation, and beyond . . . 168
VI.4 Conclusion . . . 173

References **175**

Appendices **191**

A Other research project **191**

A.1 Article: “Overexploitation can counteract top-down control and the paradox of enrichment in simple food chains” 191

Summaries and communications

Résumé en français

Dans mon travail de thèse, j'analyse la variabilité à court terme de l'abondance des populations et des communautés dans un contexte de changements à long terme de la biodiversité. En effet, face aux changements globaux, des espèces déclinent alors que d'autres augmentent, et les fluctuations environnementales subies par les populations et les communautés s'appliquent ainsi autour de tendances à long terme.

Dans un premier chapitre basé sur l'analyse des données du Suivi Temporel des Oiseaux Communs français (STOC), nous avons montré que, comparés aux habitats forestiers, les habitats agricoles sont associés à de plus fortes tendances à long terme, mais aussi à une plus forte variabilité des populations autour de leurs tendances. La richesse spécifique est associée à de plus faibles tendances mais à une plus forte variabilité des populations.

Dans un deuxième axe, nous avons utilisé des modèles stochastiques de dynamiques de populations afin d'approfondir cette apparente indépendance entre changements à long terme et variabilité à court terme. Comparées à un régime stationnaire, les tendances de population positives causent des excès de variabilité alors que les déclins causent un déficit de variabilité, mais ces déviations sont moins marquées pour des populations à reproduction rapide. La manière dont les changements à long terme se répartissent au sein des communautés peut ainsi biaiser la mesure de la variabilité.

Dans un troisième temps, nous avons travaillé à l'estimation des changements récents de la variabilité des communautés et de l'intensité des tendances de populations au cours du temps pour les oiseaux communs de France. Nos résultats montrent que les changements à long-terme de la variabilité des communautés sont en partie expliqués par les changements d'abondance relative des espèces.

Ces travaux contribuent à placer la relation entre tendances de populations et variabilité des communautés dans un cadre hors-équilibre et dépendant de l'échelle d'étude, améliorant ainsi notre compréhension des dynamiques temporelles des communautés naturelles. Ils permettent d'envisager la construction d'indicateurs de biodiversité basés sur de multiples dimensions de la stabilité écologique.

Summary

This PhD dissertation analyses the temporal variability of population and community abundance in a context of biodiversity decline. In the face of global anthropogenic pressures, some species decline while others increase. The environmental fluctuations that population and communities are subjected to thus operate around long-term trends.

In a first chapter, we analyzed time series data from the French Breeding Bird Survey (FBBS). We showed that, compared to forest habitats, farmland habitats are associated to stronger long-term trends but also to a stronger population variability around these trends.

In a second chapter, we used stochastic models of population dynamics in order to further investigate this apparent independence between long-term trends and short-term temporal variability. Compared to a stationary regime, positive population trends cause an excess of variability while declines generate variability deficits, but these deviations are weaker for fast-growing populations. The ways long-term trends are spread within communities can thus bias variability measurements.

In a third chapter, we estimated recent changes in community variability and in the strength of long-term population trends across time for wild birds in France. Our results show that long-term changes in community variability can be partially explained by changes in species relative abundances, which are driven by long-term population trends.

Overall, this work shows that the relationship between long-term population trends and temporal variability depend on the scale of study, improving our understanding of the temporal dynamics of natural communities. This paves the way for developing biodiversity indicators based on multiple dimensions of ecological stability.

Résumé court en français

Face à l'augmentation des pressions d'origine humaine sur la biodiversité, les communautés naturelles subissent des changements environnementaux à long terme ainsi que des fluctuations environnementales. Les oiseaux communs de France ne sont pas épargnés, avec de forts déclins de certaines espèces mais des augmentations d'autres ainsi qu'une variabilité inter-annuelle autour de ces tendances. Nous étudions ces deux dimensions de la réponse des communautés aux perturbations et évaluons leurs liens (i) face à l'usage des sols à l'échelle locale, (ii) indépendamment dans des modèles théoriques, et (iii) au cours du temps à l'échelle nationale. Ces travaux, en plaçant l'étude de la variabilité dans un cadre hors équilibre et en plaçant l'étude des tendances de populations dans un cadre issu de la théorie de la stabilité écologique, permettent d'envisager une attribution plus exhaustive des impacts des activités humaines sur les dynamiques temporelles de la biodiversité.

Short plain language summary

With increasing anthropogenic pressures on biodiversity, natural communities face long-term environmental changes and environmental fluctuations. Common birds of France are not spared and some species show long-term declines while others increases, as well as inter-annual variability around these trends. We study these two dimensions of ecological response to perturbations and evaluate their links (i) at a local scale with respect to land use intensity, (ii) independently in theoretical models and (iii) over time at the scale of France. This work places the study of temporal variability out of equilibrium and places the study of population trends in a framework derived from the theory of ecological stability. It thus paves the way for a more exhaustive attribution of anthropogenic impacts on biodiversity temporal dynamics.

Résumé long en français

Par les cinq grandes pressions d'origine anthropique sur la biodiversité que sont le changement d'usage des sols, le changement climatique, l'exploitation, la pollution et les invasions biologiques, les activités économiques humaines menacent non seulement de nombreuses facettes de la diversité du vivant (Díaz and Malhi 2022), mais aussi les conditions matérielles ayant permis le développement humain (Cardinale

et al. 2012) ainsi que les modes de relation des sociétés humaines aux autres êtres vivants (Himes et al. 2024). Créés dans l'objectif de préciser les relations causales entre pressions anthropiques, changements environnementaux et facettes de la biodiversité, les dispositifs de suivi de la biodiversité permettent un suivi structuré de l'abondance des espèces sauvages au cours du temps sur de larges étendues spatiales (Magurran et al. 2010). Souvent analysées en écologie de la conservation, les données issues de ces programmes montrent généralement que la perte globale d'espèces ne se traduit pas nécessairement par un déclin généralisé à l'échelle locale, mais par des tendances à long terme de déclins d'abondance des espèces subissant le plus les pressions anthropiques tandis que les populations d'espèces mieux adaptées à des environnements perturbées augmentent ou stagnent (Dornelas et al. 2014, Dornelas et al. 2023). Ces changements à long terme de la composition des communautés viennent questionner le cadre conceptuel issu de la recherche sur le lien entre la biodiversité et le fonctionnement des écosystèmes. Dans ce cadre, le nombre d'espèces d'une communauté favorise la compensation entre les réponses des espèces aux fluctuations environnementales, réduisant ainsi la variabilité temporelle de l'abondance de la communauté (Tilman 1996, Yachi and Loreau 1999, Loreau and de Mazancourt 2013). D'une part, les tendances de populations gagneraient à être complétées d'analyses portant sur la variabilité des populations autour de leurs tendances pour une vision plus exhaustive des dynamiques des populations naturelles, mais d'autre part l'étude de la variabilité temporelle s'est majoritairement intéressée à des communautés dont la composition est considérée comme une donnée fixe. Ce travail de thèse propose un cadre conceptuel unifiant ces deux facettes des dynamiques temporelles de la biodiversité ainsi que trois études des liens entre tendances de populations et variabilité des populations et des communautés.

Dans un environnement dont les paramètres biotiques et abiotiques changent au cours du temps tout en présentant une part de variation aléatoire appelée ici stochasticité, les dynamiques temporelles des systèmes écologiques intègrent l'intensité des perturbations avec la capacité des populations et des communautés à maintenir leurs propriétés face à ces perturbations, leur stabilité (Van Meerbeek et al. 2021). En particulier, la réponse d'une population à un changement environnemental à long terme peut être une tendance temporelle positive, neutre ou négative, tandis que la variabilité de l'abondance d'une population reflète l'intensité des fluctuations environnementales, mais aussi la manière dont la population y répond. La réponse de l'abondance de la communauté au régime de perturbation dépend ainsi des réponses des espèces, mais aussi de la manière dont le fonctionnement de la communauté couple

les dynamiques des populations. Déjà liées par leur capacité à comprendre la réponse des systèmes écologiques aux changements environnementaux, les études des tendances de populations et de la variabilité temporelle peuvent donc aussi être reliées dans le même cadre conceptuel où tendances et variabilités sont deux dimensions intégratives de la stabilité écologique. Les liens possibles entre tendances et variabilité sont ainsi à lier aux travaux conceptuels existants sur la dimensionnalité de la stabilité écologique, qui cherchent à quantifier la multiplicité des réponses écologiques aux perturbations (Donohue et al. 2016, Kéfi et al. 2019).

Les **méthodes générales** de cette thèse sont l'occasion de préciser les détails de l'origine des données du Suivi Temporel des Oiseaux Communs utilisées pour cette thèse, de regrouper les méthodes que nous avons utilisées pour séparer tendances et variabilité dans des données réelles ou simulées, et de partager la manière dont j'ai organisé le code informatique développé pendant cette thèse. Depuis 2001, des centaines d'observateurs et observatrices à travers la France suivent les populations d'oiseaux dans un carré de deux kilomètres de côté à proximité d'une localité de leur choix par dix points d'écoutes de cinq minutes réalisés trois fois par an au printemps (Jiguet et al. 2012). Pour les chapitres 1 et 3 de cette thèse, nous avons ajouté aux étapes de pré-traitement de données classiques réalisés par l'équipe de la plateforme Vigie-Nature une étape supplémentaire: le groupement des données des points d'écoute du même carré se trouvant dans des habitats similaires en une seule communauté (Monnet et al. 2026). Ce regroupement offre un compromis entre représentativité écologique et quantité de données disponible. En ce qui concerne les mesures de tendances et de variabilité, une première approche à l'échelle locale consiste à ajuster une régression de Poisson à la série temporelle d'une espèce au sein d'une seule communauté. Le coefficient de régression correspond à la tendance (log-)linéaire sur les années suivies, et l'écart-type des résidus de Pearson de la régression correspond à la variabilité de la série temporelle autour de sa tendance. En considérant une seule espèce observée dans plusieurs communautés, un modèle mixte généralisé avec une structure d'effets aléatoire adaptée permet d'estimer la tendance moyenne de l'espèce ainsi qu'un paramètre de variabilité temporelle. Cette méthode permet d'estimer l'incertitude du paramètre de variabilité, mais nécessite une plus grande quantité de données que la première approche et ne permet donc pas de considérer autant d'espèces. Enfin, dans des modèles théoriques, la variabilité peut être définie pour chaque pas de temps du système.

Le **premier chapitre** de cette thèse propose de démêler tendances et variabilité des populations à

l'échelle locale, au sein des communautés d'oiseaux du Suivi Temporel des Oiseaux Communs (STOC). D'une part, l'intensification de l'agriculture et l'artificialisation causent de forts déclins des espèces d'oiseaux affiliées aux milieux agricoles (Burns et al. 2021, Rigal et al. 2023), souvent insectivores (Bowler et al. 2019), mais les dynamiques locales de ces déclins mesurés à des échelles nationales ou continentales sont rarement évaluées (Johnston et al. 2025). D'autre part, les mesures de variabilité utilisées dans les études montrant un lien entre usage des sols et variabilité des populations d'oiseaux ne prennent pas en compte la part de variation temporelle expliquée par les tendances de population (Blüthgen et al. 2016, Olivier et al. 2020). Le lien entre usage des sols et "variabilité" non corrigée par la tendance peut donc être porté par les réponses à long terme des espèces, mais aussi par la variabilité des populations autour de leur tendances. Nos résultats montrent que l'habitat principal de la communauté est associé aux tendances ainsi qu'à la variabilité. Comparées à un milieu forestier, les communautés suivies dans les habitats agricoles sont composées de populations ayant des tendances plus fortes en moyenne, mais aussi de plus fortes variabilités autour de leur tendances. Tendances et variabilité répondent donc à une même pression anthropique: l'usage des sols. Cependant, en considérant uniquement les communautés agricoles, seule la variabilité est associé à des indicateurs d'intensité de l'usage des sols à l'échelle locale, qui ne permet pas d'expliquer la force des tendances locales. Après avoir pris en compte le type d'usage des sols, tendances et variabilité apparaissent ainsi comme conditionnellement indépendantes.

Dans le **deuxième chapitre**, nous approfondissons cette indépendance conditionnelle en utilisant des modèles théoriques de dynamiques stochastiques de population et de communautés (Arnoldi et al. 2019). Nous y mesurons l'écart entre la variabilité observée et la variabilité attendue en ne tenant compte que des abondances moyennes des populations au cours de la réponse à un changement brutal des conditions environnementales, une perturbation de type *press*. Pour cela, nous résumons les dynamiques aléatoires des modèles à des systèmes déterministes décrivant les changements attendus de moyenne et de variance des abondances, grâce à une approximation issue de la physique statistique (Särkkä and Solin 2019). L'approximation déterministe permet une analyse mathématique qui montre qu'à l'échelle d'une population, les perturbations qui génèrent une tendance négative causent une variabilité observée plus faible qu'attendue en régime stationnaire, alors que les tendances positives causent un excès de variabilité. Atténuées par un plus fort taux de croissance des populations, ces déviations par rapport

aux attendus stationnaires se répercutent au niveau des communautés: la variabilité de la communauté est proche de son équivalent stationnaire quand les tendances des populations sont variées. Ainsi, la manière dont la perturbation est répartie dans la distribution des abondances et des taux de croissance est importante pour prédire les déviations de variabilité des communautés. Ces résultats apportent des éléments théoriques sur l'impact des tendances de populations sur la mesure de la variabilité: même si, longtemps après une perturbation *press*, la variabilité des modèles étudiés rejoint les attendus proches de l'équilibre, des déviations transitoires se produisent.

Dans le **troisième chapitre**, nous adoptons une perspective à une plus large échelle spatiale et temporelle, en mesurant les changements temporels des tendances et de la variabilité dans le jeu de données du STOC. A de larges échelles spatiales, les trajectoires à long terme des espèces ne sont souvent pas complètement (log-)linéaires (Clark and Luis 2020, Boennec et al. 2024), et les changements temporels de variabilité sont mal connus dans des contextes hors équilibre. Dans ce chapitre, un travail théorique a été nécessaire afin d'adapter le cadre usuel de décomposition de la variabilité des communautés (Loreau and de Mazancourt 2008, Thibaut and Connolly 2013) aux estimations issues de modèles linéaires mixtes généralisés souvent utilisés pour estimer les tendances temporelles. Nous avons ensuite ajusté ces modèles aux données de suivi de 55 espèces d'oiseaux communs pour des fenêtres temporelles glissantes de 10 ans, permettant d'évaluer les changements temporels des tendances de populations, mais aussi des estimateurs de variabilité. A l'échelle des espèces, nous remarquons de nombreux changement de tendances en lien avec de possible dynamiques non linéaires, mais moins de changements de variabilité. Inversement, à l'échelle des communautés, les tendances des populations modifient la composition de la communauté moyenne, ce qui se traduit par des changements temporels de variabilité des communautés, qui décline au cours de la période. Les changements temporels de synchronie des populations suivent les changements temporels d'*evenness* des abondances relatives des espèces, tandis que les liens entre composition de la communauté et variabilité moyenne des populations sont plus difficile à détecter.

Cette thèse permet ainsi de placer l'étude de la variabilité temporelle dans un cadre hors équilibre où la composition des communautés est variable sous l'effet des tendances de populations. Dans la **discussion**, j'aborde les avantages et les défis futurs de l'approche développée lors de cette thèse, je discute des dynamiques hors équilibres dans l'étude de la stabilité, et j'envisage des perspectives de dialogues entre écologie théorique et écologie de la conservation, vers des indicateurs de biodiversité

basés sur la stabilité. (i) Considérer les tendances de populations permet de préciser les attendus à l'équilibre sur la variabilité (Chapitre 2), et interpréter les tendances de populations en mobilisant un cadre conceptuel issu de la théorie de la stabilité écologique permet de rendre compte des propriétés dynamiques des communautés écologiques (Chapitres 1 et 3). L'intrication entre échelles spatiales, écologiques et temporelle dans le déterminisme des dimensions intégratives de la stabilité écologique génère des perspectives théoriques en modélisation ainsi que des défis empiriques pour attribuer une dynamique donnée à ses déterminants anthropogéniques ou aux traits fonctionnels qui lui sont associés. (ii) Le caractère hors équilibre des trajectoires récentes de la biodiversité invite à ré-examiner la relation entre biodiversité et stabilité écologique, tout en permettant de tirer des parallèles avec l'étude des transitions catastrophiques en écologie. (iii) Les jeux de données empiriques issus des sciences participatives, par leur conséquente couverture géographique, sont un point de rencontre particulièrement prometteur pour confronter des prédictions théoriques à des systèmes empiriques dont la conservation est cruciale. Afin d'aller plus loin et de porter ce dialogue entre théorie et observation dans des arènes de négociation politique, la construction d'indicateurs de biodiversité basés sur la stabilité est prometteuse. Cependant, il faudra veiller à la pertinence, la précision, l'actualité, l'accessibilité, la comparabilité et la cohérence de tels indicateurs.

Dans l'ensemble, mon travail de thèse présente un effort de meilleure considération de la multiplicité des dynamiques temporelles de la biodiversité. Les liens entre tendances de populations et variabilité des communautés varient entre échelles et cadres d'étude, mais offrent de nombreuses perspectives en écologie des communautés, écologie de la conservation et écologie théorique.

Scientific communications

Published journal article

Guerber, J., Fontaine, C., & Thébault, E. (2026). Population trends and variability within bird communities are amplified by intense land use. *Journal of Animal Ecology, 95(6)*, 1047–1058. https://doi.org/10.1111/1365-2656.70254

Preprint

Guerber, J., Genettais, D., Fontaine, C., & Thébault, E. (2026). Population and community variability deviate from stationary expectations during transient dynamics. *bioRxiv*. https://doi.org/10.64898/2026.07.08.737188

Presentations at international conferences

Birds in farmland exhibit increased population variability beyond the impact of species population trends. SFE^2 international congress, *Société Française d'Ecologie et d'Evolution*, Lyon, 2024.

How do population and community stability change during increasing or decreasing population trends ? BES Annual Meeting, *British Ecological Society*, Edinburgh, 2025.

How do population and community stability change during increasing or decreasing population trends ? Biodiversity in Equations, *CNRS Biodiversity Theory and Modeling Research Network*, Montpellier, 2026.

I . Introduction

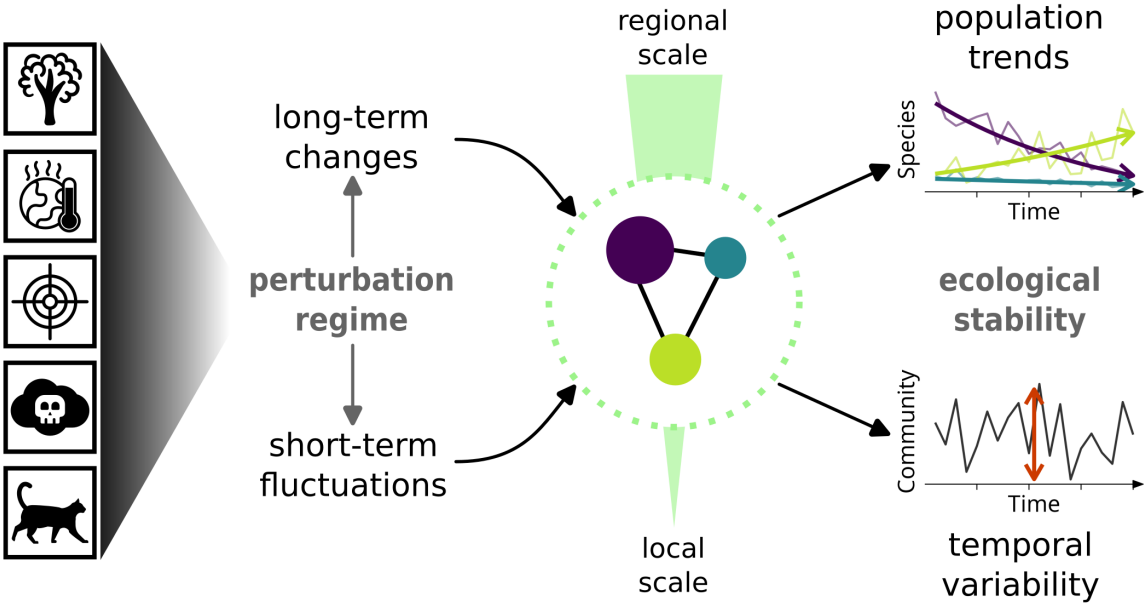

Figure I.0: **General framework.** The five main anthropogenic pressures drive changes in the perturbation regime consisting of long-term environmental changes as well as short-term fluctuations. Ecological dynamics couple these two perturbation types across geographical scales, and measured stability dimensions may reflect one or both perturbation types. Anthropogenic pressure icons modified from Bellard et al. (2022).

Biodiversity is the variety of all living beings and of the ecological complexes of which they are part. Across domains of ecology, biodiversity is studied at various organizational levels, from genetic diversity to ecosystem functioning, at all spatial extents, from local scale to the biosphere, and at many temporal resolutions, from few hours to geological time scales. Beyond their respective fascinating aspects and beyond the complexity of the interplay between these study scales, lies the consensus that modern human society is strongly and increasingly affecting biodiversity at every scale (IPBES 2019a). By the main five *anthropogenic pressures* (habitat destruction, climate change, exploitation, pollution, biotic invasions), human activities threaten the maintenance of ecological processes that shaped current biodiversity and that support the material requirements of human well-being as well as the relationships between humans and other living beings (Cardinale et al. 2012). Intrinsic, instrumental and relational values of biodiversity (Himes et al. 2024) are thus all at stake in the ongoing biodiversity crisis.

A key concern for biodiversity conservation lies in mapping the causal relationships between socio-economic drivers, anthropogenic pressures, and the various components of biodiversity across taxa and scales (Pereira et al. 2010). In that endeavour, *biodiversity monitoring* programs have been developed in order to document biodiversity change over time (Magurran et al. 2010). Often coordinated at the scale of countries or subcontinents, biodiversity monitoring schemes involve the repeated, often yearly, sampling of target groups of organisms at given locations. These valuable data sources have been accumulating proof that global biodiversity loss, *i.e.* increasing species extinctions worldwide (Díaz and Malhi 2022), translates to seemingly idiosyncratic changes in individual species' population abundances (McKinney and Lockwood 1999). As species disfavored by anthropogenic pressures decline in abundance and eventually go extinct, other species better suited to their new environmental conditions stagnate or increase in abundance (Dirzo et al. 2014, Finn et al. 2023). This is even more striking when considering natural *communities*, sets of interacting organisms from different species that co-occur at some spatial scale (Palmer and White 1994, Stroud et al. 2015). As so-called "loser" species decline and "winner" species increase, the local number of species may not necessarily change (Dornelas et al. 2014, Dornelas et al. 2023), but different communities do tend to change in composition and become increasingly similar to each other, undergoing biotic homogenization (Olden and Rooney 2006, Carroll et al. 2023). In the following, we will call these global patterns *long-term biodiversity change* and the regional and local shifts in population abundances will be designated by *long-term population trends*.

Joining ecosystem ecology with community ecology, biodiversity-ecosystem functioning research focuses on the impact of biodiversity on ecosystem-level processes (Hooper et al. 2005, Gonzalez et al. 2020). Early experimental and theoretical work in this field generated the insurance hypothesis, which states that species diversity both increases the magnitude of ecosystem properties and decreases the strength of their fluctuations, their *temporal variability* (Tilman 1996, Yachi and Loreau 1999). In species-rich communities subjected to a fluctuating environment, individual species' fluctuations can compensate for each other, reducing the variability of community abundance or community biomass. These less variable communities, because they have a high capacity to maintain their properties in the face of perturbations, are described as more *stable*, and the terms "community stability", "community constancy" and "community invariability" are often used interchangeably (Van Meerbeek et al. 2021). This rekindling of the complexity-stability debate (May 1972, Pimm 1984) generated a rich literature, especially in theoretical work, studying various aspects of ecological response to perturbations (Donohue et al. 2016, Kéfi et al. 2019). In this framework, endangering the maintenance of biodiversity poses a risk to human societies by increasing the variability of ecosystem processes and biodiversity should therefore be promoted to safeguard human well-being (Cardinale et al. 2012, Tilman et al. 2014).

The study of community invariability and the study of long-term population trends are thus naturally related by their common goal of understanding the impact of anthropogenic pressures on biodiversity. They also share their system of interest, *i.e.* population abundance across time, but typically consider it at different time scales and different spatial extents. Investigating the links between temporal variability and long-term population trends could help refining our understanding of biodiversity temporal dynamics. However, the two frameworks only rarely connect because they originate in different sub-disciplines of ecology, respectively community ecology and conservation ecology.

If temporal variability and long-term population trends were phenomenologically related, what would be the mechanism for this relationship ? If they both responded to similar anthropogenic pressures, what would be these pressures and how would temporal variability and long-term population trends co-vary across pressure gradients ? In order to be able to address these questions convincingly, a clear conceptual framework is needed to conjointly study temporal variability and long-term population trends.

In the following, I start from the theory of stability in ecology and show that existing literature presents,

despite definition issues, all the requirements for justifying the use of the term *"stability dimensions"* to designate both community (in-)variability and long-term population trends in the context of biodiversity monitoring. I expand on the study of community variability and anticipate how considering long-term population trends in this context could refine known patterns. By introducing the case study of wild bird monitoring, I review how regional long-term population trends reveal local responses of communities to anthropogenic pressures. Lastly, I summarize knowledge gaps on the relationship between our two stability dimensions and how we addressed them throughout this work.

I.1 From single perturbations to dimensions of ecological stability

From the early recognition that stability patterns are highly dependent on the definition of stability and on the way it is measured (Pimm 1984), the later profusion of stability definitions and metrics has motivated conceptual work to clarify the concept (Kéfi et al. 2019, Sánchez-Pinillos et al. 2024), drawing on theoretical and experimental results (Donohue et al. 2013, Domínguez-García et al. 2019). A precursor attempt is the article by Grimm and Wissel (1997) where, after calling ecological stability "one of the most nebulous terms in the whole of ecology", the authors propose to group the 70 stability concepts that they inventory in a reduced set of few fundamentally different properties. The concept of *stability dimensions* has later been introduced to describe this set of few properties that can explain many definitions of ecological stability (Donohue et al. 2013), and the number and relationships between stability dimensions is still up to debate (Isbell et al. 2026).

In the following section, I will try to define ecological stability dimensions in the context of biodiversity monitoring. I will first adopt a definition for ecological stability, then describe its underlying properties for simple perturbation scenarii and finally arrive to a definition of stability dimensions in the context of biodiversity monitoring.

Defining stability and its properties

The broadest definition for ecological stability is the *ability for ecological systems to maintain their function in the face of perturbations* (Van Meerbeek et al. 2021). This inclusive definition allows to bridge two schools of thought regarding ecological stability that both originate in the seminal paper by Holling (1973) : the study of *ecological resilience*, the ability for a system to maintain the relationships between its

components, and the study of *engineering resilience*, the ability for a system to return to an equilibrium condition after a disturbance (Holling 1996). While the study of engineering resilience focuses on systems close to their equilibrium (or close to a reference dynamical regime, Sánchez-Pinillos et al. (2024)), ecological resilience focuses on whether ecological systems may or may not shift to a different functioning than in their reference condition. Van Meerbeek et al. (2021) suggest to group the two definitions for resilience under the umbrella term "ecological stability" and identify five *stability properties* which, taken together, constitute ecological stability (Tab. I.1). In this framework, perturbations are any change that cause the ecological system to depart from a reference condition (Justus 2008).

Table I.1: **Stability properties.** Adapted from Van Meerbeek et al. (2021). For latitude and tolerance, the threshold designates the point at which the system can switch to different relationships between its components than in the reference condition.

Stability property	Definition
Resistance	The ability to withstand changes in environmental variable
Resilience	Rate of return to reference after a state displacement
Recovery	Ability to fully recover the reference condition
Latitude	Distance to threshold on the system variable axis
Tolerance	Distance to threshold on the environmental variable axis

A major source of complexity for estimating the ecological stability of natural communities is the multi-faceted nature of perturbations (Donohue et al. 2016). Ecological systems are affected by many environmental variables, and even for a single environmental variable, properties of the perturbations have to be considered (Sousa 1984). A fundamental distinction is whether or not a change in environmental condition is maintained in time. When a change in environmental conditions is sudden and reversed, it is called a *pulse perturbation*. When the change is maintained through time and never reversed, it is called a *press perturbation* (Donohue et al. 2016). We will call this distinction between press and pulse the *perturbation type*, although this term has also been used to describe other aspects of the perturbation (Radchuk et al. 2019).

Ecological response under different perturbation types

Stability properties are classically measured with respect to a well-identified perturbation of a single environmental variable, and not all stability properties may come into play for all perturbations (Van Meerbeek et al. 2021). For example, perturbation intensities that are too low to induce a shift in system functioning will not allow to measure latitude and tolerance. Moreover, since press perturbations are maintained in time, they never allow the system to return to the reference condition, and recovery and resilience are thus difficult to define.

As an example, consider two species whose carrying capacities linearly decrease with temperature following different slopes (Fig. I.1A). Under a pulse perturbation, the species whose carrying capacity changes the most with temperature (species 1) experiences the strongest change in abundance (Fig. I.1B). Likewise, under the same press perturbation, species 1 is the most affected by the perturbation. The resistance of the two species to the two perturbations could be measured by comparing species abundances before and during the perturbations, and would yield that species 1 is less resistant than species 2.

In natural settings, the multiplicity of perturbations faced by populations and communities is not as simple as isolated pulse or press perturbations. The notion of *perturbation regime* denotes the type, frequency, magnitude and directionality of the perturbations that a given ecological system is subjected to (Battisti et al. 2016). Ecological systems are subjected to various perturbation regimes since long before human societies were capable of strongly altering them. Natural perturbation regimes have driven the evolution of natural communities (Sousa 1984), but are now pushed to unprecedented intensities by anthropogenic pressures. For example, selection by fire regimes explains the evolution of many plant species in Mediterranean ecosystems, but fire regimes have recently been amplified by land use and climate change up to a threatening level (Pausas and Fernández-Muñoz 2012).

When communities are subjected to various pulse perturbations of varying direction, intensity and frequency, a convenient approach is to consider these perturbations as random fluctuations and to call this perturbation regime *environmental stochasticity*. Arnoldi et al. (2019) show the mathematical assumptions made by considering a perturbation regime made of multiple pulses as random environmental stochasticity. Conversely, when similar press perturbations of a given environmental variable accumulate

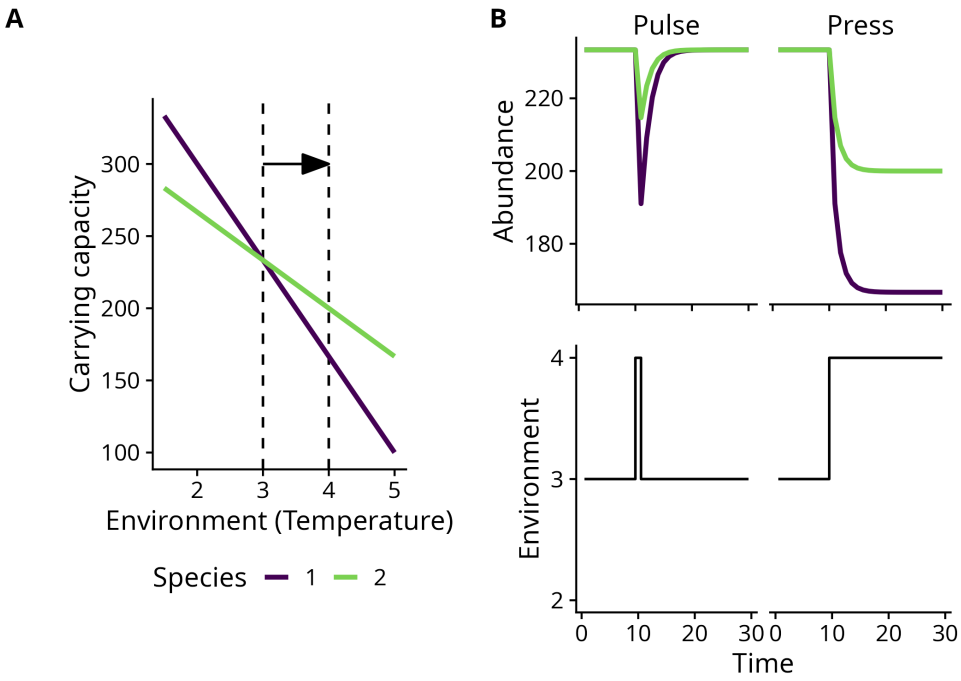

Figure I.1: **Response of two example species to simple perturbations.** (A) Carrying capacity decreases linearly with temperature. The slope of this decline (solid lines) for species 1 is twice as steep as the slope for species 2. The arrow denotes the perturbation in environmental parameter, from the reference to the perturbed condition (dashed lines). (B) Response of the two species (top) to changes in environmental conditions (bottom). Species abundances follow a discrete logistic growth with $N_{t+1} = rN_t(1 - N_t/K(T_t))$ with $r = 0.5$ for the two species. $K(T_t)$ is the carrying capacity for T_t, the temperature at time t and varies according to panel A. This example is inspired by Santisteban et al. (2012) , who show a linear negative relationship between spring temperature and annual survival of a population of red crossbill *(Loxia curvirostra)*, a forest passerine bird, in Idaho, USA.

through time, the environmental variable shows a *long-term directional change*. Others have described this perturbation regime as a separate perturbation type, the ramp perturbation (Van Meerbeek et al. 2021), but for clarity we will consider long-term environmental changes as a perturbation regime.

Fig. I.2 shows the response of the two example species from Fig. I.1 to environmental stochasticity, to long-term changes, or to both. Compared to species 2, the lower resistance to changes in temperature of species 1 is driving a stronger temporal variability under environmental stochasticity (Fig. I.2, left), and a stronger change in population abundance under long-term environmental change (Fig. I.2, middle). If the perturbation regimes had been stronger (*i.e.* more variable environment for environmental stochasticity and stronger change for long-term environmental change), the responses of both species would have been stronger. Both temporal variability and long-term population changes thus integrate the strength of the perturbation regime with intrinsic ecological stability properties.

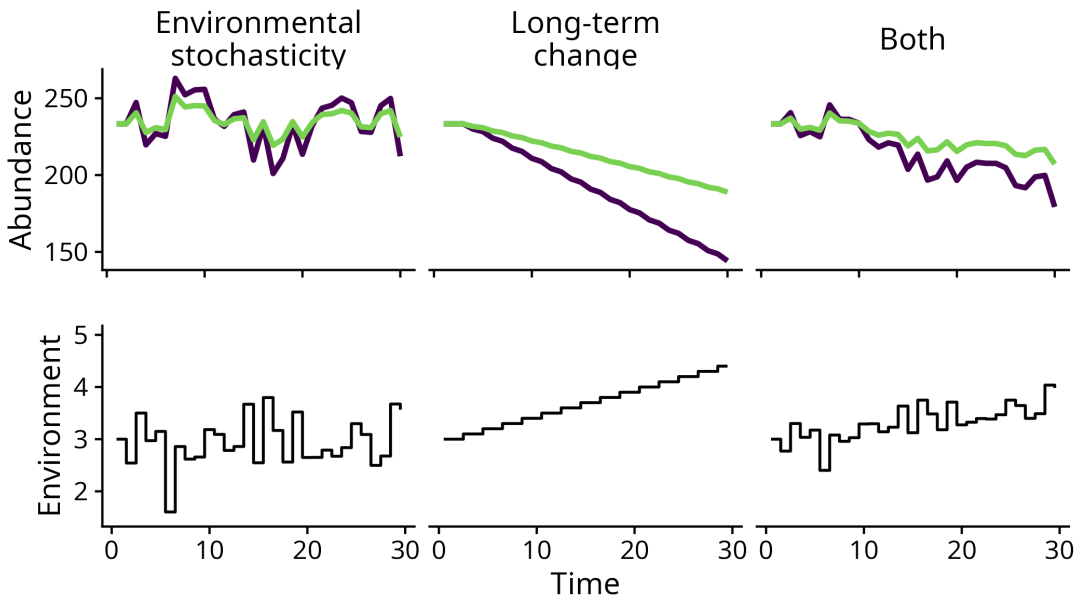

Figure I.2: **Response of two example species to three perturbation regimes.** Carrying capacity decreases with temperature, which changes through time (bottom). Time series of population abundance of two species (top). Species 1 in dark purple is less resistant to temperature change than species 2 (light green). Species abundances follow a discrete logistic growth with $N_{t+1} = rN_t(1 - N_t/K(T_t))$ with $r = 0.5$ for the two species. $K(T_t)$ is the carrying capacity for T_t.

Under both environmental stochasticity and long-term changes, ecological systems show both long-term population trends and temporal variability around these trends (Fig. I.2, right). Measuring exactly which environmental changes drive which variations in species abundances is difficult, even more so when several environmental parameters have different temporal dynamics. However, measuring two aspects of

community temporal dynamics may enable comparing ecological response across different perturbation regimes or across species. In our example, species 1 has a stronger trend and is more variable around its trend than species 2, but if they were under different environmental parameters to which they had different resistances (Polazzo et al. 2024), one could imagine all combinations of temporal variability and long-term trends for species 1 and 2. This question of **assessing if and how do variability and trends co-vary will be addressed throughout this dissertation.**

As we showed in an example scenario (Fig. I.2), under constant perturbation regime, higher temporal variability and stronger population trends can be interpreted as signs of a lower ecological stability. While they are not stability properties in a strict sense (Justus 2008), they integrate stability properties with the strength of the perturbation regimes. By definition, long-term trends are associated to a perturbation regime that operates on a longer timescale than the short-term fluctuations that generate temporal variability. Investigating both temporal variability and long-term trends in natural systems can thus provide information on ecological response to perturbations at different time scales, connecting different aspects of temporal dynamics in ecology (Hastings 2016, Gonzalez et al. 2020).

Stability and biodiversity monitoring

Natural communities are subjected to concurrent perturbation regimes of many environmental variables, some of which are driven by anthropogenic pressures (Díaz and Malhi 2022) and some of which result from feedbacks from community dynamics themselves (Pichon et al. 2026). In order to measure population and community stability properties (Tab. I.1) from biodiversity monitoring data, one would need to evaluate which exact changes in environmental variables cause which changes in demographic parameters, inducing which responses for all species' population abundances. While this is a common question in population ecology (Selwood et al. 2015), the task is daunting at the scale covered by biodiversity monitoring. However, because they integrate properties of the perturbation regimes with stability properties, temporal variability and long-term population changes can be used to quantify changes in perturbation regime or in ecological stability, allowing to describe biodiversity's response to anthropogenic drivers in a more exhaustive way than by focusing only on temporal variability or only on long-term population trends.

In our framework, we adopt the following assumptions, summarized by Fig. I.0:

- any natural community is subjected to a perturbation regime presenting an intricate mix of environmental stochasticity and long-term changes in environmental variables (Sousa 1984)
- anthropogenic pressures can change the perturbation regime by increasing or decreasing the strength of environmental stochasticity, amplifying or buffering long-term changes, or all combinations thereof (Donohue et al. 2016)
- under constant population and community stability, variations in long-term changes in population abundances or in temporal variability of natural communities can be explained by changes in properties of the perturbation regime
- under constant perturbation regime, variations in long-term changes in population abundances or in temporal variability of natural communities can be explained by changes in ecological stability

Co-occurring species in a community share environmental conditions, but may respond differently to changes in environmental variables (Polazzo et al. 2025). Under any perturbation regime, the response at the scale of community abundance then depends on the strength of individual species' responses and on how well their responses can compensate for each other (Thibaut and Connolly 2013). The temporal dynamics of a given community subjected to a given perturbation regime can thus be characterized by its long-term population trends and by its temporal variability, both at population and community scale. In the following, we will call *stability dimensions* these integrative features of community response to the perturbation regime. While they are not stability properties in a strict sense, they are indeed features of the community's ability to maintain species abundances in the face of the perturbation regime, and thus qualify for the term stability. Because long-term trends and temporal variability arise from different perturbation regime types and because they are measured differently, they are not a direct consequence of one another and therefore also qualify for the term dimension.

By investigating links between temporal variability and long-term population trends, **we will investigate the links between two integrative dimensions of ecological stability** (Donohue et al. 2013, Isbell et al. 2026). Before pointing towards existing work and knowledge gaps in the relationship between temporal variability and long-term population trends, I will expand on known mechanisms that drive population and community variability as well as known phenomena that explain long-term population trends in natural communities.

I.2 Temporal variability around an equilibrium

When studying temporal variability, the strength of short-term fluctuations in community or population abundance, it is often assumed that fluctuations occur around an equilibrium, *i.e.* a state where the system would stay if it was unperturbed. Theoreticians adopt this assumption because it enables many mathematical tools (May 1972, Arnoldi et al. 2019), experimentalists and empiricists often use detrending methods to focus on temporal variability by ruling out the impact of long-term trends on measured variability metrics (Tilman 1996, Li et al. 2021). An implicit assumption is that there is no mechanism by which ecological response to short-term fluctuations could depend on the presence of long-term trends. Fueling the diversity-stability debate, this near-equilibrium assumption has generated a rich literature with a continued dialogue between theoretical and experimental work (Lehman and Tilman 2000, Tilman et al. 2006), later joined by investigations on observational data (Blüthgen et al. 2016, Valencia et al. 2020b). While in this dissertation we will explicitly consider **how long-term population trends challenge the near-equilibrium assumption**, here I review existing theory near equilibrium.

Population variability

Taylor (1961) noticed that population variance "is proportional to a fractional power of the mean" with said fraction often between 1 and 2. In constant environments, population abundance is random when individual survival and reproduction vary randomly across individuals. This source of variation in population abundance is called *demographic stochasticity*, and yields variances that are proportional to mean abundance (Engen et al. 1998). When short-term fluctuations in environmental parameters affect all individuals in the population similarly, the variance of abundance is proportional to the square of mean abundance. Taylor's law thus arises because i) natural populations are subjected to a mixture of environmental and demographic stochasticity (Lande et al. 2003) and ii) many populations show substantial interindividual variation in response to environmental change (Violle et al. 2012, Des Roches et al. 2018).

Under environmental stochasticity, a common measurement for variability is the coefficient of variation, the ratio between temporal standard deviation and mean. Using the coefficient of variation allows to consider changes in population variability separately from changes in population mean and its ease

of measurement has favored its use in empirical studies (Kéfi et al. 2019). In linear systems close to equilibrium, the coefficient of variation of population abundance is equal to the ratio of the variance of population response to environmental fluctuations and the square root of the species' linear growth rate (Arnoldi et al. 2016, Mentges et al. 2024). Populations are thus more variable under stronger environmental stochasticity, or when they have a lower growth rate. This extends to linear approximations of non-linear systems close to their equilibrium (Arnoldi et al. 2019).

When environmental fluctuations are not modelled explicitly, the variance of the responses to short-term fluctuations in environmental parameters is often called the strength of environmental stochasticity (Arnoldi et al. 2019). This semantic simplification is harmless when a single species is considered, but when environmental stochasticity is the perturbation regime shared by several species, there is some risk of confusion between the strength of the short-term fluctuations in environmental parameters and the strength of each species' response to these fluctuations. While the former is a property of the perturbation regime alone, the latter integrates species resistances with the strength of the perturbation regime. In the example of Fig. I.2, species 1 and 2 are subjected to environmental fluctuations of the same strength, but they have different resistances to environmental changes and species 2 exhibits a lower temporal variability than species 1. The simplified definition yields that species 1 is subjected to a stronger environmental stochasticity than species 2, while actually species 1 has a higher population variability than species 2 but they are subjected to the same environmental stochasticity.

Functional traits that explain the response to fluctuating environmental variables as well as traits that explain the linearized growth rate thus conjointly define a species' response to environmental fluctuations (de Bello et al. 2021). Higher individual body mass is generally expected to decrease the linearized growth rate (Brown et al. 2004, Brose et al. 2006), but the response to fluctuations depends on which environmental parameters both vary and affect species abundances, and thus depends on taxa and perturbation regimes. For example, a fast-growing pace of life is suspected to decrease species resistance to drought in dryland plants (Campetella et al. 2020), but decreases temporal variability in generic models (Rip and McCann 2011, Greyson-Gaito et al. 2023). An example of the impact of intrapopulation variability in reproductive strategies has been shown in lizards, where high pace of life variance decreased population variability (Dochtermann and Gienger 2012). In this dissertation, we will address **the role of functional traits in the response to environmental stochasticity, but also to**

long-term environmental changes.

Community variability and the insurance hypothesis

Community variability, in the absence of long-term environmental changes, is the response of community abundance to environmental fluctuations. Since community abundance is the sum of all populations' abundances, community variability is entirely driven by the species' responses to environmental fluctuations and their correlations (Box 1). Community abundance is thus more variable if populations are more variable, or if species fluctuations occur synchronously and fail to compensate for each other. These two components of community variability are themselves driven by community composition, diversity and structure (Loreau and de Mazancourt 2013). Early biodiversity experiments indeed measured that community biomass tends to be less variable as the number of species in the community increases (Tilman and Downing 1994, Tilman 1996), a pattern now well supported across study systems both in empirical and experimental settings (Craven et al. 2018, Pennekamp et al. 2018, Xu et al. 2021). Since this contradicts models that predict a mathematical impossibility for complex unstructured random matrix models to exhibit stable equilibria (May 1972), a positive biodiversity-invariability relationship was not expected under unstructured community dynamics.

Box 1: Community variance as the variance of a sum of random variables

In a community of S species of random abundance X_i, community abundance $Y = \sum_i^S X_i$ is a sum of random variables. With ρ_{ij} the correlation coefficient between species i and species j, we can write (Loreau and de Mazancourt 2008):

$$\begin{aligned} V[Y] &= \sum_i V[X_i] + \sum_i \sum_{j \neq i} E[(X_i - E[X_i])(X_j - E[X_j])] \\ &= \sum_i V[X_i] + \sum_i \sum_{j \neq i} \rho_{ij} \sqrt{V[X_i]} \sqrt{V[X_j]} \end{aligned} \tag{I.1}$$

For a given distribution of population variances, community variance is maximal when $\rho_{ij} = 1$ for all pairs i and j and minimal when species fluctuations are fully desynchronized. Species variances thus set a range for possible values of community variance, and the location of community variance within that range is set by interspecific correlations.

Analytical decompositions of the coefficient of variation of community abundance (Thibaut and Connolly 2013, Wang et al. 2019, Zhao et al. 2022) are consequences of Equation I.1 under some assumptions for $\rho_{i,j}$. In particular, writing $V[X_i] = \sigma_i^2$ and $E[X_i] = \mu_i$, Thibaut and Connolly (2013) show that CV$[Y]$, the coefficient of variation of community abundance, can be written:

$$\mathrm{CV}[Y] = \frac{\sqrt{V[Y]}}{\sum_i \sigma_i} \sum_i \frac{\mu_i}{E[Y]} \mathrm{CV}[X_i] = \sqrt{\phi}\, \widetilde{\mathrm{CV}}_{\mathrm{pop}} \tag{I.2}$$

ϕ is the species synchrony index (Loreau and de Mazancourt 2008) and is equal to 1 when $\rho_{i,j} = 1$ for all species pairs (perfect synchrony). $\widetilde{\mathrm{CV}}_{\mathrm{pop}}$ is the abundance-weighted average population variability.

The positive biodiversity-invariability relationship was named the "insurance hypothesis" (Yachi and Loreau 1999) or the "portfolio effect" (Tilman et al. 1998). Its underlying mechanisms are separated into the *statistical averaging* effect on one side, where under independent species responses to environmental fluctuations, species richness decreases community variability because of properties of the sum of random variables with mean-variance scaling (Doak et al. 1998). On the other side, *compensatory dynamics* denote the capacity for ecological dynamics such as competitive interactions to induce negative covariances between species fluctuations (Tilman 1999). Thibaut and Connolly (2013) provided a unifying framework by writing the community coefficient of variation as the product of average population variability and the species synchrony index of Loreau and de Mazancourt (2008) (Box 1). Community variability can thus be decomposed into average population variability and species synchrony (Fig. I.3), and the portfolio effect has been shown to operate by a negative effect of species richness on species synchrony (Loreau and de Mazancourt 2008, Xu et al. 2021). Fig. I.3B shows two simulated communities with similar community variabilities, but where the underlying community variability components vary.

A recent development of the species synchrony framework allowed to partition species synchrony in explicit expressions for the statistical averaging effect and for the compensatory dynamics effect (Zhao et al. 2022). There, the statistical averaging effect is driven by the evenness of species variances while compensatory dynamics arise due to differences in species responses to environmental fluctuations and due to interspecific interactions (Danet et al. 2025). The framework can also be partitioned across spatial scales (Wang et al. 2019), yielding a general theory of how variability scales through ecological and geographical scales (Wang et al. 2017, Clark et al. 2021, Liang et al. 2025).

Community variability under anthropogenic pressures

An initial critique to early diversity-variability experiments was possible confounding effects of environmental conditions on both species richness and temporal variability (Tilman 1996). Since then, empirical

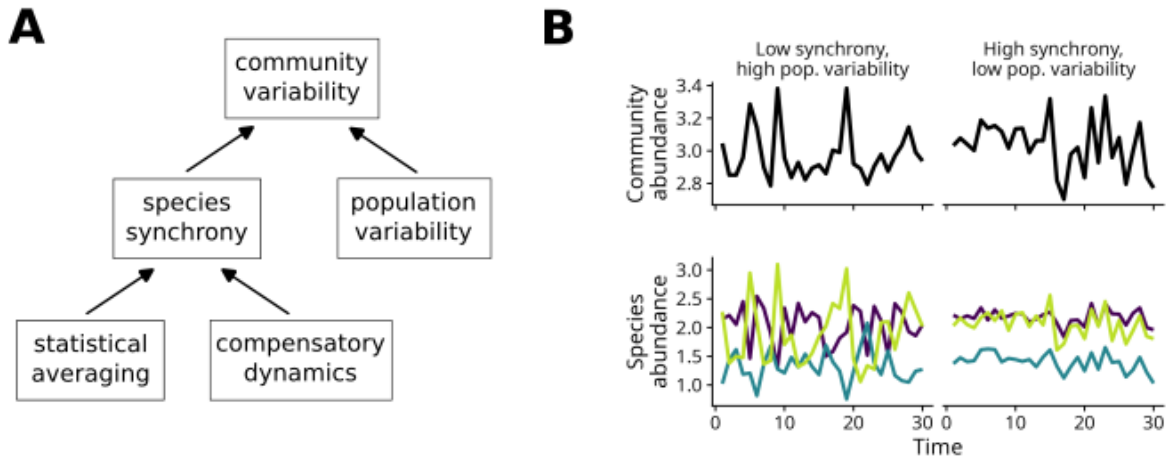

Figure I.3: **Community variability components.** (A) Sequential decompositions of community variability into community variability components. (B) Simulated communities with an adapted version of the community model in Loreau and de Mazancourt (2008), allowing to set species synchrony and species variances. Abundances are log-transformed.

and experimental tests of the insurance hypothesis often take environmental drivers into account in order to document their effects on temporal variability. For example, in plant communities, nitrogen enrichment (Zhang et al. 2016) and mean temperature (Valencia et al. 2020b) have been shown to increase community variability by increasing both synchrony and average population variability. In some cases, environmental drivers affect community variability components both directly and via effects on species diversity (Fig. I.4): Olivier et al. (2020) show that land use affects bird, bat and butterfly communities via increased population variability and increased species synchrony via decreased diversity.

However, an unresolved question is partitioning environmental effects on community variability into effects on the perturbation regime or on community stability properties via effects on community composition (Fig. I.4). In that endeavor, much progress is done by integrating the functional composition of communities and identifying which traits drive changes in community stability properties (Hillebrand et al. 2018b, Weeks et al. 2026). Just like species pace of life traits are candidates to explain population variability, the distribution of pace of life traits within communities is a strong candidate to explain community variability (de Bello et al. 2021). The diversity of species' response traits to the perturbed environmental parameters is also expected to decrease community variability (Polazzo et al. 2025). Empirical evidence in bird communities from monitoring programmes show that the diversity of traits associated to the response to short-term perturbations can decrease species synchrony (White et al. 2023), and that the community-weighted mean of a slow-fast trait continuum decrease both species synchrony and average population

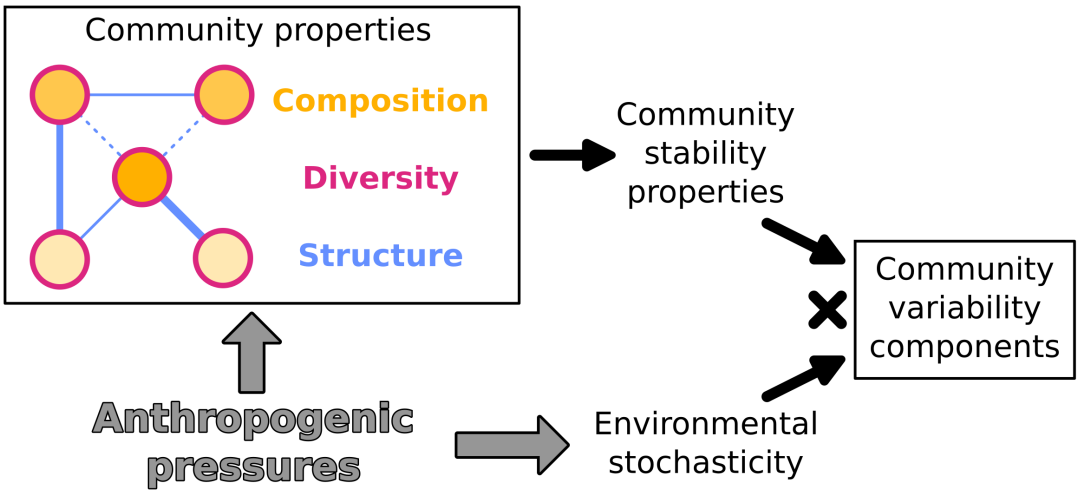

Figure I.4: **The study of community variability under anthropogenic pressures.** Elements in boxes are the most studied in the theoretical and empirical literature of the diversity-invariability relationship. Small black arrows illustrate that community composition drives community stability properties (Tab. I.1) which interact with the strength of environmental stochasticity, generating variable community abundance and its components. Since anthropogenic pressures may alter both environmental stochasticity and community properties (large gray arrows), they can affect community variability.

variability (Li et al. 2021). Note that even for a single environmental driver such as temperature, different taxa will show different responses (Rodrigues et al. 2025).

Relaxing the equilibrium assumption

The importance of long-term changes in environmental parameters for explaining temporal variability is well recognized in systems that can show critical transitions, *i.e.* large changes in functioning following a small parameter or state perturbation (Scheffer et al. 2001). There, the increasing proximity to a critical transition is accompanied by increases in temporal variability and temporal autocorrelation (Dakos et al. 2024). However, the long-term change that causes the arrival of the critical transition is typically very slow compared to system dynamics (Scheffer 2009). In these settings, long-term changes that generate long-term population trends do increase the temporal variability of the system as its resilience decreases, but the assumption of proximity to equilibrium is well respected as long as the threshold for the critical transition is not crossed.

When long-term population trends are acknowledged in studies focusing on temporal variability, it is because they recognize that the presence of long-term trends prevents the use of very simple variability measurements (Lepš et al. 2019). When taking the raw coefficient of variation of a time series that show

a long-term trend, the percentage of variance explained by the long-term trend is indeed erroneously attributed to temporal variability. For this reason, many studies that focus on temporal variability on experimental or empirical data with long-term trends use some detrending technique in order to avoid biasing their variability estimates (Tilman 1996, *e.g.* Craven et al. 2018, Danet et al. 2021). Beyond this direct measurement bias, the possibility that long-term trends might challenge the near equilibrium assumption is rarely acknowledged outside of theoretical studies (Menck et al. 2013, Arnoldi et al. 2016).

Out-of-equilibrium dynamics are indeed not often considered in the study of temporal variability. In theoretical work focusing on systems that show alternative stable states (Hastings 2004), transient dynamics may for example allow systems that have crossed a critical transition to stay in the vicinity of the now unstable reference condition (Hastings et al. 2018), with consequences on temporal variability (Arumugam et al. 2021). For well-known population dynamics models which seldom have alternative stable states, **theoretical understanding of how being far from equilibrium might affect temporal variability is lacking**. In biodiversity monitoring data, empirical studies that measure one stability dimension tend to overlook the other, making any prediction difficult. As natural perturbation regimes show both short-term fluctuations and long-term environmental changes (Donohue et al. 2016), relationships between the two stability dimensions should however be expected.

I.3 Long-term population trends across ecological scales

Under the force of natural selection, within populations, groups of individuals (including their descendents) with lower fitness will tend to decline in abundance in favor of groups better suited to environmental conditions. Over geological time scales, evolution has been registered in the fossil record, documenting how entire clades arose and eventually became replaced (Benson and Druckenmiller 2014). The focus for conservation biology is therefore not to avoid all forms of change (Robert et al. 2017), but to safeguard future change by conserving evolutionary potential (Soulé et al. 1985, Sarrazin and Lecomte 2016, Milot et al. 2020) and to understand by which mechanisms do current long-term biodiversity changes outpace their baseline counterparts (Duchenne et al. 2022, Díaz and Malhi 2022). With the current rate of species extinction estimated to be a hundred times higher than the background rate (Ceballos et al. 2015), anthropogenic pressures are causing the likely onset of a sixth mass extinction (Cowie et al. 2022).

Because they are signs of potential future species extinctions, long-term population trends are a major field of work in conservation ecology (Willis et al. 2007), with large-scale biodiversity monitoring programmes as a key data source (Lindenmayer et al. 2022). There, a main challenge lies in detecting which environmental parameters drive long-term changes (Thomas et al. 2026), which often depend on considered taxa and geographical area (Finn et al. 2023). Analysing community time series from biodiversity monitoring programmes, conservation ecologists and community ecologists have developed complementary paradigms on attributing long-term changes of many species to environmental drivers (Box 2). Conservation ecologists ask what is the long-term pattern that most species exhibit (e.g. Loh et al. 2005), which we will call the *species paradigm*. Community ecologists ask what is the long-term pattern that community-level aggregates exhibit (e.g. Dornelas et al. 2014), the *community paradigm*. The apparent contradictions between results from the two paradigms have been labelled as a biodiversity conservation paradox (Fig. I.5), but can be resolved by adopting a multi-scale framework (Hillebrand et al. 2018a, Chase et al. 2020). Both perspectives indeed contribute to the understanding of how anthropogenic pressures drive long-term changes (Fig. I.5C).

Since the empirical aspects of my PhD work analyse data from the French Breeding Bird Survey, we will adopt the case study of wild birds, especially in Western Europe. Overall, bird decline operates by declines of specialist species which induces long-term changes in community composition (Devictor et al. 2008a). The main environmental drivers of bird long-term changes in Europe are land use, especially agricultural intensification, and climate change (Gaüzère et al. 2020, Rigal et al. 2023). In this dissertation, **we will consider links between land use and both variability and population trends**, but in the following section, I review evidence of wild bird long-term trends and their drivers. I first review findings from the species paradigm and secondly from the community paradigm. Studies linking the two approaches allow for a comprehensive view of bird long-term trends, with open questions across geographical scales.

Wild birds in the Anthropocene

The passenger pigeon (*Ectopistes migratorius*) was once one of the most abundant bird species in the world. It fed on mast from the deciduous forests of North America where it was heavily hunted by settlers as massive passenger pigeon colonies offered a major natural resource (Bucher 1992). Exploitation and breeding disruption by industrialized hunting conjoined with decline in food availability generated a very

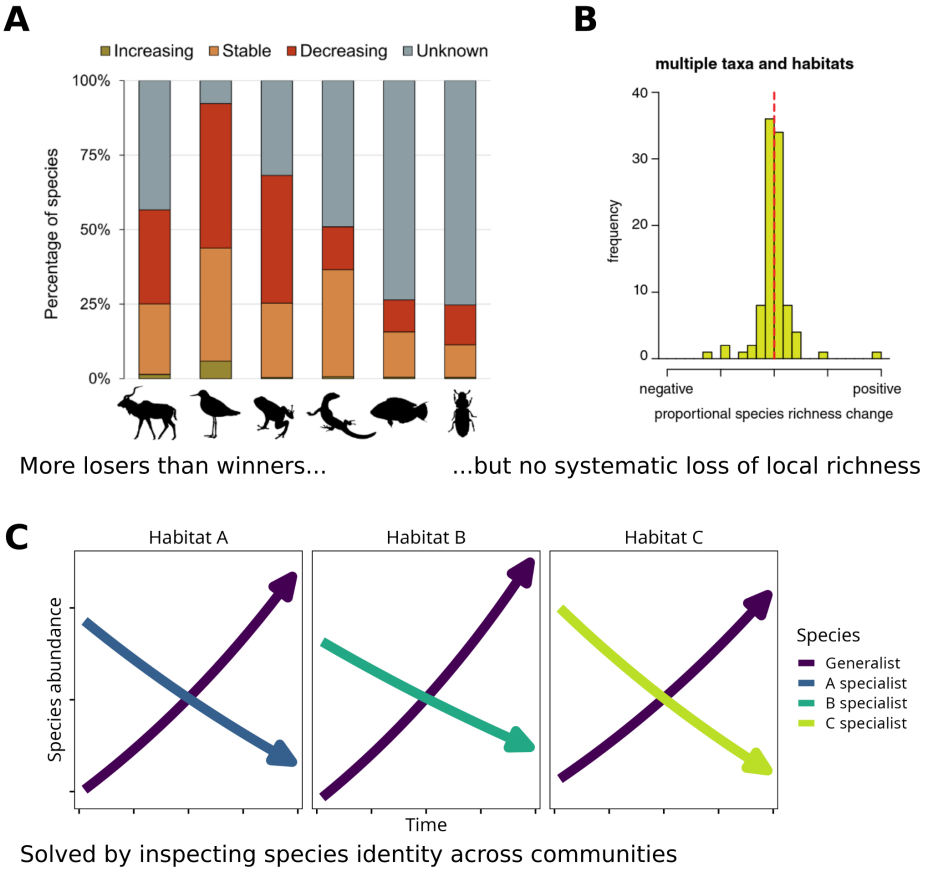

Figure I.5: **Solving the biodiversity conservation paradox.** (A) In a global database of population time series across taxa, many species show population declines while fewer increase, with substantial remaining uncertainties. Adapted from Finn et al. (2023). (B) In a global database of community time series, some communities show increases in richness while some show declines, with no shared pattern. Adapted from Vellend (2017) with the original figure in Dornelas et al. (2014). (C) As a possible solution, consider four imaginary species (different colors) spread among three habitat types with a declining specialist species each and an increasing generalist present in all three habitats. There are more species declines than increases, like in panel A, but local richness is constant through time, like in panel B.

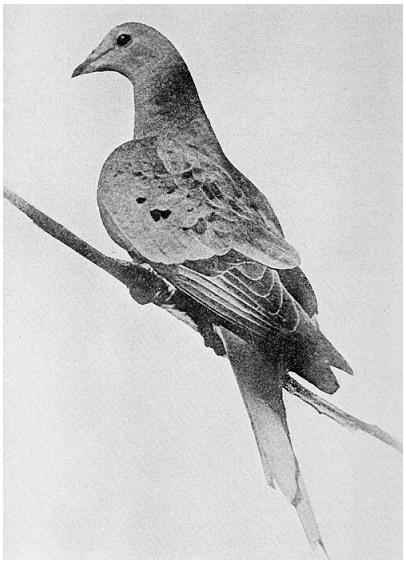

Figure I.6: **Martha, the last passenger pigeon.** Photographed by Enno Meyer in the Zoological Gardens of Cincinnati, United States, 1912 (Shufeldt 1921).

strong decline in passenger pigeon population size (Hung et al. 2014), which over the nineteenth century went from hundreds of millions of individuals to just one, named Martha, who died in 1914 (Fig. I.6). Concern about the possible extinction of the passenger pigeon arose as early as 1847 (Fuller 2015), a first example of the close link between wild birds and early concerns in biodiversity conservation. Half a century after the death of Martha, the fate of wild birds was again associated to the rise in awareness for the impact of human activities on biodiversity by Rachel Carson's *Silent spring*. There, noticing that widespread insecticide use was reducing food availability for birds, she denounced the use of pesticides as "man's war against nature" that would "still the song of birds and the leaping of fish in the streams" (Carson 1962). Over the sixty years since the publication of Carson's work, more than 50 bird species have become extinct, for a total of 216 since the 16th century, most of them endemic to islands (Kittelberger et al. 2024).

Complementary to conservation concerns, wild birds are a common study taxon in ecology with close to 10000 extant described species (Jetz et al. 2012). Because their breeding and feeding lifestyles can integrate different aspects of habitat quality and because of their relative ease of observation, the local abundance of some bird species is often used as an indicator of good local ecosystem conditions (Carignan and Villard 2002). They are involved in many ecosystem-level processes such as seed dispersal and insect population control (Sekercioglu 2006) and provide cultural contributions to human societies (Gaston et al. 2018).



Figure I.7: **A farmland specialist: the Eurasian skylark.** Solitary, ground-nesting and insectivorous, Eurasian skylarks were formerly very abundant in European farmland. Their populations are strongly declining since the last half of the 20th century (Wilson et al. 1997). Picture by Ekaterina Chernetsova.

Among the various characteristics of birds (Tobias et al. 2022), an important trait for explaining their response to perturbations is their ecological specialization (Devictor et al. 2008b). A species is classified as a specialist when it occupies a relatively narrow ecological niche (Clavel et al. 2011), and specialization therefore entails various facets and is measured in various ways (Morelli et al. 2019). The two most common are habitat breadth and diet breadth (Şekercioğlu et al. 2025), where a species that is able to occupy few habitats or relies on a few food sources is labelled as a habitat or diet specialist, respectively. A notable example of a specialist bird is the Eurasian skylark, a farmland specialist with an insectivorous diet (Fig. I.7). The evolutionary history of farmland specialist birds is closely linked to the spread of grasslands across Eurasia in the late Miocene, around 10 million years ago (Fuchs et al. 2015, Cai et al. 2021, García-Navas et al. 2024). Farmland specialist bird species therefore often have insectivorous or granivorous diets as insects and seeds were major food sources in these ecosystems. Many farmland specialist birds thus also share similar nesting, foraging and dietary behaviors. Since even species where adults are mostly granivorous rely on insects to feed their young, survival and reproduction of most farmland birds suffer from the strong declines in insect populations across Europe and North America (Wagner 2020). In the following, we will most often use the term *specialist* to denote habitat specialization, but note that habitat specialization is associated to other functional traits across species.

Means of long-term trends: the species paradigm

Agricultural practices drive long-term declines of farmland specialist bird species in Europe and North America (Donald et al. 2001, Rigal et al. 2023). In extensive agricultural landscapes, heterogeneous landscapes offered diverse food sources and habitats for farmland birds and for the insects they feed on (Benton et al. 2003). Agricultural intensification, by the increase in pesticide and fertilizer use as well as by landscape homogenization, is unsustainably affecting farmland ecosystem functioning, even threatening the conditions for long-term food production (Rasmussen et al. 2018). Farmland specialist birds increasingly find less food to support them (Wagner 2020), less fallow and hedges for shelter or nesting (Traba and Morales 2019), and suffer direct physiological effects from widespread chemical inputs (Molenaar et al. 2024). More generalist species that are able to exploit even strongly affected environments have more stable population trends (Mancini et al. 2023), while insectivorous and granivorous bird species decline in abundance (Bowler et al. 2019). Except for urban specialists, ecological specialization is linked to long-term decline (Burns et al. 2021). Other traits associated to long-term bird decline include long-range migratory behavior and adaptation to colder climates (Bowler et al. 2019).

Multi-species aggregates of long-term changes of bird population abundances by groups of habitat preference have been proposed as biodiversity indicators for evaluating agricultural policies across Europe (Gregory et al. 2004, Gregory et al. 2005). Their simplicity associated to their integrative property of reflecting how anthropogenic pressures affect different groups of birds have made the use of multi-species bird indices prevalent in studies aiming at predict the impact of climatic scenarios (Princé et al. 2013) or environmental policies on biodiversity (Princé et al. 2021, Reif et al. 2024). The PanEuropean Common Bird Monitoring Scheme publishes yearly updates of the long-term trend of Wild Bird Indices since 1980, with the 2024 update stating an average decrease of 10% for forest birds, 19% for all birds and 58% for farmland birds Fig. I.8.

Worldwide, near half of bird species decline in population abundance while half stagnate and a minority increases (Finn et al. 2023). However, measured long-term trends may vary depending on the geographical area or the scale at which the species trends are computed (Fig. I.9). A given species whose trend is increasing when estimated at a large geographical scale can decrease for some smaller geographical

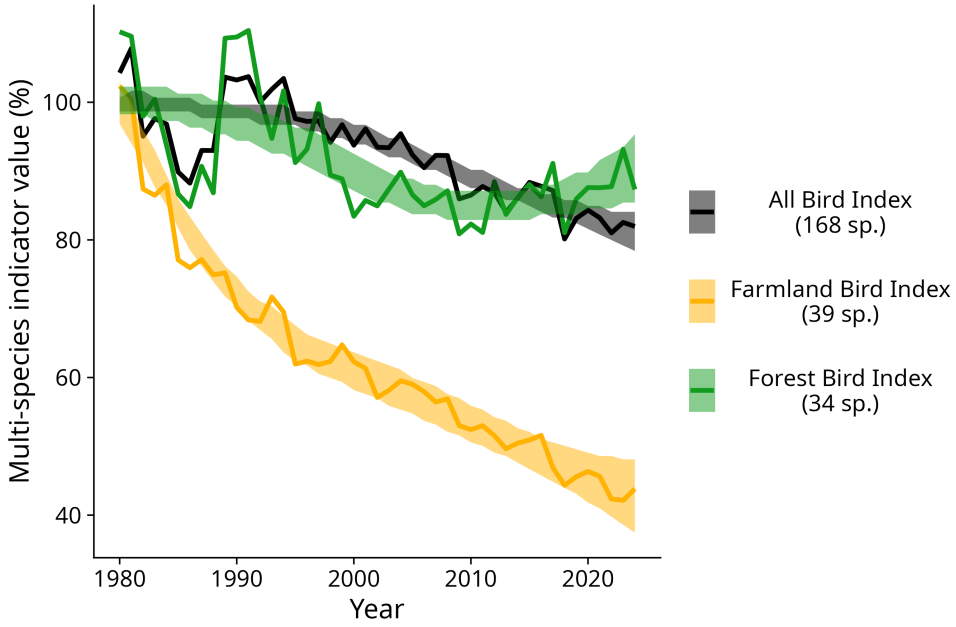

Figure I.8: **Wild bird indices from 1980 to 2024 in the PanEuropean Common Bird Monitoring Scheme.** Solid lines are each year's geometric mean of relative abundances to the reference year, across bird species groups. Shaded ribbons denoted smoothed confidence interval bounds. Data and methods from PECBMS (2025).

extents, like the northern house wren in North America (Fig. I.9, bottom). For example, Bowler et al. (2021) show different long-term trends of multi-species indicators across different European countries, but also notice consistent effects of species traits, with more positive trends for warm-dwelling species and more negative trends for farmland specialist across four countries. In order to understand these patterns, measuring how underlying anthropogenic pressures affect birds at different geographical scales is needed (Gregory et al. 2023, Gaüzère et al. 2025).

Long-term trends of means: the community paradigm

Long-term population trends reshuffle community composition, on which aggregate metrics are computed in the community paradigm (Box 2). The simplest community metric, local species richness, can exhibit positive or negative long-term trends depending on the relative importance of declines or increases (Dornelas et al. 2014), which makes it a poor indicator of community long-term processes. Decreases of specialist species and increases of generalists drive different communities to be increasingly similar, a phenomenon called biotic homogenization (Olden and Rooney 2006). Bird communities in landscapes under agricultural intensification or land artificialization follow this long-term trend, with long-term declines in spatial dissimilarity (Davison et al. 2024). Spatial scale also matters in the community paradigm

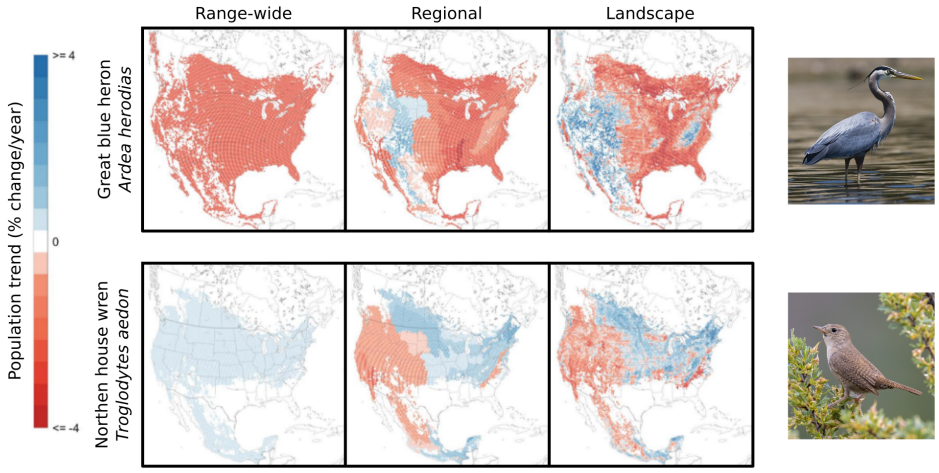

Figure I.9: **Bird population trends across geographical scales for two species.** Adapted from Johnston et al. (2025). Average population trends from 2007 to 2021 are computed across the whole North American Breeding Bird Survey (left), for every biogeographical region (middle), and across 27x27km^2 grid cells (right). Great blue heron picture by Michael L. Baird and northern house wren picture by Eric Ellingson.

(Allen et al. 2019), as local community turnover has been shown to be more closely linked to land use while turnover computed on regionally aggregated abundances was more strongly associated to climate change (Di Cecco and Hurlbert 2022).

Box 2: Two paradigms for long-term trend analyses

In biodiversity monitoring schemes, raw datasets typically contain the results of sampling several species i at sites s and times t as species abundance $X_{i,s,t}$. The sampling design usually standardises sampling effort across these three dimensions, or allows to take possible sampling effects into account. For example, for breeding bird surveys, several survey sessions each year allow to account for varying migration phenology across species (Princé et al. 2013).

In the species paradigm, a statistical model is fit on each species indepently:

$$X_{i,s,t} \sim \beta_i t \ + \ \omega_s \tag{I.3}$$

In Equation I.3, β_i is an estimator for the long-term trend of species i after taking its spatial variability into account with some terms ω_s. The distribution of β_i across species and its relationship with species traits is used to indicate which species show the most negative trends and what could be the underlying causes (*e.g.* Bowler et al. 2019).

In the community paradigm, a community-level aggregate $Y_{s,t} = f(X_{1,s,t}, X_{2,s,t}, \dots)$ is first computed, then a statistical model for the long-term trend of $Y_{s,t}$ is fit:

$$Y_{s,t} \sim \beta_s t \tag{I.4}$$

> Long-term changes of Y in community s are measured by β_s, and the distribution of β_s across sampling sites is compared to the distribution of anthropogenic pressure indicators across sites, allowing to identify possible drivers of change in community-level aggregates (*e.g.* Davison et al. 2024).

A simpler surrogate index of biotic homogenization is the community-weighted mean of ecological specialization, which tends to decline in bird communities (Devictor et al. 2008a, Gaüzère et al. 2020). Species traits associated to long-term trends in the species paradigm are therefore likely to show long-term trends in community-weighted means. Functional diversity indices, which quantify the diversity of functional traits around their community-weighted means, show more contrasted long-term trends, with increases or decreases depending on traits and metrics used (Monnet et al. 2014, Barnagaud et al. 2017). This is likely due to functional diversity metrics being numerous and difficult to relate to each other (Mouchet et al. 2010).

A positive long-term trend of a generalist species, seen as a sign of low conservation concern in the species paradigm, is thus interpreted as a sign of biotic homogenization in the community paradigm. High species richness, associated to high ecosystem functioning in community ecology, can be caused by a situation where many new generalist species are settling while declining specialists are not locally extinct yet, a phenomenon called extinction debt (Tilman et al. 1994, Kuussaari et al. 2009). Tensions in interpretation between the species and the community paradigms have been named a biodiversity conservation paradox (Vellend 2017), but we have seen that they both help to describe the same phenomenon at different scales of interest (Fig. I.5).

Long-term trends in fluctuating environments

From the perspective of estimating long-term trends at large geographical scales, local-scale environmental fluctuations are seen as noise to account for (Rueda-Cediel et al. 2018, Gregory et al. 2019). Conversely, since local community turnover is not well understood (Di Cecco and Hurlbert 2022, Davison et al. 2024), empirical studies focusing on local-scale variability tend not to focus on long-term trends. However, we have seen that long-term population trends reshuffle species composition, possibly changing community stability properties, and vulnerability to short-term fluctuations may also indicate vulnerability to long-term changes in environmental variables. As cross-scale conceptual syntheses emerge for

long-term trends (Gaüzère et al. 2025) and for community variability (Liang et al. 2025), **acknowledging several perturbation types at several spatial scales** is crucial in order to better integrate several approaches. For example, many studies of community invariability attribute an instrumental value to local biodiversity by its role in stabilizing ecosystem functions (Cardinale et al. 2012), but local biodiversity may not necessarily decrease in the Anthropocene (Dornelas et al. 2023). Conversely, multi-species indices over large spatial extents document long-term trends of groups of species that may not all co-occur at smaller spatial scales, making links to ecosystem functioning limited.

I.4 Main research questions

In this dissertation, we explore the relationships between two integrative stability dimensions, temporal variability and long-term changes in population abundances. Beyond the methodological need to account for long-term trends when measuring community variability in biodiversity monitoring data, we have seen that long-term changes in environmental conditions may alter community variability by acting both on community stability properties via community composition and on the strength of short-term environmental fluctuations. Conversely, because of its ability to integrate short-term fluctuations in environmental conditions, community variability may bring complementary information to long-term changes in biodiversity indicators, possibly more strongly linked to local short-term perturbation regimes. Moreover, theoretical expectations for links between these two integrative dimensions of ecological stability are currently lacking. The following work attempts to bridge the study of community variability with the study of long-term population changes across three study cases.

At a local scale, **how does local land use intensity affect bird population trends and bird population variability around their trends ?** Clarifying the local imprint of regional long-term population trends and how they co-vary with population variability and their common drivers is needed to understand how regional patterns translate to local scales.

In simulated stochastic communities, **is there a mechanistic link between long-term trends and measured temporal variability ?** Theoretical predictions on community variability have been made near equilibrium, making predictions on possible impacts of long-term population trends on community variability difficult.

Averaged over communities in France, **how do long-term trends and community variability vary in time ?** With long-term trends and community variability integrating intrinsic stability properties with perturbation regimes, their temporal variation at the species and at the community level can reveal temporal changes in perturbation regimes or changes in stability properties, to be compared with species traits and changes in community composition.

II . General methods

In the following, I present some overarching methodological aspects that relate to several main chapters of this dissertation. I first detail the sampling protocol and data curation process for bird data from the French Breeding Bird Survey. I then summarize the several variability measurement methods that were used across this work, in order to make comparisons between them easier. Lastly, I document some of the ideas that I used when writing software during my PhD.

II.1 The French Breeding Bird Survey

Part of the PanEuropean Common Bird Monitoring Scheme, the *French Breeding Bird Survey* (FBBS) was initiated in 1989 in order to document changes in wild bird abundances in France (Jiguet et al. 2012). A network of volunteer ornithologists, hereafter called observers, is coordinated by the wildlife protection organization “Ligue de Protection des Oiseaux” (Bird Conservation League). Some are ecologists or professional ornithologists that participate in the FBBS in their spare time, while for others ornithology is a hobby with no connection to their professional activities. Data curation is coordinated at the National Museum of Natural History by the Vigie-Nature platform. FBBS data consists of highly standardized time series of bird counts across continental France (Fig. II.1A). The sampling design was updated in 2001, which is now the most common start date for analyses on the FBBS.

Sampling protocol

Each observer is assigned a 2x2km square plot, placed randomly in the vicinity of the observer’s choice municipality. There, he or she decides on the location of ten listening points that are placed in order to represent all possible habitats in the square plot and at least 300m apart from each other (Fig. II.1B). There are three survey sessions every year, during the breeding season: in March, in April/May and in May/June. Exact survey dates vary across observers and are placed at least 4 weeks apart from each other. A given observer repeats each session around the same date each year, in good weather conditions. The first, early session was initiated in 2011 and is therefore still seldom used in long-term analyses.

A survey session starts one hour after sunrise and ends at most 4 hours after sunrise. Observers visit their ten listening points always in the same order, thus monitoring each point approximately at the same time of day at each survey session. At each listening point, during five minutes, all birds seen or heard

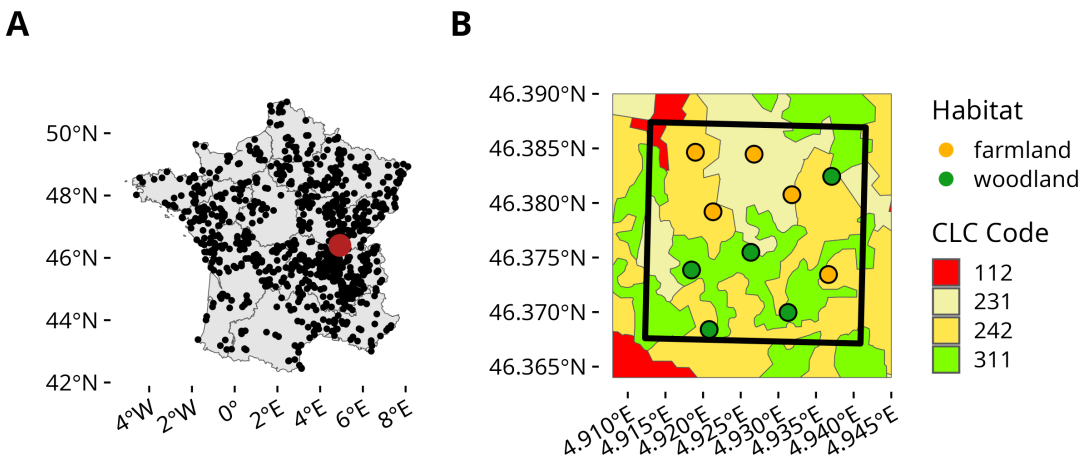

Figure II.1: **The French Breeding Bird Survey.** (A) Geographical position of square plots surveyed 10 years or more from 2001 to 2025. The red dot denotes the location of the site in panel B. (B) Example of a square plot with its 10 listening points (colored dots). Shaded areas represent land cover data from CORINE Land Cover. 112: Discontinuous urban fabric. 231: Pastures. 242: Agricultural area with complex cultivation patterns. 311: Broad-leaved forest.

are attributed to five distance classes (less than 25m, 25-100m, 100-200m, more than 200m and flyover). Birdwatching glasses can be used to identify the species of a detected individual, but are not used for helping detection. For each listening point, around ten species with a few individuals each can typically be detected over the five minutes of survey, with fewer birds detected at the listening points surveyed the later in the session. Observers also record weather information and classify the habitat at each point using standardized multi-level habitat codes. Raw data is deposited in the FBBS database via a web portal.

Data curation

Raw data from observers is curated in order to ignore entries that do not comply with the protocol's requirements. For example, listening points that are surveyed too early or too late at a given session are not included in exports. Database exports can be requested from the database manager with different levels of data aggregation, each with its associated default curation procedure, depending on analyses needs. "Raw" data exports thus include compliant bird counts across all requested distance classes, separated by listening point and by survey session (Fig. II.2A).

A second export method aggregates bird counts across distance classes and survey sessions for each point each year (Fig. II.2B). For each detected species, the general method is to first sum abundances

across distances classes below 200m and to then use the maximum of bird abundance across the two late survey sessions. Some exceptions are made depending on taxa: for raptors, swifts and swallows, the flyover distance class is also included, because these taxa are most often detected in flight. For species such as the Meadow pipit (*Anthus pratensis*) for which some populations overwinter in France and leave in Spring while some overwinter further South and breed in France, or for late-arriving migratory species such as the Northern wheatear (*Oenanthe oenanthe*), only the last survey session is considered in order to only count individuals from the breeding populations (Princé et al. 2013). This export can also be made at the scale of the square plot (Jiguet et al. 2012), which is the method used for exporting FBBS data to the PanEuropean Common Bird Monitoring Scheme, but data at the scale of the listening point offers more flexibility in analyses.

A

Site	Point	Year	Session	Habitat	<25m	25-100m	100-200m
"010101"	P01	2001	1	D1	1	0	0
"010101"	P01	2001	2	D1	1	1	2
"010101"	P02	2001	1	D2	2	1	0
"010101"	P02	2001	2	D2	0	0	1
"010101"	P01	2002	2	D1	1	1	0

B

Site	Point	Year	Sessions	Habitat	Abundance
"010101"	P01	2001	2	D1	4
"010101"	P02	2001	2	D2	3
"010101"	P01	2002	only_2	D1	2

C

Community	N_Points	Year	Sessions	Abundance
"010101_farmland"	2	2001	2	7
"010101_farmland"	1	2002	only_2	2

Figure II.2: **FBBS data curation steps for a fictitious species in a single square plot (site).** In this example, two listening points are surveyed on two sessions in 2001, but only the point P01 is surveyed in 2002 and only in the second session. (A) Raw data from observers contains bird counts in each distance class for each survey session. (B) In curated data, abundances are summed across distance classes and the maximum abundance across survey sessions is recorded. (C) In this PhD, we further aggregated counts by defining a community as a set of points from a given square plot that share the same habitat and summing abundances across points in the same community.

In this PhD work, we used an additional aggregation on point-level data, where we grouped listening points in the same square plot when they shared the same habitat, thus defining communities (Fig. II.2C). Also used in other analyses on FBBS data (Monnet et al. 2026), this method offers a good trade-off between ecological representativeness (which is higher at point level where habitat information is available

from observer data) and the data quantity which is required for fitting statistical models to time series (for many species with low abundances, point-level counts are almost distributed like categorical variables between 0, 1 and 2 birds). The number of points and the number of survey sessions considered each year are kept as variables used to account for varying sampling effort across this aggregated dataset. While the number of points a given year is directly proportional to underlying sampling effort and can thus be considered as an offset term, the number of survey sessions cannot be used as such because of the use of the maximum abundance.

II.2 Disentangling trends and variability

A major requirement in order to study possible links between long-term trends and temporal variability is to be sure that the measurement method for one of these stability dimensions does not inadvertently also measure the other. When measuring variability with the coefficient of variation over time of series with long-term trends, a time series with a stronger trend will show higher variability, which makes using the raw coefficient of variation unsuited to our research questions. Existing methods include measuring variability over short-term temporal scales by using small moving windows (Valencia et al. 2020a) or weighted temporal kernels. Another possibility is parametric or non-parametric detrending (Lepš et al. 2019, Clark et al. 2022), where a statistical model is fit on time series to estimate the relative importances of long-term and short-term variations. In parametric detrending, the maximum likelihood or posterior distribution of parameters that describe the long-term behavior of the time series is estimated. Since many studies on long-term trends, especially in the species paradigm, use log-linear mixed models in order to estimate the strength of trends (Vimont et al. 2025) and to aggregate them across species (Loh et al. 2005), we adopted this technique for the two empirical studies of this PhD work.

Here I expand on the different measurements for trends and for variability that we used across the three main chapters (Fig. II.3), taking some time to acknowledge their respective underlying assumptions and limitations. For simplicity, I will consider a single species, as the different aggregation methods for multiple species are detailed in each chapter's Methods section.

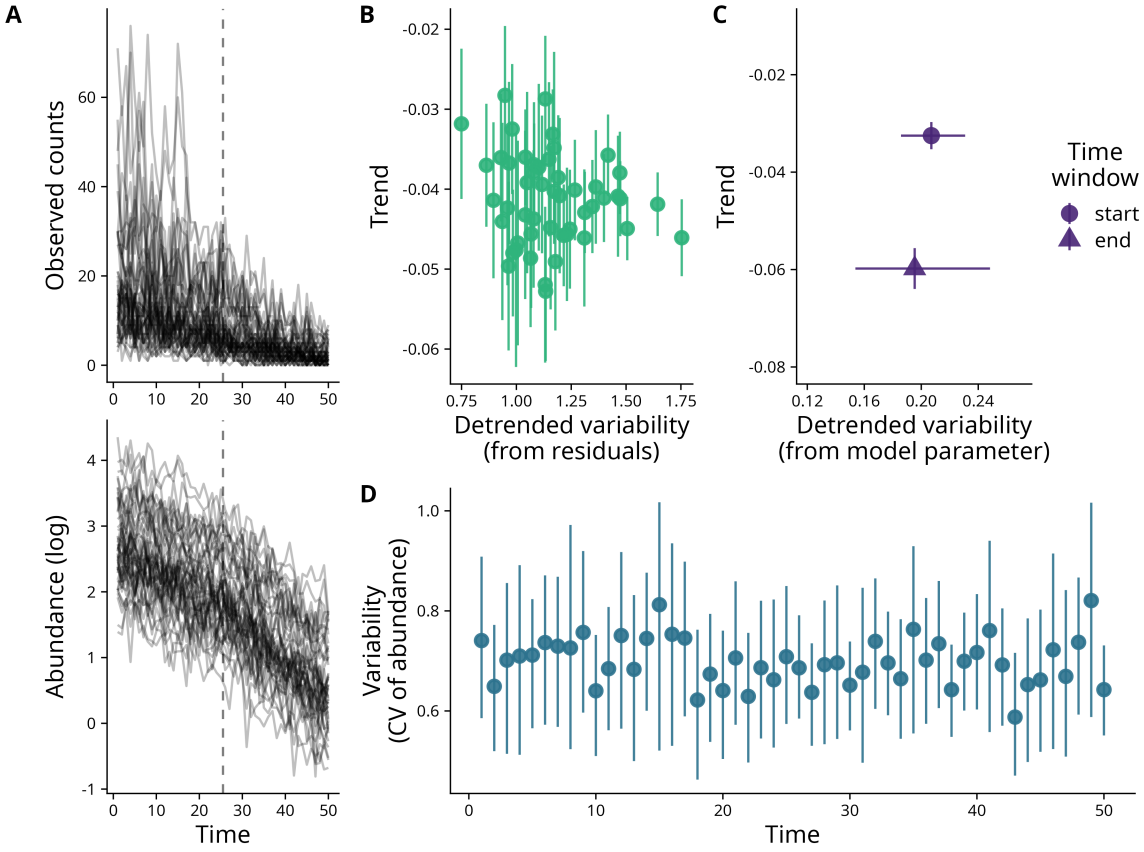

Figure II.3: **Three methods for measuring the variability of time series with long-term trends.** (A) Observed counts (top) are drawn from the Poisson distribution with expected count set as a random time-varying abundance (bottom), for 50 time series and 50 time steps. In the middle of the time series (dashed line), the trend changes, but not variability. (B) In Chapter 1, all time series are considered separately and have a trend estimator with uncertainty and a variability estimator without uncertainty after fitting model II.1. (C) In Chapter 3, time series are grouped together for estimation. Here, they are split in two time windows, before (start) and after (end) the change in trend. This allows to estimate the uncertainty in variability by fitting model II.2. (D) In Chapter 2, variability is defined for each time step around the time-varying mean of abundances. Here, uncertainty is estimated by bootstrap, but could alternatively have been estimated by taking replicate sets of panel A.

Local scale detrending

In order to focus on trends and variability at the local scale, the approach used in Chapter 1 is to consider time series from different communities independently (Fig. II.3B). For each species in a community s with p local centered covariates $x_{s,t,p}$, a log-linear model is fit for local population abundance, $X_{s,t} \sim \mathcal{P}(\lambda_{s,t})$:

$$\log(\lambda_{s,t}) = \beta_{s,0} + \beta_s\ t + \sum_p \beta_{s,p} x_{s,t,p} \tag{II.1}$$

Maximum likelihood estimates yield the most likely values for the coefficients β as well as confidence intervals. β_s is the strength of the (log-)linear long-term trend in the local species time series: on average, local mean abundance is multiplied by $\exp(\beta_s)$ from each year to the next. In order to compute variability around this long-term trend, the Pearson residuals of model II.1 are computed as: $r_{s,t} = (X_{s,t} - \hat{\lambda_{s,t}})/\sqrt{\hat{\lambda_{s,t}}}$. The variability of the local species time series is then computed as the standard deviation of $r_{s,t}$ across time, and this is repeated for all species in all communities.

This approach allows to compute trend and variability for as many local time series as possible (Fig. II.3B), even for species that are present only in a few sites. Beyond the log-linearity assumption which can be discussed, model II.1 does not allow to build a confidence interval for the variability index and does not allow to introduce too many covariates.

Detrending over several time series

In linear mixed models, random effects are used to account for non-independence between different observations. In models for species long-term trends, random effects are most often used to group observations by sampling site, accounting for unmeasured covariates that might explain differences in expected mean between different sites (Vimont et al. 2025). The variance parameter for such a random effect then describes how much unaccounted spatial variation is observed over the dataset. In Chapter 3, we extend this approach across time and measure species temporal variability as the variance parameter of a log-linear mixed model (Fig. II.3C). Here,

$$\log(\lambda_{s,t}) = \beta_0 + \beta\ t + \sum_p \beta_p x_{s,t,p} + \omega_s + \alpha_{s,t} \tag{II.2}$$

ω and α are random effects that account for spatial (ω) and temporal (α) variation that are not accounted for by spatio-temporal variation in covariates $\mathbf{x}$. Using covariance structures for ω and α can help acknowledging dependencies between observations (McGillycuddy et al. 2025). The variance parameter for $\alpha_{s,t}$ estimates the variability of abundance around the long-term trend β, with the whole dataset considered for its estimation.

Thus model II.2 allows to estimate long-term trends and temporal variability for many communities in a given time frame of FBBS data, yielding large-scale averages of the two stability dimensions (Fig. II.3C), and could allow to compare results for different sets of covariates. Our theoretical contributions in Chapter 3 show that the variance parameter for $\alpha_{s,t}$ can be analytically related to the population variability parameter as it is defined in theoretical studies (Arnoldi et al. 2016). The main difficulty with this approach is that substantial data availability is required to correctly estimate the parameters, and results therefore include fewer species than for Chapter 1.

Link between theoretical predictions and empirical measurements

In Chapter 2, using theoretical models allows to measure a time-varying variability: at each time step, the expected value for the variability of many stochastic simulations is obtained (Fig. II.3D). If a time series $(X_t)_{1\leq t}$ is produced by random draws with time-varying variance V_t, the temporal variance of X will reasonably match the temporal average of V_t only under small temporal changes in V_t. Conversely, strong changes in time-varying variance generate time series for which measuring temporal variance is only meaningful over short temporal windows. The choice of width for temporal moving windows may then influence variability measurements for systems under long-term changes in variance.

II.3 Notes on implementation

Over the course of my PhD, I tried to adopt principles of open science and reproducibility, especially with respect to code writing, organizing and sharing (Jenkins et al. 2023). Here I summarize some key aspects of software written for this work. Some are very general and may apply regardless of domains in ecology or programming languages, some are only relevant to `R` users in the context of statistical pipelines in ecology. Many and more of these principles and techniques are mentioned in the British Ecological Society Guide for Reproducible Code (Cooper and Hsing 2025), and a very good read for `R` users is the

free electronic book by Bruno Rodrigues (Rodrigues 2023). While computational reproducibility may be the most trivial aspect of reproducibility and replicability in science (Gould et al. 2025, Gómez-Llano and De Lisle 2026), it is an important first step.

Project-based workflow and version control

In order to be easily shared, all code and data relevant to a given project is grouped in the same directory so that the project file structure is conserved even if it is copied to another computer. This enables the use of relative file paths within the project, allowing code to be re-run on a different computer without needing any changes. Functions that are used at several places in the project can be placed in a `R/` subdirectory, where they will be available to be loaded as if they were part of a package and where changes to a function can apply to all steps that depend on it.

Project-based workflows also enable many other tools that have been developed for software engineering. Version control systems such as `git` can keep different code versions registered as "commits" across the development of a project, which makes it possible to roll back one or several files to earlier versions, or to conjointly develop several versions of a project with "branches". For example, a working version of a project may be kept in a "main" branch in order to regenerate figures if needed while a "feature" branch is used for development work that might break the working version. Version-controlled projects are also easier to share as `git` repositories can be uploaded online easily, for example on GitHub (see Braga et al. 2023).

Reproducible environments

The possibility for some code to run without errors on one computer but produce errors or different results on another computer is common. In `R`, four sources of variation between the environments of different users can generate such problems: the `R` version and the suite of installed `R` packages, the operating system used, and the state of `R`'s random number generator.

The `R` package `renv` allows to record which `R` version and which packages are used within one project repository, and to commit this information to version control in order to track the required environment across the development of the project. When the project is copied to another computer, a single call to `renv::restore()` allows to install the required project packages and will raise a warning if another `R`

version is detected. For reproducibility issues that are caused by differences in operating systems, `Docker` allows to generate images of common operating systems, allowing for example to run code written for Linux even on Windows machines. When some results are randomly generated but should ideally not depend on the state of the random number generator (*e.g.* point locations on jittered plots), explicitly setting its parameters allows to always generate the same "random" results.

Pipeline management, distributed computing and literate programming

Over the course of the development of a data analysis pipeline, there is a need to make sure that outputs always match the current state of code and input data, but when re-running the pipeline after a modification, it is tempting to avoid re-running the steps that take the most time to run. Keeping a mental representation of the dependencies between steps of a project in order to know when to re-run which steps is increasingly difficult as the size of the project increases. The `targets` package in `R` allows to automate this process by allowing users to define individual pipeline steps and automatically tracking each step's dependencies (Landau 2021, Brousil et al. 2023). On pipeline re-run, steps whose code and data dependencies have not changed are automatically skipped (Fig. II.4).



Figure II.4: **Example targets pipeline.** Given a targets definition file, `targets` automatically detect dependencies between pipeline steps, visualized by arrows. For example, a code change in the `stats_method1` target will cause `plots_method1`, `all_stats` and `summary_plot` to re-run, but `plots_method2` will be skipped. Squares denote "patterns", targets that are defined to map over different elements of their dependencies. Here, if the dataset in `read_data` contains information on several species and mapping is parametrized across species, each of the square targets will be run for each species. Mapping allows `targets` to distribute computations over several processors without having to rewrite underlying code.

This PhD work was granted access to the High Performance Computing resources of the SACADO MeSU platform at Sorbonne Université. Its MCMeSU supercomputer allowed to run some data analysis steps in parallel over a large number of processors in order to reduce execution time. Having organized code as project-based workflows was particularly useful then, as code and `renv` environments could be easily shared with the supercomputer via `git` and GitHub. Pipeline management by `targets` was also possible on the supercomputer, allowing to keep pipeline outputs synchronized with code versions even for computationally intensive steps.

During the process of academic writing, changes to existing data analysis results are sometimes necessary, for example changing a variable in a model formula, or more trivially resizing figure labels. Including figures and tables as steps in the project's `targets` pipeline allows them to be re-generated if they depend on modified code. Moreover, writing manuscripts with literate programming frameworks such as Quarto, allowing to mix code and text, helps continuously integrate pipeline results with the manuscript. This notably avoids having to manually copy/paste results to the manuscript document every time a code update changes figures or tables.

III . Chapter 1: Populations trends and variability are amplified by intense land use

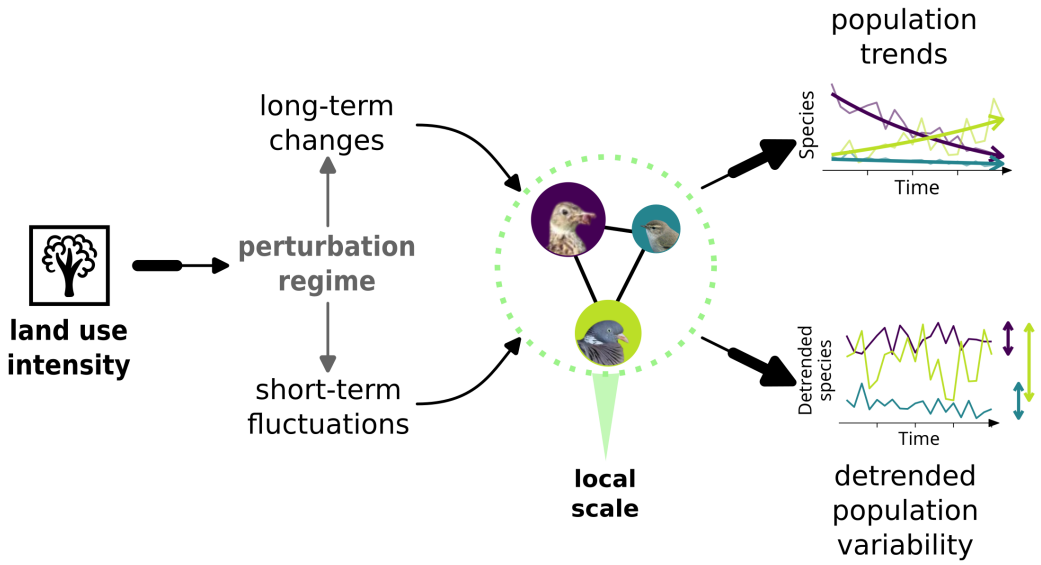

Figure III.0: **Chapter 1 in the general conceptual framework.** We measure average strength of population trends and average detrended population variability in communities from the French Breeding Bird Survey. Land use intensity is associated to stronger trends and higher variability. Here, two integrative dimensions of ecological stability thus respond to the same anthropogenic pressure. Thicker arrow parts correspond to components measured in this Chapter. Land use icon modified from Bellard et al. (2022). Bird pictures by F. Jiguet and S. Wroza.

III.1 Context and aim of the study

In Europe, urbanization and agriculture intensification both induce long-term changes in bird habitat quality (Tassin de Montaigu and Goulson 2023, Rigal et al. 2023) as well as short-term fluctuations in resource availability (Oliver et al. 2010). In local bird communities across France, Olivier et al. (2020) showed that land use intensity drives changes in bird community variability via increases in average population variability, this without considering the variation explained by local long-term population trends.

In this chapter, we disentangle long-term trends and short-term populations in local time series from the French Breeding Bird Survey and evaluate if the link between land use intensity and population variability can be explained by trends or by variability. Both stability dimensions differed across land use type while only detrended population variability was associated to changes in land use intensity within similar habitats. At a local scale, comparing different communities across France reveals that land use can be associated to concurrent changes in the two stability dimensions, which then appear independent when their common drivers are taken into account. Short-term detrended population variability appears more strongly related to the local perturbation regime than long-term population trends computed at a local scale.

This chapter was published as an article in *Journal of Animal Ecology* (Guerber et al. 2026b).

III.2 Article: “Population trends and variability within bird communities are amplified by intense land use”

Abstract

Human activities affect wild communities through significant long-term changes in population abundance as well as changes in short-term fluctuations. However, studies that focus on one of these stability components tend to overlook the other. Using community time series data from the French Breeding Bird survey, we investigate the variations of community-scale long-term changes (population trends) and short-term fluctuations (detrended variability) across habitat categories and with land use intensity, for 905 communities in continental France. We show that communities within agricultural and urban habitats were less stable than woodland communities, for both components of stability. Moreover, within habitat categories, only detrended variability increases with land use intensity, while the drivers of local long-term population changes remain to be elucidated. These findings highlight that measuring several stability dimensions provides a better understanding of the links between local land use and community temporal dynamics.

Keywords: stability, communities, land use intensity, landscape complexity, multidimensional stability

Introduction

Global biodiversity loss and increasing anthropogenic pressures due to economic activities threaten ecosystems worldwide (IPBES 2019a). Understanding how natural communities maintain their properties in the face of disturbances, i.e. how stable they are (Van Meerbeek et al. 2021), is thus key in assessing the ways present and future ecosystems may or may not continue to provide essential contributions to human societies (Cardinale et al. 2012). Since disturbances and ecological properties are multi-faceted, ecological stability is increasingly regarded as multi-dimensional (Donohue et al. 2013, Hillebrand et al. 2018b), which should be taken into consideration when assessing its drivers (Kéfi et al. 2019). However, in practice, ecologists from different fields have focused on different aspects of ecological stability, yielding different perspectives on ecosystem and bird responses to pressures.

On one side, the study of long-term changes in species population abundances, hereafter called population trends, investigates how anthropogenic pressures alter the abundance of specific populations over decades at the scale of countries and continents. These works increasingly document that while some species decline in abundance with increasing pressures, other species stagnate or even increase (McKinney and Lockwood 1999, Bowler et al. 2019). In this framework, a strongly negative temporal trend of a given species' population identifies a threat to the conservation status of the declining population (IUCN 2024), but strongly positive trends of species well suited to disturbed environments can also indicate high habitat degradation (Bowler et al. 2017, Carroll et al. 2023). While it is widely recognized that long-term changes may not always be (log-)linear (Dornelas et al. 2013, Clark and Luis 2020), measuring long-term trends as a multiplicative growth rate facilitates both comparison across species and the use of multi-species indices (Loh et al. 2005).

On another side, many studies in community ecology have focused on the mechanisms driving the temporal (in-)variability of ecosystem processes, demonstrating that more diverse communities have lower interannual fluctuations in community biomass or abundance (Tilman 1996), i.e. are less variable. This positive diversity-invariability relationship was first measured in biodiversity experiments (Tilman 1996) and has since been documented in empirical surveys of wild communities (Xu et al. 2021), supporting the idea that more diverse communities are less sensitive to perturbations. In particular, species richness promotes the asynchrony between population fluctuations, favoring the invariability of

community properties (Yachi and Loreau 1999, Thibaut and Connolly 2013).

Since long-term changes and short-term fluctuations both are components of community stability (Hillebrand et al. 2018b), there is a need to assess them in the same framework to better understand the temporal dynamics of communities. For example, to warn of a catastrophic shift in systems with alternative stable states, the long term change of an ecosystem function is not as relevant as the short term fluctuations around the trend (Scheffer 2009). Conversely, species long-term trends reshuffle the functional composition of communities, which may alter community variability (de Bello et al. 2021, Li et al. 2021). Further, the measurement of short-term fluctuations can be biased by the way long-term changes are accounted for (Lepš et al. 2019, Valencia et al. 2020a), especially when the long-term dynamics are not monotonic (Wu et al. 2007). Moreover, anthropogenic pressures may induce both long-term changes in population abundance and increase in short-term fluctuations. Conjointly measuring these two dimensions of stability would help disentangle how they relate to each other and their drivers (Donohue et al. 2013).

Charismatic as well as essential for ecosystem functioning and services (Gaston et al. 2018), common birds worldwide are threatened by anthropogenic pressures and face strong population declines (Rosenberg et al. 2019, Smith et al. 2020, Burns et al. 2021, Pollock et al. 2022), raising questions about their maintenance. In Europe, birds are especially affected by anthropization (Donald et al. 2001, Burns et al. 2021, Rigal et al. 2023) and landscape homogenization (Gaüzère et al. 2020, Vallé et al. 2023). At a regional scale, most farmland specialist bird species undergo strong declines in population abundances while populations of generalist species well suited to disturbed habitats increase (Bowler et al. 2019). Locally, this translates to changes in the average functional composition of communities (Le Viol et al. 2012, Gaüzère et al. 2020), but local population trends are rarely measured. Moreover, higher land use intensity has been shown to be associated to lower bird community stability via higher population variability (Blüthgen et al. 2016, Olivier et al. 2020). It is likely that part of this increase in population variability is due to the long-term directional trends of bird population abundances (Fig. III.1a), but it is also likely that more intense land use causes stronger disturbances on bird populations, increasing population and community variability.

There is therefore a necessity to separate bird population variability into long-term population trends on one side, and into variability around their trends on another side to understand how human activities

influence bird community dynamics. Habitat type, a key determinant of bird community composition (Reif et al. 2022), may influence both long-term changes via habitat suitability and short-term fluctuations by contrasted disturbance regimes across habitats. Indices measuring land use intensity vary in range between habitats, and habitat type may alter their relationships with bird community properties (Pellissier et al. 2017).

We measure two components of ecological stability in bird community time series from the French Breeding Bird Survey (Jiguet et al. 2012). From population abundances at the community scale, we disentangle long-term directional population changes regardless of their signs on one side, and detrended fluctuations around these changes on the other side (Fig. III.1). We then test habitat category and anthropogenic pressures as potential drivers of the two stability components. We investigate how trends and detrended variability are distributed (i) across several habitat categories and (ii) across land use intensity for communities in similar habitats, with respect to species richness. We expected destabilization of communities for both components of stability in farmland and built areas compared to woodland habitats, and destabilization of both components with more intense land use within similar habitats. Our results generally match these expectations, although only detrended variability is associated with increasing land use intensity within similar habitats. Overall, considering several components of stability helped assess the effects of habitat and land use intensity on wild bird communities and paves the way for better understanding the mechanisms at play.

Materials and Methods

Bird survey data

We used data from the French Breeding Bird Survey (Jiguet et al. 2012), a citizen science program coordinating several hundreds of volunteer ornithologists, hereafter called observers. Each observer is randomly assigned a 2x2km square plot around a chosen locality, where they place 10 listening points representative of bird habitats in the square plot, at least 300m away from each other. There are two survey sessions each year during the breeding season (in March and in April or May), where all listening points are surveyed at dawn, always in the same order. At each survey session and at each listening point, all individual birds heard or seen in a time frame of five minutes and a distance from the observer of 200m or less are logged, and observers describe the surrounding habitat with seven categories (Tab. III.S1).

Raw data from observers is then curated by the Vigie-Nature platform at the French National Natural History Museum (see Princé et al. 2013 for details). For listening points that were surveyed during both survey sessions of a given year, each species' curated abundance for that year is its maximum abundance over the two survey sessions. At the time when data was extracted from the survey database (January 2025), available survey years spanned from 2001 to 2023. Since no animals were manipulated, no ethical approval was required for this study.

We grouped habitat description from observers in broader habitat categories focusing on points located in woodland, farmland and built habitats, the categories with the most available data (Tab. III.S1, Fig. III.S1). Since landscape at a small spatial extent is a major driver of bird community composition (Morelli et al. 2013, Adler and Jedicke 2022), we define a bird community as the bird individuals recorded in the set of listening points from a square plot that belong to the same habitat category. This leads to up to three bird communities per square plot, one for each of the three habitat categories. This definition of community offers a good trade-off between ecological representativeness and data quantity required to compute local species abundance trends.

To ensure sufficient sampling coverage to fit the local species trends, we subsetted the French Breeding Bird Survey data using several criteria (Tab. III.S2). We excluded points for which the habitat description changed over time or with inconsistent geolocalization. From the three habitats of interest (farmland, woodland and built habitats), we retained only communities with 3 listening points or more and surveyed 9 years or more in total between 2001 and 2023. Within each community, we only kept the time series of species that were present in at least half of survey years, yielding 24743 population time series from 961 communities surveyed between 9 and 23 years (Tab. III.S2, Fig. III.S2). Because this last filtering step might cause an underestimation of community species richness by excluding rare species, we computed mean species richness per community before applying this criterion. For each community, we counted all species with at least one individual each year, and averaged these yearly counts across survey years.

Measuring two components of stability

We quantified two aspects of population stability at the community level. For each community, we measured (i) how strong are population trends and (ii) how variable the population time series are around their respective trends, using a residuals-based approach (Lepš et al. 2019). Because long-term changes

in communities consist of both negative and positive population abundance changes (McKinney and Lockwood 1999), we consider populations with strong changes in abundance as unstable (for their long-term change component), regardless of the direction of these changes. Therefore, a community is destabilised when its populations have strong trends (negative or positive) or when its populations have high detrended variability, i.e. strongly fluctuate around their respective trends.

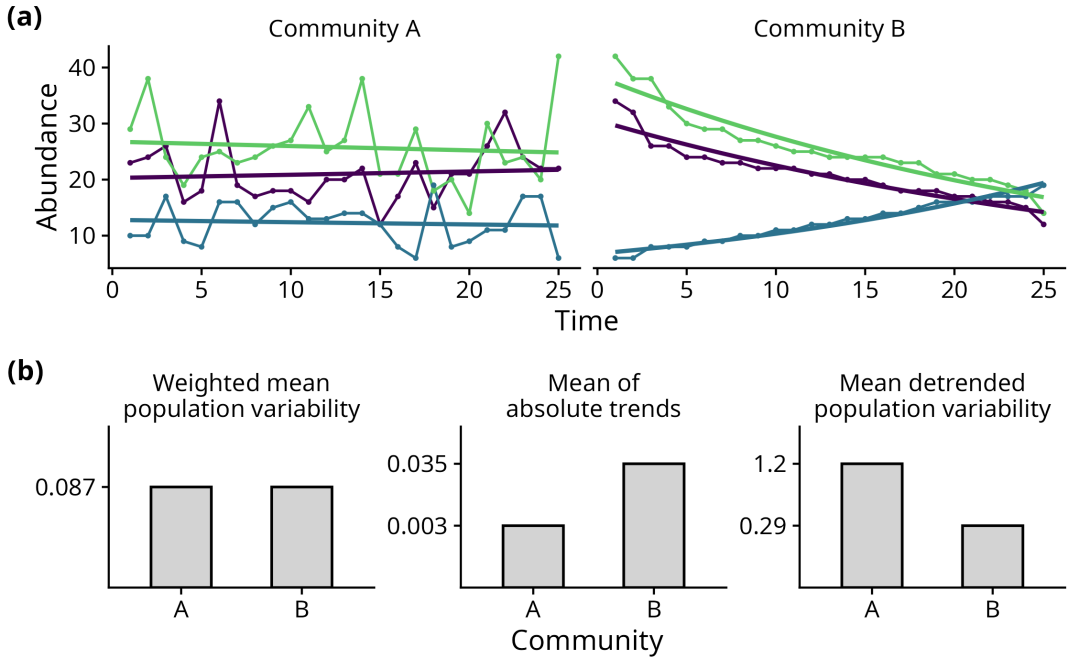

Figure III.1: **Separating long-term trends and detrended variability in communities.** (a) Time series of two simulated communities with three species each. Colours represent different species, with raw abundance as lines with dots and Poisson regression fits of abundance against time as thick lines. (b) Resulting community-level metrics, comparing a measure of population variability without detrending (left) with our two stability components (middle and right). Vertical axes in panel (b) are log-scaled.

To do so, for each species time series in each community, we fit a Poisson regression of abundance against time, controlling for the number of listening points as an offset term and for the number of survey sessions as a fixed effect term if it varied across the duration of the community's survey (63.8% of time series). Species local trend $\beta_{i,s}$ at community i for species s was the maximum likelihood estimator of the Poisson regression, on the natural logarithmic scale. We also recorded the Pearson residuals $r_{i,s,t}$ of the regression (at time t, $r_{i,s,t} = \frac{y_{i,s,t} - \hat{y_{i,s,t}}}{\sqrt{\hat{y_{i,s,t}}}}$ with $y_{i,s,t}$ and $\hat{y_{i,s,t}}$ the observed and fitted values, respectively), defining species detrended variability $\sigma_{i,s}$ as the standard deviation of $r_{i,s,t}$ in the local species time series. Using Pearson residuals allows to detrend the time series without introducing strong dependence on the mean of the original survey for the resulting detrended variability index. After data filtering, most local Poisson regressions converged and produced reliable local estimators, except for 16 excluded time

series (Tab. III.S2, fifth row).

For each community, species trends were averaged using the arithmetic mean of their absolute values, yielding the mean of absolute trends $\tilde{\beta}_i = \frac{1}{N_i} \sum_s |\beta_{i,s}|$ with N_i the number of available time series for community i. Similarly, the mean detrended population variability $\bar{\sigma_i}$ was obtained by averaging all species' detrended variabilities. Thus, each community was characterised by two stability measures, one for each of the two stability components (Fig. III.1b). To compare mean population variability with and without detrending, we compared our metric with the abundance-weighted mean population coefficient of variation (Thibaut and Connolly 2013), widely used in diversity-variability studies.

Land use intensity data

We characterise land use intensity for each community using human footprint (*i.e.* landscape anthropization) and landscape complexity data, both known to affect bird communities (Gaüzère et al. 2020, Olivier et al. 2020). An intense land use is thus associated with high human footprint and low landscape complexity.

We used the Human Impact Index (HII) from the Human Footprint database (Sanderson et al. 2022), available as a 300m resolution yearly raster. This index aggregates nine indices of land anthropization such as infrastructure density, human population and nighttime lighting, which provides a simple measure of how strongly any location is impacted by human activities (Venter et al. 2016). For each listening point, we averaged the HII value of the corresponding raster cell for all years between 2001 and 2014, and averaged the HII values over all listening points of each community, yielding a single HII value per community. The end date of 2014 was chosen because of a change in HII methods from 2015 onwards (Sanderson et al. 2022). For 56 communities, HII values were unavailable, yielding a final subset of our dataset with 905 communities, representing a total of 2.3397×10^4 time series for 160 species (Tab. III.S2). As a supplementary analysis, because a community in a given location can be influenced by pressures in the surrounding area, we also extracted HII values in circular buffers of 5, 10, and 25km radius around each community.

For landscape complexity, we downloaded land use data from the CORINE Land Cover database, available through the Copernicus Land Monitoring Service (https://land.copernicus.eu/en), which maps landscape elements wider than 100m into 43 land use classes for the years 2000, 2006, 2012 and 2018.

Around each listening point, we drew a 250m-radius circular buffer and extracted the surface proportion of each land use category within the union of the buffers of all listening points in each community. We averaged land use proportions across the four releases for each community. Landscape complexity was then calculated as the Shannon entropy of the averaged land use proportions in the community's buffer.

Statistical analyses

Statistical analyses, as well as data processing steps described above, were carried out in R version 4.5.0 (R Core Team 2024), with the help of the `targets` package for pipeline management (Landau 2021).

To compare stability components across habitats, we fit two log-linked linear mixed effects models using `glmmTMB` (Brooks et al. 2017). Explanatory variables included habitat category and the number of listening points in the community. We included a random effect for square plot identity after comparing with several alternative residual structures using restricted maximum likelihood (Zuur et al. 2009). Goodness-of-fit was checked by computing χ^2 tests against alternative fixed effects structures (adding habitat category always significantly improved the fit), and we further checked model quality by inspecting standardised residuals using `DHARMa` (Hartig et al. 2024). Accounting for distance-based autocorrelation required a more complex modelling framework (Anderson et al. 2024), but did not qualitatively change the estimates from the models (Fig. III.S3, Fig. III.S5). We therefore only present results from the less complex `glmmTMB` model.

To explain the variation of stability components among communities from a given habitat, we separately analysed each habitat category. Because land use intensity may be linked to stability but also to species richness, which can in turn impact stability, we estimate these indirect (via species richness) and direct links with a structural equation model (SEM) fit using `piecewiseSEM` (Lefcheck 2016). Stability components were log-transformed before fitting the SEM. All linear models within the SEM were fit using `nlme` (Pinheiro et al. 2025) with an exponential spatial correlation structure. Model quality was tested with Fisher's C statistic (Shipley 2000), failure to reject the null hypothesis meaning that the model structure is not rejected by the data.

Results

Without detrending, mean population variability is correlated with the mean of absolute population trend (Fig. III.2, top) across all bird communities in our dataset, as expected (Fig. III.1). This correlation was removed when using the mean detrended population variability (Fig. III.2, bottom), indicating that our method is efficient at disentangling variability and long-term population changes. In what follows, we focus on mean detrended population variability and mean population trend as two independent components of population stability in communities.

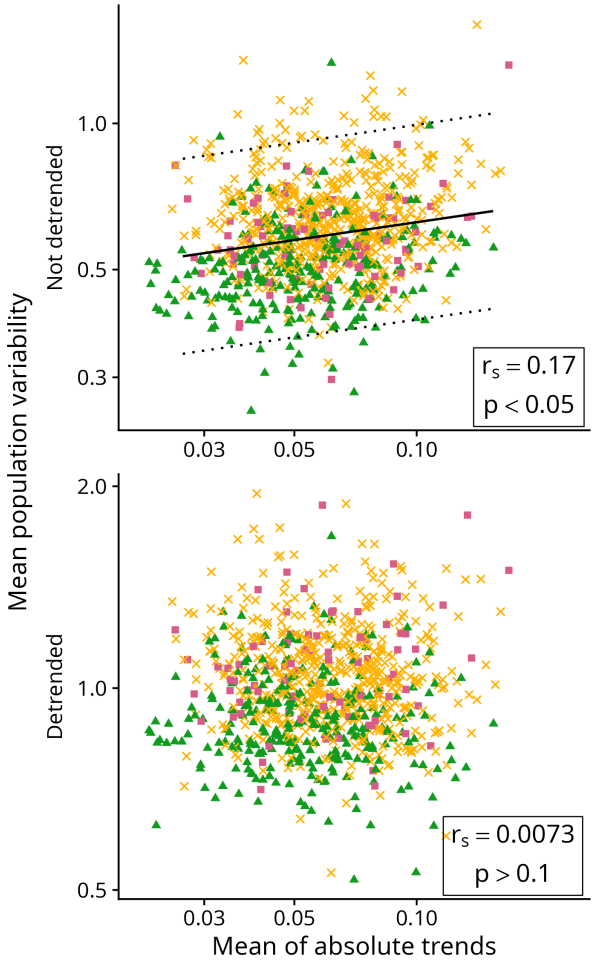

Figure III.2: **Correlation between the mean of absolute trends and mean population variability without (top) and with detrending (bottom).** Plot insets show the test statistics of Spearman's rank correlation tests between the mean of absolute trends and each population variability metric. For the panel with a significant correlation, linear regression fit (solid line) and 95% prediction intervals (dashed lines) are displayed. Green triangles, yellow crosses and red squares denote communities in woodland, farmland and built areas, respectively.

Both components of bird population stability vary across habitat categories. For mean detrended variability, bird communities from farmland and built areas are less stable than those from woodland

(Fig. III.3, left). Bird communities in farmland also have higher mean of absolute trends than those in woodland, while bird communities from built areas cannot be significantly distinguished from the other categories (Fig. III.3, right). This indicates that within farmland, on average, bird communities are made of populations with both stronger trends and higher variability around their trends compared to communities in woodland. Bird populations from communities in built areas are also more variable around their trends than populations from woodland, but do not have significantly stronger trends. Accounting for variations in stability components linked to the differences in land use intensity and species diversity across habitat categories does not suppress the effects of habitat category (Fig. III.S4), but increases the quality of the model, as measured by its Akaike and Bayesian information criteria (Tab. III.S3).

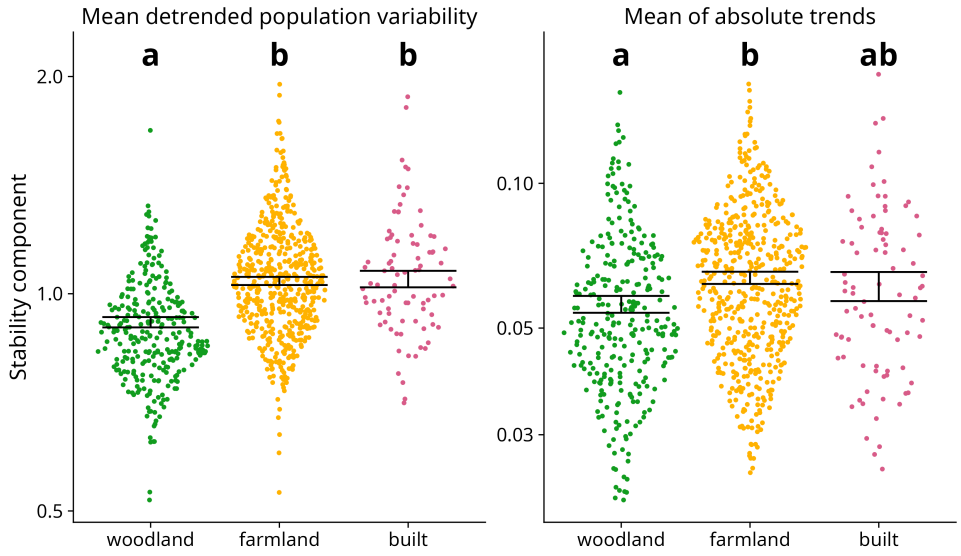

Figure III.3: **Stability components across habitat category.** Dots show computed values for mean detrended population variability (left) and the mean of absolute trends (right). For each stability component, black error bars show confidence intervals for the estimated marginal means for each habitat category in the fitted model, controlling for the number of listening points and with a random effect for square plot identity. Groups sharing the same letter cannot be significantly distinguished from each other after Tukey's p-value adjustment for multiple comparisons with a 5% threshold.

Looking at variations in the two stability components within each habitat type, we found that they do not have the same response to land use intensity. Strikingly, changes in human impact index and landscape complexity are mostly associated to changes in mean detrended population variability, but not to changes in the mean of absolute trends (Fig. III.4). This discrepancy between stability components as well as the signs of significant effects are both consistent across habitat categories, although habitat categories with less data exhibit fewer significant effects (Fig. III.4).

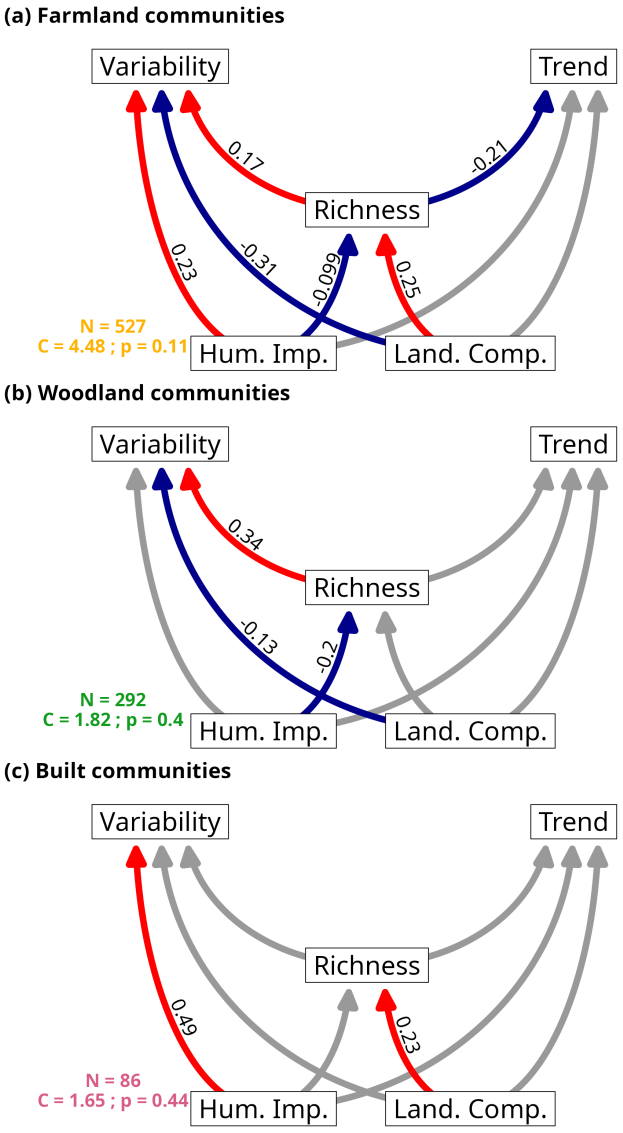

Figure III.4: **Stability components across land use intensity for the three habitat types.** Positive (respectively negative) significant effects in the structural equation models are represented in red (resp. blue) with standardised effect size as a text annotation, and non-significant tested relationships are represented in grey. Annotations in the bottom-left corners denote number of communities (N) and outputs of the Fisher's C test on 2 degrees of freedom for each subset of communities. Land use intensity variables are abbreviated as *Hum. Imp.* for human impact index and *Land. Comp.* for landscape complexity.

For communities in both farmland and built habitats, we found a total positive relationship between human impact index and mean detrended population variability, indicating that populations are more variable around their trends in communities where human footprint is stronger (Fig. III.4a and c). This effect is partly mitigated for communities in farmland by an indirect negative link via species richness (Fig. III.4a). For woodland communities, human impact index had a stabilizing effect on mean detrended population variability via this same indirect link through species richness (Fig. III.4b). Landscape complexity had a stabilizing effect on mean detrended population variability in farmland and woodland communities (Fig. III.4a and b). For farmland communities, the effect of landscape complexity was again partially mitigated by an indirect positive effect via species richness, but the total effect was negative (Fig. III.4a). Overall, higher land use intensity is associated with increased detrended population variability.

For all three habitat types, variation in the mean of absolute population trends could not be attributed to direct effects of human impact index or landscape complexity (Fig. III.4). However for farmland communities, the habitat category with the most data, higher species richness is associated to lower mean of absolute trends. Since the effect of human impact index (resp. landscape complexity) on species richness is significant and negative (resp. positive), land use intensity thus has an indirect destabilizing effect on the mean of absolute trends via its effect on richness (Fig. III.4a). All else being equal, populations in farmland bird communities with more species have weaker population trends on average, but are more variable around these trends.

Discussion

We show that two components of the (in)stability of bird communities, average long-term population changes and average short-term population fluctuations, can be disentangled and that both differ across habitat categories. Agricultural and built habitats were associated to lower stability than woodland for the two components. Furthermore, our analysis allows linking local land use intensity to short-term detrended population fluctuations, but the drivers of long-term changes in local-scale population abundance within communities remain elusive.

The two components of community stability vary among habitats

Our results indicate that the two stability components of bird communities we studied are similarly related to habitat category. Communities in farmland and built areas host less stable bird populations than woodland because populations in farmland have both stronger trends and stronger variability around their trends, and populations in built areas are more variable around their trends.

The differences in short-term population fluctuations among habitats we find corroborate previous studies (Blüthgen et al. 2016, Olivier et al. 2020) and suggest that farmland and built areas are subject to stronger disturbance regimes than woodland habitats. Habitat loss and pollution are indeed known to affect bird populations both in farmland and in built areas (Busch et al. 2020, Tassin de Montaigu and Goulson 2023). These factors are already well-known as drivers of long-term changes in bird communities (Benton et al. 2002, Stanton et al. 2018, Rigal et al. 2023), but it is also likely that they drive interannual population variability. For example, Meyer et al. (2019) show that crop rotation generates interannual variability in the composition of arthropod communities, a major food resource for farmland birds. This variability in drivers could then generate more short-term fluctuations in bird population abundance.

Our finding that farmland bird communities have stronger long-term changes in population abundance than woodland communities adds a local and community-scale perspective to previous results at continental scale across Europe (Bowler et al. 2019, Burns et al. 2021, Rigal et al. 2023) and North America (Saunders et al. 2022, Johnston et al. 2025). Stronger population trends in local farmland communities hints at stronger species reshuffling in these communities, which can cause biotic homogenization if many specialist species are replaced by a few increasing generalists (Devictor et al. 2008a, Le Viol et al. 2012). A similar pattern is expected for built areas (Devictor et al. 2008a, Davison et al. 2024). However, trends in built areas appear intermediate between woodland and farmland but not significantly different from either, likely due to smaller sample size and to the fact that “built” sites can include isolated buildings within farmland or woodland rather than strictly urban areas.

Contrasted responses of stability components to varying land use intensity within habitats

Within a single habitat category, short-term fluctuations and long-term changes respond differently to land use intensity, with a higher land use intensity associated to higher detrended variability only. This

effect (or lack thereof) was generally consistent across habitat categories, with losses of significance for habitat categories with lower statistical power. The effect of land use intensity on short-term fluctuations was expected. Landscape complexity indeed increases the number of micro-habitats available to birds for nesting and foraging, improving their resilience to perturbations (Smith et al. 2022) as well as promoting their diversity (Morelli et al. 2013). Similarly, landscape anthropization is expected to decrease bird richness (Lu et al. 2024) and increase bird community variability (Olivier et al. 2020, Smith et al. 2022).

Strikingly, the variables we used to characterize local land use intensity fail to explain the strength of long-term population changes, for all three habitat categories. Davison et al. (2024) reported strong temporal turnover (i.e. changes in species composition over time) in Danish bird communities at local scale, but found it only weakly associated to local land use or climate descriptors. This puzzling mismatch between local long-term community reshuffling and local habitat anthropization corroborates our findings. Since natal and breeding bird dispersal can span several kilometers (Fandos et al. 2023), effects of spatial scale may be at play here (Di Cecco and Hurlbert 2022). However, complementing our analyses by accounting for human footprint at a larger scale around each community did not allow us to corroborate this hypothesis, with non-significant effects of human impact index over a 10km radius around each community (Fig. III.S6). Including weather and climate variables may also help explaining more variance in the mean of absolute population trends (Lehikoinen et al. 2016, Stephens et al. 2016, Gaüzère et al. 2020).

In farmland communities, species richness is negatively associated with the mean of absolute trends. Investigating the mean of absolute trends under null assumptions supports that this link is not artefactual (Fig. III.S7), and may instead reflect that communities with good habitat quality can support more species while also having weak population trends. As previous studies report inconsistent links between richness and population variability (Danet et al. 2021, Xu et al. 2021), further work is needed to test whether such variation arises from differing effects of richness on either long-term population changes or on short-term population fluctuations.

Separating short-term fluctuations from long-term changes

We disentangle mean detrended variability from the mean of absolute trends and do not find any significant correlation between them, arguing for the multi-dimensionality of ecological stability (Donohue et al. 2013).

Conversely, without detrending, these two components of stability would seem significantly correlated with each other.

By considering short-term fluctuations as deviations around long-term trajectories, we bridge two perspectives: studies of long-term changes that overlook short-term fluctuations (e.g. Bowler et al. 2019, Burns et al. 2021) and studies of short-term fluctuations that rarely account for long-term trends (e.g. Blüthgen et al. 2016, Olivier et al. 2020), or do account for trends but do not relate them to short-term fluctuations (Tilman 1996, Valencia et al. 2020a, Danet et al. 2021). Jointly studying these components of stability, we show that they are similarly affected by habitat category but also that they respond differently to local land use intensity. Note that in our method, long-term trends are log-linear, making all non-linear changes (e.g. quadratic, Pélissié et al. 2024) contribute to detrended variability. Estimating to which extent mean detrended variability represents interannual fluctuations and not more complex non-linear temporal patterns would require inspecting the residuals of the underlying 23397 time series models.

While our results on the mean of absolute trends seem robust to propagating the uncertainty in local species trends to our statistical analyses (Figs. SIII.8-SIII.12), uncertainty in detrended variability is not directly measurable in our framework. It could be estimated by more advanced statistical modelling, e.g. by modelling mean detrended variability as the variance parameter of a structured temporal random effect (Brooks et al. 2017). Using hierarchical models could further refine our estimates by taking the observation process (e.g. bird detectability and observer effect) as well as spatial autocorrelation into account directly in the estimation of local population trends (Smith et al. 2024, Nabias et al. 2024). This is likely to produce lower estimates of detrended variability than in our methods, but we anticipate that it should not be strongly biased by land use intensity. Alternative detrending methods such as three-term local variance (Lepš et al. 2019, Valencia et al. 2020a) could refine our estimates of detrended variability by accounting for non-linear long term changes, but cannot calculate population trends directly. The use of empirical dynamical modelling, a more advanced set of methods for non-linear time series analysis, could help disentangle short-term fluctuations from non-linear long-term changes but may require time series with low noise levels (Clark et al. 2022).

Perspectives for community dynamics in a changing world

Our results support that the maintenance of the provisioning of ecosystem function and services by birds is threatened by land management (Rosenberg et al. 2019) as land use is associated with altered bird population stability with respect to both long-term changes and short-term fluctuations, provided that detrended variability captures short-term fluctuations well enough. In systems with alternative stable states, strong short-term variability around long-term trends is an early warning sign of ecosystem shifts (Scheffer 2009). Conversely, strong population trends indicate strong compositional shifts within communities (Dornelas et al. 2014), raising questions about the adaptation of novel community assemblages to current and future environmental changes (Carroll et al. 2023). In our study, considering two dimensions of ecological stability (Donohue et al. 2013, Hillebrand et al. 2018b, Kéfi et al. 2019) helped paint a more complete picture of the links between land use and bird community dynamics. Together with recent evidence of long-term changes in bird populations, we anticipate that taking into account several dimensions of stability across space and time will help to analyze valuable biodiversity monitoring data. This should be joined with increasingly available spatio-temporal data on the pressures affecting biodiversity, towards a more exhaustive understanding of the ways wild communities respond and will respond to present and future anthropogenic pressures.

Acknowledgments

This work was granted access to the High-Performance Computing resources of the SACADO MeSU platform at Sorbonne Université. The authors thank Benoît Fontaine (MNHN) and Lorraine Delthel (LPO) for coordinating the French Breeding Bird survey, supported by Ligue de Protection des Oiseaux, Office Français de la Biodiversité and MNHN. We thank the hundreds of volunteer observers who participate in the survey.

Conflict of Interest

The authors declare no relevant conflict of interest.

Author Contributions

Josquin Guerber, Colin Fontaine and Elisa Thébault conceptualized the study. Josquin Guerber analysed the data, visualized the results and wrote the first draft. All authors contributed to reviewing and editing the drafts.

Data accessibility statement

Raw bird survey data, processed land use and population variability data as well as code to reproduce the manuscript's analyses are available from the Dryad Digital Repository https://doi.org/10.5061/dryad.2rbnzs82z (Guerber et al. 2026c). The code is also accessible in a GitHub repository (https://github.com/jguerber/birdpopvar). Raw land use data is accessible via the CORINE Land Cover database (https://land.copernicus.eu/en/products/corine-land-cover). Raw human footprint data is available via the Human Footprint database (https://wcshumanfootprint.org/data-access).

III.3 Supplementary Information for Chapter 1

III.S1 Supporting information on the bird dataset

Table III.S1: **Grouping of habitat categories from raw observer data into wider classes.** For each observer habitat category, percentages report how many of the 2499973 bird abundance records in the raw survey were recorded in this habitat category, before any other data filtering. More details about habitat categories are available in French at https://www.vigienature.fr/fr/bilans-et-resultats.

Observer habitat category	Habitat category	Used (% of dataset)
A - Forest (trees higher than 5m)	woodland	yes (25%)
B - Shrubland and young forests	woodland	yes (4.5%)
C - Meadows, marshes and heathlands	other	no (4.1%)
D - Agricultural land	farmland	yes (47%)
E - Urban, suburban and rural built areas	built	yes (15%)
F - Water bodies and wetlands	other	no (3.6%)
G - Coastal and terrestrial rocky areas	other	no (0.36%)

Table III.S2: **Filtering community time series data.** Number and proportion of time series, communities and species at each subsequent data filtering step (see Material and Methods).

	Communities	Time series	Species
Available FBBS communities	8493 (100%)	273486 (100%)	331 (100%)
Habitats of interest	7445 (88%)	243337 (89%)	315 (95%)
Survey coverage	961 (11%)	50978 (19%)	278 (84%)
Abundant enough species	961 (11%)	24743 (9%)	168 (51%)
Convergent local trends	961 (11%)	24727 (9%)	167 (50%)
Correct pressure data	905 (11%)	23397 (9%)	160 (48%)

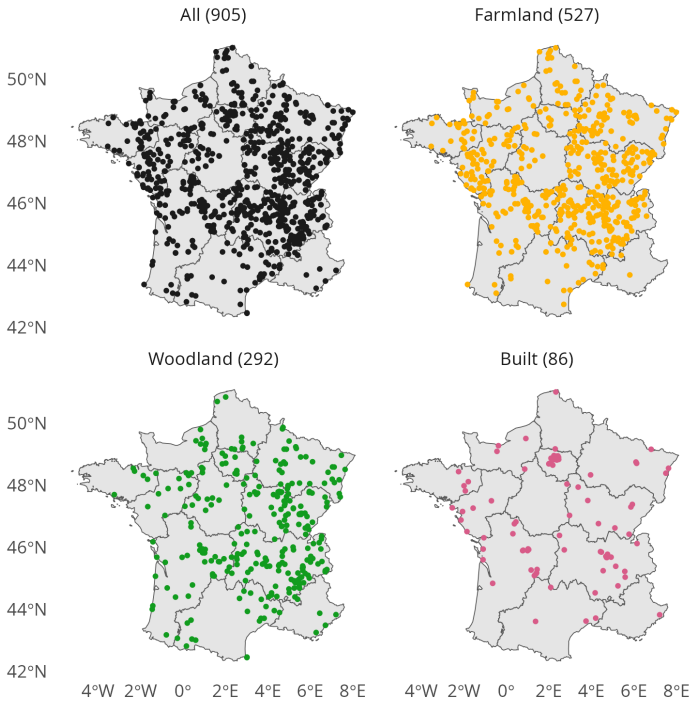

Figure III.S1: **Spatial distribution of communities used in statistical analyses.** Rights to the shapefile of the French regions are reserved to the contributors of OpenStreetMap under the Open Database License (ODbL).

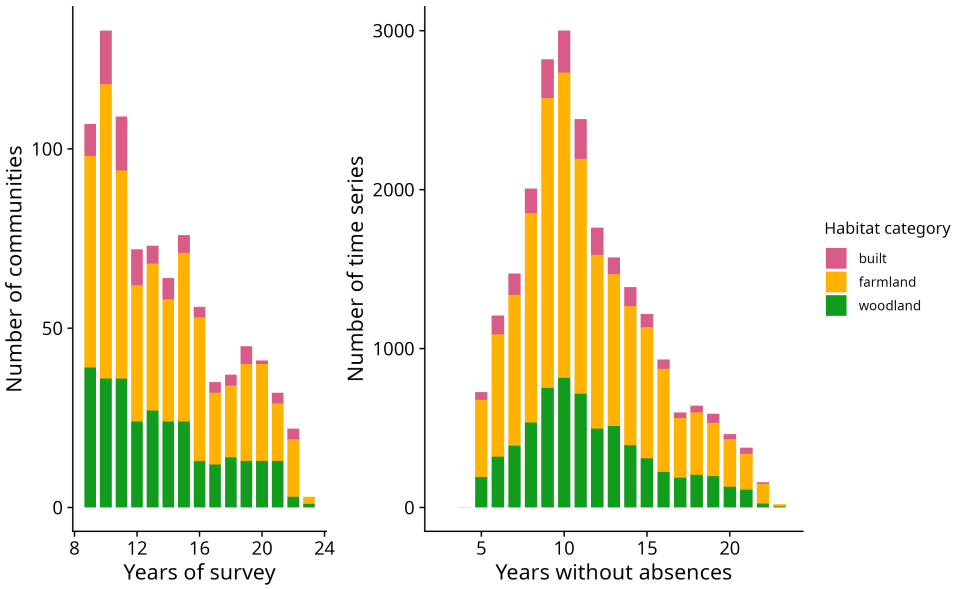

Figure III.S2: **Distribution of the number of years of survey for each community (left) and of the number of years without null abundance for each species time series (right) in the final dataset.** Mean (standard deviation): 13.7(3.81) (left); 11.4(3.92) (right).

III.S2 Supporting analyses

III.S2.1 Model validation

For each stability index, full generalised linear mixed models (GLMM) were fit with and without square identity as a random intercept using restricted maximum likelihood in `glmmTMB`. The best-fitting model always included the random intercept. All models presented in Tab. III.S3 include square identity as a random intercept and were fit using unrestricted maximum likelihood (Zuur et al. 2009). We detail the maximum likelihood estimates of the model for habitat category for each stability index in Fig. III.S3, and the estimates for the full models (also including anthropogenic pressure indices and species richness as fixed effects) in Fig. III.S4.

Table III.S3: **Model selection table for variability (left) and average absolute trend (right) across habitats.** The full model included human impact, landscape complexity, species richness, number of points and habitat category as fixed effects, with a random effect for square plot identity. For each model and stability components, we report the corresponding information criteria values as well as the number of estimated parameters (df). Bold text in cells show the minimum value of each information criterion for each stability index.

		Variability		Trend		
	df	AIC	BIC	AIC	BIC	Fixed effects
Full	9	**-899**	**-856**	**-4455**	**-4412**	All
Habitat controlled	6	-844	-815	-4438	-4409	Habitat category and number of points
No ecology	4	-634	-615	-4411	-4391	Number of points by community
Null	3	-487	-473	-4411	-4396	None (intercept only)

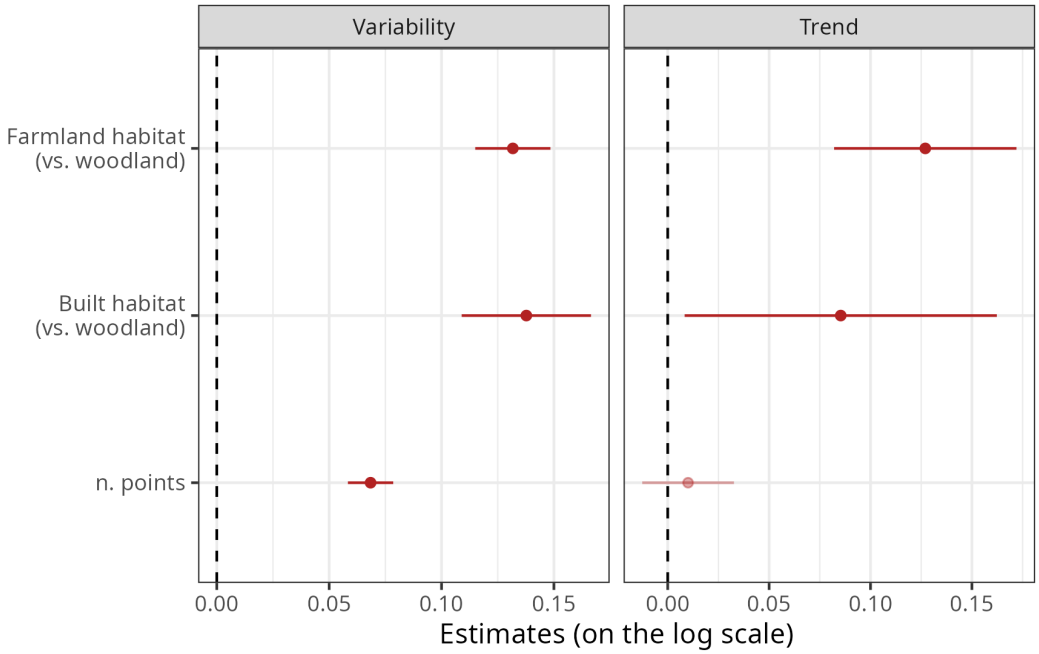

Figure III.S3: **Parameter estimates for the fixed effects for mean detrended variability (left) and mean of absolute trends (right).** Points represent the estimates of the effects of each variable on the stability index and segments represent the 95% confidence interval around them. Red (respectively blue) colours indicate positive (resp. negative) effects. Non-significant effects (Wald approximation) are transparent.

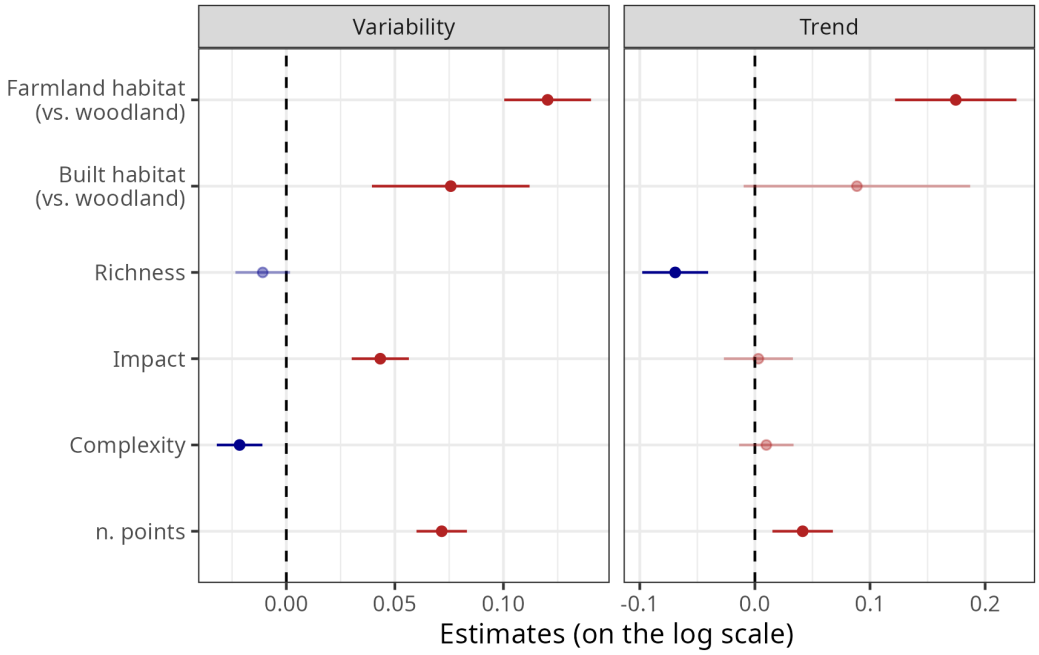

Figure III.S4: **Parameter estimates for the fixed effects for mean detrended variability (left) and mean of absolute trends (right) in a model accounting for land use intensity and species richness.** Points represent the estimates of the effects of each variable on the stability index and segments represent the 95% confidence interval around them. Red (respectively blue) colours indicate positive (resp. negative) effects. Non-significant effects (Wald approximation) are transparent.

III.S2.2 Spatial autocorrelation

As shown in Tab. III.S4, residuals of the GLMM for habitat category display signs of distance-based autocorrelation. We refit the models with `sdmTMB`, including spatial random effects. In this framework, the correlation between the observed values at two observations is expected to decrease with increasing geographical distance between the observation points (in our case, the communities). In `sdmTMB`, spatial random effects are fit using a triangulated mesh that approximates the spatial structure of the data, and we chose 10km as the cutoff distance for the mesh. This allowed to fit the model while efficiently accounting for spatial autocorrelation (Tab. III.S4). However, since the parameter estimates for the fixed effects as well as their significance are similar between the classical GLMM (Fig. III.S3) and the spatial GLMM (Fig. III.S5), we present only the results and methods for the classical GLMM in the main manuscript text.

Table III.S4: **Spatial autocorrelation of residuals from the two models**. For each stability index, we compare the observed spatial autocorrelation of the residuals of the full model (Moran's I) fit as a classical generalised linear mixed model (with `glmmTMB`) or as a spatial GLMM (with `sdmTMB`) to the expected distribution of Moran's I under the null assumption of no spatial autocorrelation. Since the geographical coordinates are the same for the two stability indices, the null distribution is the same for variability as for trends. Bold values indicate that the observed Moran's I significantly deviates from the null distribution (two-sided).

	Observed I			
	(with glmmTMB)	(with sdmTMB)	Expected null I (mean)	(sd)
Variability	**-0.13**	-0.0067	-0.0011	0.0095
Trend	**0.018**	-0.007	-0.0011	0.0095

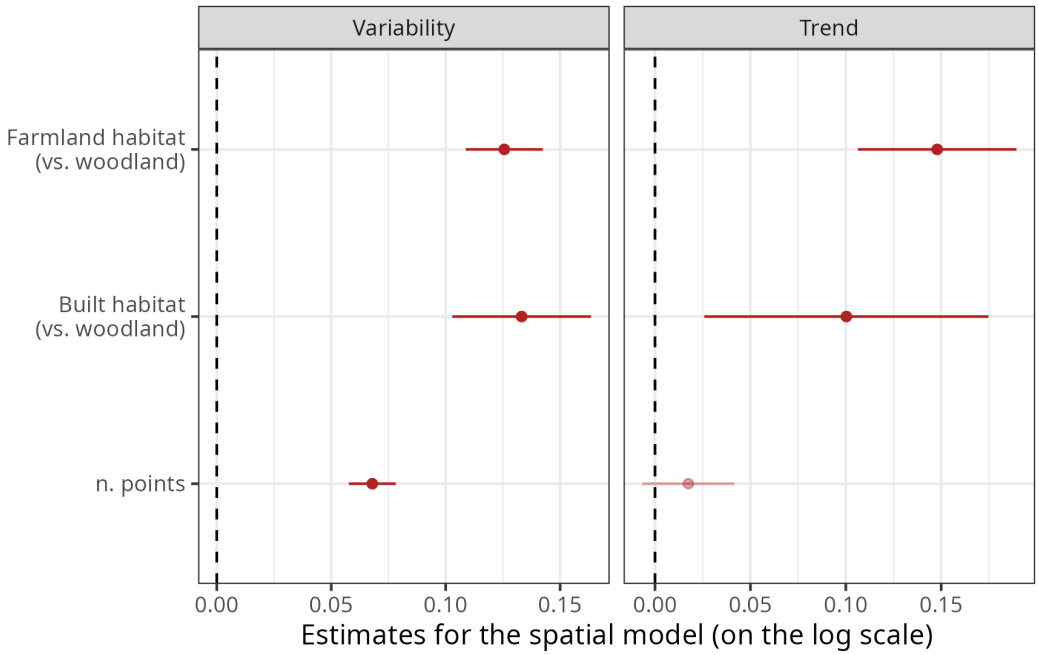

Figure III.S5: **Parameter estimates for the fixed effects for mean detrended variability (left) and mean of absolute trends (right) in the spatial GLMMs.** Points represent the estimates of the effects of each variable on the stability index and segments represent the 95% confidence interval around them. Red (respectively blue) colours indicate positive (resp. negative) effects. Non-significant effects (Wald approximation) are transparent.

III.S2.3 Sensitivity to the spatial scale of anthropogenic pressures

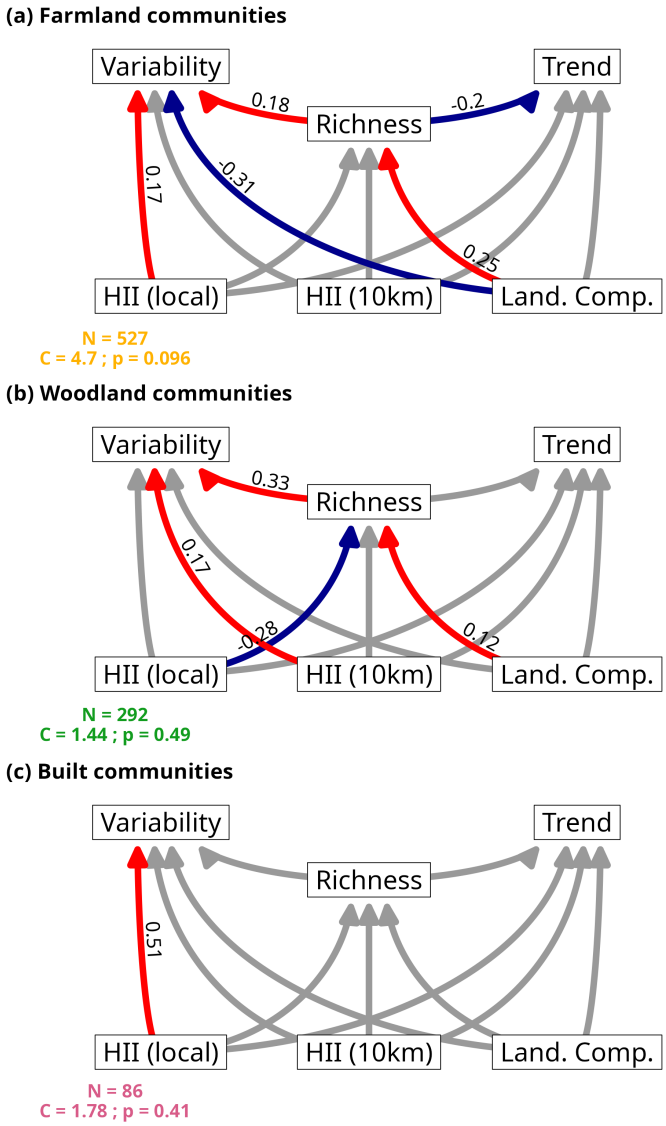

Figure III.S6: **Stability components across land use intensity with human impact in a 10km radius.** Positive (respectively negative) significant effects in the structural equation models are represented in red (resp. blue) with standardised effect size as a text annotation, and non-significant tested relationships are represented in grey. Annotations in the bottom-left corners denote number of communities (N) and outputs of the Fisher's C test on 2 degrees of freedom for each subset of communities. *HII*: human impact index, *Land. Comp.*: landscape complexity.

III.S2.4 Relationship between species richness and the mean of absolute trends

We numerically and mathematically check that the observed negative link between species richness and the mean of absolute trends is not artefactual, *i.e.* does not arise from simple null assumptions about the mean of absolute trends.

Proof

Consider a community with S species. Assume that for any species i, the species trend β_i follows a normal distribution with mean 0 and standard deviation σ_β. We derive the expected value for the mean of absolute trends $\tilde{\beta} = \frac{1}{S}\Sigma_i^S|\beta_i|$. $|\beta_i|$ follows a half-normal distribution, which has an expected value of $\mathbb{E}[|\beta_i|] = \sigma_\beta \frac{\sqrt{2}}{\sqrt{\pi}}$ (Leone et al. 1961). If the species trends are independent, $\mathbb{E}[\tilde{\beta}] = \frac{1}{S} S\, \mathbb{E}[|\beta_i|] = \sigma_\beta \frac{\sqrt{2}}{\sqrt{\pi}}$.

The mean of absolute trends is thus expected to be proportional to the variance of the underlying species trend distribution within the community, without direct link to the species richness.

Numerical illustration

Although there can be substantial variation around the expected value, the mean of absolute trends under a null assumption does not show a clear pattern along varying species richness (Fig. III.S7).

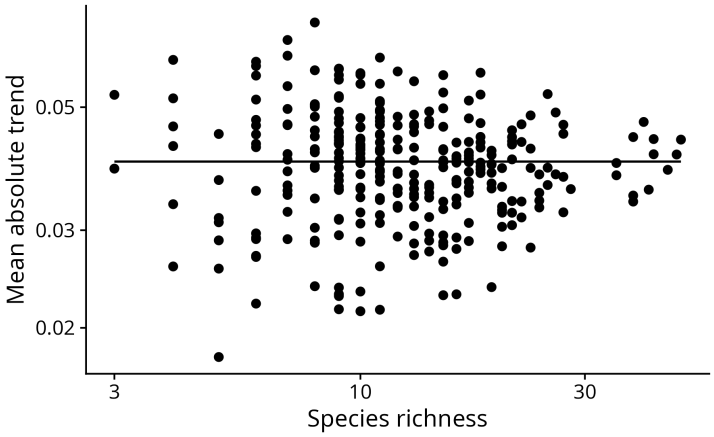

Figure III.S7: **Mean of absolute trends in simulated communities with different species richness.** 300 communities are simulated by sampling the number of species according to a log-Normal distribution with scale 2.5 and range 0.5, rounded to the nearest integer. Species trend standard deviation was set to $\sigma_\beta = 0.05$. The solid line indicates the expected value $\sigma_\beta \sqrt{2/\pi}$.

Link to uncertainty propagation

Now assume that σ_β is the result of both the ecological variance of species trend σ_e^2 and the uncertainty of the measurement of the species trend σ_u^2, *i.e.* $\sigma_\beta^2 = \sigma_e^2 + \sigma_u^2$. The expected value for $\tilde{\beta}$ when considering

only σ_e^2 is therefore lower than the expected value when considering both σ_e^2 and σ_u^2.

Under an uncertainty propagation method, communities with higher uncertainties in species trends are thus likely to show higher values of the mean of absolute trends than communities with lower species trend uncertainty. Moreover, communities with higher uncertainties in species trends are also more likely to have higher values of mean detrended variability, because the maximum likelihood estimator for the standard error of the trend is closely related to residual standard deviation. Observing a statistical association between mean of absolute trends and mean detrended variability is therefore likely under propagation of species trend uncertainty (see Section III.S2.5 of the Supporting Information).

III.S2.5 Propagating the uncertainty in species trend estimation

Method description

In the main methods, each local species time series model (hereafter called trend model) yields a maximum likelihood estimator (MLE) of local species trend $\beta_{i,s}$ and we compute a detrended variability $\sigma_{i,s}$ using the residuals from each trend model. $\beta_{i,s}$ and $\sigma_{i,s}$ values are aggregated within each community by the mean of absolute trends $\tilde{\beta}_i$ and the mean detrended variability $\bar{\sigma}_i$. The variations of these population variability components are then investigated across habitat categories and across anthropogenic pressures within habitat categories (hereafter called the ecological models). By only considering the MLE-based values for $\tilde{\beta}_i$ and $\bar{\sigma}_i$, the uncertainty for fixed effects in the ecological models is likely underestimated. Here we present a Monte Carlo approach (Soldaat et al. 2017, Li et al. 2019) to assess the magnitude of this underestimation by propagating trend model error to the $\tilde{\beta}_i$ values and then to the ecological models.

The trend models return a MLE for the uncertainty associated to $\beta_{i,s}$, which we call $S_{i,s}$, the standard error MLE for $\beta_{i,s}$. Because the detrended variability values $\sigma_{i,s}$ are based on the spread of the residuals of the trend models, their estimation does not yield any error term and the approach we propose therefore only propagates uncertainty via the mean of absolute trends.

The uncertainties of the trend models were propagated by simulating $R = 10000$ replicates of the species trend dataset. For each replicate dataset r, each species trend is resampled according to its estimated error, i.e. $\beta_{i,s,r} \sim \mathcal{N}(\beta_{i,s}, S_{i,s}^2)$ (Fig. III.S8, step 1). Aggregating by community and by replicate yields R datasets of simulated values of the mean of absolute trends $\tilde{\beta_{i,r}}$ (Fig. III.S8, step 2). These datasets are then used in the ecological models across habitats and across pressures within habitats. For each fixed effect in the ecological models run on the simulated dataset r, a MLE coefficient value C_r is associated to a MLE standard error E_r (grey slope and area in Fig. III.S8, step 3). Under the assumption that the real coefficient C is normally distributed, the mean value of C_r across all replicates, $\bar{C}$, is the most likely value for the fixed effect. There are three sources of variance for C around $\bar{C}$: (i) the Monte Carlo error (MCE) of C_r across all replicates, sd_C, (ii) the mean error estimated by the ecological model $\bar{E}$ and (iii) the MCE of E_r across all replicates, sd_E (Fig. III.S8, step 4 and 5). Assuming a normal distribution for C, a reasonable interval for the real value of C considering all replicates thus is the 95% interquantile of

$\mathcal{N}(\bar{C}, \text{sd}_C^2 + \bar{E}^2 + \text{sd}_E^2)$. This interval can be compared to the 95% interquantile of $\mathcal{N}(\bar{C}, \text{sd}_C^2)$, which only takes into account the uncertainty in C originating from the propagated trend model errors.

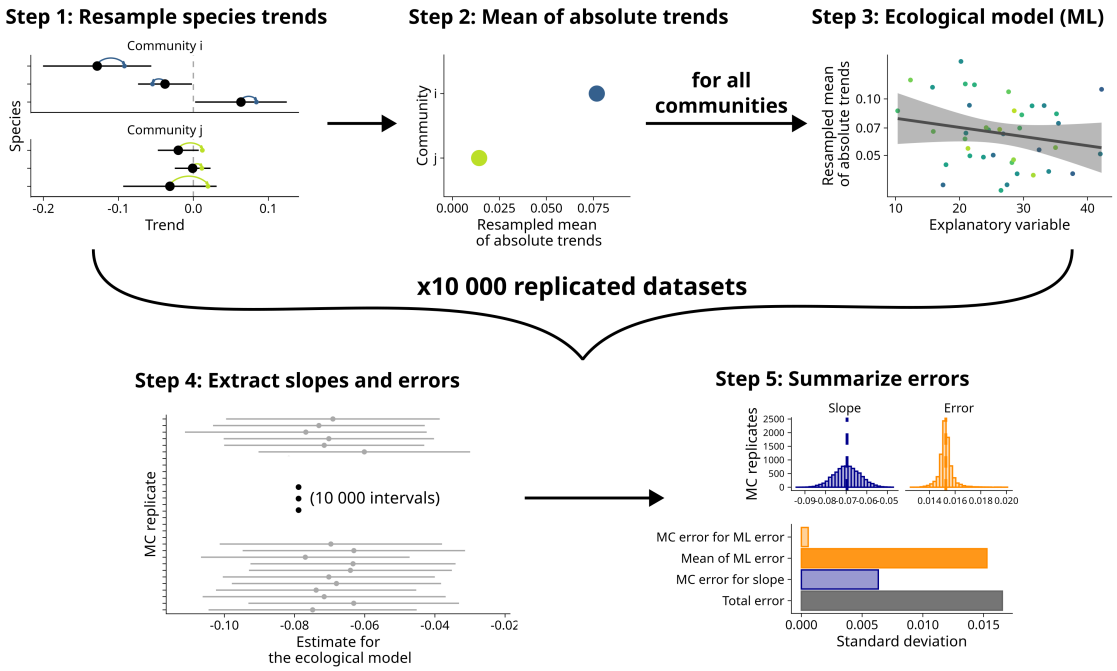

Figure III.S8: **Summary of the Monte Carlo method for uncertainty propagation for a single model coefficient.** Step 1: We resample (colored points) species trends accordind their estimated values (black points) and standard errors (black lines). Step 2: we aggregate them using the mean of absolute trends. Step 3: Repeating steps 1-2 for all communities, resampled values of the mean of absolute trends can be used in an ecological model, which produces an estimate (slope of grey line) associated to an error term (grey area). Step 4: Repeating steps 1-3 for R replicates, we produce R intervals for each estimate in the ecological model. Step 5: We get an MC distribution for the slope and for its associated error (top). The total error for the slope thus takes into account the MC error for the slope, but also the mean ML error and its MC error.

Results for the GLMM

For the GLMM considering the variation in mean of absolute trends across habitat categories, uncertainty propagation still allows to detect that populations in farmland have stronger trends than populations in woodland. This is somewhat visible by inspecting the propagated intervals for the mean of absolute trends across habitats (Fig. III.S9), and is clearer on the estimated credible intervals for each coefficient of the GLMM across habitat categories as well as the similar GLMM controlling for anthropogenic pressures (Fig. III.S10). For both models (top and bottom of Fig. III.S10), the full MC interval for the comparison of the mean of absolute trends between farmland and woodland communities indeed does not include zero, consistent with the interval in the method without uncertainty propagation (ML). The intervals for the other model coefficients are also consistent between the two methods, with full MC intervals slightly wider than ML intervals. Note that comparing the ML and the MC intervals in Fig. III.S10 hints that the uncertainty originating in trend model error is much smaller than the uncertainty originating in the spread of the MLE mean of absolute trends values.

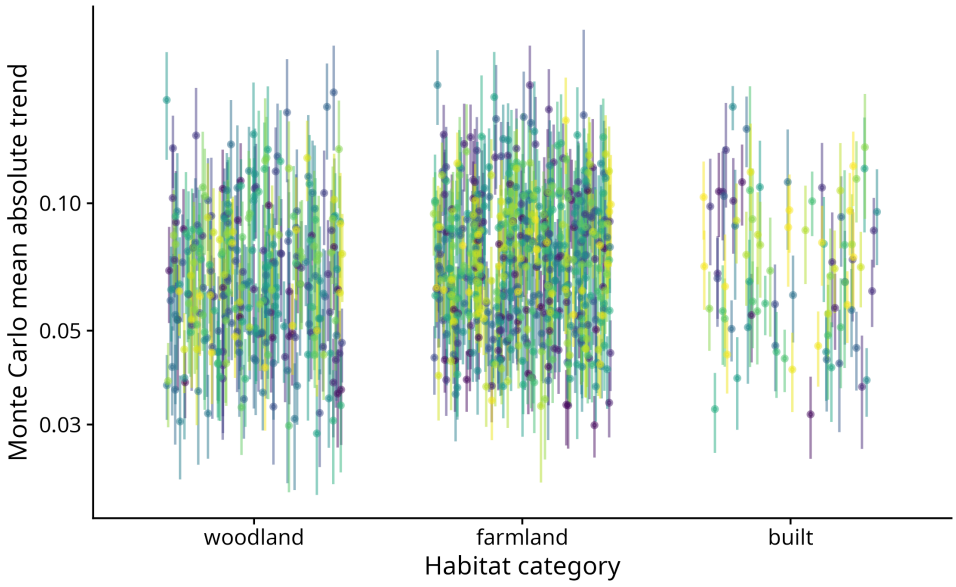

Figure III.S9: **Mean of absolute trends (dots) and their Monte Carlo 95% interquantile ranges (lines) across habitat categories.** Different colors denote different communities. Notice the logarithmic scale on the vertical axis. Intervals were obtained using 10000 simulated datasets.

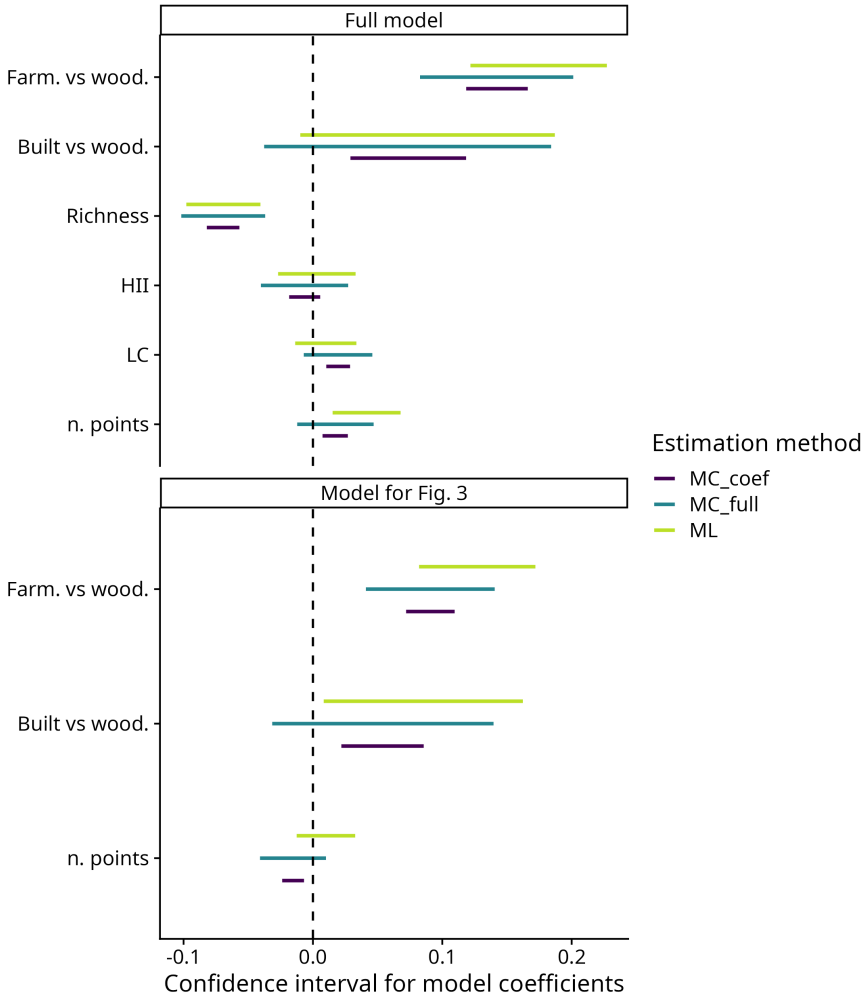

Figure III.S10: **Estimated intervals for each fixed effect in the models explaining the variation of the mean of absolute trends across habitat categories.** Intervals were estimated without Monte Carlo resampling (ML), with resampling but without the uncertainty estimated by the GLMM (MC_coef), and with propagated uncertainties in coefficients and GLMM errors (MC_full). Each GLMM was run on 10000 simulated datasets, out of which 7894 and 8928 models converged without errors for the top and bottom GLMM, respectively.

Results for the structural equation models

For the structural equation models, propagating error from the species trend models only slightly increases the errors for the paths including the mean of absolute trends (Fig. III.S11). The Monte Carlo interval for the negative link between species richness and the mean of absolute trends in farmland communities does not include zero, the results are thus consistent with the results without uncertainty propagation. An unexpected outcome of Monte Carlo error propagation to the SEMs is that the Monte Carlo interval for the goodness-of-fit criteria indicates that the SEM structure is rejected by the resampled data (Fig. III.S12), i.e. a rejection of the conditional independence of mean detrended variability and mean of absolute trends under uncertainty propagation. This can be explained by the fact that uncertainty in the trend estimate is related to detrended variability, which biases the test of conditional independence under uncertainty propagation (see Section III.S2.4 of the Supporting Information).

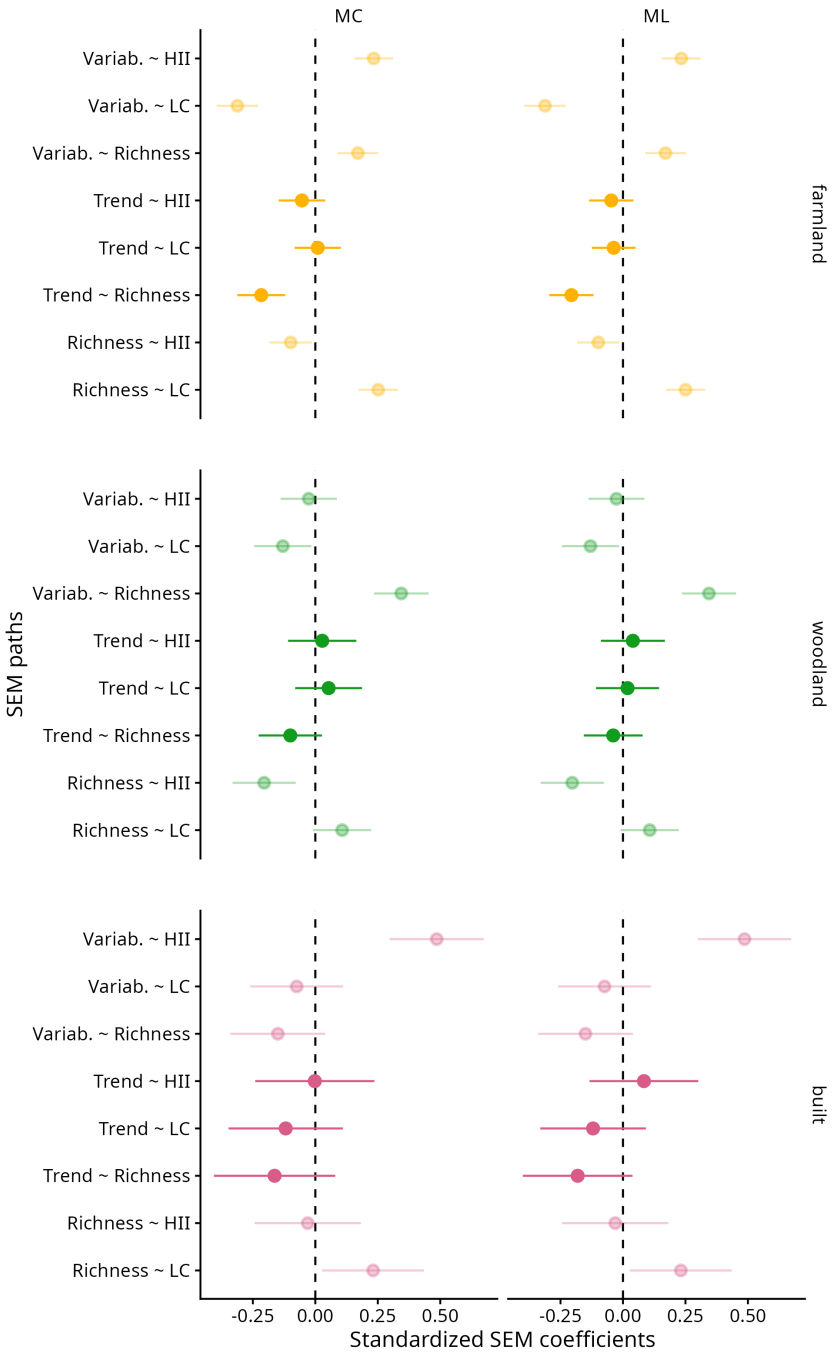

Figure III.S11: **Estimated intervals for standardized structural equation model (SEM) coefficients with full Monte Carlo propagation of trend model error (left) and without (right).** Transparent colors indicate paths that do not incorporate the mean of absolute trends (Trend), whose intervals in the two estimation methods are therefore identical. For Monte Carlo estimation, SEMs were fit on 10000 simulated datasets, of which 9982, 9522 and 9778 SEMs converged for farmland, woodland and built communities, respectively. Variab.: mean detrended variability.

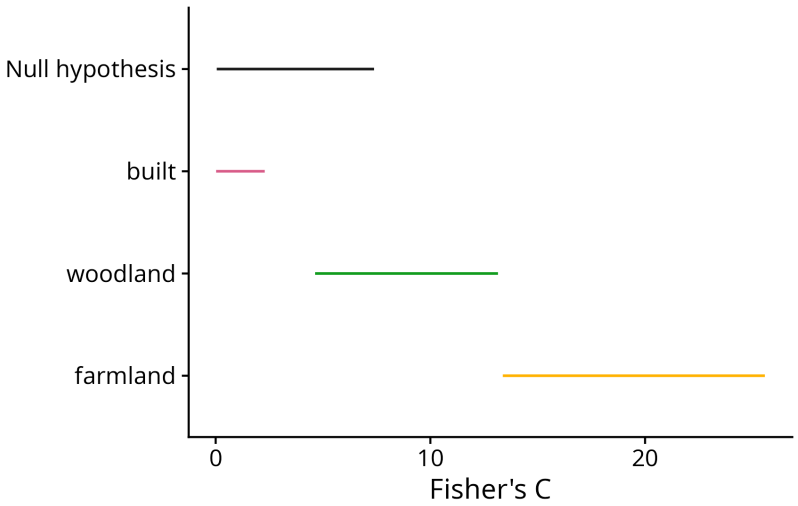

Figure III.S12: **95% interquantiles for Fisher's C across the structural equation models on resampled datasets (colors) compared to the 95% interquantiles for Fisher's C under the null hypothesis (gray).** SEMs were fit on 10000 simulated datasets, of which 9982, 9522 and 9778 SEMs converged for farmland, woodland and built communities, respectively.

IV . Chapter 2: Press perturbations induce transient changes in temporal variability

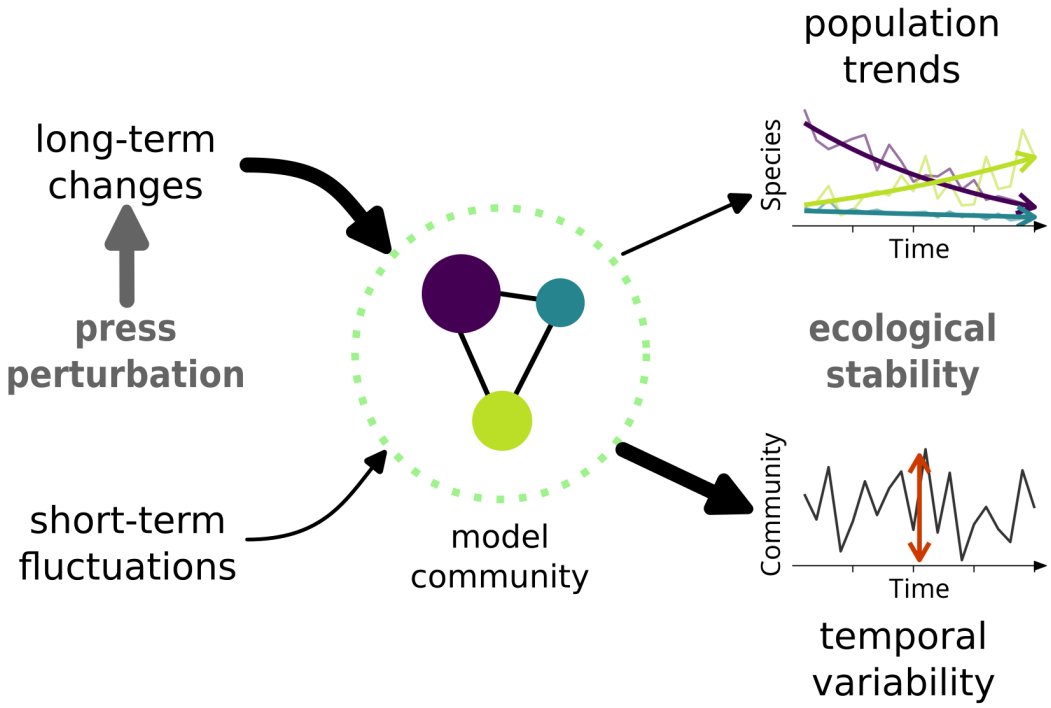

Figure IV.0: **Chapter 2 in the general framework.** By introducing known press perturbations in stochastic population and community dynamics models, we show that transient changes in variability deviate from what could be expected from stationary regimes based on population means. Thicker arrows denote the main relationship investigated in this Chapter.

IV.1 Context and aim of the study

In Chapter 1, we measured that average population trends and detrended population variability at a local scale shared a common driver, land use intensity, but could not identify any further relationship between these two integrative stability dimensions. In order to clarify if this may be due to a lack of statistical power needed to detect a relationship that should otherwise be expected, we turned to mathematical models of stochastic population and community dynamics.

In this chapter, we revisit stochastic counterparts of well-known population and community dynamics models, the logistic growth and the competitive Lotka-Volterra model, and build analytical approximations in order to measure variability far from equilibrium. By introducing known press perturbations in these models, we show that variability is expected to show stronger changes during transient regimes than what could be expected based on the changes in means. Communities subjected to both long-term environmental changes and environmental stochasticity are thus expected to exhibit temporal variability values that cannot be explained only by their stationary response to environmental stochasticity. At the community level, these deviations affect species synchrony as well as average population variability. Our approach also allows us to quantify such deviations and thus to anticipate that their small magnitude will likely make their detection in biodiversity monitoring data difficult.

This chapter was submitted to *The American Naturalist* in July 2026 and is available online as a preprint (Guerber et al. 2026d).

IV.2 Article: "Population and community variability deviate from stationary expectations during transient dynamics"

Abstract

Under complex perturbation regimes, biodiversity dynamics show temporal variability in species and community abundance around long-term population trends. Many species indeed show long-term declines while other species increase, putting natural communities far from stationary regimes, while variability is often studied near equilibrium. We contribute to bridging this gap by investigating population and community variability during long-term trends caused by press perturbations in stochastic models of population dynamics. By estimating the deterministic changes in mean and variance during the transient regime, we show that population variability deviates from stationary expectations. Moreover, the deviation strongly depends on the sign of the population trends: increases generate excesses of variability while declines generate deficits. Scaling up to community variability, we propose a decomposition of community variability deviation, allowing to highlight that community variability in the transient regime depends on how the press perturbation is distributed within species relative abundances and growth rates. These results challenge the equilibrium assumption and open new perspectives for the study of the variability of ecological systems under multiple perturbation types.

Keywords: ecological stability, population trends, logistic growth, interspecific competition, stochastic differential equations, moment closure

Introduction

Understanding how ecological systems respond to perturbations is critical in assessing threats to the maintenance of ecosystem functioning (Cardinale et al. 2012). Short-term fluctuations in environmental conditions generate variable population and community abundances (Tilman 1996, Engen et al. 1998), and anthropogenic pressures cause many wild species to decline in abundance while other species increase (McKinney and Lockwood 1999, Dornelas et al. 2014). While empirical and experimental approaches have proposed different ways to disentangle temporal variability from so-called long-term population trends (Hillebrand et al. 2018b, Lepš et al. 2019, Clark et al. 2022), theoretical understanding of how temporal variability might be affected by long-term population trends is lacking. In some situations, these two components of ecological stability appear correlated (Donohue et al. 2013), but no underlying mechanisms for such correlation have been proposed.

Temporal variability encapsulates both the intensity of environmental stochasticity as well as the ecological system's intrinsic ability to recover from perturbations (Arnoldi et al. 2019, Van Meerbeek et al. 2021). Because of this dual property as well as its ease of measurement, temporal variability has received considerable theoretical and empirical attention (Kéfi et al. 2019). There, temporal variability is often measured as the coefficient of variation, the ratio of temporal standard deviation to temporal mean, yielding an adimensional index of how variable a system is compared to its magnitude (Tilman 1996). A common framework for investigating temporal variability is to think of small perturbations affecting a system close to its equilibrium (Lundberg et al. 2000, Arnoldi et al. 2019). Following this near-equilibrium assumption, most studies rule out the impact of long-term population trends on the measured variability by studying a stationary regime (Arnoldi et al. 2019, Danet et al. 2025) or by detrending time series prior to variability analysis (Craven et al. 2018, Li et al. 2021). Under anthropogenic pressures, long-term population trends challenge the near-equilibrium assumption, with shifts in community composition being the most empirically supported aspect of recent biodiversity changes at local scales (Carroll et al. 2023, Dornelas et al. 2023). While the importance of non-equilibrium dynamics is increasingly recognized in ecological theory (Hastings et al. 2018), they are not often combined with the study of temporal variability. A reason for this theoretical gap lies in the fact that the most commonly used mathematical methods for studying the stability of dynamical systems require to linearize the system's dynamics around the

equilibrium, which is only reasonable if the system stays in the close vicinity of its equilibrium.

The near-equilibrium assumption has yielded a general theory of how temporal variability scales across spatio-temporal and ecological dimensions (Clark et al. 2021). Temporal variability of population and community abundance has been shown to vary with the strength of stochasticity (Arnoldi et al. 2019) and with species growth rate (Mentges et al. 2024). Moreover, the near-equilibrium assumption has also enabled the development and mechanical understanding of the insurance hypothesis (Yachi and Loreau 1999), which states that the variability of community abundance or biomass declines with the number of species in the community (Tilman 1996, Pennekamp et al. 2018). Community abundance is more variable when the species' population abundances are more variable, or when the species-level fluctuations are synchronized and fail to compensate for each other (Loreau and de Mazancourt 2008, Thibaut and Connolly 2013). Biodiversity has been shown to promote the evenness of species variances, decreasing species synchrony and thus stabilizing communities (Zhao et al. 2022), while interspecific competition tends to increase population variability (Ives et al. 1999). Understanding how these mechanisms could operate far from equilibrium is a critical step towards better understanding the temporal dynamics of natural communities.

In this study, we implement long-term trends in stochastic population and community dynamics models as responses to press perturbations, *i.e.* sudden and maintained changes in carrying capacity (Van Meerbeek et al. 2021, Lajaaiti et al. 2025). Our approach relies on deterministic approximations for the changes in the mean and variance of a process described by a stochastic differential equation, called moment closure approximations (Särkkä and Solin 2019). In the biochemical literature, these approximation methods have enabled exploration of the role of stochastic phenomena in cell biology (Schnoerr et al. 2017), including in the case of transient dynamics (Zechner et al. 2012). While they have been known for some time in ecology (Lande et al. 2003, Nåsell 2003), moment closure approximations are rarely used in the context of population dynamics models. Here we use such approximations in order to summarize stochastic dynamics during the long-term trends into simple, deterministic indices for population and community variability far from equilibrium.

We revisit classical findings on temporal variability of population and community abundance in the context of long-term trends caused by press perturbations. At the population level, we investigate how properties of the press perturbation and population growth rate drive temporal variability during long-term trends.

We then explore how the variability of a simple community is affected by the diversity of individual species' responses to the press perturbation and by how these responses depend on species abundances and growth rates, this with and without interspecific competition. This work extends current knowledge on population and community variability to contexts with transient dynamics and paves the way for better inference of ecological stability and perturbation regime from variability data.

Methods

Mathematical framework

In a community of S species under environmental stochasticity (Engen et al. 1998, Lande et al. 2003, Arnoldi et al. 2019), population abundances are the result of community dynamics (drift) and stochastic pulse perturbations (diffusion). In continuous time, this translates to some stochastic differential equation system of the form:

$$\mathrm{d}\mathbf{X_t} = f(\mathbf{X_t})\mathrm{d}t + G(\mathbf{X_t})\mathrm{d}\boldsymbol{W_t} \tag{IV.1}$$

$\mathbf{X_t} = (X_1(t), X_2(t), \ldots, X_S(t))$ is the vector of population abundances at time t, f encapsulates the deterministic community dynamics and G represents how small short-term perturbations modelled as infinitesimal Wiener process increments $\mathrm{d}\mathbf{W_t}$ affect the different species. For simplicity, we will call f the deterministic term and G the stochastic term, but notice that G itself is not random and only $G(\mathbf{X_t})\mathrm{d}\boldsymbol{W_t}$ is.

For any stochastic process that can be written as Equation IV.1, stochastic calculus allows to approximate the changes in the statistical moments of $\mathbf{X_t}$ as an ordinary, deterministic differential equation system (see supplemental Section IV.S1 for an overview). In particular, our moment closure approximation relies on linearizing the deterministic term around the (time-varying) mean of the stochastic process instead of linearizing it around a fixed point (Särkkä and Solin 2019). The approximation thus does not only hold in a stationary regime near an equilibrium, but also during transient regimes. Moreover, the mean and variance of species abundance can be studied as numerical solutions of ordinary differential equations instead of the sample mean and variance of many simulations of the stochastic process (Fig. IV.1).

Mean and variance of a single population

For a single population with a carrying capacity K and a logistic growth rate r under environmental stochasticity of strength σ_e, Equation IV.1 simplifies to:

$$\mathrm{d}X_t = rX_t(1 - \frac{X_t}{K})\mathrm{d}t + \sigma_e X_t \mathrm{d}W_t \tag{IV.2}$$

Under the moment closure approximation (supplemental Section IV.S1.2), the dynamics of the mean and variance of population abundance, μ_t and V_t, can be described as:

$$\begin{aligned} \frac{\mathrm{d}\mu_t}{\mathrm{d}t} &= r\mu_t\left(1 - \frac{\mu_t}{K}\right) - \frac{r}{K}V_t \\ \frac{\mathrm{d}V_t}{\mathrm{d}t} &= 2rV_t(1 - 2\frac{\mu_t}{K}) + \sigma_e^2(V_t + \mu_t^2) \end{aligned} \tag{IV.3}$$

System IV.3 holds during transient regimes but also allows setting $\frac{\mathrm{d}\mu_t}{\mathrm{d}t} = \frac{\mathrm{d}V_t}{\mathrm{d}t} = 0$ in order to calculate (μ^*, V^*), the mean and variance of X_t in the stationary regime. Conversely, for any observed mean value μ_t, the same system can be solved for $(\hat{K}(\mu_t), \hat{V}(\mu_t))$, with $\hat{K}(\mu_t)$ the carrying capacity required to observe a stationary regime of mean $\hat{\mu}$, with variance $\hat{V}(\mu_t)$. We call $\widehat{V}(\mu_t)$ the stationary expectation for variance at mean μ_t, it is the variance that the population would have if it was in a stationary regime at mean μ_t.

A given population of mean μ_t thus has three associated values for variance: V_t, the observed variance according to the moment closure approximation; $\hat{V}(\mu_t)$, the stationary expectation for variance at μ_t; and V^*, the variance in the stationary regime. Note that $V^* = \hat{V}(\mu^*) = \lim_{t\to\infty} V_t$. Because V_t (resp. V^*) is always roughly proportional to μ_t^2 (resp. μ^{*2}), we compute variability as the coefficient of variation of X_t, *i.e.* $\mathrm{CV}_t = \frac{\sqrt{V_t}}{\mu_t}$ (see supplemental Section IV.S2.1 for derivation).

Long-term trends as responses to press perturbations

We model long-term population trends as the transient response of the population to a press perturbation, *i.e.* to a sudden and maintained change in carrying capacity (Lajaaiti et al. 2025). Press perturbations that decrease the carrying capacity generate decreasing population trends, while press perturbations that increase K generate increasing trends.

Starting from a stationary regime with $K = K_0$ for time $t < t_d$ corresponding to mean and variance $(\mu^*, V^*)_{|K=K_0}$, we introduce a press perturbation by setting $K = K_d$. The relative strength of the press perturbation is defined as $\delta = \frac{K_d - K_0}{K_0}$. A single simulation of Equation IV.2 shows how a single replicate population reacts to the press perturbation (one single black line in Fig. IV.1A). We first assess the approximation provided by Equation IV.3 for the mean and variance of population abundance as it responds to a press perturbation. To do so, we compare the (deterministic) expected mean and variance provided by Equation IV.3 with the distribution of observed mean and variance obtained from simulating Equation IV.2. To estimate these distributions across the transient regime, we first compute the mean and coefficient of variation of a single batch of simulations (e.g. 50 simulations of population dynamics in Fig. IV.1) for each time step. This measures the changes in mean and variability of populations in this batch across time. Second, the distributions of mean and coefficient of variations at each time step can be estimated by simulating many batches, called replicates, and are then compared to their approximate expected values after converting variances from Equation IV.3 to variabilities (Fig. IV.1B).

Over the course of transient dynamics following the press perturbation, X_t will converge to a new stationary regime $(\mu^*, V^*)_{|K=K_d}$ if the population does not become extinct and if the parameter values allow the moment closure approximation. For all values of μ_t during the transient dynamics, we compute a stationary expectation for variability $\widehat{\mathsf{CV}}(\mu_t) = \sqrt{\widehat{V}(\mu_t)}/\mu_t$, which corresponds to the coefficient of variation that the population would have if it was in a stationary regime at mean μ_t. The deviation of the variability of X_t from a stationary regime at a given time can be computed as the log-ratio between CV_t and $\widehat{\mathsf{CV}}(\mu_t)$. This deviation can then be integrated over the course of the transient regime:

$$D = \int_{t_d}^{+\infty} \log(\frac{\mathsf{CV}_t}{\widehat{\mathsf{CV}}(\mu_t)})\mathrm{d}t \tag{IV.4}$$

Positive values of D indicate an overall excess of variability over the transient regime compared to stationary expectations, while negative values indicate an overall lower variability.

Community variability in the transient regime

For community dynamics, we set the deterministic term in Equation IV.1 as the generalized Lotka-Volterra system (Lotka 1925, Volterra 1928). We use its formulation from Bunin (2017):

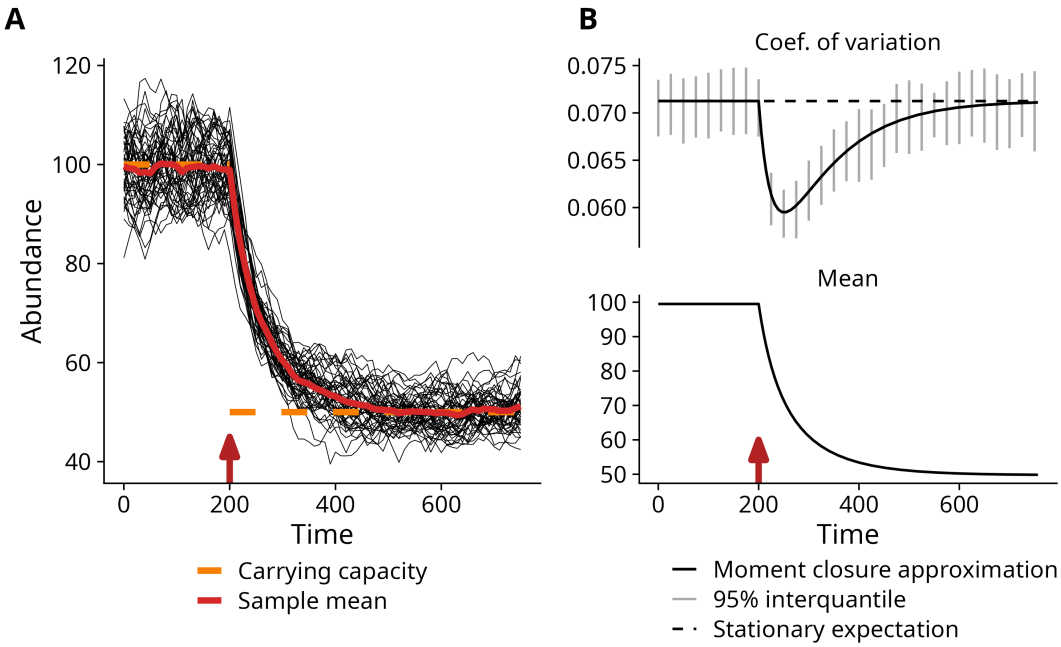

Figure IV.1: **Population dynamics with a stochastic logistic growth under a press perturbation.** (A) 50 numerical simulations of the stochastic logistic growth with a press perturbation from $t_d = 200$ (red arrow) onwards. (B) Solution of the moment closure approximation for coefficient of variation (top) and mean (bottom). Gray vertical intervals on the top panel indicate the 95% interquantile for 50 replicates of the coefficient of variation computed across 500 stochastic simulations. The corresponding intervals for the mean had negligible sizes. The dashed black line indicates the stationary expectation for the coefficient of variation. K_0, K_d, r and σ_e were set to 100, 50, 0.01 and 0.01, respectively.

$$f_i(\mathbf{X_t}) = \frac{r_i}{K_i} X_i(K_i + \mathbf{A}\mathbf{X_t}) \tag{IV.5}$$

The interaction matrix $\mathbf{A}$ encapsulates each species' effect on the abundances of all species (including itself). We set $A_{ii} = -1$ for all i to ensure that, without any interspecific interactions, each species reaches its carrying capacity K_i. Off-diagonal terms can be set at will or randomly chosen, but only some ranges or distributions will allow for asymptotic coexistence (Bunin 2017, Barbier et al. 2018). With environmental stochasticity acting independently on each species with constant strength, the stochastic term is $G(\mathbf{X_t}, t) = \sigma_e \operatorname{diag}(\mathbf{X_t})$.

We approximate Equation IV.5 by a deterministic differential equation system for $\boldsymbol{\mu_t}$ and $\boldsymbol{\Sigma_t}$, the vector of means and the variance-covariance matrix of $\mathbf{X_t}$ (supplemental Section IV.S1.2, Equation IV.S5). Because $\boldsymbol{\Sigma_t}$ is symmetric, this is a system of $S + S(S+1)/2 = S(S+3)/2$ equations. Therefore, while the system remains numerically solvable, it quickly becomes analytically untractable as the number of species increases. For any parameter combination, the means and variance-covariance matrix in the stationary regime, $(\boldsymbol{\mu}^*, \boldsymbol{\Sigma}^*)$, can be computed numerically and for any observed value for means $\boldsymbol{\mu_t}$, one can try to compute the carrying capacities $\hat{\mathbf{K}}(\boldsymbol{\mu_t})$ that allow for a stationary regime with population means $\boldsymbol{\mu_t}$. The corresponding variance-covariance matrix is called $\widehat{\boldsymbol{\Sigma}}(\boldsymbol{\mu_t})$, the stationary expectation for the variance-covariance matrix at means $\boldsymbol{\mu_t}$. For some values of $\boldsymbol{\mu_t}$, solutions for $\widehat{\boldsymbol{\Sigma}}(\boldsymbol{\mu_t})$ may not exist (in these cases, because of the values of the other parameters, there is no $\hat{\mathbf{K}}$ such that a stationary regime is possible at these means).

Community mean $\mu_c(t)$ and variance $V_c(t)$ can be obtained by summing all elements of $\boldsymbol{\mu_t}$ and $\boldsymbol{\Sigma_t}$, respectively. Moreover, the stationary expectation for community variance, $\hat{V}_c(\boldsymbol{\mu_t})$, can be computed by summing the elements of $\widehat{\boldsymbol{\Sigma}}(\boldsymbol{\mu_t})$. At a given vector of population means $\boldsymbol{\mu_t}$, $\hat{V}_c(\boldsymbol{\mu_t})$ is the variance that the community would have if the system was in a stationary regime at population means $\boldsymbol{\mu_t}$. The total deviation in community variability from stationary expectation across the transient regime, D_c, can thus be defined similarly to Equation IV.4:

$$D_c = \int_{t_d}^{+\infty} \log\left(\frac{\mathsf{CV}_c(t)}{\widehat{\mathsf{CV}_c}(\widehat{\boldsymbol{\mu}} = \boldsymbol{\mu_t})}\right) \mathrm{d}t \tag{IV.6}$$

In order to pinpoint the underlying drivers of D_c, we use two subsequent decompositions of the community coefficient of variation $\mathsf{CV}_c(t) = \sqrt{V_c(t)}/\mu_c(t)$. From Thibaut and Connolly (2013), $\mathsf{CV}_c(t) = \mathsf{CV}_p(t)\sqrt{\phi(t)}$, with CV_p the average of species coefficients of variation weighted by species' relative abundances and ϕ the species synchrony index of Loreau and de Mazancourt (2008). Moreover, following Zhao et al. (2022) and with $s_{ii}(t)$ the variance of species i (*i.e* the i-th diagonal element of $\boldsymbol{\Sigma_t}$),

$$\frac{1}{\sqrt{\phi(t)}} = \mathsf{SAE}(t)\mathsf{CPE}(t) = \frac{\sum_i \sqrt{s_{ii}(t)}}{\sqrt{\mathrm{tr}(\boldsymbol{\Sigma_t})}} \frac{\sqrt{\mathrm{tr}(\boldsymbol{\Sigma_t})}}{\sqrt{V_c(t)}} \tag{IV.7}$$

The statistical averaging effect ($\mathsf{SAE}(t)$) accounts for how aggregating species with uncorrelated fluctuations reduces overall community variability, and the compensatory dynamics effect ($\mathsf{CPE}(t)$) accounts for the reduced variability introduced by negative temporal covariances among species (Zhao et al. 2022). By definition, communities with uneven species variances have a low statistical averaging effect. For each of $\mathsf{CV}_p(t)$, $\mathsf{SAE}(t)$ and $\mathsf{CPE}(t)$, the corresponding expectation under a stationary regime at means $\boldsymbol{\mu_t}$ can be computed from $\widehat{\boldsymbol{\Sigma}}(\boldsymbol{\mu_t})$. Each component of community variability is then assigned a total deviation across the transient regime, and all their deviations sum to the total deviation in community variability:

$$\begin{aligned} D_c &= \int_{t_d}^{+\infty} [\log(\frac{\mathsf{CV}_p(t)}{\mathsf{SAE}(t)\mathsf{CPE}(t)}) - \log(\frac{\widehat{\mathsf{SAE}}(\boldsymbol{\mu_t})\widehat{\mathsf{CPE}}(\boldsymbol{\mu_t})}{\widehat{\mathsf{CV}_p}(\boldsymbol{\mu_t})})]\mathrm{d}t \\ &= \int_{t_d}^{+\infty} \log(\frac{\mathsf{CV}_p(t)}{\widehat{\mathsf{CV}_p}(\boldsymbol{\mu_t})})\mathrm{d}t - \int_{t_d}^{+\infty} \log(\frac{\mathsf{SAE}(t)}{\widehat{\mathsf{SAE}}(\boldsymbol{\mu_t})})\mathrm{d}t - \int_{t_d}^{+\infty} \log \frac{\mathsf{CPE}(t)}{\widehat{\mathsf{CPE}}(\boldsymbol{\mu_t})}\mathrm{d}t \\ &= D_{\mathsf{pop}} - D_{\mathsf{sae}} - D_{\mathsf{cpe}} \end{aligned} \tag{IV.8}$$

Community variability thus deviates from stationary expectations either because mean population variability, statistical averaging or compensatory dynamics deviate from their stationary expectations. Excesses of statistical averaging effect or of compensatory dynamics effect generate deficits of community variability.

Press perturbation scenarii and numerical analysis

To explore the deviation of population variability from stationary expectations, we explore the effects of the relative press perturbation δ and the population growth rate r on D by numerically solving equation IV.3. For all values of μ_t across time in the numerical solution, we compute the stationary expectation for population variability $\widehat{\mathsf{CV}}(\mu_t)$ using system IV.3, which allows to compute D (Equation IV.4) by numerical

integration between perturbation time t_d and the end of simulation time.

In order to investigate the impact of press perturbations on community variability, we focus on a community with two species with $A = \left(\begin{smallmatrix} -1 & -\alpha \\ -\alpha & -1 \end{smallmatrix}\right)$, *i.e.* symmetric competitive interactions of strength α. The vector of carrying capacities before the press perturbation, $\mathbf{K_0} = (K_{0,1}, K_{0,2})$ is set such that the $K_{0,1} > K_{0,2}$. The first species thus is the most abundant in the community before the press perturbation. Together with the vector of growth rates $\mathbf{r}$, α and $\mathbf{K_0}$ define the community context in which the press perturbation is introduced. We used community contexts with or without interspecific competition and with equal or different growth rates across species. Since higher population growth rate is generally associated with higher carrying capacity (Brown et al. 2004), r_1/r_2 was set equal to $K_{0,1}/K_{0,2}$ for contexts where growth rates were different across species.

Setting the relative press perturbation to be equal in magnitude $|\delta|$ across species, there are four different ways to introduce a press perturbation, which we call perturbation scenarii. First, the two species can have the same response to the press perturbation, which can be negative or positive. This defines the "increase" scenario with $\boldsymbol{\delta} = (|\delta|, |\delta|)$ and the "decrease" scenario with $\boldsymbol{\delta} = (-|\delta|, -|\delta|)$. In the two other scenarii, the response to the press perturbation varies across species. The "divergence" scenario is defined with $\boldsymbol{\delta} = (|\delta|, -|\delta|)$, *i.e.* the carrying capacity of the abundant species increases and the other decreases. Conversely, the "convergence" scenario is defined with $\boldsymbol{\delta} = (-|\delta|, |\delta|)$, the carrying capacity of the more abundant species is decreased and the carrying capacity of the less abundant species is increased.

We applied the four perturbation scenarii to the community contexts using the moment closure approximation, by numerically solving Equation IV.S5. For each combination of perturbation scenario and community parameters, we recorded species means and variance-covariance matrices across time and computed the stationary expectations for the community variability components at each time step, which we then summarized using D_c, D_{pop}, D_{sae} and D_{cpe} (Equation IV.8).

Symbols used throughout the Methods section are summarized in Tab. IV.1. Stochastic differential equation systems were simulated in the Julia programming language using the `DifferentialEquations.jl` framework (Datseris 2018) and the SRIW1 algorithm (Rößler 2010) with a fixed time step of $\mathrm{d}t = 1/25$ and t from 0 to 1000 with press perturbations at $t_d = 200$. Ordinary differential equation systems were

solved using the `scipy` suite for the Python language, with an adaptive time step. Over all numerical simulations, parameter values were chosen in order to observe noticeable long-term trends after press perturbations while also ensuring (i) that replicate populations did not go extinct for stochastic simulations and (ii) that a stable fixed point of Equation IV.3 existed before and after the press perturbation for the chosen parameters. Results were visualised using the `ggplot2` package in the R programming language. The manuscript was written as a `Quarto` project.

Table IV.1: **List of symbols.** Non-bold symbols in parentheses are the one-dimensional counterparts of each bold symbol. They are used for the stochastic logistic growth of single populations while bold symbols are used for the generalized Lotka-Volterra system modelling community dynamics. In the column "Dimension", for functions, the left-hand side of the arrow is the dimension of the domain of the function and the right-hand side is the dimension of its destination set. Throughout the text, symbols with a hat $\widehat{\ }$ denote the stationary expectation for their measured quantity.

Symbol	Description	Dimension
S	Number of species	scalar
$\mathbf{X_t}$ (X_t)	Species abundances at time t	S (1)
$\boldsymbol{\mu_t}$ (μ_t)	Population means at time t	S (1)
$\boldsymbol{\Sigma_t}$ (V_t)	Variance-covariance matrix of abundance at time t (variance at time t)	$S \times S$ (1)
$\boldsymbol{r}$ (r)	Species growth rates	S (1)
$\boldsymbol{K}$ (K)	Species carrying capacities	S (1)
σ_e	Strength of environmental stochasticity	scalar
f	Deterministic dynamics term	$S \to S$
G	Stochastic dynamics term	$S \to S \times S$
CV_t	Coefficient of variation of population abundance at time t	scalar
D	Total deviation in population variability	scalar
$\mathsf{CV}_c(t)$	Coefficient of variation of community abundance at time t	scalar
D_c (D_{cmp})	Total deviation in community variability (in community variability component cmp)	scalar
t_d	Time point where the press perturbation is introduced	scalar
$\boldsymbol{\delta}$ (δ)	Relative strength of the press perturbation	S (1)

Results

Population model

During the transient regime after a press perturbation, population variability deviates from its stationary expectation (Fig. IV.1). This is noticeable over many samples from the stochastic logistic growth, and the moment closure approximation allows to reproduce this effect in a deterministic setting (Fig. IV.1B). With the parameters used to produce Fig. IV.1, this deviation is a deficit of variability, and the coefficient of variation reaches down to a value 10% lower than its value if the population was in a stationary regime.

Positive press perturbations, *i.e.* press perturbations that increase the carrying capacity, generate excesses of population variability during the positive transient trends in abundance (Fig. IV.2A, green lines). Conversely, negative press perturbations generate deficits of variability during the negative long-term trends (Fig. IV.2A, orange lines). Equation IV.3 allows to construct the phase space for mean and variance of population abundance after the press perturbation (supplemental Section IV.S2.1). The relative position of the stationary expectation for variance (dashed line on Fig. IV.2B) and of the variance

isocline (blue line on Fig. IV.2B) explain that an increase (resp. decrease) in mean comes with a stronger increase (resp. decrease) in variance, ultimately causing an excess (resp. a deficit) of coefficient of variation. Since variability thus does not depend only on the mean abundance but also on the press perturbation, observed variability (solid thin lines on Fig. IV.2B) deviates from its stationary expectation. In other words, during transient dynamics, population variability does not stay at its stationary expectation dictated by the mean abundance, but also depends on the sign and strength of the press perturbation that generated the transient dynamics. This results in a deviation from the stationary expectation for variability. Mathematical analysis justifies that the excess (resp. deficit) of population variance for positive (resp. negative) press perturbations is a general result that does not depend on parameter values (supplemental Section IV.S2.2).

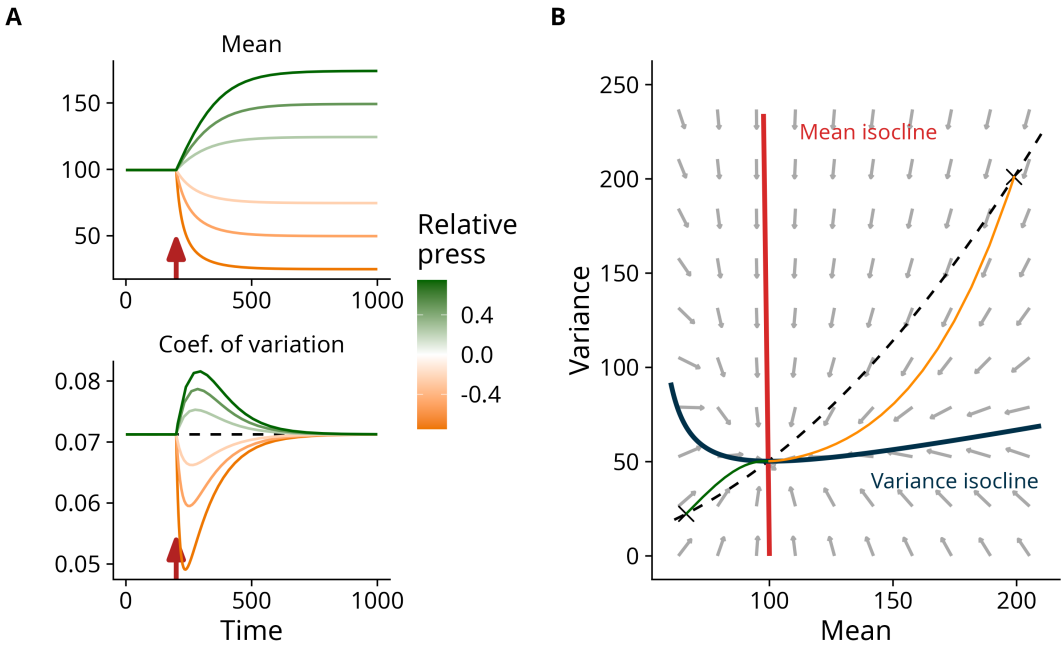

Figure IV.2: **Change in mean and coefficient of variation of population abundance with the sign of the press perturbation for the stochastic logistic growth.** (A) In the moment closure approximation, different press perturbations initiated from $K_0 = 100$ at $t_d = 200$ (red arrows) induce different responses of mean and coefficient of variation (colored lines). The dashed line shows the stationary expectation for variability. (B) Deterministic phase space for variance and mean for $K_d = 50$. The dashed line shows the stationary expectations for variance at each possible mean value. The two crosses are the initial conditions for the green and yellow lines (example trajectories respectively for a population increase and decrease). Grey arrows show the direction of the instantaneous dynamics for mean and for variance across the phase space. r and σ_e were both set to 0.01.

Integrating the deviation in population variability over the whole duration of the transient regime confirms that the magnitude of the deviation depends on the relative strength of the press perturbation and not on initial carrying capacity (Fig. IV.3A). Comparing absolute values, for a given strength of press perturbation,

deviations appear stronger for declines than for increases. Regardless of its sign, total deviation in variability is amplified by stronger environmental stochasticity and buffered by increasing population growth rate (Fig. IV.3B).

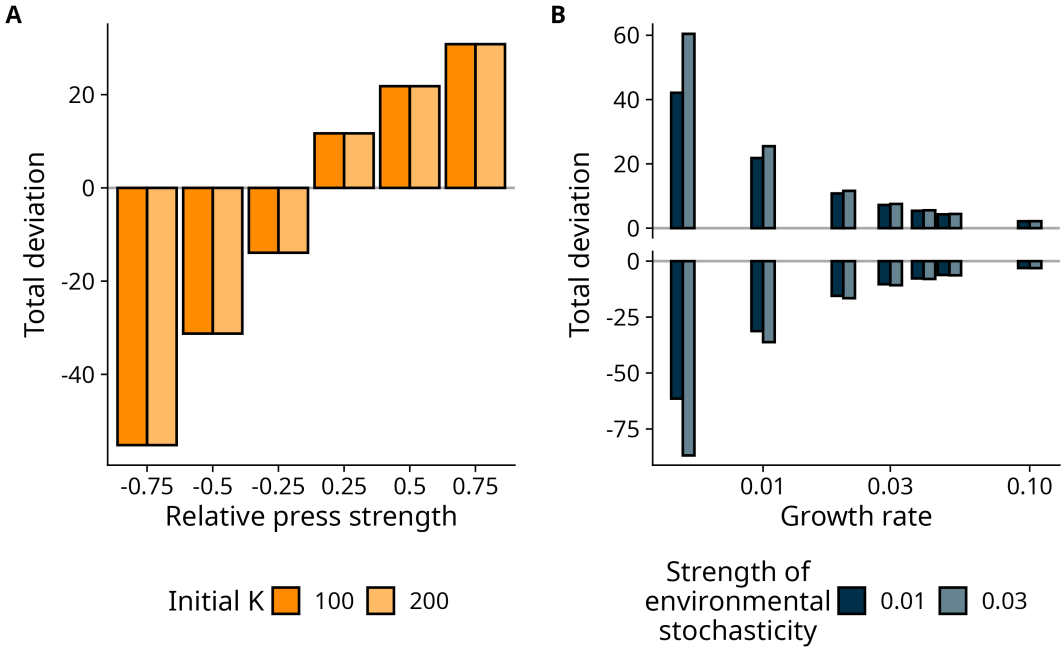

Figure IV.3: **Response of total deviation in population variability from its stationary expectation for the stochastic logistic growth.** (A) Total deviation is measured for different relative press strengths δ and initial carrying capacities K_0 and (B) for different values of the species growth rate r and environmental stochasticity strength σ_e. Panel (A) is generated with r and σ_e set as 0.01 and panel (B) is generated with K_0 as 100 and δ as 0.5 (top part) or -0.5 (bottom part). The horizontal axis of panel (B) is log-scaled.

Community model

The moment closure approximation for mean and variance combined with the decomposition of deviation in community variability allows to study community variability during the transient regime after a press perturbation (Fig. IV.4). In this example, a community of two species with uneven carrying capacities and moderate interspecific competition undergoes a press perturbation with the “divergence” scenario. At the population level, the rarer species has a strong negative deviation in population variability and the more abundant species has a less intense positive deviation in population variability (Fig. IV.4A). However, the deviation of the most abundant species dominates and community variability during the transient is higher than its stationary expectation.

This effect can be explained by the deviations in average population variability and statistical averaging effect (Fig. IV.4B). Because average population variability is weighted by relative abundances, the deficit of

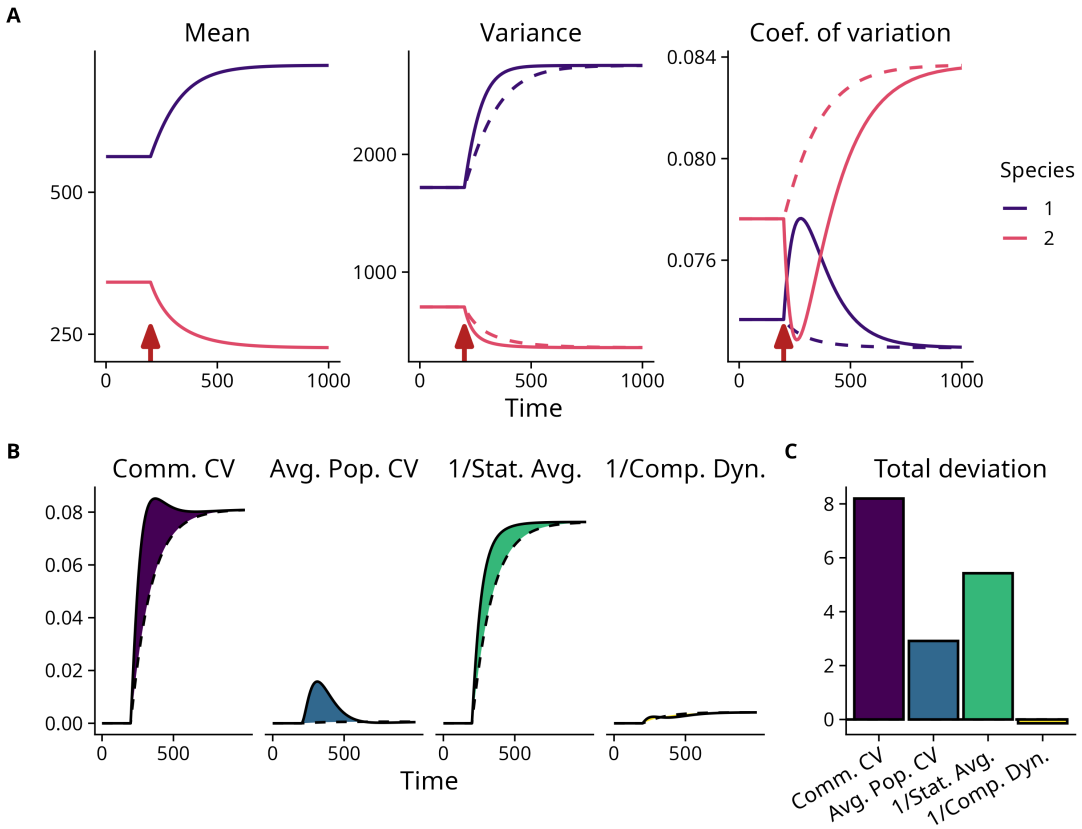

Figure IV.4: **Decomposing community variability during transient dynamics following a press perturbation.** (A) Moment closure approximation for means, variances and coefficients of variation for a community of two species undergoing a press perturbation at $t_d = 200$ (red arrows). Dashed lines indicate, for a given timepoint, the stationary expectations for variances or variabilities (see Methods). (B) Community variability components (solid lines) and their stationary expectations (dashed lines), computed from the moment closure approximation. Components are divided by their values before the press perturbation and logged in order to bring all components to the same vertical scale. Shaded areas denote the total deviations to the stationary expectations. (C) Integrals across time of each community variability component. For all panels, $\mathbf{K_0} = (600, 400)$; $r_1 = r_2 = 0.01$; $\boldsymbol{\delta} = (0.25, -0.25)$; $\sigma_e = 0.01$ and $\alpha = 0.1$. Stat. Avg.: statistical averaging effect. Comp. Dyn.: compensatory dynamics effect.

population variability of the decreasing rarer species does not fully compensate for the excess of variability of the increasing and abundant species. Moreover, the evenness of species variances decreases faster than it would if it followed stationary expectations (Fig. IV.4A, middle), yielding a deficit in statistical averaging effect (Zhao et al. 2022) which contributes positively to the deviation in community variability. The remaining component of community variability, the compensatory dynamics effect, is the component that reacts the least to the press perturbation, with a low negative value.

The interactions among the spread of the press perturbation within the community, the underlying community's abundance distributions and the growth rate distributions generate rich patterns, even for simple two-species communities. Scenarii where the two species share the same response to the press perturbation generate the strongest absolute deviations in community variability, for "increase" and for "decrease" (Fig. IV.5). In these settings, positive responses expectedly generate positive community variability deviations and negative responses generate negative community variability deviations. Since variance evenness does not change much during the transient dynamics, these deviations are mostly driven by deviations in average population variability. When the two species do not have the same growth rate, the population trend of the faster-growing, more abundant species happens slightly more quickly than that of the slower-growing, rarer species. This mismatch of the relative speeds of the species' transients generate subtle changes in the evenness of species mean abundances and slightly stronger changes in the evenness of species variances, causing small deviations in statistical averaging effect (Figures IV.S1 and IV.S2).

In the "convergence" and "divergence" scenarii, where responses to press are opposite between the two species, the deviations of community variability from the stationary expectation are weaker than in the other scenarii, regardless of their sign (Fig. IV.5). In contexts where the two species share the same growth rate (left half of Fig. IV.5), the community deviation is driven by the population trend of the most abundant species, via both the deviation in average population variability and the deviation in statistical averaging effect. In the "convergence" scenario, deviations in community variability components are negative but small in magnitude, because the deviations in average population variability and in statistical averaging effect change sign across time (Fig. IV.S3, top half). This is due to the community crossing the point at which the rarer species, because of the press perturbation, becomes the more abundant one.

Adding interspecific competition when the two species have the same growth rates, the deviation in

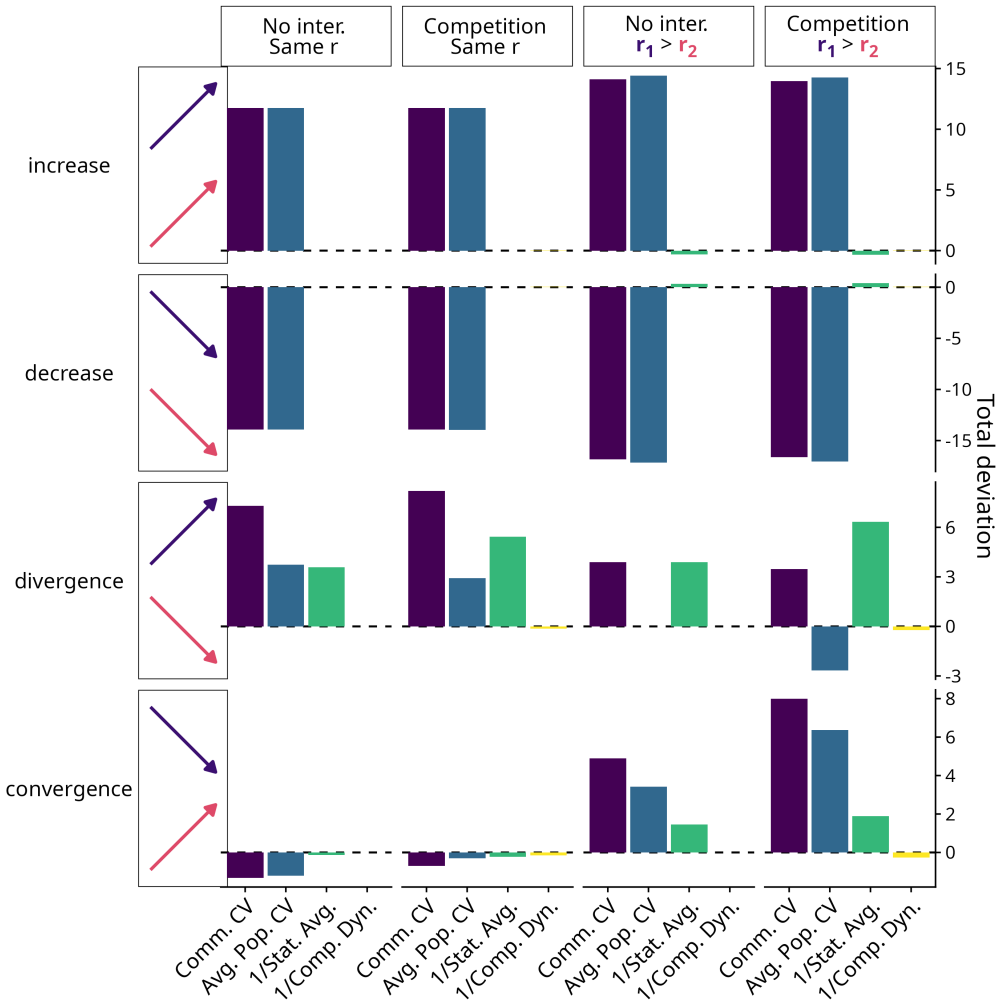

Figure IV.5: **Impact of press perturbations (rows) on community variability during transient dynamics for different community contexts (columns).** In each panel, total deviations from the stationary regime are reported for community variability and its components. Press perturbation scenarii are noted by colored arrows and represent different values of the relative perturbation vector $\boldsymbol{\delta}$, namely from to top bottom: $(0.25, 0.25)$, $(-0.25, -0.25)$, $(0.25, -0.25)$ and $(-0.25, 0.25)$. For community contexts, $\mathbf{K_0} = (600, 400)$ for all panels, with varying interspecific competition strength (No inter.: $\alpha = 0$; Competition: $\alpha = 0.1$) and varying relative species growth rates (Same r: $r_1 = r_2 = 0.01$; r1 > r2: $\mathbf{r} = (0.01, 0.0066)$). Stat. Avg.: statistical averaging effect. Comp. Dyn.: compensatory dynamics effect.

average population variability is decreased in the “divergence” scenario while the deviation in inverse statistical averaging is increased (left half of Fig. IV.5). Conversely, in the “convergence” scenario, adding interspecific competition increases the deviation of average population variability while the deviation in inverse statistical averaging stays similar. Inspecting the temporal change of each variability component (Figs. IV.S3-IV.S4) reveals that this arises because, with interspecific competition, in the later part of the transient dynamics the components take more time to reach their stationary values than without competition. When a component’s deviation keeps the same sign across the transient regime, its deviation is thus amplified (*e.g.* statistical averaging in Fig. IV.S3). Conversely, when a component’s deviation in the beginning of the transient is opposite to its deviation in the end of the transient regime, the deviation is amplified (resp. buffered) by interactions if the end (resp. the beginning) of the transient regime dominates the integral. See for example the contrast between inverse statistical averaging in the first and in the second columns of Fig. IV.S3 (amplification) as opposed to the contrast between average population variability in the first and in the second columns of Fig. IV.S4 (buffering). Small deviations in compensatory dynamics effect occur only in the presence of interspecific competition, and always contribute negatively to the deviation in community variability.

In the community contexts with different growth rates across species (right half of Fig. IV.5), the rarer, slower-growing species takes more time to reach its stationary mean than the more abundant, faster-growing species. This increases the contribution of the rarer species to the average population variability deviation, increasing total deviation in community variability in the “turnover” scenario but reducing it in the “divergence” scenario. Again, interspecific competition exacerbates the patterns in the end of the transient regimes. Contrastingly to all other cases, in the right half of the third row of Fig. IV.5, total deviations in average population variability and in inverse statistical averaging effect are both noticeable but have opposed signs. There, the positive deviation in inverse statistical averaging explains the positive deviation in community variability (see Fig. IV.S3).

Discussion

Our results reveal that the temporal variability of populations and communities subjected to a press perturbation as well as short-term environmental stochasticity deviates during transient dynamics from what could have been expected near equilibrium, under environmental stochasticity alone. Moreover,

the distribution of the responses to the press perturbation among species within communities alters how community variability deviates from its stationary expectation, depending on which of the abundant or rare species is the one that increases or decreases. While these results are well in line with the framework that variability reflects a system's inherent stability in a given perturbation context (Arnoldi et al. 2019), our results clearly illustrate how the response to press perturbations interacts with the response to environmental stochasticity. Especially, the dependence of population variability deviation to the direction of the long-term trend was not predicted by classical methods that linearize community dynamics around a fixed point. Since we show that long-term changes in mean abundance impact the variability around these changes, these two dimensions of ecological stability appear fundamentally related (Donohue et al. 2013).

Our findings at the scale of population variability resonate with increasing efforts to consider transient dynamics in population biology (Ezard et al. 2010). By estimating population projection matrix models for many wild species and comparing the corresponding stability metrics with the species' long-term growth, Gamelon et al. (2014) found that declining populations may be more efficient at buffering disturbances than increasing populations. This corroborates our findings in a different conceptual and methodological framework (Stott et al. 2011). An intuition for explaining this phenomenon lies in the asymmetry of the stability landscape of the logistic growth around the carrying capacity (Dennis et al. 2016). Above carrying capacity (and thus during a decline), the stability landscape is steeper, pulling the population to its equilibrium faster than if it was below carrying capacity. This was never detected in studies using the near-equilibrium assumption because linearization around the carrying capacity implies a symmetric stability landscape.

We predict that in communities where species share a common negative response to a press perturbation, such as microcosm warming experiments (Pennekamp et al. 2018), measured community variability could reflect lower values than expected near equilibrium. Our results show that such situations pose a risk of overestimating ecological stability for such communities, or underestimating the strength of environmental stochasticity.

Extending our approach to more complex communities is key in understanding when strong deviations in population and community variability can be expected. Just like the number of species generally dampens community variability via an increase in the diversity of responses to environmental fluctuations

(Loreau and de Mazancourt 2013, Polazzo et al. 2025, Danet et al. 2025), we expect that increasing the number of species will dampen the deviation of community variability to its stationary expectation via an increase in the diversity of responses to the press perturbation. Even in that case, quantifying deviations from stationary expectations would remain helpful to investigate the relationship between the number of species and the average population variability (Xu et al. 2021, Danet et al. 2025). Interspecific competition has been shown to affect community variability (Loreau and de Mazancourt 2008) and asymptotic response to press perturbations (Lajaaiti et al. 2025). Here we illustrate that competition also affects transient dynamics by slowing down the long-term trends in the end of the response to the press perturbation, altering community variability deviation. Extending our approach to different types of interactions and community structures could help uncover how long-term changes cascading through ecological networks could affect variability measurements (Duchenne et al. 2020, Danet et al. 2021).

Species long-term trends are associated to specific functional trait combinations that determine species responses to anthropogenic pressures (Henn et al. 2024). Notably, from metabolic scaling and evolutionary trade-offs, species that reproduce faster tend to exhibit higher population abundances while also having smaller body size (Brown et al. 2004). Moreover, large body size is linked to high extinction risk (Chichorro et al. 2019). The population abundance of large-bodied species is thus expected (i) to be lower on average, (ii) to be more variable because they have a lower growth rate and (iii) to be more likely to decline. Many natural communities are thus expected to follow the “divergence” scenario of our study, where community variability is always higher than expected near equilibrium (Fig. IV.5). For some taxa, other traits than body size may explain the response to pressures, such as insectivory in the case of wild birds (Bowler et al. 2019) or habitat specialization generally (Chichorro et al. 2019). Identifying the traits responsible for ecological stability is at the core of bridging advances in functional ecology with ecological stability theory (Lavorel and Garnier 2002, de Bello et al. 2021). By showing that deviations in community variability can arise from the co-occurence of traits associated to long-term trends and traits associated to variability, we support this framework across perturbation types.

Whether or not these deviations in population and community variability could actually be detected in biodiversity survey data and correctly attributed to long-term population changes is not easily predictable. Firstly, our predictions only consider press perturbations as abrupt changes in carrying capacity, while real-world perturbations applied to ecological systems also change in time (Díaz and Malhi 2022, Jaureguiberry

et al. 2022), and may affect not only to the carrying capacity but also the strength of environmental stochasticity itself (Seddon et al. 2016, Vázquez et al. 2017). Secondly, even for population variability, the deviations from stationary expectations that we observe have a small magnitude. Since measuring variability out of equilibrium is a challenge in itself (Clark et al. 2022), detecting changes in variability may be even more difficult, especially for systems under different stochasticity types (Engen et al. 1998, Arnoldi et al. 2019). In supporting analyses, we extend our methods to demographic and migration stochasticity, and we show that our results for environmental stochasticity also hold for demographic stochasticity (supplemental Section IV.S3, Fig. IV.S5).

Moment closure approximations in ecology have first been introduced in birth-death models, where the probability of demographic events is modelled explicitly (Nåsell 2003, Newman et al. 2004). They prove a valuable tool for studying stochastic systems, even if they remain approximations (see Marrec et al. 2023), which could be made more accurate by also modelling the temporal dynamics of the skewness rather than only the mean and variance (Nåsell 2003). In our methods, the moment closure approximation holds only when stochasticity strength and growth rate are not too high, which is an expected limitation. Simulation studies could help better quantifying the magnitude of the error associated to our approximation, but may hit the limitation that numerical methods for integrating stochastic differential equations also rely on approximations (e.g. Rößler 2010). Aside from generating useful insights for ecological variability, moment closure approximations also generate predictions for the means of ecological properties and could help further reveal how stochasticity shapes ecological systems, near or far from equilibrium (Shoemaker et al. 2020).

The importance of transient phenomena in ecology has been proposed for a long time (Hastings 2004), but their study has been restricted to a few particular settings such as systems with alternative stable states (Scheffer 2009, Hastings et al. 2018). We show that out-of-equilibrium dynamics can also matter for systems usually studied near equilibrium, and where transient dynamics are generated by abrupt changes in parameter values. Overall, our results reveal a mathematical relationship between two dimensions of ecological stability and call for further investigation of the impact of long-term population trends on population and community variability. Under multiple perturbation regimes at multiple time scales (Hastings 2016), the fact that community variability integrates intrinsic ecological properties with the strength of several perturbation types is an avenue towards building biodiversity indicators that

accurately reflect the intensity of anthropogenic perturbations across ecological and geographical scales.

Acknowledgements

We thank Jean-François Arnoldi for valuable advice on mathematical methods. This work was supported by Agence Nationale de la Recherche (ANR) under grant number ANR-23-CE02-0030.

Author Contribution Statement

JG, DG, CF and ET conceptualized the study. DG and JG conducted mathematical analyses. DG wrote Python code and JG wrote Julia code. DG and JG visualized the results. JG wrote the original draft and all authors contributed to review and editing.

Code Accessibility Statement

All code required to reproduce the results as well as simulated data are available on Zenodo (access link available on request) and in a GitHub repository (will be made public after acceptance).

IV.3 Supplementary Information for Chapter 2

IV.S1 Mean and variance of stochastic differential equations

In this appendix section, we detail how stochastic calculus theory is used to build deterministic approximation for the statistical moments of the solution of stochastic differential equations.

IV.S1.1 Previous mathematical results

Definitions. Let $\mathbf{X_t}$ a stochatic (Itô) process of dimension S. Let $p_X(\mathbf{X}, t)$ the probability density of $\mathbf{X_t}$ at time $t \in \mathbb{R}^+$. Let $X_{t,i}$ the i-th component of $\mathbf{X_t}$.

Let $\boldsymbol{\mu_t} = \mathbb{E}[\mathbf{X_t}]$ the expectation of $\mathbf{X_t}$ and let $\boldsymbol{\Sigma_t} = \mathbb{E}[(\mathbf{X_t} - \boldsymbol{\mu_t})(\mathbf{X_t} - \boldsymbol{\mu_t})^T]$ the S by S variance-covariance matrix of $\mathbf{X_t}$.

∇ is the vector differential operator, *i.e.* for ϕ a (differentiable) function of S variables $(x_1, \dots, x_S)$, $\nabla\phi = (\frac{\partial\phi}{\partial x_1}, \dots, \frac{\partial\phi}{\partial x_S})$.

We consider the stochastic differential equation (SDE) in Equation IV.1:

$$\mathrm{d}\mathbf{X_t} = f(\mathbf{X_t}, t)\mathrm{d}t + G(\mathbf{X_t}, t)\mathrm{d}\boldsymbol{W_t} \tag{IV.S1}$$

f is a twice differentiable vector-valued function, G is a matrix-valued function. $p_X(\mathbf{X}, t)$ satisfies the Fokker-Planck-Kolmogorov equation, which is a partial differential equation. While it is exact, it is not easily solvable even for simple functions f and G (Särkkä and Solin 2019). In the following, we present existing results that allow to build an approximation for the change in time of the statistical moments of $\mathbf{X_t}$.

Itô's lemma. Let $\phi(\mathbf{X_t}, t)$ any scalar function of the process $\mathbf{X_t}$. The Itô stochastic differential equation for ϕ is given by:

$$\mathrm{d}\phi = \frac{\partial\phi}{\partial t}\mathrm{d}t + (\nabla\phi)^T\mathrm{d}\mathbf{X_t} + \frac{1}{2}\,\mathrm{tr}[(\nabla\nabla^T\phi)\mathrm{d}\mathbf{X_t}\mathrm{d}\mathbf{X_t}^T] \tag{IV.S2}$$

This equation can then be expanded using Equation IV.S1 with the following rules for mixed differentials:

$\mathrm{d}\mathbf{W_t}\ \mathrm{d}t = \mathbf{0}\ ;\ \mathrm{d}t\ \mathrm{d}\mathbf{W_t} = \mathbf{0}\ ; \mathrm{d}\mathbf{W_t}\mathrm{d}\mathbf{W_t}^T = \mathrm{d}t.$

General formula. Applying Itô's lemma on Equation IV.S1 with $\phi(\mathbf{X_t}) = X_{t,i}$ (for elements of $\boldsymbol{\mu_t}$) and $\phi(\mathbf{X_t}) = X_{t,i}X_{t,j} - \mu_{t,i}\mu_{t,j}$ (for elements of $\boldsymbol{\Sigma_t}$) and taking the expectation yields (Särkkä and Solin 2019):

$$\begin{aligned}\frac{\mathrm{d}\boldsymbol{\mu_t}}{\mathrm{d}t} &= \mathbb{E}[f(\mathbf{X_t}, t)] \\ \frac{\mathrm{d}\boldsymbol{\Sigma_t}}{\mathrm{d}t} &= \mathbb{E}[f(\mathbf{X_t}, t)(\mathbf{X_t} - \boldsymbol{\mu_t})^T] + \mathbb{E}[(\mathbf{X_t} - \boldsymbol{\mu_t})f(\mathbf{X_t}, t)^T] + \mathbb{E}[G(\mathbf{X_t}, t)G(\mathbf{X_t}, t)^T]\end{aligned} \tag{IV.S3}$$

When f is non-linear, the first two terms of the time-derivative of $\boldsymbol{\Sigma_t}$ can depend not only on $\mathbb{E}[\mathbf{X_t}]$ and $\mathbb{E}[\mathbf{X_t}^2]$, but also on statistical moments of $\mathbf{X_t}$ of higher order than 2, which time-derivatives then depend on even higher order moments, and so on.

Moment closure approximation. To close this relationship, we use a first-order linearization of f around $\boldsymbol{\mu_t}$ in the expression for the time-derivative of $\boldsymbol{\Sigma_t}$ (Särkkä and Solin 2019). $f(\mathbf{X_t}, t)$ is approximated by $f(\boldsymbol{\mu_t}, t) + \mathbf{F}(\boldsymbol{\mu_t}, t)(\mathbf{X_t} - \boldsymbol{\mu_t})$ if $\mathbf{F}(\boldsymbol{\mu_t}, t)$ is the Jacobian matrix of $f(., t)$ evaluated in $\boldsymbol{\mu_t}$, and Equation IV.S3 thus yields:

$$\begin{aligned}\frac{\mathrm{d}\boldsymbol{\mu_t}}{\mathrm{d}t} &= \mathbb{E}[f(\mathbf{X_t}, t)] \\ \frac{\mathrm{d}\boldsymbol{\Sigma_t}}{\mathrm{d}t} &\approx \mathbb{E}[\mathbf{F}(\boldsymbol{\mu_t}, t)(\mathbf{X_t} - \boldsymbol{\mu_t})(\mathbf{X_t} - \boldsymbol{\mu_t})^T] + \mathbb{E}[(\mathbf{X_t} - \boldsymbol{\mu_t})(\mathbf{F}(\boldsymbol{\mu_t}, t)(\mathbf{X_t} - \boldsymbol{\mu_t}))^T] + \\ &\quad \mathbb{E}[G(\mathbf{X_t}, t)G(\mathbf{X_t}, t)^T] \\ &= \mathbf{F}(\boldsymbol{\mu_t}, t)\boldsymbol{\Sigma_t} + \boldsymbol{\Sigma_t}\mathbf{F}(\boldsymbol{\mu_t}, t)^T + \mathbb{E}[G(\mathbf{X_t}, t)G(\mathbf{X_t}, t)^T]\end{aligned} \tag{IV.S4}$$

Note that this first-order approximation relies on the assumption that $\mathbf{X_t}$ stays relatively close to $\boldsymbol{\mu_t}$. In our study cases, since G never includes powers of $\mathbf{X_t}$ higher than 1, expressions of $\mathbb{E}[G(\mathbf{X_t}, t)G(\mathbf{X_t}, t)^T]$ never require high order moments of $\mathbf{X_t}$ and therefore we can keep their exact expression even in the approximated system.

Stationary regime. $\mathbf{X_t}$ reaches a stationary regime when its probability distribution is constant in time. In the moment closure approximation, the fixed points $(\boldsymbol{\mu}^*, \boldsymbol{\Sigma}^*)$ of system IV.S4, *i.e.* the values for means and variance-covariance matrix elements for which $\frac{\mathrm{d}\boldsymbol{\mu_t}}{\mathrm{d}t} = \frac{\mathrm{d}\boldsymbol{\Sigma_t}}{\mathrm{d}t} = 0$, are approximations to the statistical moments of the stationary distribution of $\mathbf{X_t}$ (Särkkä and Solin 2019).

IV.S1.2 Applications to ecological modelling

Stochastic logistic growth. X_t is a scalar representing the population abundance of a single species, $f(X_t, t) = f(X_t) = rX_t(1-\frac{X_t}{K})$, and $\boldsymbol{\mu_t}$, $\boldsymbol{\Sigma_t}$ and $G(X_t, t)$ are scalars written μ_t, V_t and $g(X_t)$, respectively. Under environmental stochasticity, $g(X_t) = \sigma_e X_t$ (Arnoldi et al. 2019) and μ_t and V_t thus satisfy Equation IV.3. See Section IV.S3 for different types of stochasticity.

Generalized Lotka-Volterra system. With f set according to the generalized Lotka-Volterra model with interaction matrix $\mathbf{A}$ (Equation IV.5) and under environmental stochasticity for G, Equation IV.S4 becomes:

$$\begin{aligned}\frac{\mathrm{d}\boldsymbol{\mu_t}}{\mathrm{d}t} &= \mathrm{diag}(\boldsymbol{\mu_t})(\mathbf{r} + \mathbf{A}\boldsymbol{\mu_t}) + \mathrm{diag}(\boldsymbol{A\Sigma_t}) \\ \frac{\mathrm{d}\boldsymbol{\Sigma_t}}{\mathrm{d}t} &= \mathbf{F}(\boldsymbol{\mu_t})\boldsymbol{\Sigma_t} + \boldsymbol{\Sigma_t}\mathbf{F}(\boldsymbol{\mu_t})^T + \sigma_e^2\,\mathrm{diag}[\mathrm{diag}(\boldsymbol{\mu_t})\boldsymbol{\mu_t} + \mathrm{diag}(\boldsymbol{\Sigma_t})]\end{aligned} \tag{IV.S5}$$

Here, when $\mathbf{v}$ is a vector, we note $\mathrm{diag}(\mathbf{v})$ the matrix whose diagonal elements are the elements of $\mathbf{v}$ and when $\mathbf{M}$ is a matrix, $\mathrm{diag}(\mathbf{M})$ is the vector whose elements are the elements of the principal diagonal of $\mathbf{M}$. Thus $\mathrm{diag}(\mathrm{diag}(\mathbf{v})) = \mathbf{v}$ but $\mathrm{diag}(\mathrm{diag}(\mathbf{M}))$ replaces all off-diagonal terms of $\mathbf{M}$ by zero.

$\mathbf{F}(\boldsymbol{\mu_t})$ is the Jacobian matrix of f evaluated at $\boldsymbol{\mu_t}$. Setting all diagonal elements of $\mathbf{A}$ to -1 (see Methods), $F_{ii}(\boldsymbol{\mu}) = r_i(1 - 2\frac{\mu_i}{K_i})$ and $F_{ij}(\boldsymbol{\mu}) = A_{ij}r_i\frac{\mu_i}{K_i}$.

From numerical solutions of Equation IV.S5, mean community abundance μ_c and expected community variance V_c can each be computed for any time point as the sum of all elements of $\boldsymbol{\mu_t}$ and of $\boldsymbol{\Sigma_t}$, respectively.

IV.S2 Supplemental analyses

IV.S2.1 Analytical results for the stochastic logistic growth

Stationary regime. Setting $\frac{\mathrm{d}\mu_t}{\mathrm{d}t} = \frac{\mathrm{d}V_t}{\mathrm{d}t} = 0$ in Equation IV.3 and solving for (μ^*, V^*) yields three possible fixed points. The first is the trivial fixed point $(\mu^*, V^*) = (0, 0)$.

If $\mu^* \neq 0$ and $V^* \neq 0$, we get:

$$\begin{cases} V^* = \mu^*(K - \mu^*) \\ 0 = 2\mu^{*2} - 3K\mu^* + K^2(1 + \frac{\sigma_e^2}{2r}) \end{cases} \tag{IV.S6}$$

Therefore μ^* has two candidate values, $\mu^* = \frac{3}{4}K \pm \frac{1}{4}K\sqrt{1 - 8\frac{\sigma_e^2}{2r}}$. Nåsell (2003) show that the smallest of these values can be ruled out as spurious (i.e. it is not a possible stationary mean for the stochastic process), which leaves the fixed point where μ^* is close to but still smaller than K. When σ_e^2 is too high, the system approaches a saddle-node bifurcation where the fixed points vanish.

Isoclines equations. From above, the isocline for the mean satisfies $\frac{\mathrm{d}\mu_t}{\mathrm{d}t} = 0 \iff V = \mu(K - \mu)$ (red thick line on Fig. IV.2B).

For the variance isocline (blue thick line on Fig. IV.2B),

$$\begin{aligned} \frac{\mathrm{d}V_t}{\mathrm{d}t} = 0 &\iff V(2r(2\frac{\mu}{K} - 1) - \sigma_e^2) = \sigma_e^2\mu^2 \\ &\iff V = \mu^2 \frac{\sigma_e^2}{2r(2\frac{\mu}{K} - 1) - \sigma_e^2} \end{aligned} \tag{IV.S7}$$

If $\mu = \mu^*$, this formulation for V^* makes it easier to see that $V^* \approx \mu^{*2}\frac{\sigma_e^2}{2r - \sigma_e^2}$ than by substituting the analytical expression for μ^* in Equation IV.S6.

IV.S2.2 Comparison between the stationary regime and the isocline for variance

Here we show that the relative positions of the stationary expectation for variance (dashed line) and of the variance isocline (blue line) always matches Fig. IV.2.

We consider a trajectory $\{(\mu_t, V_t)\}_{t>t_d}$ where the mean and variance of the stochastic logistic growth converge towards their stationary regime (μ^*, V^*).

For any mean value μ_t, the stationary expectation for variance, $\hat{V}(\mu_t)$, is the variance that the system would have if it was in a stationary regime at mean μ_t. It is obtained by setting $\frac{\mathrm{d}V_t}{\mathrm{d}t} = \frac{\mathrm{d}\mu_t}{\mathrm{d}t} = 0$ in Equation IV.3 and solving it for $(\hat{K}(\mu_t), \hat{V}(\mu_t))$, with $\hat{K}(\mu_t)$ the carrying capacity required to observe a stationary regime at mean μ_t.

Using the result of Section IV.S2.1, we can also define $V_{iso}(\mu_t)$, the nullcline for variance, *i.e.* the value of V_t for which $\frac{\mathrm{d}V_t}{\mathrm{d}t} = 0$. Graphical analysis shows that $\frac{\mathrm{d}V_t}{\mathrm{d}t} > 0$ when $V_t > V_{iso}(\mu_t)$. Notice that, by definition, $\hat{V}(\mu^*) = V_{iso}(\mu^*)$.

We need to prove that, when the mean is above (resp. below) its stationary value, the variance isocline is below (resp. above) the stationary expectation. We detail the proof for a negative long-term trend, *i.e* we show that $\mu_t > \mu^* \implies V_{iso}(\mu_t) < \hat{V}(\mu_t)$.

Let α such that $\mu^* = K\alpha$. According to the solution of Equation IV.S6, $\alpha = 3/4 + 1/4\sqrt{1 - \frac{4\sigma^2}{r}}$ and thus $3/4 < \alpha < 1$. Also note that according to the same system, $\mu_t = \hat{K}(\mu_t)\alpha$.

Thus $\mu_t > \mu^* \implies \hat{K}(\mu_t)\alpha > K\alpha \implies \hat{K}(\mu_t) > K$.

From Equation IV.S7, $\hat{V}(\mu_t)(2r\ (2\frac{\mu_t}{\hat{K}(\mu_t)} - 1) - \sigma_e^2) = \sigma_e^2\mu_t^2 = V_{iso}(\mu_t)(2r(2\frac{\mu_t}{K} - 1) - \sigma_e^2)$. If $\hat{K}(\mu_t) > K$ then, since all coefficients are strictly positive, $V_{iso}(\mu_t) < \hat{V}(\mu_t)$.

IV.S2.3 Supplemental figures

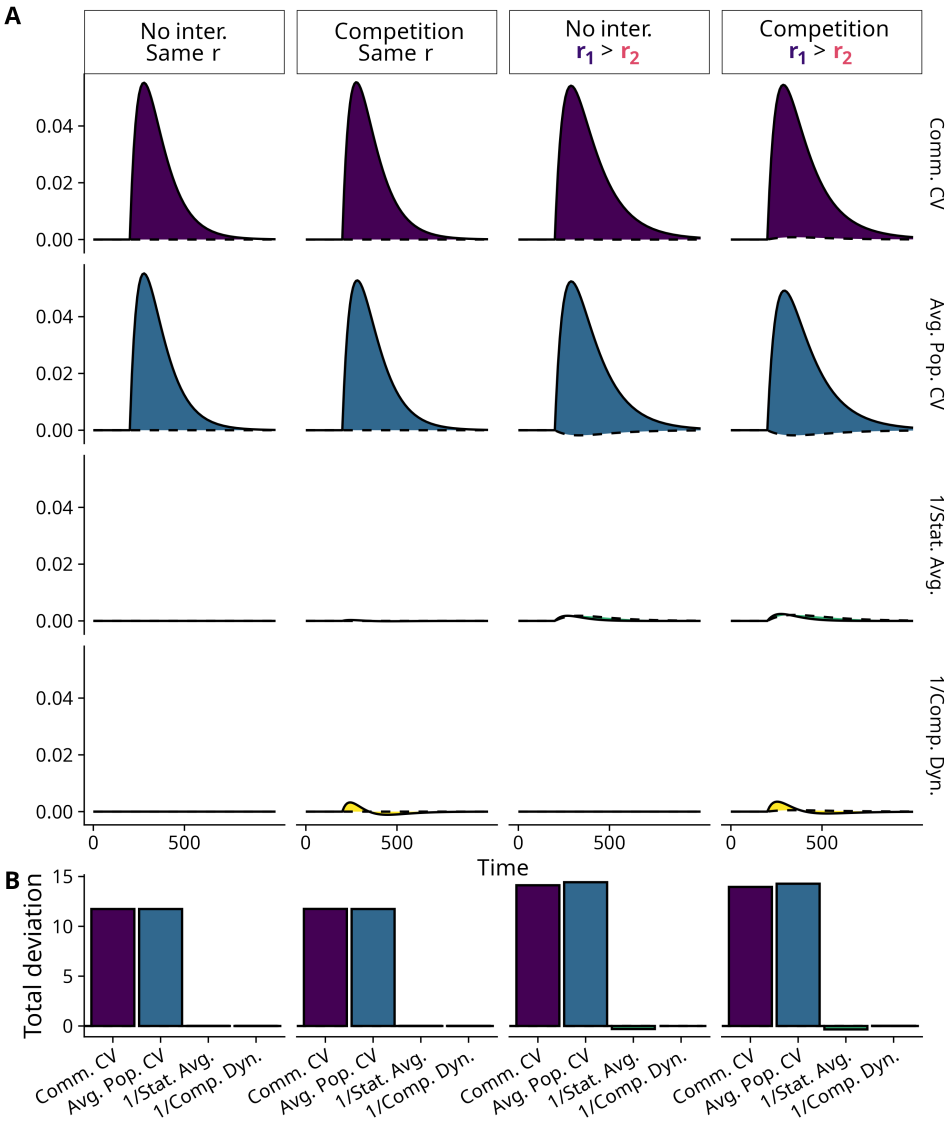

Figure IV.S1: **Detail on the impact of the "increase" press perturbation in different community contexts.** Time series and total deviations correspond to the first row of Figure 5. In the "increase" scenario, both species increase under the press perturbation, *i.e.* $\boldsymbol{\delta} = (0.25, 0.25)$. Community contexts (different columns) correspond to the different columns in Figure 5.

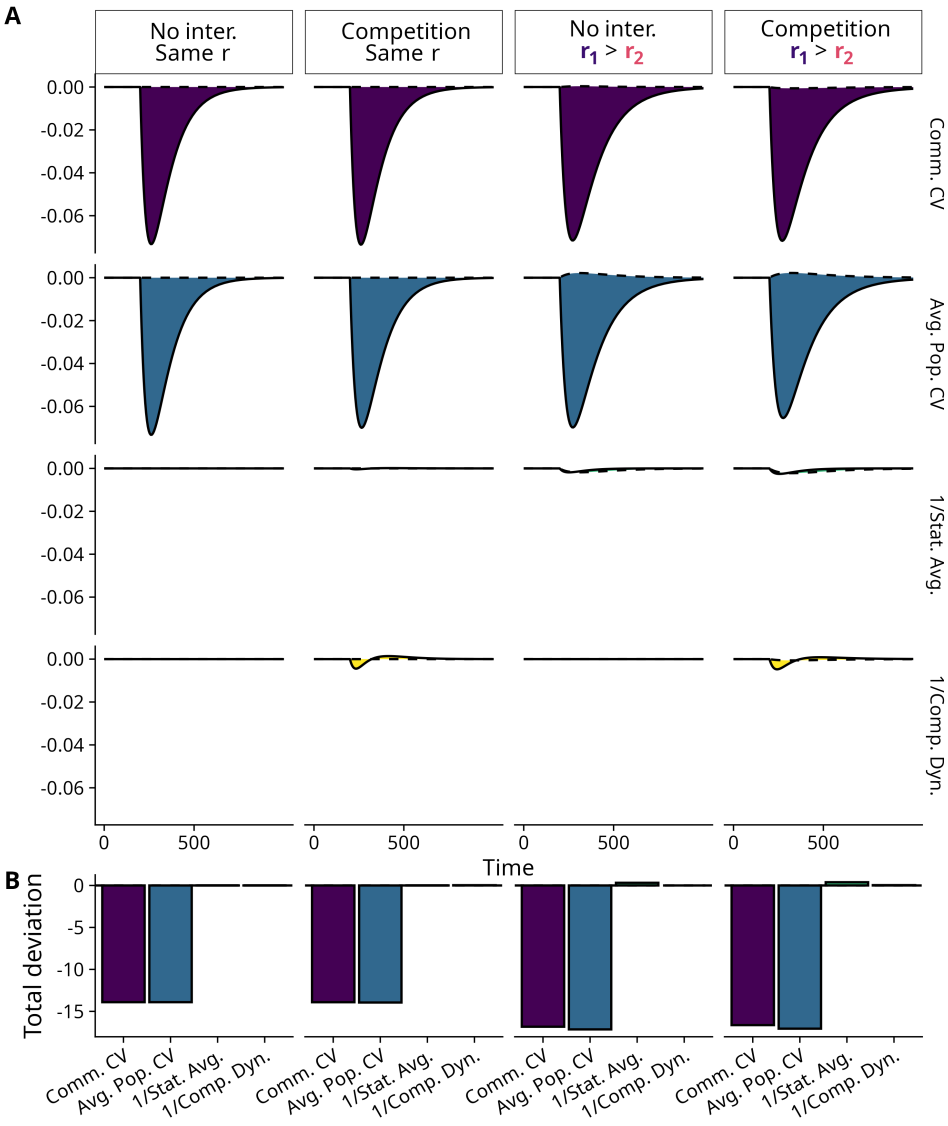

Figure IV.S2: **Detail on the impact of the "decrease" press perturbation in different community contexts.** Time series and total deviations correspond to the second row of Figure 5. In the "decrease" scenario, both species decline under the press perturbation, *i.e.* $\boldsymbol{\delta} = (-0.25, -0.25)$. Community contexts (different columns) correspond to the different columns in Figure 5.

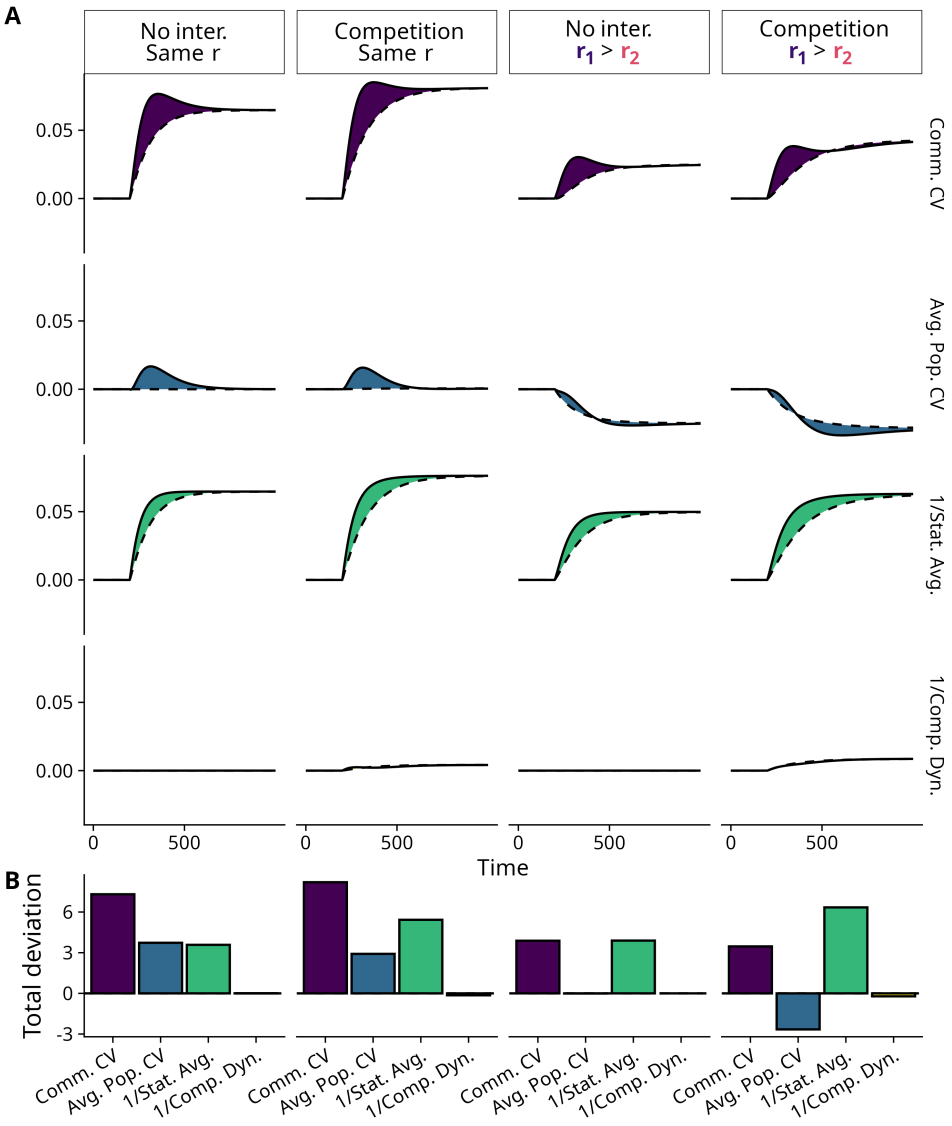

Figure IV.S3: **Detail on the impact of the "divergence" press perturbation in different community contexts.** Time series and total deviations correspond to the third row of Figure 5. In the "divergence" scenario, the most abundant species increases and the rarer species declines, *i.e.* $\boldsymbol{\delta} = (0.25, -0.25)$. Community contexts (different columns) correspond to the different columns in Figure 5.

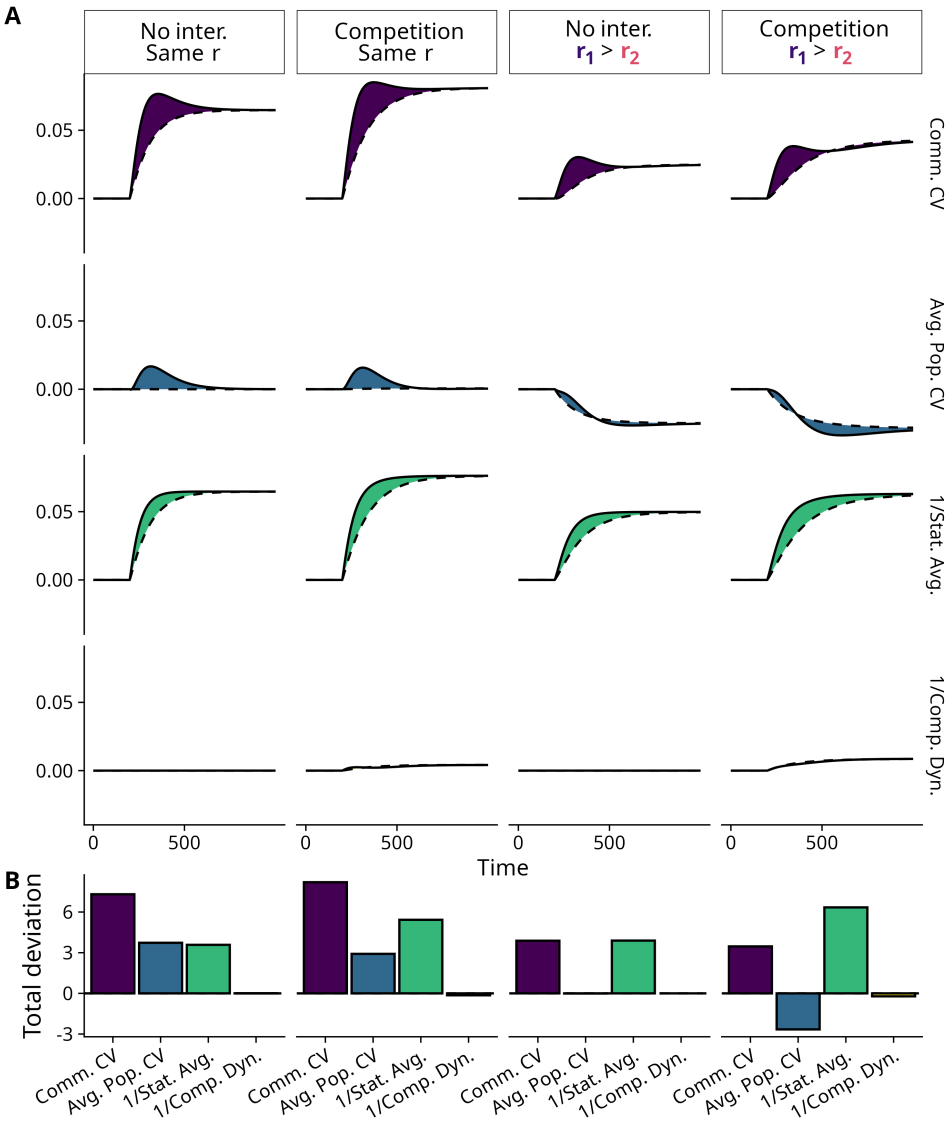

Figure IV.S4: **Detail on the impact of the "convergence" press perturbation in different community contexts.** Time series and total deviations correspond to the last row of Figure 5. In the "convergence" scenario, the most abundant species declines and the rarer species increases, *i.e.* $\delta = (-0.25, 0.25)$. Community contexts (different columns) correspond to the different columns in Figure 5.

IV.S3 Extensions to different stochasticity types

Following Arnoldi et al. (2019), Equation IV.1 can translate several types of stochasticity by introducing a parameter γ, the stochasticity type, in order to change the scaling of the diffusion function with population abundance. Namely, for independent species-level perturbations, $G_\gamma(\mathbf{X_t}, t)_i = \sigma_\gamma X_i(t)^\gamma$. For environmental stochasticity, $\gamma = 1$ (see Methods). Setting $\gamma = \frac{1}{2}$ corresponds to demographic stochasticity and $\gamma = 0$ to stochasticity due to immigration and emigration (Arnoldi et al. 2019).

IV.S3.1 Relationship between stationary mean and variance

For a single population, Equation IV.S4 yields:

$$\begin{aligned} \frac{\mathrm{d}\mu_t}{\mathrm{d}t} &= r\mu_t\left(1-\frac{\mu_t}{K}\right) - \frac{r}{K}V_t \\ \frac{\mathrm{d}V_t}{\mathrm{d}t} &= 2rV_t(1-2\frac{\mu_t}{K}) + \sigma_\gamma^2\mathbb{E}[X_t^{2\gamma}] \end{aligned} \tag{IV.S8}$$

For $\gamma = 1/2$, and solving Equation IV.S8 for the stationary regime yields $\mathbb{E}[X_t^{2\gamma}] = \mu_t$ and $V^* \approx \mu^* \frac{\sigma_d^2}{2r}$. For $\gamma = 0$, $\mathbb{E}[X_t^{2\gamma}] = 1$ and $V^* \approx \frac{\sigma_m^2}{2r}$.

Standardizing population variance by population mean thus must take a different shape depending on the type of stochasticity, for which we propose a coefficient of variation that depends on γ:

$$\mathrm{CV}_\gamma = \frac{\sqrt{V}}{\mu^\gamma} \tag{IV.S9}$$

Note that, under environmental stochasticity, CV_γ is the classical coefficient of variation used in the main manuscript.

IV.S3.2 Decomposing the generalized coefficient of variation

In the framework of Thibaut and Connolly (2013), the (classical) coefficient of variation of community abundance can be decomposed as the product of the average population coefficient of variation with the population synchrony index of Loreau and de Mazancourt (2008), ϕ. In the following, we derive the same decomposition for any positive value of γ.

Now with V_c the variance of the abundance a community composed of S species under stochasticity type

γ, with $\mu_c = \sum_{i=1}^{S} \mu_i$ the average of community abundance. V_i denotes the variance of the abundance of species i. Loreau and de Mazancourt (2008) define the species synchrony ϕ as:

$$V_c = \phi(\sum_{i=1}^{S} \sqrt{V_i})^2 \tag{IV.S10}$$

Taking the square root of Equation IV.S10 and dividing by μ_C^{γ}, the generalized coefficient of variation of the community's abundance is:

$$\mathrm{CV}_{\gamma,c} = \sqrt{\phi} \sum_i \frac{\sqrt{V_i}}{\mu_C^{\gamma}}$$

Following Thibaut and Connolly (2013), multiplying the fraction inside the sum by $\mu_i^{\gamma}/\mu_i^{\gamma}$ yields:

$$\mathrm{CV}_{\gamma,c} = \sqrt{\phi} \sum_i \left(\frac{\mu_i}{\mu_c}\right)^{\gamma} \frac{\sqrt{V_i}}{\mu_i^{\gamma}}$$

Writing p_i the relative (average) abundance of species i in the community, i.e. $p_i = \frac{\mu_i}{\mu_c}$, we get:

$$\mathrm{CV}_{\gamma,c} = \sqrt{\phi} \sum_i p_i^{\gamma} \mathrm{CV}_{\gamma,i} \tag{IV.S11}$$

The average population variability from Thibaut and Connolly (2013) thus has different weights depending on stochasticity type. Note that under environmental stochasticity, $\gamma = 1$ and Equation IV.S11 is the result of Thibaut and Connolly (2013).

Statistical averaging effect and compensatory dynamics effects from Zhao et al. (2022) (see Methods) depend only on population and community variances, not on means, and can thus be used regardless of the stochasticity type.

IV.S3.3 Long-term trends under different stochasticity types

Because of the varying importance of p_i for the average population coefficient of variation, rare species increasingly drive the (generalized) community coefficient of variation as stochasticity type goes from environmental, to demographic, to migration. The population-level coefficients of variation of rare species

are indeed decreasingly weighted by their low relative abundance, increasing their contribution.

In order to illustrate this, for the most simple community context of Fig. IV.5, we vary the stochasticity type (and the formulae for community variability components) for each of the four press perturbation scenarii (Fig. IV.S5). For example, in the “divergence” scenario under migration stochasticity, the population variability deficit of the decreasing rare species completely compensates the population variability excess of the increasing abundant species. This is less the case for demographic stochasticity, and even less for environmental stochasticity (Fig. IV.S5). The increase and decrease scenarii are not affected by stochasticity type.

This result is already known near equilibrium (Arnoldi et al. 2019), but must be taken into consideration before applying our framework to real biodiversity data: the main stochasticity type can yield different dependences of community variability to the way long-term trends are spread between the distributions of species abundances and growth rates.

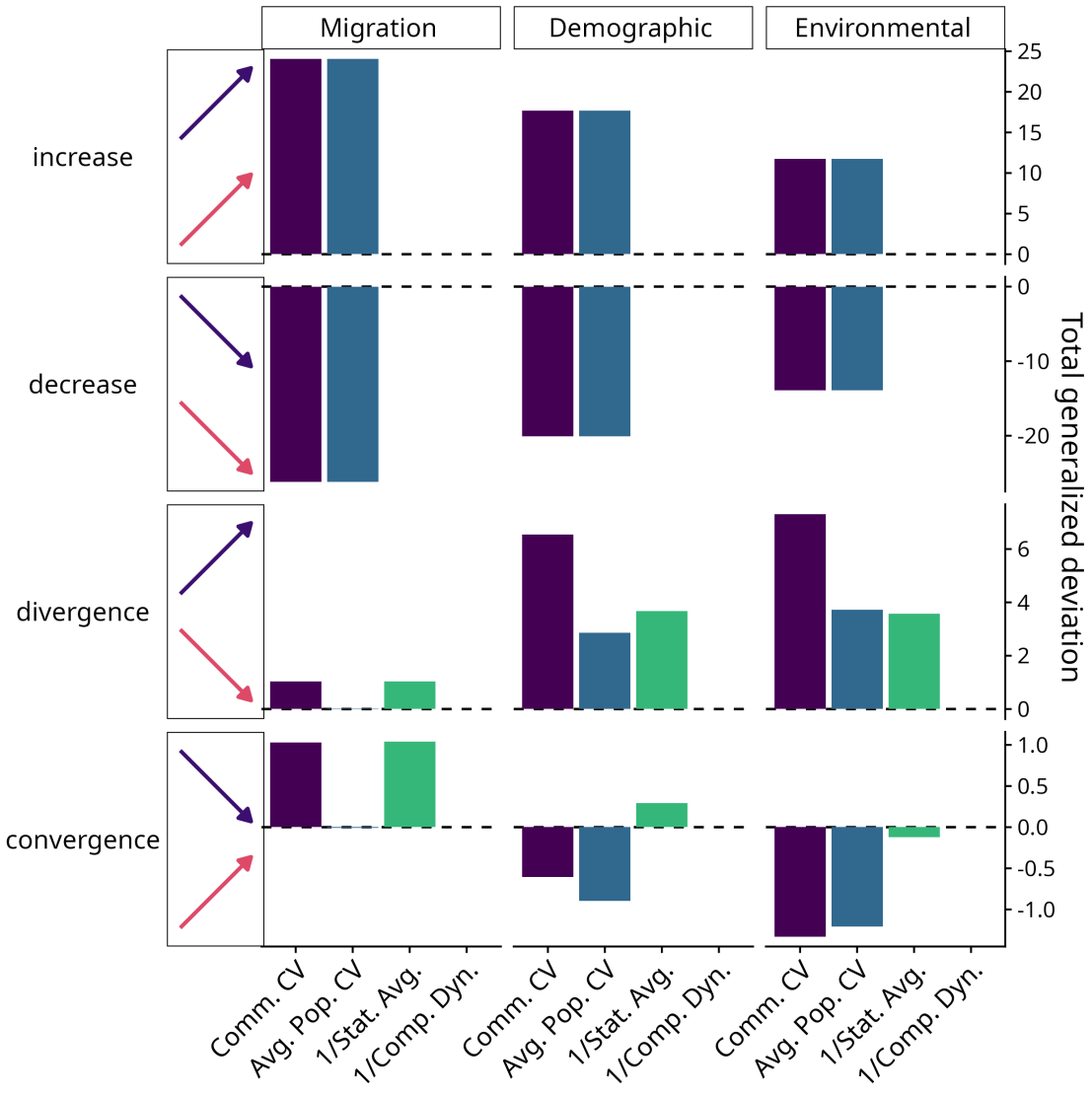

Figure IV.S5: **Impact of stochasticity type on total deviation from stationary expectation.** The most simple community context is shown, with $\mathbf{K_0} = (600, 400)$; $r_1 = r_2 = 0.01$ and $\alpha = 0$. σ_γ is set to 0.01 for all stochasticity types. Average population coefficient of variation is computed according to Equation IV.S11.

V . Chapter 3: Temporal changes in integrative stability dimensions

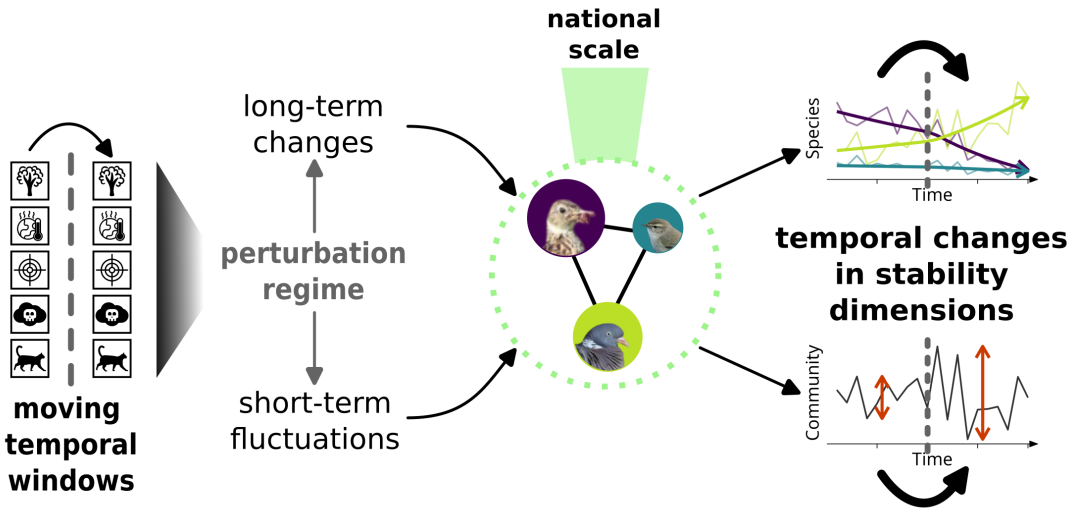

Figure V.0: **Chapter 3 in the general framework.** Over time, anthropogenic pressures may change, altering the perturbation regime that bird communities are subjected to. We measure changes across moving windows in trends and variability (thicker arrows) at species and community levels in the French Breeding Bird Survey data. Anthropogenic pressure icons modified from Bellard et al. (2022). Bird pictures by F. Jiguet and S. Wroza.

V.1 Context and aim of the study

In Chapters 1 and 2, we compared communities from different local land use contexts or under different simulated perturbations, which has classically been more associated to the study of temporal variability. In this Chapter, we measure the temporal changes of bird long-term population trends and bird temporal variability across 10-year moving windows at the national scale in France, a scale which has mostly been associated to the study of long-term population trends.

A requirement for that was to see how the classical framework for decomposing community variability into species synchrony and average population variability (Thibaut and Connolly 2013) could be translated to parameters estimated from statistical models usually built for the estimation of national-scale long-term population trends. In this updated framework, changes in species population trends are more pronounced than changes in population variability, but the impact of long-term trends on community composition coincides with changes in community variability. While the role of candidate response traits remains elusive, this Chapter opens new perspectives for assessing changes in perturbation regimes or ecological stability at large geographical scales.

Work in progress

Some additional work is still envisioned before submitting this last chapter to a journal, namely:

- Investigating different multi-trait indices of sensitivity to long-term changes and to environmental fluctuations. The traits we considered for now, ecological specialization and slow-fast pace of life, do not explain individual species' responses in a satisfactory manner.
- Evaluating the relative contributions of land use change and climate change to detected patterns by accounting for these drivers' effects on local bird abundance across species
- More sensitivity analyses to check that observed patterns do not come from the spurious influence of individual species' or spatial subsets of the dataset.

V.2 Article: “Temporal changes of trends and variability of bird communities over 25 years in France”

Abstract

As two integrative dimensions of ecological stability, bird long-term population trends and community variability are the ecological response to the multi-faceted perturbation regimes faced by bird communities. Over the 25 years covered by bird community time series data of the French Breeding Bird Survey, temporal changes in trends or variability can thus reflect changes in perturbations at different time scales and changes in ecological stability, but are not often documented. We measure trends and variability for species abundances and for total community abundance across moving 10-year temporal windows over continental France. Community-level variability components reflect changes in community composition better than community-level trend components, but temporal changes in species trends are more frequent than changes in species variability. Species estimated abundance is associated to lower variability while the slow-fast life history continuum and ecological specialization fail to capture residual variation in trends or variability. This work hints at complex scale interplays in the drivers of community-level variability and trends, calling for better integration of stability-based frameworks in the investigation of bird temporal dynamics across perturbation scales.

Keywords: community variability, population trends, slow-fast continuum, bird monitoring

Introduction

As anthropogenic pressures threaten bird communities worldwide, understanding bird temporal dynamics is key in assessing the maintenance of ecosystem functioning (Şekercioğlu et al. 2004, Cardinale et al. 2012), and can reveal threats to species conservation (Buckland et al. 2005). In the face of multi-faceted perturbation regimes (Donohue et al. 2016, Van Meerbeek et al. 2021), bird communities respond to long-term environmental changes and environmental stochasticity by long-term changes in population abundances and temporal variability of population and community abundance, two integrative dimensions of bird community stability (Fig. V.1A). However, the temporal dynamics of environmental parameters are not constant through time. For example, under climate change, average temperature is rising, but extreme weather events are also more likely to occur (Garcia et al. 2014). Investigating how the temporal dynamics of bird abundance change over time across perturbation regimes is thus needed for painting a comprehensive picture of bird response to changing perturbation regimes.

Since perturbation regimes as well as the ability for ecological systems to respond to perturbations can both change with time, changes in bird integrative stability dimensions are expected. Compared to baseline conditions, a change in community variability or community trend can occur (i) because the perturbation regime has changed, (ii) because population or community stability has changed or likely (iii) both (Fig. V.1). However, this has been rarely studied. Bird population trends are most often assessed for the longest possible time frame and temporal changes in bird community variability are not well known as many empirical studies rely on space-for-time substitution (*e.g.* Blüthgen et al. 2016). Temporal changes in trends are investigated by assessing signs of non-linearity in average population trajectories (Boennec et al. 2024) or by measuring log-linear trends over different periods (Reif et al. 2024, Vimont et al. 2025). They reveal that many bird populations have trajectories that cannot be summarized as a log-linear trend only, with for example more than a quarter of bird species showing signs of non-linearity in a global population database (Clark and Luis 2020). For variability, an existing attempt notices that long-term changes in the functional composition of bird communities coincides with an increase in community variability in the North American Breeding Bird Survey (Li et al. 2021). Conjointly measuring changes in variability and in trends may thus both further document the complexity of natural population and community dynamics and pave the way for understanding the underlying mechanisms.

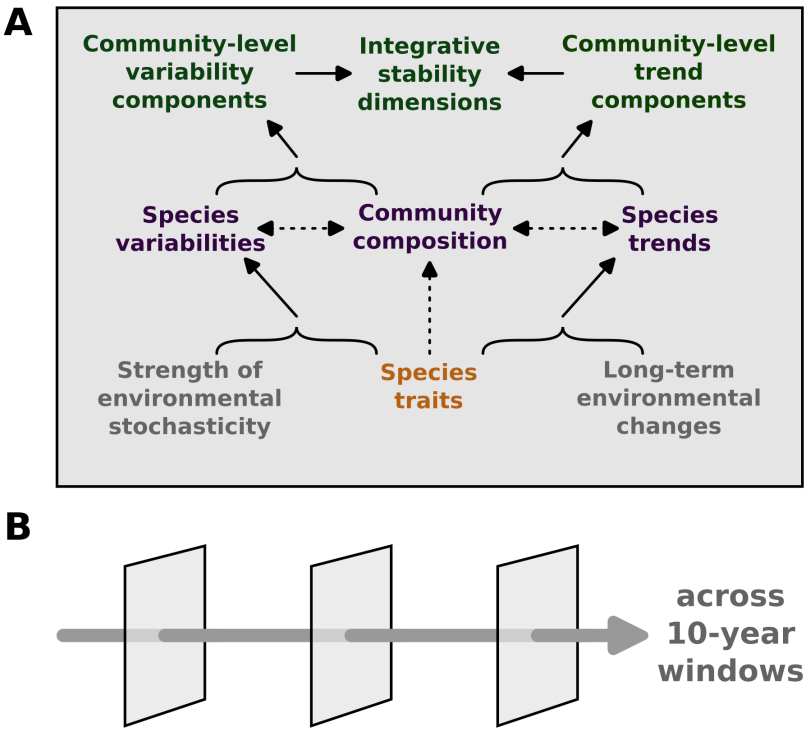

Figure V.1: **A conceptual framework for measuring changes in integrative stability dimensions.** (A) Summary of definitions (solid arrows) and likely relationships (dashed arrows). All named categories may entail several components. Different colors denote different organizational levels: assessing green categories requires information on community temporal dynamics, purple categories on species temporal dynamics and abundances, gray on the environmental variables that species respond to, and orange on species traits. (B) In this paper, we measure community stability dimensions and their underlying components across moving temporal windows.

Over Europe and North America, bird monitoring programmes provide structured datasets allowing to estimate long-term trends and variability of bird abundance as well as the environmental drivers of bird abundance (Sauer et al. 2013, Brlík et al. 2021). These have led to accumulating evidence that agricultural intensification drives population declines of insectivorous species associated to farmland (Donald et al. 2001, Barnes et al. 2016, Bowler et al. 2019, Rosenberg et al. 2019). Moreover, cold-dwelling species decline locally (Gaüzère et al. 2020) as their geographical ranges shift northwards (Zurell et al. 2024). Conversely, populations of warm-dwelling, omnivorous species or species well suited to disturbed habitats stagnate or increase (Bowler et al. 2019, Gaüzère et al. 2020, Rigal et al. 2023). Bird population variability has also been linked to land use (Olivier et al. 2020, Guerber et al. 2026b) and climate (Li et al. 2021). Land use change in Europe slightly decelerates since the year 2000 (Winkler et al. 2021) while climate change has been accelerating in the last 50 years (Smith et al. 2015) and climate stochasticity is expected to increase (Garcia et al. 2014). Other environmental parameters affecting bird abundance in Europe such as pesticide contamination (Molenaar et al. 2024, Monnet et al. 2026) and hunting (Grzegorczyk et al. 2024) are also likely to vary in time, for example as legislation changes (Perrot et al. 2025). The exact impact on birds of the combination of these changes in perturbation regimes is difficult to disentangle.

However, integrative stability dimensions contain information on how bird communities respond to these complex changes. At the species level (Fig. V.1A), long-term population trends integrate long-term changes in environmental variables with species' response to these changes. Similarly, temporal variability integrates the strength of environmental fluctuations with ecological systems' ability to recover from these fluctuations (Arnoldi et al. 2019). Habitat specialist birds and insectivores are expected to have decreasing population trends while populations of habitat and diet generalists are expected to increase (Bowler et al. 2019, Rigal et al. 2023), however possible temporal changes in species trends are less documented (but see Vimont et al. 2025). For population variability, demographic rates set by life history traits drive population response to environmental stochasticity (Sæther et al. 2016). Particularly, species with a faster pace of life tend to reproduce faster and are thus able to compensate for environmental fluctuations more quickly than slower species, reducing their population variability (Mentges et al. 2024). Over large geographical scales, meta-population dynamics can also buffer local fluctuations, decreasing local population variability (Abbott 2011, Wang and Loreau 2016). These biotic drivers of species trends

and variability, if they undergo temporal changes or if the perturbation regime changes, can propagate to stability changes at the community level.

The variability of community abundance is indeed the outcome of species variabilities, mediated by species relative abundances, functional composition as well as functional diversity (Craven et al. 2018, Zhao et al. 2022, White et al. 2023). In order to understand these effects, theoretical works have built a solid framework decomposing community variability into interpretable mechanistic components, called hereafter the species synchrony framework. There, community abundance is more variable if species are more variable on average and if species' fluctuations fail to compensate for each other (Loreau and de Mazancourt 2008, Thibaut and Connolly 2013). Species synchrony, the degree to which species responses to environmental fluctuations occur synchronously, can be further decomposed into a statistical averaging effect and a compensatory dynamics effect (Doak et al. 1998, Zhao et al. 2022). For trends, theoretical work is less developed and there is no similar analytical decomposition of the temporal trend of community abundance, the trend of the sum of all considered species' abundance (Davison et al. 2024). A candidate underlying component is the mean of the absolute values of species trends (Guerber et al. 2026b), which gives the expected strength of the trend of a species sampled randomly within the community. As we have seen above, changes in community-level trends and variability components thus integrate changes in species stability and changes in community composition (Fig. V.1).

A prerequisite to conjointly study temporal changes in trends and in variability from biodiversity monitoring is to adopt a measurement method that allows to measure these two stability dimensions separately while still allowing the mechanistic decompositions of community variability in the species synchrony framework. While residuals-based methods (Lepš et al. 2019, Guerber et al. 2026b) adequately separate trends and variability, the application of these methods for decomposing community variability into population variability and species synchrony remains limited. This is likely partly explained by the lack of a full theoretical understanding of how to unite the species synchrony framework with detrending methods in the context of counting data. One of the basic assumptions in the species synchrony framework is indeed that the response of abundance to environmental stochasticity varies proportionately to squared abundance (Engen et al. 1998, Loreau and de Mazancourt 2008). This assumption justifies the use of the coefficient of variation for measuring variability in abundance (Tilman 1996, Arnoldi et al. 2016). However, usual counting processes measure the outcome of a counting process conditionally on real

abundance (Buckland 2001), which generates variances in count that are proportionate to mean count, with some overdispersion. Partitioning count variance into its environmental and counting-process origins is therefore not trivial and requires further developments to see how it scales from species to community level.

Using bird community time series data of the French Breeding Bird Survey (Jiguet et al. 2012) from 2001 to 2025, we conjointly estimate variability-based and trend-based integrative stability dimension metrics at the scale of continental France over 10-year moving temporal windows. We do so after clarifying the mathematical assumptions underlying the measure of population variability as well as the use of the species synchrony framework in the context of count data. Joining observed long-term patterns at the community level with underlying species-level integrative stability dimensions as well as compositional and functional biodiversity components allows to evaluate how changes in stability dimensions can be linked to changes in community stability properties (Fig. V.1). Overall, we reveal changes in community variability tightly linked to changes in the average community composition while highlighting the importance of integrating changes in species trends in a wider community stability framework.

Material and methods

Overview

We assess temporal changes in integrative community stability dimensions for birds in France by measuring them across sixteen 10-year moving temporal windows from years 2001-2010 to years 2016-2025. For both species and community count data and for each 10-year moving window, we fit a Poisson-log-Normal count model that estimates species and community trends, variabilities and abundances over France (Fig. V.2A-B). These output datasets are then visualized at several organizational levels across moving windows, investigating changes in different aspects of the conceptual framework in Fig. V.1. More precisely, changes in community-level stability components are estimated from community output datasets, while data from species-level model outputs is required for assessing changes in species-level trends and variability as well as changes in components of the species synchrony framework (Fig. V.2B). In addition, estimated species abundances for each moving window are used in combination with functional traits data to assess changes in community composition. Lastly, in order to better interpret how community composition alters community-level stability components, we also estimate how population

stability dimensions are influenced by species abundance and traits, using data for all years of the survey (Fig. V.2C). Each of the two parts of Fig. V.2 requires some mathematical background in order to see how quantities of interest can be properly estimated from count data.

Bird data

We used data from the French Breeding Bird Survey (Jiguet et al. 2012), from 2001 to 2025. In this bird monitoring scheme, hundreds of volunteer observers are each assigned a square plot of 2x2km near a location of their choice across France. There, they place 10 listening points in habitats representing the diversity of bird habitats within their square plot, at least 300m apart from each other. Twice a year during the breeding season (in April/May and in May/June), they visit their listening points and record all birds heard or seen during five minutes. Across years, sampling sessions are repeated around the same dates and listening points are always surveyed in the same order, one to four hours after sunrise. Observers also classify the habitat at each listening point with fine habitat classes which we grouped between “woodland”, “farmland”, “built” or “other” (Guerber et al. 2026b). Raw survey data is curated by the Vigie-Nature platform at the National Museum of Natural History (Paris), were each species’ yearly curated count at each point is the maximum recorded count across the available survey sessions (Princé et al. 2013).

As a tradeoff between ecological relevance and data quantity, we defined a community as a set of listening points from the same square plot that share their habitat category. Each year, for all species recorded in a community, we used the sum of curated counts across the community’s points as species count. In a given community, counts of species that were absent a given year but present other years were set to zero in the absence years. If a species was never recorded in a community, the community was not included in abundance data for this species.

Functional traits data

Pace of life traits were extracted for all species in the French Breeding Bird Survey that are known to have established breeding populations in France (Dupuy and Sallé 2022), from the trait table published by Storchová and Hořák (2018). We complemented missing traits for some species with the BIRDBASE trait table (Şekercioğlu et al. 2025). We extracted life span, mean body mass, average clutch size,

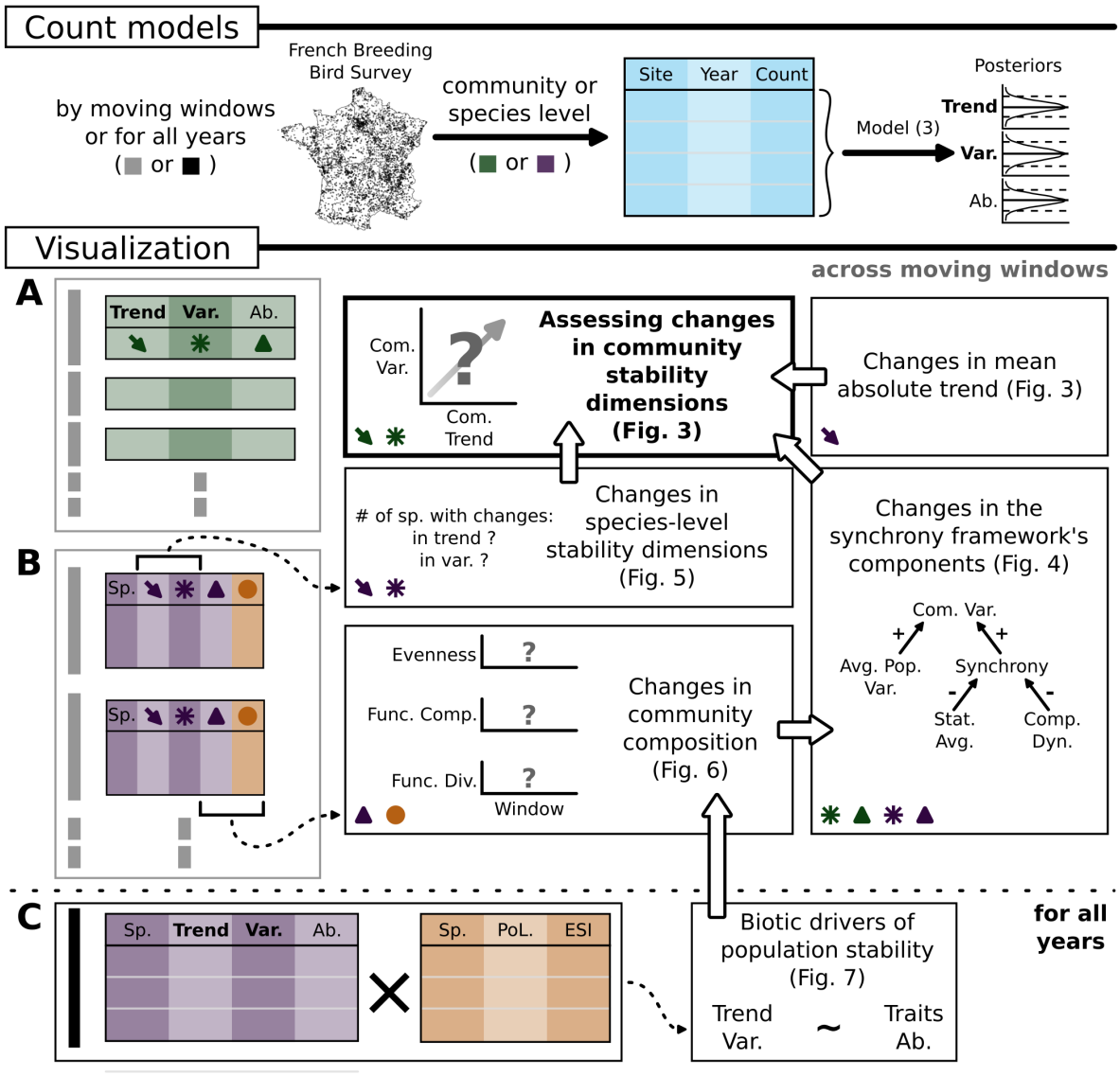

Figure V.2: **From bird data to understanding changes in integrative stability dimensions.** For count models, bird data is filtered for years in each moving 10-year window (gray) or for 2001-2025 (black). Count models yield posterior distributions for trend, variability (Var.) and abundance (Ab.). For visualization, letters denote: (A) community-level model outputs across moving windows, (B) species-level model outputs across moving windows, (C) species-level model outputs for all survey years. In each box for visualization across moving windows, colored icons in the bottom left corner indicate which information is used from which output dataset. The box at the start of an open large arrow can help the interpretation of the box at the arrow's end. Green, purple and orange datasets denote community-level model outputs, species-level model outputs and species trait information, respectively. Sp.: species. PoL.: pace of life. ESI: Ecological Specialization Index.

average brood number and fledging period. Missing trait information for 36 traits and species (mostly for life span which was missing for 30 species) was completed using the Handbook of the Birds of the World for 10 trait values (Hoyo et al. 2013), by using information from closely related species for 9 trait values, and using the collaborative ornithological portal `oiseaux.net` for 17 trait values. The two parasitic cuckoo species (*Clamator glandarius* and *Cuculus canorus*) never build nests and their brood number is therefore not defined (Hoyo et al. 2013): we assigned them the mean brood number across species. After log-transforming body mass, we summarized pace of life traits by Principal Component Analysis (Li et al. 2021). The first principal component accounted for 50.8% of total variance across 265 species (Fig. V.S2). It was negatively correlated with high life expectancy, high mean body mass and fledging period while positively correlated with clutch size and brood number, well representing the slow-fast pace of life continuum with low values for species with slower paces of life and high values for "faster" species.

We checked for social behavior during the breeding season in the trait table from Storchová and Hořák (2018), classifying species with colonial or semi-colonial nesting as gregarious. Four introduced species were missing from Storchová and Hořák (2018), which we complemented by checking the Handbook of the Birds of the Worlds (gregarious: *Euodice malabarica*, *Threskiornis aethiopicus*; non-gregarious: *Serinus corsicana*, *Leiothrix lutea*). Ecological specialization was assessed with the Ecological Specialization Index extracted from BIRDBASE, which equally weights habitat and diet specialization obtained from large-scale sources (Kittelberger et al. 2024, Şekercioğlu et al. 2025).

Count models

For a single time series, we conform to previous definitions (Engen et al. 1998, Arnoldi et al. 2016) and define temporal variability υ as the coefficient of variation of abundance. When true abundance is unknown but sampled by a counting process, we show that temporal variability can be estimated from random effect parameters of a Poisson log-linear mixed model such as those usually used in estimating long-term population trends (Section V.S1). We then detail how these models were used on French Breeding Bird Survey data.

Mathematical background: Trends and variability in the Poisson-log-Normal model

In a typical bird survey protocol, observers count birds during short sessions that are repeated across years at each sampling location. Recorded species abundance therefore is not sampled from the distribution of local population size, but is the result of a stochastic counting process. The variance of recorded abundance across several years thus depends on "true" population variability but also on the variance generated by the counting process. In order to measure trends and variability from counting data over several temporal windows, there is therefore a need for a detrending method able to partition the total observed variation into the variation explained by the trend, by population variability and by the variance of the counting process. We do so in the convenient setting of the Poisson counting process.

From a probabilistic perspective (parameters are known), if true population variability (*sensu* Arnoldi et al. 2016) is υ, we show that recorded species counts X follow (Section V.S1.2):

$$\begin{aligned} X &\sim \mathcal{P}(\lambda) \\ \log(\lambda) &\sim \mathcal{N}(\beta, \sigma^2) \\ \upsilon &= \sqrt{\exp(\sigma^2) - 1} \approx \sigma \end{aligned} \tag{V.1}$$

X thus follows a mixed Poisson distribution with the distribution of λ as its mixing distribution (Karlis and Xekalaki 2005). Since λ follows a log-Normal distribution with scale β and range σ, the distribution of X is called a Poisson-log-Normal (Aitchison and Ho 1989). The Poisson-log-Normal model is known in ecology from a statistical perspective (parameters estimated from data), as a generalized linear (mixed) model which is often used to estimate long-term population trends from count data over sites and sampling times (Stoehr and Robin 2026). In these settings, expected count at site s and time t $\lambda_{s,t}$ depends on the fixed log-linear effects of covariates $\mathbf{x}_{s,t}$ as well as spatial random effects ω_s and spatio-temporal random effects $\alpha_{s,t}$:

$$\begin{aligned} X_{s,t} &\sim \mathcal{P}(\lambda_{s,t}) \\ \log(\lambda_{s,t}) &= \mathbf{x}_{s,t}\boldsymbol{\beta} + \omega_s + \alpha_{s,t} \end{aligned} \tag{V.2}$$

We show that the standard deviation parameter for $\alpha_{s,t}$ is an estimator of population variability υ (Section V.S1.2) and check that realistic dataset sizes allow satisfactory estimation of υ by a simulation analysis (Section V.S2, Fig. V.S1). When covariates include the centered sampling time t, the corresponding

element of the coefficients vector β is the estimated log-linear long-term trend of population abundance. Fitting model V.2 on count data thus allows to estimate long-term population trends and population variability while controlling for the effects of spatio-temporal covariates on population abundance.

Fitted count models

We restricted our analyses to species that were abundant enough for population variability to be reliably estimated (Section V.S2), *i.e.* for which all 10-year moving windows contained more than a thousand non-zero counts. We also excluded gregarious species, for which detection of a single individual is strongly dependent on detection of other individuals. In total, we used data for a total of 55 species, for which the number of non-zero counts in the moving windows ranged from 1018 (*Pyrrhula pyrrhula*, 2015-2024) to 24519 (*Turdus merula*, 2016-2025). Community count was set as the sum of the 55 species' counts in each community.

For all selected species' counts and for community count, for each of the 16 moving windows and for all available years (Fig. V.2), we fit a Poisson-log-Normal model with a fixed year effect and a temporal random effect in order to estimate trend and detrended temporal variability. There, the recorded count $X_{s,t}$ at site s on time t is given by model V.2. In order to consider varying sampling effort across communities, we added the log-transformed number of listening points as an offset term $O_{s,t}$. Covariates $\mathbf{x_{s,t}}$ included an intercept term, the centered year, the realized survey sessions each year (two, only April/May or only May/June), and the habitat category of the community with woodland communities as base factor level. Including the habitat category ensures that trend and variability estimation is not confounded by temporal changes of the repartition of survey coverage across habitats. Unaccounted spatial variation in average count was accounted for by a plot-level random intercept $\omega_{p(s)} \sim \mathcal{N}(0, \sigma^2_\omega)$.

With the log-linear trend estimated by the fixed effects, the standard deviation of $\alpha_{s,t}$ measures the detrended temporal variability of the time series, averaged over the considered dataset. $\alpha_{s,t}$ was estimated with an autoregressive first-order covariance structure (AR1), meaning that parameters ϕ and σ_{AR} were fit such that $\alpha_{s,t} = \phi\alpha_{s,t-1} + \epsilon_t \ ; \ \epsilon_t \sim \mathcal{N}(0, \sigma^2_{\mathsf{AR}})$. The stationary variance of $\alpha_{s,t}$, σ^2_α, is equal to $\sigma^2_{\mathsf{AR}}/(1-\phi^2)$. While a single variability value σ_α is estimated for each model, realizations of the AR1 process are assumed to be independent across communities.

The full model formula for species or community count $X_{s,t}$ in community s on year t therefore was:

$$\begin{aligned} X_{s,t} &\sim \mathcal{P}(\lambda_{s,t}) \\ \log(\lambda_{s,t}) &= O_{s,t} + \mathbf{x_{s,t}}\boldsymbol{\beta} + \omega_{p(s)} + \alpha_{s,t} \\ \omega_p &\sim \mathcal{N}(0, \sigma^2_\omega) \\ \alpha_{s,t} &\sim \text{AR1}(\rho, \sigma_{\text{AR}}); \text{ repeated at each } s \end{aligned} \tag{V.3}$$

We checked that realistic dataset sizes allow model V.3 to correctly estimate detrended variability on simulated community data in a Bayesian framework (Section V.S1.2). Outputs of count models were checked to verify that the posterior 95% interquantiles for the σ_α parameter were between 0.01 and 3, corresponding to sane ranges for variability, and that the width of the posterior 95% interquantiles did not exceed five times their mode, a sign of bad precision of the posterior density. Fixed effects coefficients were checked for some species to verify that they corresponded to the ecology of each species, but subsequent analyses focused on the posterior distributions of β_i, the fitted species log-linear trend, υ_i, the fitted species variability, and μ_i the fitted species abundance, computed from the intercept and the variability parameter (Section V.S1.1). Their community-level counterparts are noted as υ_c, β_c and μ_c.

Temporal changes in integrative stability dimensions

At the species level, each species' trend and detrended variability reflect the species' response to its perturbation regime. Changes in these species-level integrative stability dimensions can thus be directly assessed from species count model outputs (Fig. V.2B). At the community level, changes in community trend and community detrended variability can be assessed from community count model outputs (Fig. V.2A), and can also be compared to changes in their underlying components. For community detrended variability, the species synchrony framework (Loreau and de Mazancourt 2008, Thibaut and Connolly 2013, Zhao et al. 2022) can be used to see how changes in community variability can be explained by changes in average population variability, species synchrony, statistical averaging effect, or compensatory dynamics effect (Fig. V.2). Because community composition is associated to several community-level variability components (Li et al. 2021, Zhao et al. 2022), we also assess changes in community composition. For correct interpretation of these indices, verifying if species traits and abundance are well linked to species stability dimensions is needed.

Mathematical background: Community variability for mixed Poisson distributions

In the species synchrony framework, community-level variability components are measured using abundance time series from approximately Gaussian data. Here we adapt these metrics to measuring population and community temporal variability from counting data. When S species' counts X_i follow Poisson-log-Normal distributions, community count $Y = \sum_i X_i$ approximately also follows a Poisson-log-Normal distribution, but with different parameters (Section V.S1.3). Community variability v_c (respectively species variabilities v_i) are measured by fitting model Equation V.2 on community time series (resp. on species time series). We show that this still allows for the decomposition of community variability into species synchrony $\sqrt{\phi}$ and abundance-weighted average population variability v_{pop}. With species and community average abundances μ_i and μ_c, we show that (Section V.S1.3):

$$v_c = \left(\sum_i \frac{\mu_i}{\mu_c} v_i \right) \sqrt{\phi} = v_{\text{pop}} \sqrt{\phi} \tag{V.4}$$

We use the same conceptual definition for species synchrony $\sqrt{\phi}$ as Loreau and de Mazancourt (2008), it is the ratio between community variability and the variability that a community with the same species variances would have if all species environmental fluctuations were synchronized. Our proof relies on two convenient properties of mixed Poisson distributions (Karlis and Xekalaki 2005). Firstly, the variance of a mixed Poisson distribution is equal to its mean plus the variance of its mixing distribution. Thus, letting λ_i and λ_c the (random) expected counts for X_i and Y, $V[Y] = E[Y] + V[\lambda_c]$ and $V[X_i] = E[X_i] + V[\lambda_i]$. Secondly, the covariance between species counts X_i and X_j is equal to the covariance between species expected counts, $\text{Cov}[X_i, X_j] = \text{Cov}[\lambda_i, \lambda_j]$.

Following Zhao et al. (2022), species synchrony $\sqrt{\phi}$ can be further decomposed into the product of the strengths of statistical averaging (SAE) and compensatory dynamics (CPE). The statistical averaging effect accounts for the statistical effects of the number of species and of the evenness of species variances on reducing v_c. It is the ratio between average population variability and $v_{c|\text{ ip.}}$, the value that community variability would have if species responses to environmental fluctuations were independent. The compensatory dynamics effect can be estimated with the remaining part of $1/\sqrt{\phi}$ (Zhao et al. 2022). If species responses to environmental fluctuations are independent, $\text{Cov}[\lambda_i, \lambda_j]_{|\text{ ip.}} = 0$. Therefore,

$v_{c|\text{ ip.}} = \sqrt{\sum_i \left(\frac{\mu_i}{\mu_c}\right)^2 v_i^2}$ (Section V.S1.3), and total community variability v_c is decomposed as:

$$v_c = \frac{v_{\text{pop}}}{\text{SAE CPE}} \text{ ; SAE} = \frac{v_{\text{pop}}}{v_{c|\text{ ip.}}} \tag{V.5}$$

Visualization: Combining count model outputs across ecological scales

Community trend and community detrended variability are directly estimated from fitting model V.3 on community time series for each moving window. We further decomposed them into variability and trend components that relied on species variability, trend and average abundance estimates. For the trend component, we computed the average across species of the absolute values of each species' trends, *i.e.* the mean absolute trend. It is the expected strength of the trend of a species drawn uniformly among all species. For variability components, we used the average population variability and species synchrony (Equation V.4) as well as the statistical averaging effect and the compensatory dynamics effects (Equation V.5). Using a Bayesian framework allows to propagate uncertainties in parameters from the species models for the computation of multi-species indices by sampling from the posterior distribution. For example, the mean absolute trend is computed as $\bar{\beta}_{\text{abs}} = 1/S \sum_i |\beta_i|$. A sample r from each species' posterior distribution is used to compute a sample for $\bar{\beta}_{\text{abs}}$: $\bar{\beta}_{\text{abs},r} = 1/S \sum_i |\beta_{i,r}|$. Over many samples, the distribution of propagated values $(\bar{\beta}_{\text{abs},r})_{1 \leq r \leq R}$ captures the uncertainty in the mean absolute trend $\bar{\beta}_{\text{abs}}$ originating from uncertainties in each species trend β_i. We call such distributions the propagated posterior distributions in order to distinguish them from posterior distributions that are directly computed by fitting model V.3. We used $R = 10000$ samples.

In order to assess changes in each species' trends and variability while still keeping an overarching perspective, we assess, for each species and each species-level stability dimension, if 95% interquantiles across all moving window all overlap a consensus credibility interval. The consensus credibility interval is the interval between the medians of the lower and upper bounds of all intervals across moving windows. While not offering any possibility for statistical testing, this method allows to evaluate, for any species and for each of species trend and species variability, if estimations for some moving windows stand out from the other moving windows. For trends and for variability, we then count the numbers of species for which at least one moving window does not overlap the consensus interval. Counting species numbers

was complemented by inspecting examples of species temporal changes in variability. Among other examples that we checked, we chose to present the strongly declining Eurasian skylark (*Alauda arvensis*) and European greenfinch (*Chloris chloris*) as well as the increasing common wood pigeon (*Columba palumbus*) and stagnating song thrush (*Turdus philomelos*) (Fontaine et al. 2020).

Community composition metrics were computed from fitted species abundance values μ_i, with uncertainty propagation. The evenness of fitted species relative abundances was computed with Shannon evenness $H = -\sum_i p_i \log(p_i)$ with $p_i = \mu_i / \sum_i \mu_i$. To compute changes in functional composition, we used species slow-fast continuum values and averaged it across species, weighted by p_i. We call this index the community weighted mean (CWM), but note that here averaging occurs on species' fitted average abundances, not on individual communities. Functional diversity of average composition (FD) was computed using Rao's quadratic entropy (Rao 1982). Functional distance between species i and j, d_{ij} was the euclidean distance between their slow-fast continuum values and FD $= \sum_i \sum_j p_i p_j d_{ij}$. It is the expected functional distance between two individuals in a community with relative abundances $(p_i)_{1 \leq i \leq S}$.

The links between species abundances and species traits on one side and population trend and detrended population variability on the other side were assessed using Structural Equation Modelling with the R package `piecewiseSEM` (Lefcheck 2016). In order to maximize accuracy in trend and variability estimation, we used trend and variability from species count models fit for all available years (Fig. V.2C).

All statistical analyses and visualizations were carried out in R version 4.5.0 (2025-04-11). Posterior distributions for species and community count model parameters were estimated under the Integrated Nested Laplace Approximation using the `inlabru` package (Bachl et al. 2019), a user interface for `R-INLA` (Rue et al. 2017). We used the `targets` package for pipeline management (Landau 2021).

Results

Across moving windows, the trend of total bird community abundance and the detrended variability of total bird community abundance have different temporal dynamics (Fig. V.3). Bird detrended community variability estimated declines over the study period, during which community trend goes from positive to negative values (Fig. V.3).

Considering underlying community-level trend and variability components, for community trend, the mean

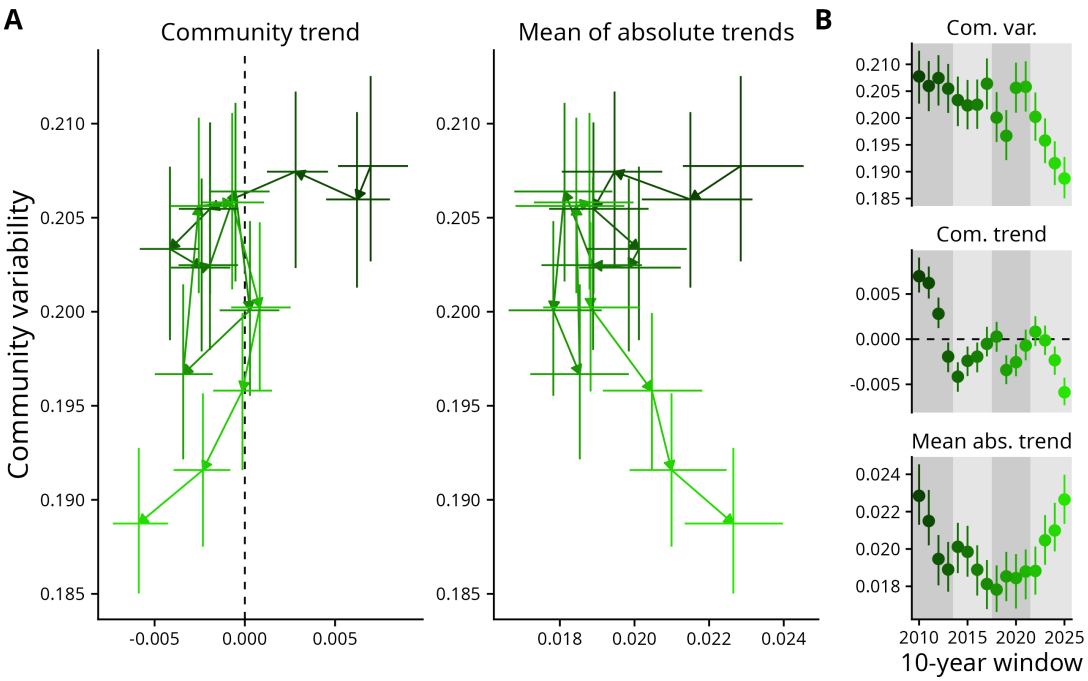

Figure V.3: **Changes in community stability dimensions across moving windows.** (A) Community variability across community trend and mean absolute trend for all moving windows. Consecutive moving windows are linked by arrows. For each stability component, line intervals indicate the 95% interquantile range of the posterior distribution (for community variability and community trend), or of the propagated posterior distribution (for mean absolute trend). They intersect at the corresponding posterior modes. (B) Stability metrics across moving windows for all stability metrics of panel A. Years indicate the last year of each 10-year moving window.

of absolute species trends first declines then increases (Fig. V.3). For detrended community variability, the components of the species synchrony framework show different temporal changes. Abundance-weighted average population variability indeed declines across the study period while species synchrony increases and then declines (Fig. V.4). For the components of species synchrony, no change in compensatory dynamics effect can be detected, while statistical averaging effect varies oppositely to variation in species synchrony (Fig. V.4). The overall decline of community variability is thus explained by an overall decline in average population variability to which an onset of a decline in species synchrony is added from the 2012-2021 window onwards, sharpening the decline in community variability.

At the species level, changes in species-level stability dimensions are more noticeable for trends than for variability (Fig. V.5A): significant differences in variability across moving windows occur only for 11 species out of a total of 55, while differences in trends occur for 41 species. Most species thus do not show significant changes in variability while they show some significant change in trend, but all combinations are found across the species list (Fig. V.5B). Many species with changes in trend show complex patterns across moving windows. For example, the declining Eurasian skylark (*Alauda arvensis*) shows overall

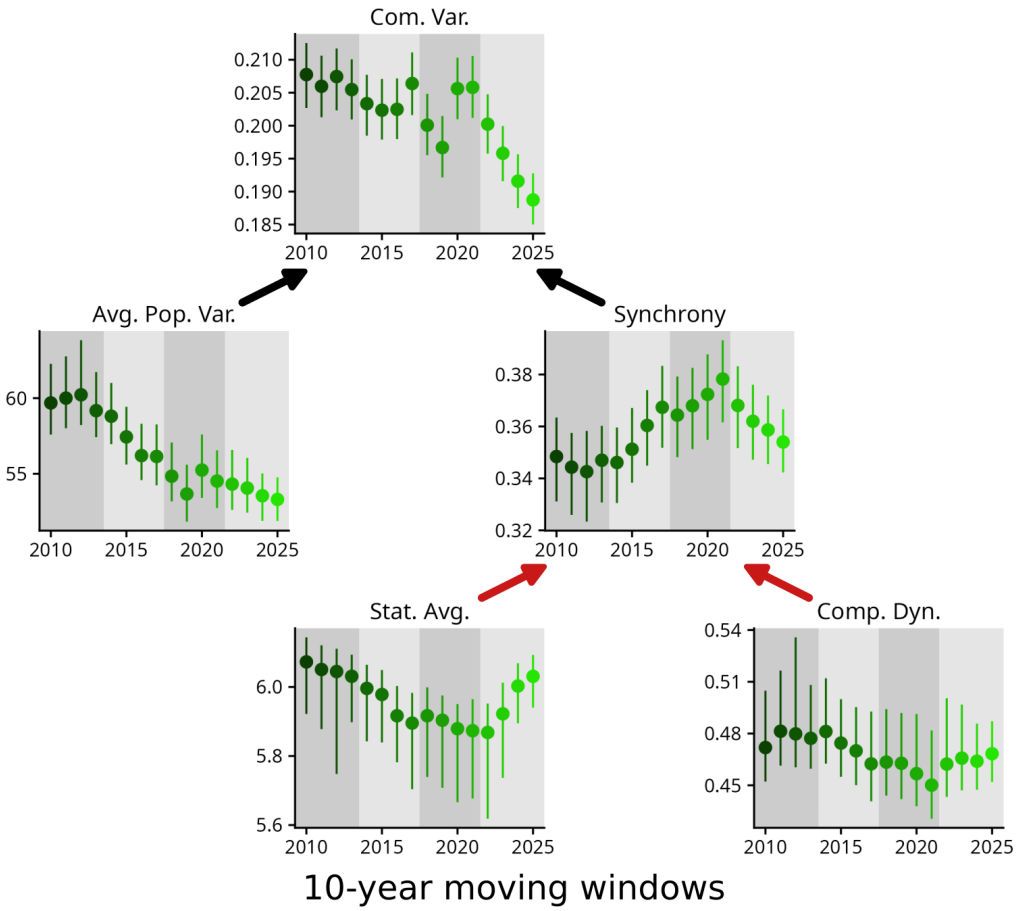

Figure V.4: **Changes in components of detrended community variability across moving windows.** For each moving window, line intervals indicate the 95% interquantile range of the posterior distribution (for community variability), or of the propagated posterior distribution (for the other components). Points indicate the posterior or propagated posterior modes. Black arrows indicate positive analytical relationships while red arrows indicate negative analytical relationships. Years indicate the last year of each 10-year moving window. Com. Var.: community variability. Avg. Pop. Var.: average population variability. Stat. Avg.: statistical averaging effect. Comp. Dyn.: compensatory dynamics effect.

negative 10-year trends, but trends for later moving windows are closer to zero (Fig. V.5B).

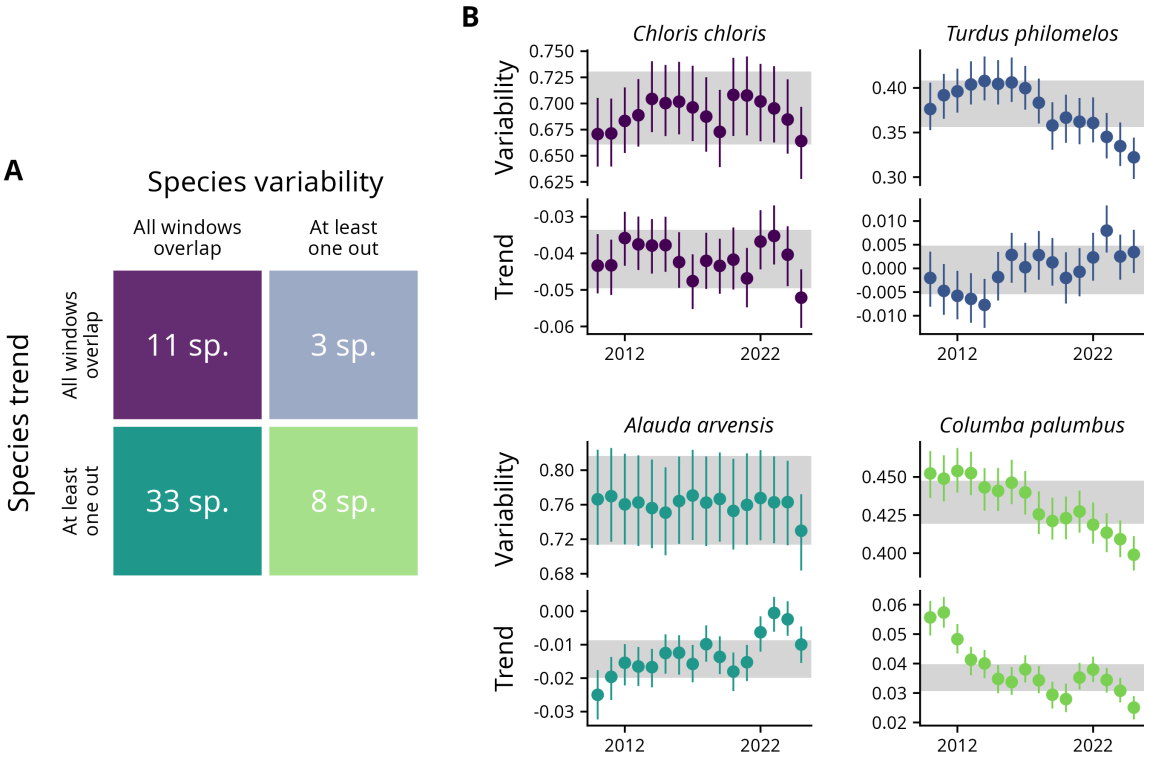

Figure V.5: **Summary of changes in species-level stability dimensions.** (A) Numbers of species for which trend or detrended variability all overlap their consensus interval (All windows overlap) and for which at least one moving window does not overlap the consensus interval (At least one out). (B) Example of trends and variability across moving windows for all possible cases in panel A. Colors and panel positions match those in panel A. Grey ribbons indicate the consensus intervals, delimited by the medians of the lower and upper bounds of all moving window's 95% interquantile of the posterior distribution (vertical lines). Years indicate the last year of 10-year moving windows.

For community composition over moving windows, count model outputs only allow to compute metrics on species' estimated average abundances (Fig. V.2B), meaning that we measure the composition of the average community across France in each moving window. The evenness of species relative abundances declines, then increases (Fig. V.6). The community-weighted mean of the slow-fast continuum decreases, meaning that the average community is increasingly dominated by slower species, while the functional diversity of the slow-fast continuum increases (Fig. V.6). Since faster species are expected to have lower population variability, the decline in community weighted mean of the slow-fast continuum would predict an increase in average population variability, but we observe a decrease (Fig. V.4). However, here changes in evenness coincide well with changes in the statistical averaging effect, with a change in direction at the 2011-2020 moving window (Fig. V.4). The lack of theoretical predictions on the links between community composition and community trend makes them difficult to be compared.

In order to precise possible links between changes in community composition and changes in community

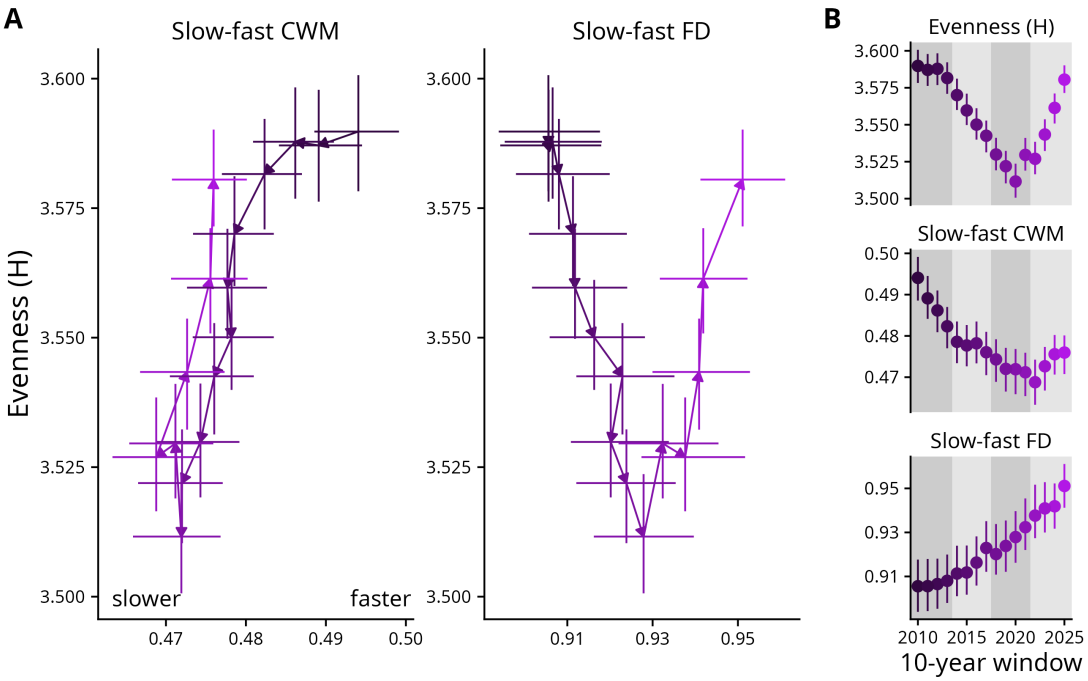

Figure V.6: **Changes in community composition across moving windows.** (A) Evenness of fitted abundances across community-weighted mean (CWM) and functional diversity (FD) of the slow-fast continuum for all moving windows. For slow-fast CWM, lower values indicate communities dominated by slower species. Consecutive moving windows are linked by arrows. For each community-level metric, line intervals indicate the 95% interquantile range of its propagated posterior distribution. Lines intersect at the corresponding posterior modes. (B) Community-level composition metrics across moving windows for all metrics in panel A. Years indicate the last year of each 10-year moving window. On both panels, the dashed line indicates a null community trend.

stability components, we estimate how species abundance and species traits are related to species stability over the whole dataset. Structural equation modelling reveals that more abundant species are less variable, but after accounting for this relationship we do not find a significant direct association between the slow-fast continuum and species variability (Fig. V.7). Many declining species in our species list have a fast pace of life while there is no such pattern for ecological specialization (Fig. V.7B), but after accounting for abundance the effect on pace of life on trend is not significant (Fig. V.7A). No direct significant relationship between species stability and ecological traits was thus detected (Fig. V.7). Since selected traits and species abundances are not strongly associated to species trends, linking community composition to community trend and to the mean absolute trend is not straightforward.

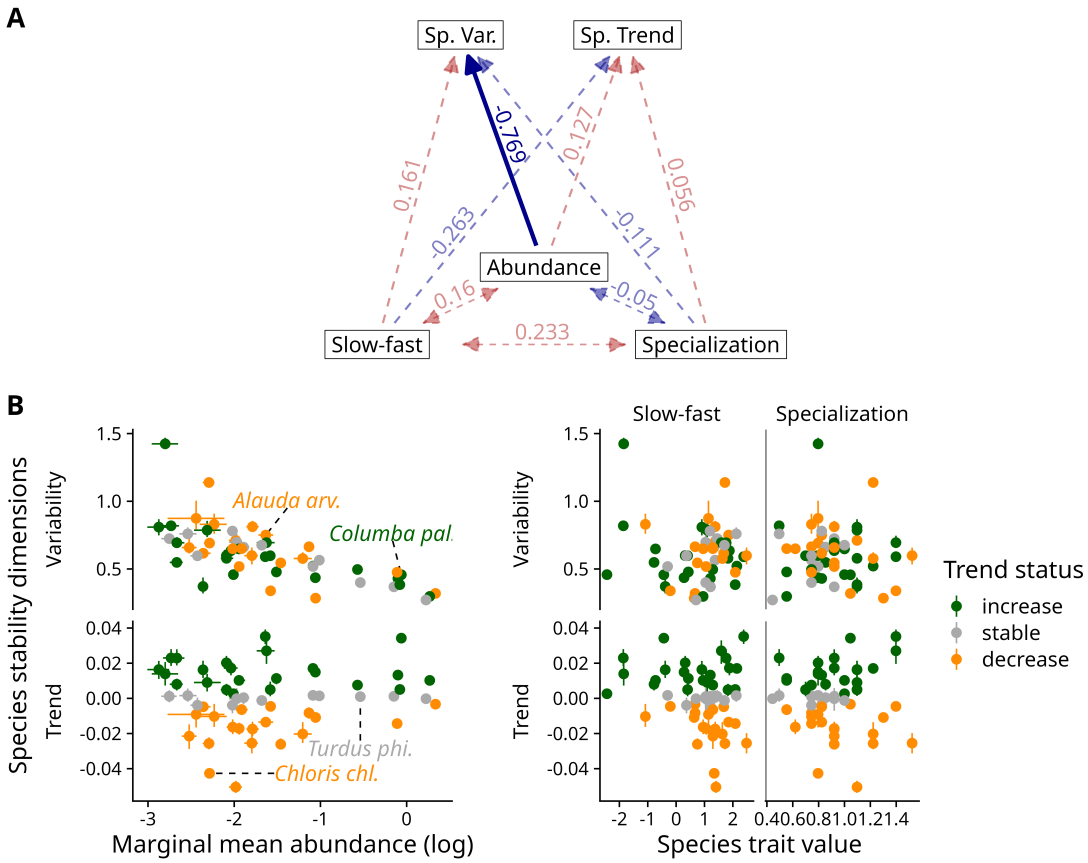

Figure V.7: **Links between species abundance or functional traits and species-level stability dimensions.** (A) Structural Equation Model (SEM) linking species slow-fast continuum (slower species have lower values), fitted abundance and ecological specialization (generalist species have lower values) to species detrended variability and species trend over all dataset years. Bidirectional arrows denote correlated error terms while unidirectional arrows denote direct SEM effects. Non-significant paths (5% confidence threshold) are shown with transparent dashed lines. Standardized SEM coefficients are reported for each path, with positive coefficients in red and negative in blue. Fisher's C criterion for global goodness-of-fit was 0.61 on 2 degrees of freedom ($p > 0.5$). (B) Scatter plots of raw species stability data corresponding to unidirectional SEM paths with species abundance (left) or functional traits (right) as predictors.

Discussion

We document temporal changes in trends and variability for bird populations and communities of the French Breeding Bird Survey. Temporal changes in community variability components appear related to changes in average community composition, especially changes in evenness, which are themselves the results of population trends. Conversely, changes in trends at both species and community levels only weakly coincide with the variables we studied, calling for further investigations.

Functional traits, species abundance and two stability dimensions

Drawing links between species functional traits and ecological stability is suggested as a key to bridging advances in functional ecology with ecological theory (de Bello et al. 2021), but the empirical patterns we find do not match expectations. We indeed do not measure significant associations of species traits and species-level stability dimensions after accounting for estimated species abundance, which has a strong negative association to species variability (Fig. V.7). The negative relationship between estimated abundance and variability was expected as species with high national-level abundances are associated with numerous suitable habitats and therefore have many opportunities to compensate environmental fluctuations. For example, Cuervo and Møller (2013) measure that European bird populations in countries closer to the latitudinal edges of their distributions, where they are rarer, are more variable. However, a positive abundance-trend relationship could have been expected as long-term trends benefit abundant generalist species (Devictor et al. 2008a) and population trends were expected to be associated to ecological specialization (Devictor et al. 2008b, Bowler et al. 2019).

While previous studies found significant links between functional community composition and variability, in our analysis these links are more elusive both at the species and at the community levels. By comparing communities in different locations, Li et al. (2021) measure that bird communities dominated by faster species have lower average population variability and lower species synchrony. Moreover, White et al. (2023) measure that functional diversity based on several ecological generalism traits increases population variability and decreases species synchrony. While both these studies did not present results at the level of species, our observed mismatch between traits and stability at the species level is not solved at the community level either. Li et al. (2021) detected an increase of bird community variability over time, in line with slower communities, while we also measure slower communities but coinciding

with a puzzling decrease in bird community variability. Including more traits in our analyses could help further investigate the relationship of traits with integrative stability dimensions, but this may encounter the same hurdle of the strong influence of estimated species abundance in explaining variation in species variability. Similarly, including more species in conjoint analyses of ecological traits and species-level stability dimensions could help, but may come at the price of less reliable estimation, especially for temporal variability (Section V.S2).

Species trends change more than species variabilities

The non-linearity of many bird population trends is expected (Clark and Luis 2020, Boennec et al. 2024), but complicates comparisons across species and hinders the interpretation of changes in multi-species trend indices. Even species that have similar responses to a given long-term environmental changes may respond with different time lags (Gaüzère and Devictor 2021), and national-level analyses may hide spatially-varying population trends (Johnston et al. 2025). However, explicitly considering community-level trends as the outcome of species response to a particular perturbation regime may help clarify these patterns in the future. As adapting our framework to spatial subsets of the French Breeding Bird Survey dataset may cause insufficient data quantity, leveraging bird time series datasets at the scale of Europe (Brlík et al. 2021) could be a way to evaluate if changes in species trends come from shared changes in long-term perturbation regimes across countries or seem idiosyncratic. This also calls for a better theoretical understanding of long-term population trends across spatial scales, with most related ecological stability literature focusing on the spatial scaling of temporal variability (Wang et al. 2017, Liang et al. 2025). Our theoretical contributions allow us to better acknowledge the underlying hypotheses of variability measurements (Section V.S1.4) and we hope that it can be the starting point for improved theoretical understanding of population trends in meta-community frameworks (Gaüzère et al. 2025).

For changes in species variabilities, a majority of species having non-significant change in population variability hints at a constant strength of environmental stochasticity. However, a lack of change at the national scale may hide opposed changes at finer geographical scales. For example, compared to forests, both agricultural and urban habitats are associated to higher population variability (Olivier et al. 2020, Guerber et al. 2026b). Since some areas across France see a decline in agricultural areas with reforestation and some other areas face increasing urbanization (Kuemmerle et al. 2016), opposed

effects on species perturbation regime may compensate each other at the scale of France. Efforts to describe changes in bird abundances across geographical scales through time are emerging (Gaüzère et al. 2025), and extending these approaches to the study of population and community variability is needed. Notice that the 11 species who do show significant changes in variability all show declines in variability with overall positive or stable long-term population trends (Fig. V.S3), which could indicate a species-level temporal relationship of increasing regional abundance causing a decrease in population variability.

Changes in community-level stability dimensions

With overall constant species-level variabilities, measured changes in community-level variability components can be partially explained by changes in facets of community composition that drive community stability (Fig. V.8). Our study highlights both the importance of species' abundance evenness in explaining changes in species synchrony via the statistical averaging effect (Zhao et al. 2022) and the importance of average population variability in driving community variability patterns (Danet et al. 2025). With limited association between our choice of species traits and species-level stability dimensions, comparing changes in functional diversity indices and changes in community stability dimensions is not straightforward. We report an increase in the functional diversity of the slow-fast continuum which coincides with a decline in average population variability (Fig. V.6), although previous studies did not find a strong link between them (Li et al. 2021, Rodrigues et al. 2025). Another possible effect of species abundance evenness on variability arises after assessing links between species abundance and species variability. Since abundant species are indeed less variable on average (Fig. V.7), decreasing evenness, *i.e.* relatively lower abundance for rare species, is expected to be associated with decreasing average population variability, which is only the case before the 2011-2020 moving window (Fig. V.4). Many of our results at the community level show a change in direction after the 2011-2020 moving window, which could indicate some temporal change of some national-scale environmental drivers, but remains puzzling.

Investigating changes in community-level trend components does not benefit from the same depth of theoretical tools as community-level variability components. Moreover, since species-level trends also change, community-level changes in 10-year trends are difficult to interpret. Overall, noticing temporal changes in trends are in line with recent calls to embrace the presence of non-linear trajectories in large population and community datasets (Boennec et al. 2024). These temporal changes in trends are

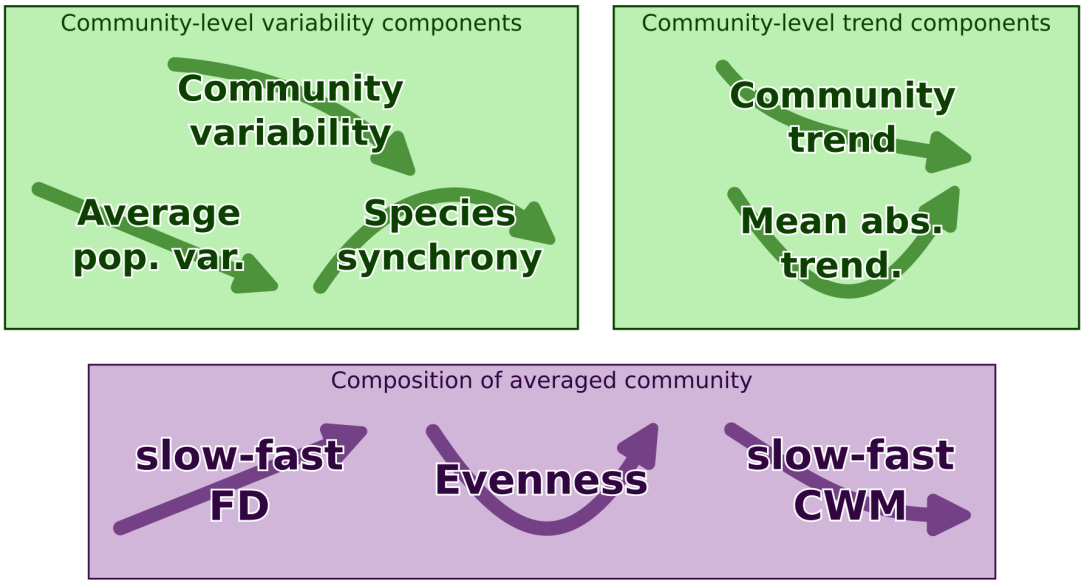

Figure V.8: **Summary of temporal changes in community-level stability dimensions and community composition.** The horizontal direction represents the 10-year moving windows (further right is later) while the vertical direction represents each community-level metric's magnitude (further up is higher). For the slow-fast community weighted mean (CWM), lower values represent slower communities.

particularly important to acknowledge when they generate inconsistencies between long-term patterns observed over different time frames (Duchenne et al. 2022). Statistical methods built for non-linear, out-of-equilibrium trajectories (*e.g.* Clark et al. 2022) may help precising known patterns (Rigal et al. 2023). However, they may be more difficult to compare with existing work on multi-species trend indices in conservation ecology, which inherit from log-linear modelling (Buckland et al. 2005, Loh et al. 2005). Estimating log-linear trends over moving windows or, alternatively, using temporally-weighted regression (Nguyen et al. 2025) offers a convenient middle ground for estimating parameters with well-known interpretations while still allowing to consider non-linear temporal variation.

Current limitations and perspectives

A strong assumption in the count models that we used is that the impact on our estimates of changes in detectability across species is limited. For species-level models, this is reasonable as the detection probability is simplified out of the estimators for trends and for variability (Section V.S1.2), although only if it is constant across years for a given species. However, when summing counts from different species or using estimated abundances in community-level indices, the contribution of easily detectable species is artificially increased while the contribution of inconspicuous species is artificially decreased. Moreover, species detectability is related (i) to species traits (Johnston et al. 2014), with large species

being generally more detectable (Sólymos et al. 2018), and (ii) to bird habitats in which sampling occurs with more detectable birds in open habitats (Morelli et al. 2022). Accounting for detectability in our framework is possible by implementing distance sampling methods (Buckland et al. 2015, Nabias et al. 2025), but they require several observations every year and are therefore not directly compatible with usual data curation methods for French Breeding Bird Survey data. Including more species from our dataset with less reliable trend and variability estimation shows robust patterns for community variability and community trend, but shows an increase in the mean absolute trend after 2011-2020 (Fig. V.S4).

Accounting for known spatially and temporally varying drivers of bird abundance such as land use, temperature and primary productivity is the step forward in order to link observed changes in stability dimensions with the actual anthropogenic pressures that drive the underlying perturbation regimes (Northrup et al. 2019). Together with considering several spatial scales (Di Cecco and Hurlbert 2022), this is necessary for refining observed patterns and could help to identify traits responsible for temporal changes in stability dimensions. We indeed did not find evidence for links of measured stability dimensions with the slow-fast continuum or with ecological specialization. However, we predict that the differences in estimated variability and trend before and after, for example, accounting for temperature, should be related to species' thermal tolerance.

Overall, we show that integrative dimensions of ecological stability are closely related as temporal changes in community composition, which are consequences of bird population trends, can partly explain temporal changes in community variability. Temporal changes in 10-year trends are more elusive to explain, because of lacking theoretical expectations but also likely because of spatial heterogeneity in changes of the perturbation regimes. Building on existing conceptual work (Van Meerbeek et al. 2021, Isbell et al. 2026), our framework thus allows to evaluate the dimensionality of ecological stability across time (Donohue et al. 2013). More conjoint work in conservation and theoretical ecology is needed in order to clarify variation in integrative stability dimensions, across drivers and spatio-temporal scales (Wolkovich et al. 2014, Hastings 2016), but also for other taxa than birds (Troudet et al. 2017).

Acknowledgments

We thank the hundreds of volunteer ornithologists who participate in data collection in the French Breeding Bird Survey, supported by Muséum National d'Histoire Naturelle, Office Français de la Bidiversité and Ligue de Protection des Oiseaux. The survey is coordinated by Benoît Fontaine and Lorraine Delthel. This work was granted access to the High Performance Computing resources of the SACADO MeSU platform at Sorbonne Université. We thank Stéphane Robin for advice on the Poisson-log-Normal model.

Data availability

Since work on this Chapter is still in progress, data and code will be made available after finalization.

Author contributions

JG, CF and ET conceptualized the study. JG conducted the analyses and visualized the results. JG wrote the first draft and all authors contributed to review and editing.

V.3 Supplementary Information for Chapter 3

V.S1 Mathematical justifications

V.S1.1 Properties of the log-Normal distribution

Mean, variance and coefficient of variation. Let λ follow a log-Normal distribution, *i.e.* $\log(\lambda) \sim \mathcal{N}(\beta, \sigma^2)$. Recall that:

$$E[\lambda] = \exp(\beta + \sigma^2/2) = \mu_{\mathsf{LN}}$$

$$V[\lambda] = \mu_{\mathsf{LN}}^2(\exp(\sigma^2) - 1)$$

When the parameters are known, the coefficient of variation of λ is thus $\mathsf{CV}(\lambda) = \sqrt{\exp(\sigma^2) - 1}$.

Multiplication by a constant. If $\log(\lambda) \sim \mathcal{N}(\beta, \sigma^2)$, then $\log(a\lambda) \sim \mathcal{N}(\beta + \log(a), \sigma^2)$ for any non-zero positive constant a.

First-order Normal approximation. We rewrite $\log \lambda$ as $\beta + \epsilon$ with $\epsilon \sim \mathcal{N}(0, \sigma^2)$. When σ is small,

$$\lambda = \exp(\beta + \epsilon) \approx \exp(\beta)(1 + \epsilon)$$

Thus λ is approximately normally distributed with mean $E[\lambda] \approx \exp(\beta) = \mu_{\mathsf{N}}$ and $V[\lambda] \approx \mu_{\mathsf{N}}^2\sigma^2$. The first-order approximation yields simpler expressions for the moments of λ and still verifies $V[\lambda] \propto E[\lambda]^2$.

V.S1.2 Defining variability in Poisson count models

Variability definition. Consider a population of size N in a stationary regime under environmental stochasticity. Arnoldi et al. (2016) show that population variance $V[N]$ is proportional to its squared expected value $E[N]^2$ with a factor υ^2, the strength of the population's response to environmental stochasticity. υ is the variability of the population, which can be measured by the coefficient of variation of abundance time series if true abundance is observed.

Variability for count data. A counting protocol is repeated at each time step t with a constant effort to count individuals from a population of size N. Given the abundance N_t at time step t and assuming that all individuals are detected with probability p, the count at time step t, X_t, approximately follows a

Poisson distribution with rate $\lambda_t = pN_t$. If the probability distribution for N is constant, we have $V[\lambda] = p^2V[N] = p^2\upsilon^2E[N]^2 = \upsilon^2E[\lambda]^2$. Moreover, if N is log-normally distributed, *i.e.* $\log(N) \sim \mathcal{N}(\beta_N, \sigma^2)$, then $\log(\lambda) \sim \mathcal{N}(\beta_N + \log(p), \sigma^2)$. Writing $\beta = \beta_N + \log(p)$, X is distributed according to model 1 from the main text and $\upsilon = \mathrm{CV}(\lambda) = \sqrt{\exp(\sigma^2) - 1}$ (Section V.S1.1).

Abundance covariates. The effects of c spatio-temporally varying covariates $\mathbf{x_{s,t}}$ on abundance are typically modelled as log-linear fixed effects. At sampling site s and time point t, $\log(N_{s,t}) = \log(\hat{N_{s,t}}) + \alpha_{s,t}$, with $\log(\hat{N_{s,t}}) = \mathbf{x_{s,t}}\boldsymbol{\beta} + \omega_s$. The vector $\boldsymbol{\beta}$ contains the fixed effects coefficients, ω_s is a random intercept that accounts for between-site variation in abundance, and the variance of $\alpha_{s,t}$, σ^2_α, accounts for temporal variation in population abundance at site s that is not accounted for by the other effects. Conditionally on fixed and spatial random effects, we still have $V[N_{s,t}] = \hat{N_{s,t}}^2\upsilon^2$ with $\upsilon = \sqrt{\exp(\sigma^2_\alpha) - 1}$ from the variance of a log-Normal variable. Under the counting protocol defined above, expected count $\lambda_{s,t} = pN_{s,t}$ satisfies $\log(\lambda_{s,t}) = \log(p) + \log(\hat{N_{s,t}}) + \alpha_{s,t}$. Since the additive constant $\log(p)$ will only change the value of the intercept term in $\boldsymbol{\beta}$, fitting $\log(\lambda_{s,t}) = \mathbf{x_{s,t}}\boldsymbol{\beta} + \omega_s + \alpha_{s,t}$ allows to measure population variability υ from the standard deviation parameter of the temporal random effect.

V.S1.3 Variability of the sum of Poisson-log-Normal variables

Sum of Poisson-log-Normals. The distribution f of two random variables X_1 and X_2 is *reproducible* when $X_1 + X_2$ is also distributed according to f, possibly with different parameters. A mixed Poisson distribution is reproducible when its mixing distribution is itself reproducible (Karlis and Xekalaki 2005). Since a common approximation for the distribution of the sum of log-normally distributed variables is the log-normal distribution (Dufresne 2004), the Poisson-log-Normal mixture is approximately reproducible.

Community abundance. As per the main Methods, let species counts X_i follow Poisson-log-Normal distributions with expected counts λ_i and population variabilities $\upsilon_i = \mathrm{CV}(\lambda_i)$. We also define $\mu_i = E[\lambda_i]$, the average expected species counts. Let community count $Y = \sum_i X_i$ and assume (see above) that Y also follows a Poisson-log-Normal distribution with expected count λ_c, community variability υ_c and average community count μ_c. Note that, from expectation and variance of a sum of random variables and

from the covariance of mixed Poisson distributions:

$$E[Y] = E\left[\sum_i X_i\right] = \sum_i E[X_i] = \sum_i E[\lambda_i]$$

$$V[Y] = \sum_i V[X_i] + \sum_i \sum_{i \neq j} \mathsf{Cov}[\lambda_i, \lambda_j]$$

Species synchrony. Let $\upsilon_{c|\text{ synchr.}} = \mathsf{CV}(\lambda_{c|\text{synchr.}})$ the variability that the community would have if, all else being equal, species' environmental fluctuations were perfectly synchronized. In that case, $\mathsf{Cov}[\lambda_i, \lambda_j]_{|\text{synchr.}} = \sqrt{V[\lambda_i]V[\lambda_j]}$ for all species pairs i and j (Loreau and de Mazancourt 2008). Community variance under perfect synchrony, $V[Y_{c|\text{ synchr.}}]$ is thus written:

$$\begin{aligned} V[Y_{c|\text{ synchr.}}] &= \sum_i V[X_i] + \sum_i \sum_{j \neq i} \sqrt{V[\lambda_i]V[\lambda_j]} \\ \iff V[\lambda_{c|\text{ synchr.}}] &= \sum_i \sqrt{V[\lambda_i]}\sqrt{V[\lambda_i]} + \sum_i \sqrt{V[\lambda_i]} \sum_{j \neq i} \sqrt{V[\lambda_j]} \\ &= \left(\sum_i \sqrt{V[\lambda_i]}\right)^2 = \left(\sum_i \mu_i \upsilon_i\right)^2 \end{aligned}$$

Taking the square root and dividing by $E[Y] = \mu_c$,

$$\upsilon_{c|\text{ synchr.}} = \sum_i \frac{\mu_i}{\mu_c} \upsilon_i$$

This is the abundance-weigthed average population variability (Thibaut and Connolly 2013), but using species variabilities measured from the Poisson-log-Normal model. Observed community variability υ_c can thus be decomposed as:

$$\upsilon_c = \left(\sum_i \frac{\mu_i}{\mu_c} \upsilon_i\right) \sqrt{\phi_\lambda} = \upsilon_{\text{pop}} \sqrt{\phi_\lambda}$$

The index $\sqrt{\phi_\lambda}$ is 0 if species fluctuations perfectly compensate for each other and 1 under perfect synchrony. Here, the subscript λ clarifies that expressions for computing μ_i, μ_c and υ_i from estimated parameters will depend on which distribution is adopted for λ, but we write $\sqrt{\phi}$ in the main text where λ is assumed to be log-Normal.

Statistical averaging effect. $\upsilon_{c|\text{ ip.}}$, the variability that the community would have if species' fluctuations were independent, can be computed similarly to $\upsilon_{c|\text{ synchr.}}$. There, $\mathsf{Cov}[\lambda_i, \lambda_j]_{|\text{ ip.}} = 0$. Thus,

$$
\begin{aligned}
V[\lambda_{c|\text{ ip.}}] &= \sum_i V[\lambda_i] \\
&= \sum_i \mu_i^2 \upsilon_i^2 \\
\iff \upsilon_{c|\text{ ip.}} &= \sqrt{\sum_i \frac{\mu_i^2}{\mu_c^2} \upsilon_i^2}
\end{aligned}
$$

This allows to compute the strength of the statistical averaging effect as $\text{SAE} = \frac{\upsilon_{\text{pop}}}{\upsilon_{c|\text{ ip.}}}$. Notice that, when species counts are perfectly even, *i.e.* $\mu_i = \mu_c/S$ with S the number of species,

$$
\begin{aligned}
\text{SAE}_{|\text{ even means}} &= \frac{\sum_i \upsilon_i / S}{\sqrt{\sum_i \upsilon_i^2 / S^2}} \\
&= \frac{\sum_i \upsilon_i}{\sqrt{\sum_i \upsilon_i^2}}
\end{aligned}
$$

Further, if all species variabilities are equal to υ_{pop}, then $\text{SAE}_{|\text{ even means and variabilities}} = \sqrt{S}$. Just like shown by Zhao et al. (2022) for true abundance data, the statistical averaging effect thus inherently accounts for the effect of the number of species and of the evenness of species counts and variabilities on community variability.

V.S1.4 Link to the coefficient of variation

Here we compare our approach with measuring population variability from the coefficient of variation of observed counts distributed according to model 1 from the main methods.

Single species. For X following a Poisson-log-Normal (Equation 1) and using the variance formula for the mixed Poisson distribution (Section V.S1.2),

$$
\begin{aligned}
V[X] &= E[X] + V[\lambda] \\
&= E[\lambda] + \upsilon^2 E[\lambda]^2 \\
\iff \text{CV}(X) &= \sqrt{\frac{1}{E[\lambda]} + \upsilon^2}
\end{aligned}
\tag{V.S1}
$$

When expected count is high, which is the case for community counts, $\text{CV}(X)$ well approximates υ. However, for low mean counts, $\text{CV}(X)$ overestimates variability, and the lower the mean count, the stronger the variability overestimation.

Community variability. Now consider S species with abundances X_i and $Y = \sum_i X_i$, with variabilities υ_i and υ_c. We write species means $\mu_i = E[X_i]$ and community mean $\mu_c = E[Y]$. Also let $\sigma_i = \sqrt{V[X_i]} = \sqrt{\mu_i + \upsilon_i^2 \mu_i^2}$ and $\sigma_c = \sqrt{V[Y]} = \sqrt{\mu_c + \upsilon_c^2 \mu_c^2}$. In the classical species synchrony framework, $\phi_{\text{LdM}} = \frac{\sigma_c^2}{(\sum_i \sigma_i)^2}$. From Equation V.S1 above,

$$\sqrt{\phi_{\text{LdM}}} = \frac{\sqrt{\mu_c(1 + \upsilon_c^2 \mu_c)}}{\sum_i \sqrt{\mu_i(1 + \upsilon_i^2 \mu_i)}}$$

With the average population coefficient of variation weighted by relative average counts $\text{CV}_{\text{pop}} = \sum_i \frac{\mu_i}{\mu_c} \sqrt{\frac{1}{\mu_i} + \upsilon_i^2}$, we still have $\text{CV}_{\text{pop}} \sqrt{\phi_{\text{LdM}}} = \sqrt{\frac{1}{\mu_c} + \upsilon_c^2} = \text{CV}[Y]$, *i.e.* the result of Thibaut and Connolly (2013). However community coefficient of variation and its two components do not match their counterparts from Section V.S1.3. For illustration, in the perfect mean and variabilities evenness case where $\mu_i = \mu_c / S$ and $\upsilon_i = \upsilon_{\text{pop}} \forall i$ and under perfect community synchrony, community variability is equal to υ_{pop} and therefore $CV(Y)_{|\text{ synchr.}} = \sqrt{\frac{1}{\mu_c} + \upsilon_{\text{pop}}^2}$. Moreover, for equal means and equal variabilities,

$$\text{CV}_{\text{pop}|\text{ synch.}} = \sum_i \frac{1}{S} \sqrt{\frac{S}{\mu_c} + \upsilon_{\text{pop}}^2} = \sqrt{\frac{S}{\mu_c} + \upsilon_{\text{pop}}^2} > \upsilon_{\text{pop}}$$

$$\sqrt{\phi_{\text{LdM}|\text{ synch.}}} = \frac{\sqrt{\frac{1}{\mu_c} + \upsilon_{\text{pop}}^2}}{\text{CV}_{\text{pop}|\text{ synch.}}} < 1$$

In this case, community coefficient of variation is higher than community variability, and its components are overestimated (for the weighted average coefficient of variation) or underestimated (for species synchrony from coefficient of variations). Again when mean species counts are high, CV_{pop} and $\sqrt{\phi_{\text{LdM}}}$ converge towards their counterparts from Section V.S1.3.

V.S2 Method validation

We used simulated data in order to check that model (2) allowed to correctly estimate temporal variability for short but spatially-replicated time series.

Data simulation. Synthetic data was drawn following model (2) with constant sampling effort. Additionally to time, a fixed categorical effect was included in the covariates. In real data, between-site variability often arises because of unmeasured environmental variables that influence species counts. Since these environmental variables are often spatially correlated, ω_s was sampled from a Gaussian random field of known variance parameter σ_ω, with site locations uniformly attributed across the field's boundaries. Temporal variation was incorporated as the sum of a known long-term trend β_1 and of a first-order autoregressive process generated with known stationary variance σ^2_α. Combinations of low or high between-site variability and low or high temporal variability were investigated.

Model fitting. For each parameter combination, 200, 500 or 1000 time series with 10 time steps were simulated. Dataset size was thus 2000, 5000 or 10000 observations. Model (1) was fit on each dataset in a Bayesian framework under the Integrated Nested Laplace Approximation using `inlabru` (Bachl et al. 2019). After fitting the model, quantiles of the posterior distributions for all parameters were recorded. Dataset sampling followed by model fitting was replicated 100 times for each combination of parameters and dataset size for a total of 2400 estimations. Estimation was deemed reliable when the width of the 95%-interquantiles of the posterior distribution for σ_α was less than 5 times its mode and the mode was higher than 0.05 but lower than 2. Rates of unreliable estimation ranged from 0 to 34.5% based on parameter values (Fig. V.S1). Within reliable estimates, we labelled as errored the estimations for which the 95% posterior interquantile range did not include the true value of σ^2_α.

Results. Estimation performs the best when temporal variability is high and between-site variability is low, and always improves with dataset size (Fig. V.S1). When both between-site and temporal variabilities are low, error rates are high even at high dataset size when estimates become more reliable (Fig. V.S1, top left). High temporal variability is associated to fewer unreliable estimations regardless of between-site variability, but when between-site variability is high the error rates can be high, even for high temporal variability (Fig. V.S1, bottom right). Fixed effects coefficients were easier to estimate than random effects parameters.

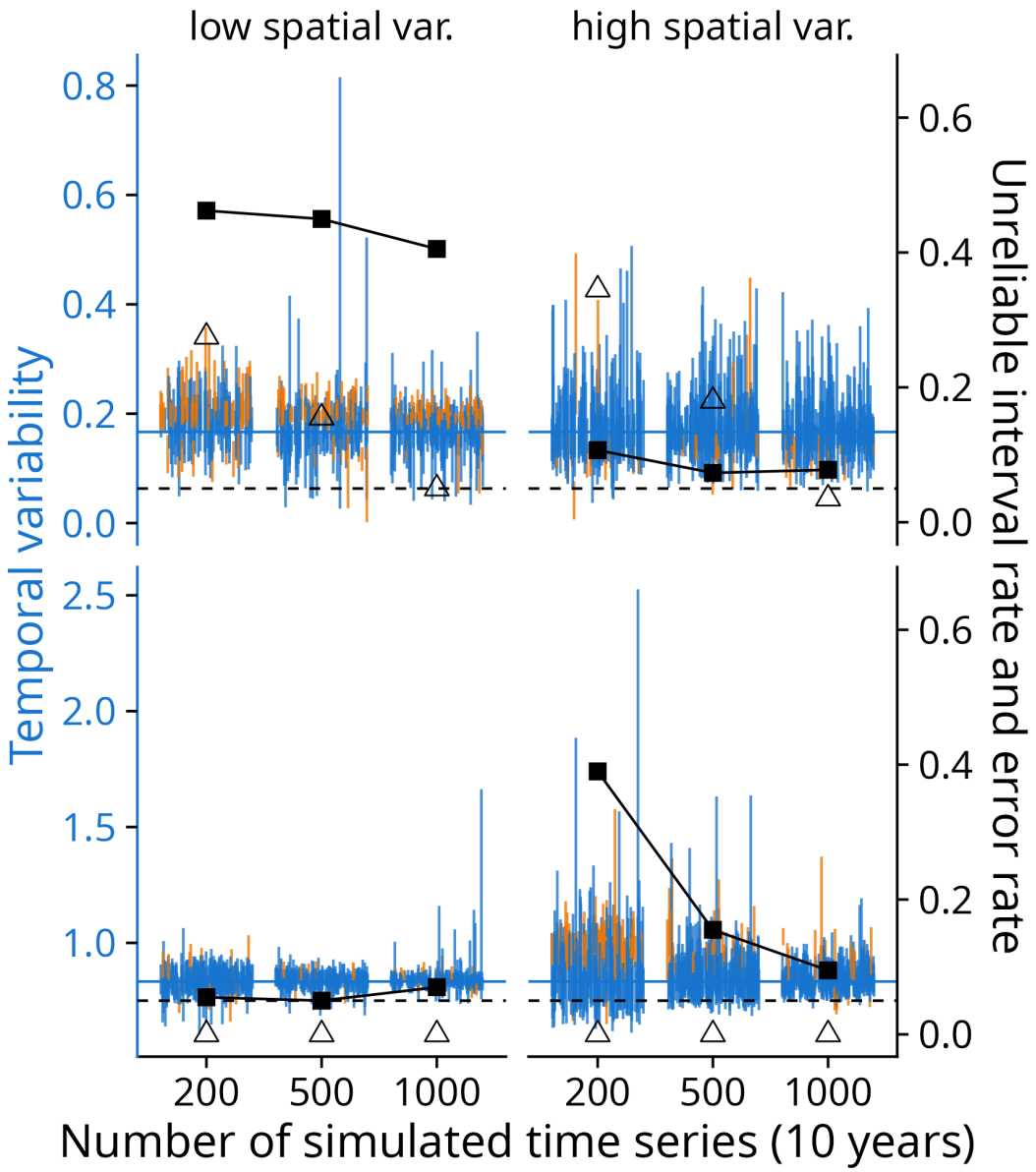

Figure V.S1: **Temporal variability estimation for low (top row) and high (bottom row) temporal variability.** Colored elements are on the scale of estimated temporal variability. Vertical intervals are 95% posterior interquantiles for the temporal variability parameter for "reliable" estimations only. They are colored in blue when they contain the true values (horizontal solid lines) and colored in orange if not. Black-and-white elements are proportions. For each parameter combination, open triangles denote the proportion of unreliable estimations for temporal variability. Filled squares denote the proportion (within the reliable estimations) of intervals that do not include the true value. The horizontal dashed black lines indicates 0.05, a 5% error or unreliability rate.

V.S3 Supplemental figures

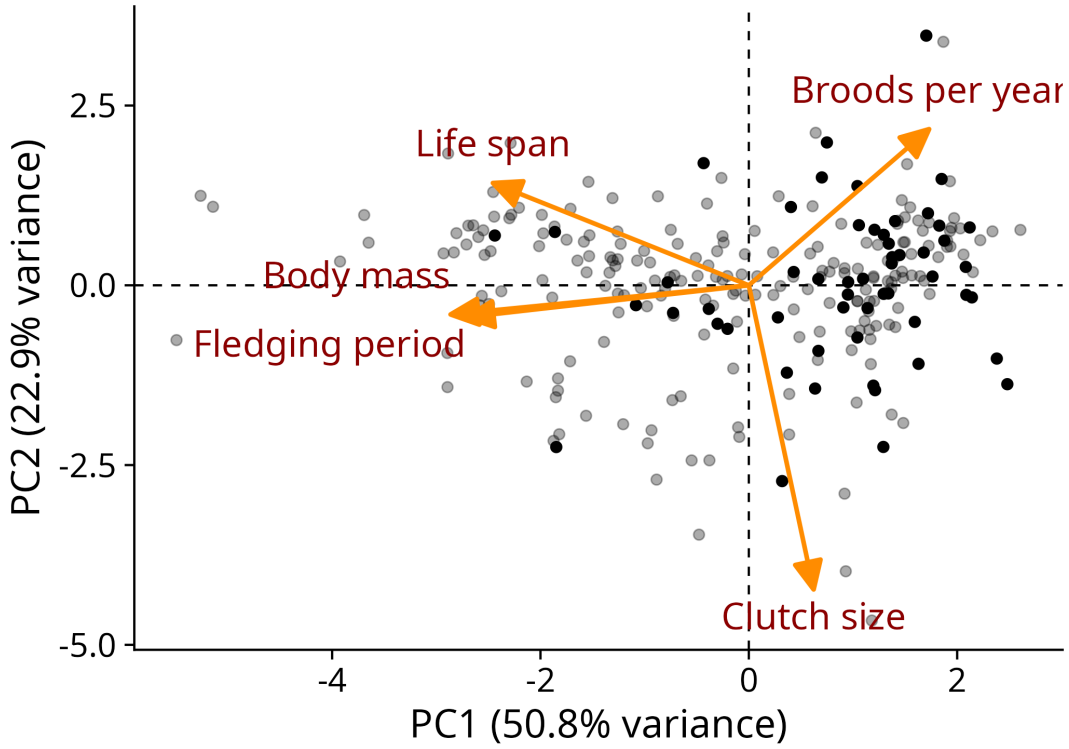

Figure V.S2: **Principal component analysis (PCA) of bird life history traits for bird species nesting in France.** Dots correspond to species scores in the PCA for the 55 species list used in further statistical analyses (solid dots) and the other 210 species (semi-transparent dots). Orange arrows are labelled with the underlying traits they correspond to and indicate the trait's rotation value in the PCA, stretched with a factor 5. Dashed lines indicate the horizontal and vertical axes, for which PC values are zero.

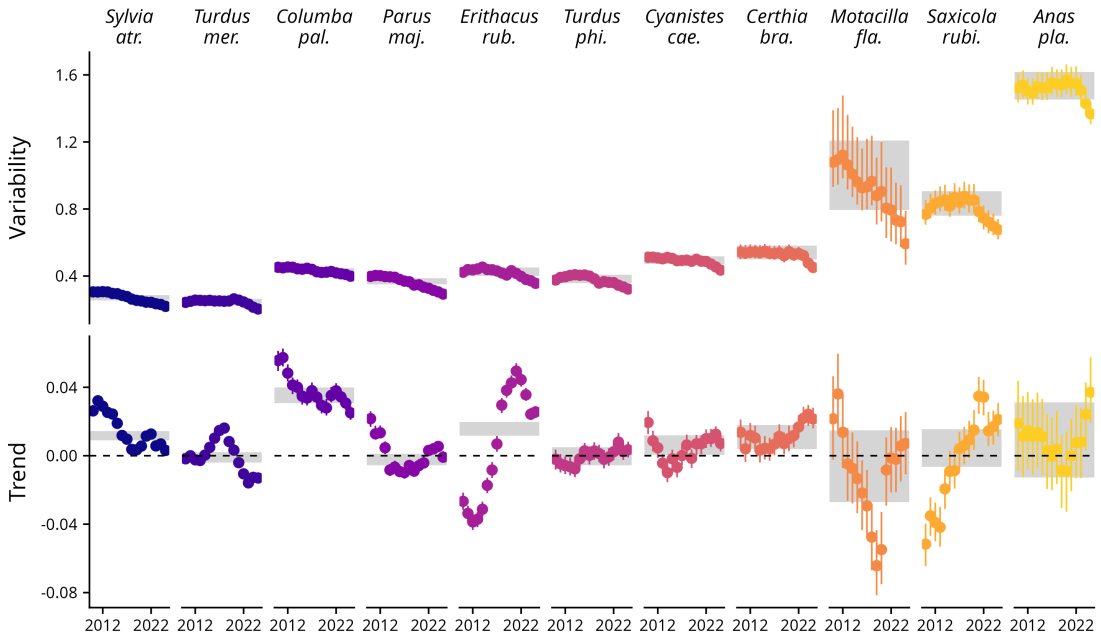

Figure V.S3: **Variability and trend for species with detected change in variability.** Line intervals are 95% interquantiles of the posterior distributions for 10-year trend and for detrended variability, with points at the modes of the posteriors. For each species and each stability dimension, the grey ribbon shows the interval delimited by the medians across windows of the lower and upper 95% quantiles of the posteriors. Species are ordered from left to right by order of decreasing data availability over the whole dataset.

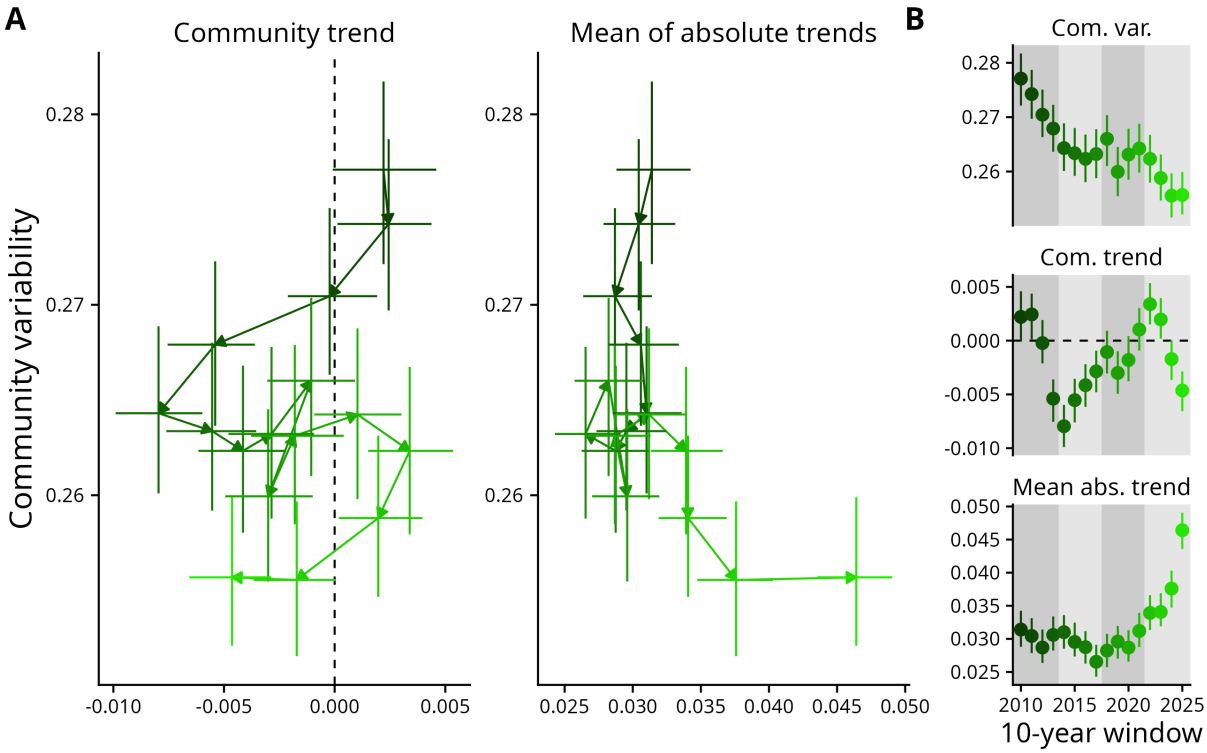

Figure V.S4: **Changes in community stability dimensions across moving windows for more species.** 108 (2011-2020) to 122 species (2016-2025) are considered for computing community variability and trend and mean of absolute trends for each moving window. (A) Community variability across community trend and mean absolute trend for all moving windows. Consecutive moving windows are linked by arrows. For each stability component, line intervals indicate the 95% interquantile range of the posterior distribution (for community variability and community trend), or of the propagated posterior distribution (for mean absolute trend). They intersect at the corresponding posterior modes. (B) Stability metrics across moving windows for all stability metrics of panel A.

VI . Discussion

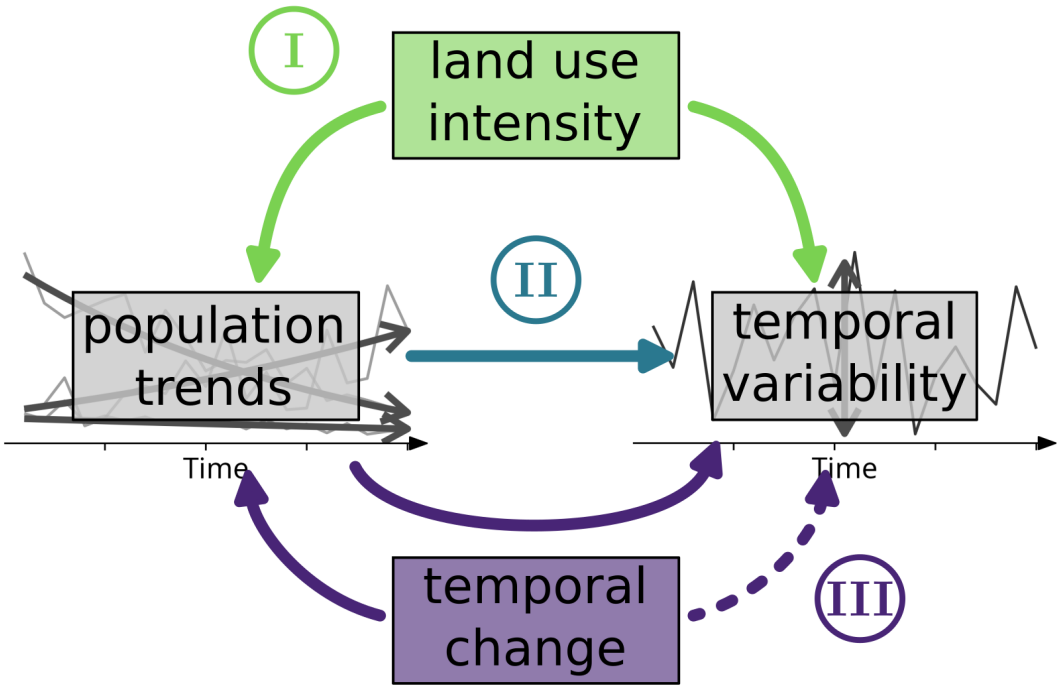

Figure VI.0: **General summary of results.** (I) Trends and variability share a common variation with land use intensity in Chapter 1. (II) In Chapter 2, press perturbations that cause trends in stochastic models are expected to cause changes in variability. (III) Over moving windows in Chapter 3, trends change over time and generate changes in community composition, driving changes in community variability.

In this thesis, we bring long-term population trends and temporal variability in a unified conceptual framework where both are integrative dimensions of ecological stability in the face of long-term changes and stochasticity of environmental conditions. Our main contribution thus lies in tackling the fact that natural communities' response to environmental stochasticity occurs around long-term trajectories generated by long-term changes in environmental conditions. Across study scales, the links between these dimensions varies. At a local scale in bird communities across France, land use intensity is associated to stronger trends and stronger variability (Chapter 1). In a theoretical model, long-term environmental change induces not only population trends but also transient changes in variability (Chapter 2). Finally, at the scale of France, temporal changes in community variability can be linked to changes in averaged community composition, which are generated by population trends (Chapter 3). Trends and variability are therefore linked in complex relationships across spatio-temporal and ecological scales (Fig. VI.0). Considering them as such opens new perspectives for analyzing biodiversity monitoring data and for developments in ecological theory. We have indeed seen that long-term trends and temporal variability allow to detect changes in ecological response to complex perturbations across scales. In this section, I discuss our results and their possible developments, notably possible ways to progress from pattern detection to mechanistic understanding and discussing how our conceptual framework relates to existing work. I then discuss considering ecological stability far from equilibrium and, finally, I share perspectives from joining community ecology with conservation ecology.

VI.1 Conjointly measuring trends and variability to better understand biodiversity dynamics

In the following, I first discuss how our efforts to consider long-term population trends relate with existing studies of temporal variability. Conversely, I expand on how perspectives from ecological stability can shed light on existing work on multi-species trends. Conjointly, trends and variability offer a multi-dimensional view of ecological response to perturbation regimes, and I discuss how this could be translated in existing frameworks in community ecology. In this endeavour, I expand on the questions of the interplay of spatio-temporal scales and of the role of functional traits in complex perturbation regimes as crucial research avenues both in community ecology and in biodiversity conservation.

Detrending temporal variability

In the study of temporal variability in ecology, our work is, to our knowledge, a first attempt at considering long-term trends not as biases to correct for (Lepš et al. 2019, Valencia et al. 2020a), but as valuable ecological information (Chapters 1 and 3). Moreover, we show that measuring the long-term trend can help generate predictions on the strength of temporal variability (Chapter 2). Since changes in community composition are widespread in natural communities (Dornelas et al. 2023), tackling long-term population trends brings the study of temporal variability in a more realistic setting. In multi-faceted perturbation regimes, community response to perturbations occurs at different time scales and thus different aspects of community stability may be responsible for responding to different aspects of the perturbation regime. The question of the apparent independence between trends and variability is then crucial. Our empirical work indeed points towards conditional independence between stability dimensions after accounting for their shared determinants in Chapter 1, and also in Chapter 3 when assuming that temporal changes represent changes in multiple anthropogenic drivers. Contrastingly, our theoretical work predicts a mechanistic influence of trends on variability (Chapter 2). If transient changes in variability are proven to be negligible in real-world systems, then community stability can be assessed for long-term changes and for environmental stochasticity separately, but interactions between integrative stability dimensions should otherwise be considered.

For disentangling population variability from long-term trajectories, it is important to acknowledge that (log-)linear detrending, the method we used in this thesis (Chapters 1 and 3), is but one option in a vast range of detrending methods in ecological time series analysis. In extensions of the generalized linear mixed model, polynomial effects and smoothing splines can be used to estimate complex shapes of long-term trajectories (Fewster et al. 2000, Rigal et al. 2020). In state space modelling, temporal dynamics can be fitted as any deterministic population growth model (de Valpine and Hastings 2002), with extensions to many observation models (Knape et al. 2011). In empirical dynamic modeling, no hypothesis on the shape of temporal dynamics is required (Sugihara et al. 2012). Total observed variance can then be decomposed into process noise, observation error and deterministic component (Clark et al. 2022). However, results of non-parametric methods are complex to interpret and to summarize across different species, and state-space models require substantial data quantity (Auger-Méthé et al. 2021).

Simulation-based studies could be an occasion to try these different data analysis methods in the context of the specific problem of disentangling long-term trajectories from population variability. Fundamental results on properties of the actual process are important, but drawing simulations from an observational model conditioned on the true process is the next step in order to evaluate how they could be detected in real-world data. This is needed in order to build more adequate comparisons between empirical and theoretical settings, and could stimulate the consideration of long-term trajectories in theoretical perspectives.

Stability-based view of multi-species trend indices

Conversely, integrating theory from ecological stability can help guiding the interpretation of long-term population trends, even more so for multi-species trend indices. From estimates of several log-linear population trends at large scales, the most frequent multi-species index is the geometric mean of relative abundance compared to an initial condition (Buckland et al. 2005, Loh et al. 2005). Since it translates to the mean of population trends estimated on a logarithmic scale (Vimont et al. 2025), we will hereafter call it the *mean trend*. For a given pool of species, the mean trend thus represents the expectation for the value obtained by drawing a single species at random from the pool and measuring its trend, which is often misinterpreted by non-specialists. For instance, in a recent newspaper article covering an updated estimate of the mean trend of birds in France (Le Monde-AFP 2026), the mean trend is interpreted by the journalists as the trend of community abundance. For diverse communities such as wild birds, where different species have different responses to long-term environmental changes (Vimont et al. 2025), increasing trends of some species and declining trend of others will compensate for each other's contributions to the mean trend. It is then very well possible to observe strong community composition changes with a mean trend close to zero, or even an increasing mean trend in the presence of many declining species (Grzegorczyk et al. 2025). A common method is then to compute the mean trend for groups of species within the species pool that share a common trait (Bowler et al. 2019), like the Farmland Bird Index (Gregory et al. 2005), which is the mean trend of a set of farmland specialist bird species.

For a given set of species, stability-based trend indices bring complementary information to the mean trend (Fig. VI.1). The trend of the total abundance of the community considers each species' relative

abundance, and thus may be driven by the trends of the most abundant species. However, since the total number of individuals is a fundamental facet of local biodiversity, its trend is an important facet of community change (Gaüzère et al. 2025). In fitted estimates from Chapter 3, there are two periods where the mean trend for 55 species of birds in France is slightly positive but close to zero: for moving windows 2001-2010 to 2003-2012 and for 2013-2022 to 2016-2025 (Fig. VI.1B). These periods are respectively characterized by a positive community trend and a strong but declining mean absolute trend for the first period, and a negative community trend with increasing mean absolute trend for the second period (Fig. VI.1B). The difference in the sign of community trend between the two periods may indicate that in the first period, many abundant species increase, while in the second period many abundant species decrease. Moreover, in both periods the changes in the mean absolute trend are consistent with changes in the strength of community trend, which means that changes in trends are shared across the species abundance distribution (mismatches and their eventual directions would indicate that changes in trend disproportionately affect rare or abundant species). Comparing the mean absolute trend (for Chapters 1 and 3) or the trend of total community abundance (for Chapter 3) for different species groups and measuring individual species' contributions to these indices is possible (Gaüzère et al. 2019). This may help verifying these supplemental interpretations of community-level trend variations from Chapter 3.

Under ever-increasing anthropogenic pressures, a high mean absolute trend in a given (meta-)community may indicate a more concerning situation than another community with a lower mean absolute trend, but this general interpretation may not hold across all settings. Effective species-targeted conservation efforts drive strong positive population trends, which can contribute positively to the mean absolute trend. For example, due to population reinforcement programmes (Bonnet-Lebrun et al. 2025), the French population of the white stork *Ciconia ciconia* is estimated to have been multiplied by a factor of almost 7 (confidence interval: [2.7;16.2]) between 2001 and 2019 (Fontaine et al. 2020). However, in Chapter 1, the observed increase of the mean absolute trend in farmland and urban areas compared to forests is well in line with the interpretation that "stronger trends means increased perturbations" and that these perturbations should be curbed to conserve biodiversity. Verifying the general interpretation that increased mean absolute trend in disturbed habitats is driven by increases in generalist species and decreases in specialist species could be carried out by more closely inspecting each species' contribution to patterns from Chapter 1. In Chapter 3, we notice that the mean absolute trend, after declining before 2020, is

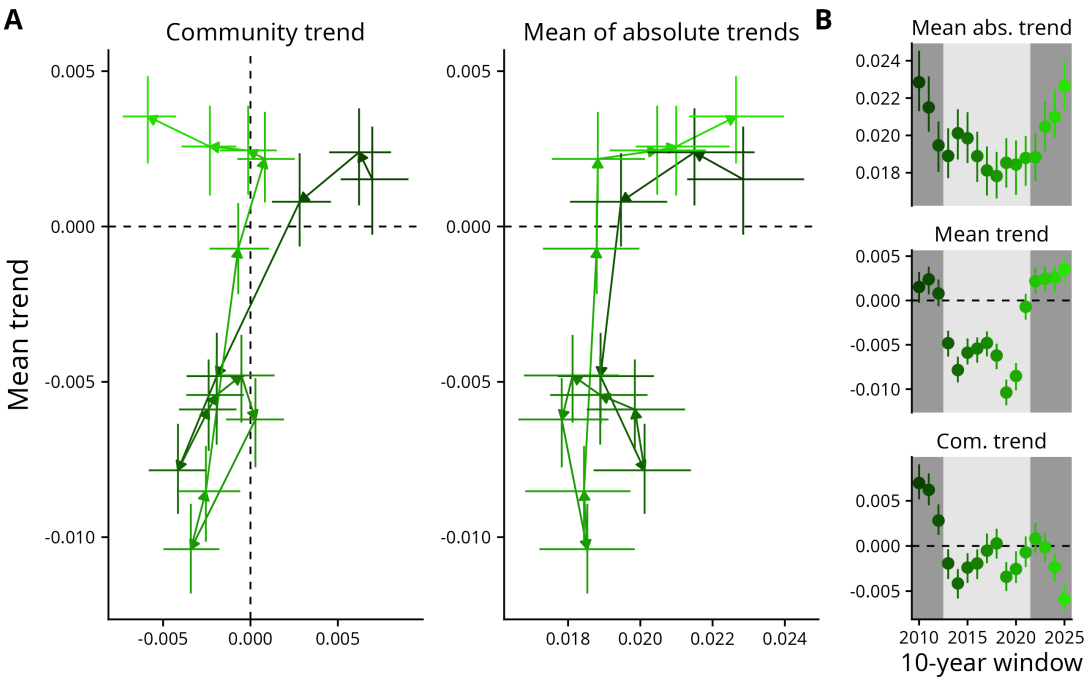

Figure VI.1: **Supplementary result of Chapter 3: mean trend and community-level trend components across all moving windows.** Data from the French Breeding Bird Survey, see Methods in Chapter 3. (A) Mean trend across community trend and mean absolute trend for all moving windows. (B) Trend metrics across moving windows for all metrics from panel A. Periods highlighted in dark gray have similar mean trend values but different patterns for the two other community-level trend components. See Chapter 3 for method details.

on a recent increasing trajectory associated to declines of abundant species. Here again, inspecting species contributions to aggregated metrics and confronting them with expert knowledge on bird temporal dynamics may guide more precise interpretations. In both Chapters, the mean absolute trend allows to assess how the perturbation regime is affecting the community as a whole, which is less direct for the mean trend.

Ecological response across spatio-temporal scales

Under multi-faceted perturbation regimes (Fig. VI.2) for which individual species' responses are difficult to measure, unraveling integrative dimensions of ecological stability offers a way to assess how anthropogenic pressures impact biodiversity dynamics. However, the multi-scale nature of ecological systems under complex perturbations remains a conceptual challenge. In Chapter 1, we see that both trends and variability are associated to the type of land use, a plot-level environmental variable (Fig. VI.2C), but that only variability was associated to differences in surrounding landscape-level land use intensity. At a national scale in Chapter 3, we notice temporal changes in species-level trends coinciding with

changes in community-level variability indices. Our results therefore contribute to filling some existing conceptual gaps, as studies on long-term trends usually focus on species at large geographical scales and studies on temporal variability mostly focus on community-level variability components at landscape or plot level. Extensions of our approaches may allow to better understand these scaling effects (Fig. VI.3), but progress is needed in our understanding of how perturbations spread in space and in driver attribution across scales.

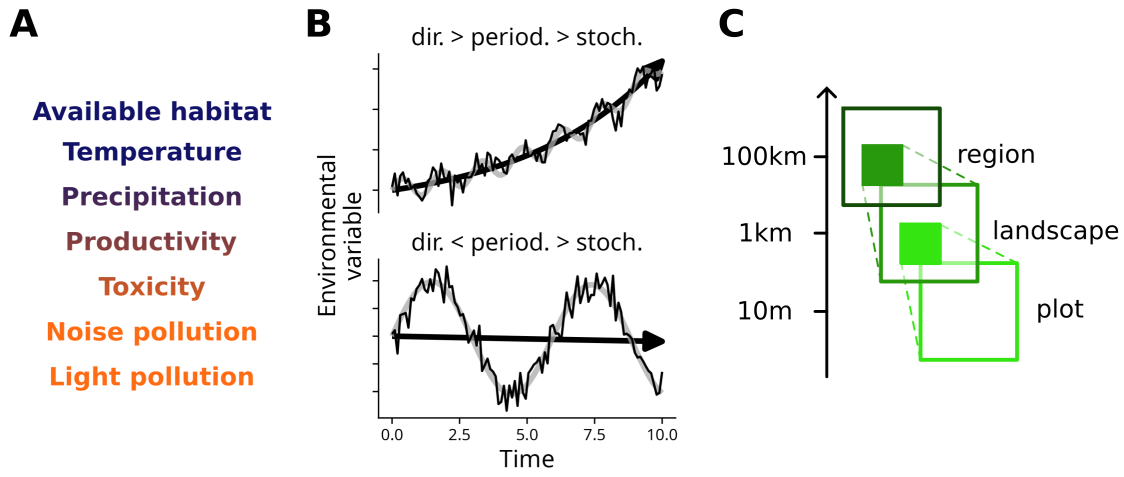

Figure VI.2: **Complex perturbation regimes.** (A) Multiple environmental variables conjointly act on ecological systems, with possible feedbacks. (B) Different temporal dynamics of perturbations. The temporal variation of a given variable can be directional (dir.), periodic (period.) or stochastic (stoch.), and the relative influences of these components can vary across environmental variables or scales. In the top panel, directionality dominates while in the bottom panel, periodicity dominates, with similar strength of stochasticity in the two panels. (C) Spatial scales of perturbations. A spatially-varying pressure at a large scale can be assumed constant at a smaller scale (*e.g.* mean precipitation varies across bioregions but is similar among nearby plots), but local perturbation regimes can be propagated to larger scales by species dispersal.

A general expectation from the theory of ecological stability is that variability decreases as the scale used to aggregate abundances increases: it is the invariability-area relationship (Wang et al. 2017). It is explained by the expectation that spatial synchrony, the synchronicity across space of a given species' local responses to environmental fluctuations (Wang et al. 2019), decreases with geographical scale as considering larger spatial extents increases the probability to cover areas with desynchronized environmental fluctuations. Moreover, as the number of species also typically increases with geographical extent, the diversity-instability relationship propagates across geographical scales (Liang et al. 2025). However, long-term changes in environmental conditions are expected to be shared across larger geographical extents than environmental fluctuations, and we detect long-term changes in community variability components likely caused by long-term population trends (Chapter 3). Relaxing the equilibrium

assumption in models describing the invariability-area relationship is needed in order to understand how the spatial scaling of the temporal dimensions of the perturbation regime (Fig. VI.2B) affects the spatial scaling of multiple integrative stability dimensions. A starting point could be based on similar approaches as those in Zelnik et al. (2018), where disturbances of varying spatial extents are introduced in a landscape with a fluctuating environment. The inclusion of perturbation scenarii across spatial scales in the models from Chapter 2 will likely increase their complexity beyond the point where analytical approximations are feasible, but numerical investigation could reveal helpful patterns.

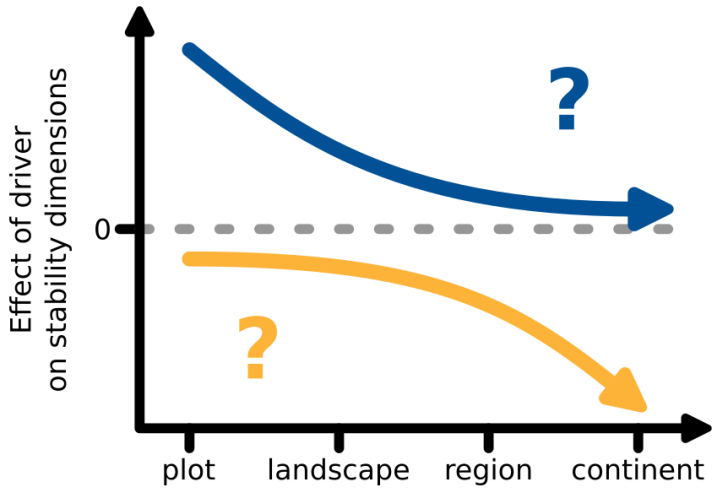

Figure VI.3: **Driver effect on stability dimensions across scales.** The blue arrow denotes a strong positive effect at local scales that becomes weaker at larger geograhical extents, while the orange arrow denotes a negative effect amplified at higher geographical scales. Inspired from Gaüzère et al. (2025), who use a similar representation of driver effects on community composition at several scales.

Temporal and spatial scales do not only add up, they are intertwined in how anthropogenic drivers affect the perturbation regime, and in how species respond to perturbations. These scaling effects may be one of the reasons for our difficulty to predict trends and variability from species traits both at species and community levels (Chapter 3). As an example anthropogenic driver, I will consider land artificialization, a component of land use change that reduces habitat availability for many bird species (Batáry et al. 2018). At the scale of the European Union, current policies have the goal to reduce net artificialization to zero by 2050 (European Commission 2021). Member states then integrate this objective in their national legislation, which is a first scale effect: policies adopted to meet the 2050 objective vary across European states. In France, the 2021 “Climate and Resilience” law sets a regulatory framework on artificialization that allows policies to differ across administrative regions and across municipalities within regions based on past efforts to curb artificialization as well as local socio-economic contexts (Ministère de la Transition

écologique 2023). The long-term change in available bird habitat due to artificialization is thus expected to differ across countries and, within countries, across administrative layers, that each correspond to increasingly smaller spatial scales (Fig. VI.2C). When a given plot becomes built up, dispersal may allow birds to settle in neighboring habitats, but this is only possible if the landscape contains enough suitable habitat (Şekercioğlu et al. 2015). Long-term change in bird habitat availability at the landscape scale will depend on the municipality policy, and change at the regional scale will depend on the administrative region's policy. Moreover, if other environmental conditions (*e.g.* climate) restrict a species' geographical range, dispersal to less artificialized plots may not be possible. Therefore, even species that share their response to a single environmental variable may not follow the same temporal dynamics if their geographical distributions make them subjected to different perturbation regimes of their common driver.

Functional traits under complex perturbation regimes

In the response-effect trait framework, the response of ecosystem function to perturbations is driven by the coupling between species' traits that explain the response and species' traits that are responsible for a given ecosystem function (Lavorel and Garnier 2002). In complex perturbation regimes, traits responsible for the response to the environmental variables that change in the long term may also be responsible for the response to the fluctuating environmental variables, and the coupling between these response traits and effect traits can drive the temporal dynamics of ecosystem functioning (Fig. VI.4). In the case of wild bird communities, the current state of our work in Chapter 3 shows that identifying these traits is more difficult than expected, although strong correlations between various bird traits are expected at macroevolutionary scales (Pigot et al. 2020).

In order to better identify the traits associated to long-term trends or to temporal variability, one of the missing links is the impact of environmental variables on species demographic rates. This caveat could be filled by comparing results from the French Breeding Bird Survey dataset that we used and its "FBBS-Capture" programme, a yearly capture-mark-recapture campaign across France. Using this dataset, Thépault et al. (2025) show that the *reproductive output* of birds in France generally increases with spring temperature, but can decrease in already warm regions. Moreover, they show that, among migratory species, only species that migrate over short distances benefit from warm temperatures in early spring. Also using "FBBS-Capture" data, Ghislain et al. (2024) notice that yearly variations in *survival*

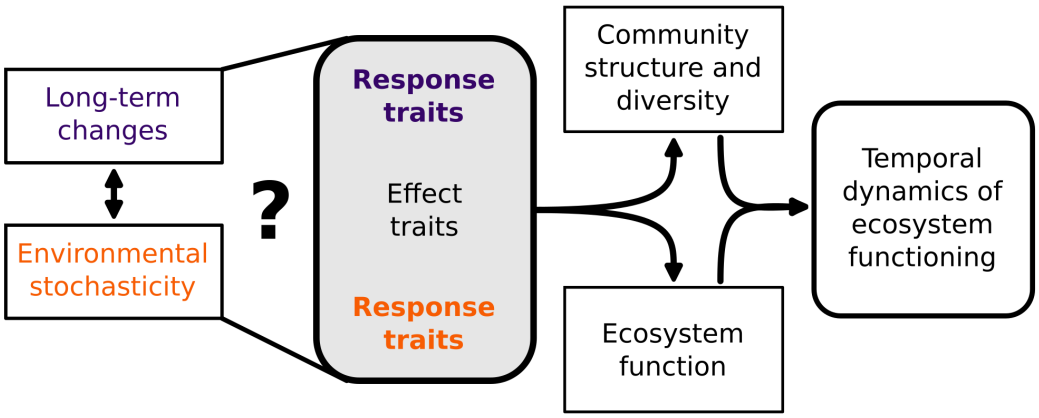

Figure VI.4: **The response-effect framework under long-term changes and environmental stochasticity.** Adapted from Lavorel and Garnier (2002).

rate are synchronous across species, without being driven by yearly climate anomalies and regardless of their migratory behaviour. The difference in results between these two studies shows the possibility that a given environmental variable (here, climate anomalies) or a given trait (here, migratory behaviour) may not affect all demographic rates in the same way. This could be modelled in extensions of our approach in Chapter 2 by introducing perturbations on survival or reproduction parameters, and empirical validation could benefit from integration of work on demographic rates with the measurement of integrative stability dimensions of abundance. In Integral Population Models, demographic rates and abundance can be estimated conjointly (Merow et al. 2014, Doak et al. 2021), and variability parameters could be integrated by writing adequate random effects. Seeing which environmental variables influence which demographic rates and how this translates to changes in population abundance would provide a stronger mechanistic background to the measurement of integrative stability dimensions, but propagating these findings to (meta-)communities may prove difficult.

VI.2 Ecological stability out of equilibrium

Even outside evolutionary perspectives, the absence of a fixed equilibrium in ecological processes is well recognized (Oro and Martínez-Abraín 2023), but the mathematical and conceptual convenience of considering fixed equilibria has generated a gap between working hypotheses in theoretical ecology and real-world situations (Kéfi et al. 2019). Although equilibrium-based ecological theory has a substantial predictive power (*e.g.* Liang et al. 2025), it is likely that observed variation in empirical patterns is not

entirely caused by measurement error and could partly be explained by out-of-equilibrium dynamics.

Diversity and stability out of equilibrium

In existing investigations of the mechanisms of the diversity-invariability relationship in empirical communities, long-term population trends have largely been neglected (Lepš et al. 2019, Xu et al. 2021). In Chapter 1, we notice a positive relationship between species richness and bird detrended population variability. This corroborates previous findings (White et al. 2023), but we do so in a setting where we explicitly separate population variability from trends (Lepš et al. 2019). We also notice a negative relationship between local species richness and the average strength of local population trends among farmland bird communities, which is robust to uncertainty propagation. If this relationship is not explained by confounding factors like unmeasured habitat quality or changes in perturbation regime (Chapter 1), the underlying mechanisms of such a negative diversity-trend relationship are unknown. Interspecific competition is expected to increase population variability (Ives et al. 1999), and is therefore likely to also increase the strength of long-term population trends (Chapter 2), but more thorough theoretical work is needed.

Moreover, if the two integrative stability dimensions also interact at some scale (Chapters 2 and 3), then known experimental designs and long-term datasets which allowed to investigate the diversity-invariability relationship, as in Xu et al. (2021), could be revisited in order to measure long-term population trends and assess their impact. Compared to biodiversity monitoring datasets, experimental designs may also be more likely to meet the assumption that perturbation regimes are constant across tested diversity levels (Wang et al. 2021). This makes them suitable to further investigation of residual association between trends and variability after their common drivers have been considered. Since environmental stochasticity has also been shown to influence species persistence (Adler and Drake 2008), trends and variability could then have complex positive feedback relationships, with possible hysteresis hindering the return to reference dynamical conditions (Pichon et al. 2026). Integrating several perturbation regimes in dynamical models of perturbed communities could help evaluating the possibility for such feedbacks and ultimately enhance our understanding of the stability of ecological systems. Depending on which value systems would prefer to conserve stability to long-term changes or stability to environmental stochasticity, different environmental management priorities could then be acknowledged.

Theory for out-of-equilibrium dynamics

In theoretical ecology, the study of transient dynamics is closely associated to the study of systems with alternative stable states (Hastings et al. 2018), with long transients as a peculiar phenomenon where systems can stay far from their equilibrium for significant lengths of time (e.g. Arumugam et al. 2021). There, stochastic dynamics allow or prevent long transients depending on the relative time scales of deterministic and stochastic dynamics (Shoemaker et al. 2020, Hastings et al. 2021). Our work in Chapter 2 illustrates the other end of the problem: in systems with a single stable state, variability can be reduced or enhanced depending on properties of the press perturbation that generated the transient regime. Strikingly, both phenomena relate to the shape of the potential function of the system's deterministic dynamics (Box 3). In stochastic systems, quasi-potentials allow to describe the potential function while taking stochasticity into account, and could be a powerful framework to join work on long transients with our theoretical models (Nolting and Abbott 2016).

Box 3: The potential function and the stability landscape

For a given deterministic system, the potential function is a function whose partial derivatives across the state space's dimensions give the opposite of the system's dynamics. It is the mathematical concept behind the intuition where dynamical systems' states are seen as marbles rolling on a stability landscape, as the slope of the potential function can be interpreted as the "slope" of the stability landscape (Dakos and Kéfi 2022).

With a one-dimensional state variable x and a dynamical system F, the potential function P is defined as:

$$\frac{\mathrm{d}x}{\mathrm{d}t} = F(x)$$

$$F = -\frac{\partial P}{\partial x}$$

In Chapter 2, lower values of the potential function of the deterministic dynamics when the population is below carrying capacity generate higher variability for population increases, while higher values of the potential function above carrying capacity generate variability deficits during declines. For long transients (Hastings et al. 2018), low values of the potential function in some directions of the parameter space cause slow transient dynamics.

Throughout this dissertation, we often assumed that long-term changes are intense and fast enough

to move communities far from their hypothetical equilibria, which is debatable for many systems. On the other side of the spectrum, the impact of very slow long-term change on ecological stability is extensively studied in the context of critical slowing down (Scheffer 2009). There, systems with alternative stable states become increasingly less able to recover from perturbations as a catastrophic shift to another stable state approaches (Scheffer et al. 2001). Under environmental stochasticity, this loss of stability as the tipping point becomes closer translates into measurable changes in integrative stability dimensions like an increase in temporal autocorrelation of system state concurrent with changes in temporal variance (Dakos et al. 2012). Long-term trends and population variability can thus be related because of critical slowing down under slow environmental change, related because of the confounding effect of common anthropogenic drivers (Chapters 1 and 3), or related because of transient dynamics under fast environmental change (Chapter 2).

The question of the interrelations between long-term population trends and temporal variability thus is, from a theoretical point of view, a question of the temporal dimensionality of the perturbation regime (Fig. VI.2B). From a conservation point of view, if and how management decisions can efficiently address different aspects of the perturbation regime is an open question (Hastings 2016). As we show with bird temporal dynamics, advanced empirical knowledge of the systems of interest is required to assess which perturbation scales are at play, which then helps generating predictions on ecological responses. However, we have seen that both empirical and theoretical challenges remain in the detection and understanding of ecological response out of equilibrium.

VI.3 Ecological theory, biodiversity conservation, and beyond

Biodiversity monitoring datasets provide substantial data quantity on ongoing biodiversity dynamics, allowing to test ecological hypotheses while also addressing pressing biodiversity conservation issues (*e.g.* Olivier et al. 2020). In this dissertation, we were able to investigate the relationships between two integrative dimensions of ecological stability in bird communities, over different geographical scales. In the following, I discuss my experience working with large datasets to connect theoretical ecology, empirical community ecology and biodiversity conservation. Finally, I discuss what is still needed in order to go from detecting patterns of ecological stability dimensions to building operational stability-based biodiversity indicators.

Empirical datasets in the theory-observation dialogue

Not all theoretical work in ecology has the maturity required to be directly comparable with empirical settings, and even fewer are able to actually predict real-world patterns. Well-known exceptions include the Yellowstone trophic cascade after wolf reintroduction (Ripple and Beschta 2012a, Ripple et al. 2025), or the positive relationship between island size and species richness in island biogeography (Whittaker et al. 2017). During my Master's studies, I was lucky to be part of the empirical validation of one of these theoretical frameworks that see themselves well reflected in empirical data. With increasing aridity, the changes in the spatial patterns of drylands vegetation in satellite imagery remarkably matched the changes predicted by mechanistic models of biotic interactions (Kéfi et al. 2007, Kéfi et al. 2024). This agreement between model predictions and observed patterns involved adequate measurement methods (for this work, see above in Section VI.1, "Detrending temporal variability") as well as good understanding of the fundamental mechanisms that drive the pattern of interest.

Table VI.1: **When theory and observation match.** Spatial patterns of drylands vegetation are predicted with a cellular automaton model, and empirically measured from satellite imagery. Adapted from Kéfi et al. (2024).

Spatial pattern metric	Effect of aridity (theory)	Effect of aridity (empirical)
Maximum vegetation patch size	↘↘	↘↘
Patch size distribution slope	↘↘	↘↘
Patch size distribution cutoff	↗	↗
Bare soil connectivity	↗↗	↗↗
Spectral density ratio	↗↗	↗
Spatial variance	↗↗	↗↗

In the case of bird temporal dynamics, the difficulty in explaining dynamical patterns from biodiversity monitoring data partly lies in the fact that the fundamental drivers of population dynamics act at the level of individuals. For example, the per capita growth rate in the logistic growth is a representation for the average individual's contribution to population abundance (Lande et al. 2003), but does not fully account for many demographic phenomena. The empirical side of this question lies in disentangling which functional traits explain environmental impact on which demographic parameters, but theoretical

work is also needed in order to better integrate demography in the study of community stability under complex perturbation regimes (see Section VI.1, “Functional traits under complex perturbation regimes”). Improving our mechanistic understanding of temporal dynamics will help to generate more testable hypotheses and go from pattern detection to causal attribution.

In that endeavor, large-scale biodiversity monitoring datasets are very valuable as their substantial sampling effort allows testing for even small effects, but as we have seen above, meaningful interpretation of detected patterns tests rely on good mechanistic understanding. Volunteer-based biodiversity monitoring programmes like the French Breeding Bird Survey have substantial geographical coverage and allow to engage already knowledgeable citizens in the scientific process. Other structured volunteer-based biodiversity monitoring programmes coordinated at the National Museum of Natural History follow the temporal dynamics of natural plant (Martin et al. 2019), bat (Froidevaux et al. 2025) and butterfly communities (Agnoux et al. 2026), with most analyses focusing on the estimation of long-term population trends. As we have seen that links between long-term trends and temporal variability can vary across ecological scales, it is likely that they also vary across considered taxa. In order to estimate population and community detrended variability for other taxa than birds, integrating less structured sampling protocols may help increasing data availability (Nabias et al. 2025, Agnoux et al. 2026), but will require adequate statistical modelling.

Towards stability-based biodiversity indicators ?

The capacity for integrative stability dimensions to reflect the ecological response to complex perturbation regimes makes them candidates as indicators of the dynamic response of biodiversity to natural and anthropogenic perturbation regimes. Ecological indicators, or biodiversity indicators, are simple indexes that summarize the available information on an ecological situation in order to guide policy decisions (Levrel et al. 2007). The concept of indicator comes from the social sciences, with the rise of “national statistics” generating indicators on the socio-economic situation like the national debt, the unemployment rate or the Human Development Index (Custodio et al. 2023). For biodiversity indicators, they are the meeting point of ecological indexes built by ecologists and political decision-making. In socio-economic policy, Desrosières (2003) summarize quality criteria for indicators (Tab. VI.2), which can also be applied in environmental policy. Ecological indicators of good quality should therefore be relevant, precise, timely,

accessible, comparable and coherent. I discuss some aspects of what it would take for stability-based indicators to meet these criteria.

Table VI.2: **Criteria for the quality of an indicator.** Definitions adapted and translated from French to English from Desrosières (2003).

Criterion	Definition
(i) *relevance*	An indicator is relevant when it fills the needs of its users
(ii) *precision*	An indicator is precise when its estimated value is close to the true unknown one
(iii) *timeliness and punctuality*	An indicator is timely when the timeline of its estimation is coherent with policy timelines
(iv) *accessibility and clarity*	An indicator is accessible when its presentation allows correct interpretation by users
(v) *comparability*	An indicator is comparable when its interpretation is equivalent when measured at another time and geographical location
(vi) *coherence*	An indicator is coherent when, measured from different sources, its interpretation stays similar

One could reasonably argue that suggesting novel indicators from the ecological side of conservation sciences only, without consulting with potential users, as I'm doing now, is one of the mechanisms that prevents satisfying the relevance criterion (Sébastien et al. 2017). However, the increasing recognition that conservation should be concerned with ecosystem processes that cannot be summarized only by fixed states (Harmsen and Foster 2014, Oro and Martínez-Abraín 2023), but requires evaluating dynamical properties (Carpenter et al. 2015), has not been translated in many ecological indicators. For example, in the 27 indicators used by the Intergovernmental Panel on Biodiversity and Ecosystem Services to evaluate temporal change in nature contributions to people (IPBES 2019b p. 23), only two refer to dynamical conditions ("stability of land use and land cover" and "ability of ecosystems to absorb and buffer hazards"). The will to maintain ecosystem dynamics while guaranteeing ecological stability could emerge as a narrative for environmental policies capable of embracing the dynamic properties of life (Sarrazin and Lecomte 2016), for which stability-based biodiversity indicators could thus be very relevant.

A critical question in the precision, comparability and coherence of stability-based biodiversity indicators will be the choice (or lack of choice) of a reference dynamical condition. The scarcity of documented

ecological time series before the last half of the twentieth century already is a problem for building reference conditions for indicators based on abundance (Magurran et al. 2010, Duchenne et al. 2022). It is thus even more problematic for building reference values for population trends or for temporal variability, which requires several consecutive measurements. For birds, historical accounts of bird local abundance before the modernization of agriculture exist (Shrubb 2003), but reviewing historical sources in search for information on variability or trends in order to infer responses to historical perturbation regimes is a difficult task. Alternatively, eco-evolutionary models integrating both speciation and community dynamics may help building expectations for variability and trends given past environmental scenarios.

For indicators based on the strength of population trends, an added difficulty for precision lies in the directionality of these trends. For example, landowner and writer Isabella Tree reports population increases of formerly locally extinct turtle doves (*Streptopelia turtur*) after implementing rewilding practices at landscape scale on her family's estate (Tree 2018). Evidence shows that rewilding practices are indeed favorable for biodiversity (Hart et al. 2023), but they would likely show signs of strong reshuffling of local community composition. Implementing some kind of directionality in indexes based on the strength of population trends is therefore needed for correct interpretation as a biodiversity indicator. However, under changing environments, deciding on a reference state for the direction of community reshuffling is debatable (Carroll et al. 2023).

For timeliness, once the methodology of an ecological indicator is decided, updating its status in a timely manner after data collection is possible. However, stability-based indicators would always require to consider data from several years in order to measure trends and variability. Substantial time lag between eventual policy implementation and subsequent change in stability-based indicator value is thus expected, even more than for abundance-based indicators (Watts et al. 2020). The accessibility of stability-based indicators will likely rely on substantial efforts of co-constructing narratives on the dynamic properties of ecological systems. Moreover, on the technical side, summarizing complex dynamics is likely to be difficult to document and to convey to users.

In adaptive co-management, a multitude of stakeholders interact and implement policies that are constantly evaluated and discussed based on the information gained during and after policy implementation (Levrel 2007). With stability-based indicators, negotiating arenas would gain information not only on current states and their capacity to fulfil the legitimate stakeholders' needs, but also on dynamical

properties of ecological systems. The time scales of ecological dynamics and their associated risks to stakeholders could then be considered in policy design. This process could then allow to iteratively bring human activities to a sustainable pathway while conserving the capacity to adapt to unforeseen changes. However, a major requirement for these decision processes to success is the just consideration of each stakeholder's needs, which is hindered by social inequalities (Ruano-Chamorro et al. 2023).

VI.4 Conclusion

In this discussion, we have seen that measuring two integrative dimensions of ecological stability allows a better understanding of biodiversity dynamics, paving the way for better driver attribution across scales and study systems. Moreover, the recognition of out-of-equilibrium dynamics in ecological systems often assumed to follow static equilibria bridges the gaps between well-established conceptual frameworks and empirical settings. Increasing dialogues between community ecology and conservation ecology deepens our understanding on biodiversity dynamics, and can help building biodiversity indicators that reflect the dynamic properties of ecological systems.

Overall, this work contributes to tackling the multi-dimensionality of ecological response to complex perturbation regimes in the case of bird temporal dynamics in France and in theoretical approaches. Theoretical understanding on how multiple perturbation regimes may interact across geographical scales is needed for better prediction of stability patterns, and empirical challenges lie in attributing dynamical patterns to species traits and to anthropogenic drivers. While the level of proof required to justify profound change in our interactions with our abiotic and biotic environment is more than met (IPBES 2019b), current environmental value systems and power relationships put the biosphere on a critically unsafe trajectory (Richardson et al. 2023). New indicators, new ways to measure biodiversity dynamics, or new conceptual syntheses are not a prerequisite to initiating social change, and highlighting the complexity of biodiversity dynamics must not be used to cast doubts on the clear unsustainability of current human activities (Saunders et al. 2025). By contributing to unravel fascinating aspects of the functioning of life, my PhD work and those of many others do help deepening existing knowledge, but more importantly add novel items in the ever-increasing list of how much is at stake in the current environmental crises.

References

Abbott, K. C. 2011. A dispersal-induced paradox: Synchrony and stability in stochastic metapopulations. - Ecol. Lett. 14: 1158–1169.

Abrams, P. A. 1993. Effect of increased productivity on the abundances of trophic levels. - Am. Nat. 141: 351–371.

Adler, P. B. and Drake, J. M. 2008. Environmental variation, stochastic extinction, and competitive coexistence. - Am. Nat. 172: E186–E195.

Adler, K. and Jedicke, E. 2022. Landscape metrics as indicators of avian community structures – a state of the art review. - Ecol. Indic. 145: 109575.

Agnoux, S., Fontaine, B., Dozières, A., Jeanmougin, M., Schmucki, R., Vimont, M. and Martin, G. 2026. Contribution of citizen sciences to the production of butterfly species long-term trends. - Insect Conserv. Diversity 19: 828–844.

Aitchison, J. and Ho, C. H. 1989. The multivariate Poisson-log normal distribution. - Biometrika 76: 643–653.

Allen, D. C., Bateman, H. L., Warren, P. S., de Albuquerque, F. S., Arnett-Romero, S. and Harding, B. 2019. Long-term effects of land-use change on bird communities depend on spatial scale and land-use type. - Ecosphere 10: e02952.

Anderson, S. C., Ward, E. J., English, P. A., Barnett, L. A. K. and Thorson, J. T. 2024. sdmTMB: An R package for fast, flexible, and user-friendly generalized linear mixed effects models with spatial and spatiotemporal random fields. - bioRxiv

Archer, S. R., Andersen, E. M., Predick, K. I., Schwinning, S., Steidl, R. J. and Woods, S. R. 2017. Woody plant encroachment: Causes and consequences. - In: Briske, D. D. (ed), Rangeland systems: Processes, management and challenges. Springer Cham, pp. 25–84.

Arditi, R. and Ginzburg, L. R. 1989. Coupling in predator-prey dynamics: Ratio-Dependence. - J. Theor. Biol. 139: 311–326.

Arnoldi, J.-F., Loreau, M. and Haegeman, B. 2016. Resilience, reactivity and variability: A mathematical comparison of ecological stability measures. - J. Theor. Biol. 389: 47–59.

Arnoldi, J.-F., Loreau, M. and Haegeman, B. 2019. The inherent multidimensionality of temporal variability: How common and rare species shape stability patterns. - Ecol. Lett. 22: 1557–1567.

Arumugam, R., Lutscher, F. and Guichard, F. 2021. Tracking unstable states: Ecosystem dynamics in a changing world. - Oikos 130: 525–540.

Auger-Méthé, M., Newman, K., Cole, D., Empacher, F., Gryba, R., King, A. A., … Thomas, L. 2021. A guide to state–space modeling of ecological time series. - Ecol. Monogr. 91: e01470.

Bachl, F. E., Lindgren, F., Borchers, D. L. and Illian, J. B. 2019. Inlabru: An R package for Bayesian spatial modelling from ecological survey data. - Methods Ecol. Evol. 10: 760–766.

Barbier, M. and Loreau, M. 2019. Pyramids and cascades: A synthesis of food chain functioning and stability. - Ecol. Lett. 22: 405–419.

Barbier, M., Arnoldi, J.-F., Bunin, G. and Loreau, M. 2018. Generic assembly patterns in complex ecological communities. - PNAS 115: 2156–2161.

Barnagaud, J.-Y., Gaüzère, P., Zuckerberg, B., Princé, K. and Svenning, J.-C. 2017. Temporal changes in bird functional diversity across the United States. - Oecologia 185: 737–748.

Barnes, M. D., Craigie, I. D., Harrison, L. B., Geldmann, J., Collen, B., Whitmee, S., … Woodley, S. 2016. Wildlife population trends in protected areas predicted by national socio-economic metrics and body size. - Nat. Commun. 7: 12747.

Batáry, P., Kurucz, K., Suarez-Rubio, M. and Chamberlain, D. E. 2018. Non-linearities in bird responses

across urbanization gradients: A meta-analysis. - Global Change Biology 24: 1046–1054.
Battisti, C., Poeta, G. and Fanelli, G. 2016. Heterogeneity, Dynamism, and Diversity of Natural Systems. - In: Battisti, C. . . . Fanelli, G. (eds), An Introduction to Disturbance Ecology: A Road Map for Wildlife Management and Conservation. Springer International Publishing, pp. 1–6.
Bellard, C., Marino, C. and Courchamp, F. 2022. Ranking threats to biodiversity and why it doesn't matter. - Nat. Commun. 13: 2616.
Benson, R. B. J. and Druckenmiller, P. S. 2014. Faunal turnover of marine tetrapods during the Jurassic–Cretaceous transition. - Biol. Rev. 89: 1–23.
Benton, T. G., Bryant, D. M., Cole, L. and Crick, H. Q. P. 2002. Linking agricultural practice to insect and bird populations: A historical study over three decades. - J. Appl. Ecol. 39: 673–687.
Benton, T. G., Vickery, J. A. and Wilson, J. D. 2003. Farmland biodiversity: Is habitat heterogeneity the key? - Trends Ecol. Evol. 18: 182–188.
Bertness, M. D., Brisson, C. P., Coverdale, T. C., Bevil, M. C., Crotty, S. M. and Suglia, E. R. 2014. Experimental predator removal causes rapid salt marsh die-off. - Ecol. Lett. 17: 830–835.
Bezanson, J., Karpinski, S., Shah, V. B. and Edelman, A. 2012. Julia: A Fast Dynamic Language for Technical Computing. - arXiv
Bideault, A., Galiana, N., Zelnik, Y. R., Gravel, D., Loreau, M., Barbier, M. and Sentis, A. 2021. Thermal mismatches in biological rates determine trophic control and biomass distribution under warming. - Glob. Change Biol. 27: 257–269.
Blüthgen, N., Simons, N. K., Jung, K., Prati, D., Renner, S. C., Boch, S., . . . Gossner, M. M. 2016. Land use imperils plant and animal community stability through changes in asynchrony rather than diversity. - Nat. Commun. 7: 10697.
Boennec, M., Dakos, V. and Devictor, V. 2024. Non-linearity and Temporal Variability Are Overlooked Components of Global Vertebrate Population Dynamics. - Divers. Distrib. 30: e13932.
Bonnet-Lebrun, A.-S., Lemaire-Patin, R., Gendre, N., Dugué, H., Dupuy, J., Pedespan, A., . . . Barbraud, C. 2025. Habitat availability is insufficient to explain regional variations in white stork breeding habitat preference. - Oikos 2025: e11214.
Bowler, D. E., Hof, C., Haase, P., Kröncke, I., Schweiger, O., Adrian, R., . . . Böhning-Gaese, K. 2017. Cross-realm assessment of climate change impacts on species' abundance trends. - Nat. Ecol. Evol. 1: 0067.
Bowler, D. E., Heldbjerg, H., Fox, A. D., de Jong, M. and Böhning-Gaese, K. 2019. Long-term declines of european insectivorous bird populations and potential causes. - Conserv. Biol. 33: 1120–1130.
Bowler, D., Richter, R. L., Eskildsen, D., Kamp, J., Moshøj, C. M., Reif, J., . . . Voříšek, P. 2021. Geographic variation in the population trends of common breeding birds across central Europe. - Basic Appl. Ecol. 56: 72–84.
Braga, P. H. P., Hébert, K., Hudgins, E. J., Scott, E. R., Edwards, B. P. M., Sánchez Reyes, L. L., . . . Crystal-Ornelas, R. 2023. Not just for programmers: How GitHub can accelerate collaborative and reproducible research in ecology and evolution. - Methods Ecol. Evol. 14: 1364–1380.
Brlík, V., Šilarová, E., Škorpilová, J., Alonso, H., Anton, M., Aunins, A., . . . Klvaňová, A. 2021. Long-term and large-scale multispecies dataset tracking population changes of common European breeding birds. - Sci. Data. 8: 21.
Brooks, M. E., Kristensen, K., van Benthem, K. J., Magnusson, A., Berg, C. W., Nielsen, A., . . . Bolker, B. M. 2017. glmmTMB balances speed and flexibility among packages for zero-inflated generalized linear mixed modeling. - R J. 9: 378–400.
Brose, U., Williams, R. J. and Martinez, N. D. 2006. Allometric scaling enhances stability in complex food webs. - Ecol. Lett. 9: 1228–1236.
Brousil, M. R., Filazzola, A., Meyer, M. F., Sharma, S. and Hampton, S. E. 2023. Improving ecological data science with workflow management software. - Methods Ecol. Evol. 14: 1381–1388.
Browning, T. J. and Moore, C. M. 2023. Global analysis of ocean phytoplankton nutrient limitation reveals high prevalence of co-limitation. - Nat. Commun. 14: 5014.
Brown, J. H., Gillooly, J. F., Allen, A. P., Savage, V. M. and West, G. B. 2004. TOWARD A METABOLIC THEORY OF ECOLOGY. - Ecology 85: 1771–1789.
Bucher, E. H. 1992. The Causes of Extinction of the Passenger Pigeon. - In: Power, D. M. (ed), Current Ornithology. Springer US, pp. 1–36.
Buckland, S. T. 2001. Introduction to distance sampling : Estimating abundance of biological populations. - Oxford University Press.
Buckland, S. T., Magurran, A. E., Green, R. E. and Fewster, R. M. 2005. Monitoring change in biodiversity through composite indices. - Phil. Trans. R. Soc. B 360: 243–254.

Buckland, S. T., Rexstad, E. A., Marques, T. A., Oedekoven, C. S., et al. 2015. Distance sampling: Methods and applications. - Springer.
Bunin, G. 2017. Ecological communities with lotka-volterra dynamics. - Phys. Rev. E 95: 42414.
Burns, F., Eaton, M. A., Burfield, I. J., Klvaňová, A., Šilarová, E., Staneva, A. and Gregory, R. D. 2021. Abundance decline in the avifauna of the european union reveals cross-continental similarities in biodiversity change. - Ecol. Evol. 11: 16647–16660.
Busch, M., Katzenberger, J., Trautmann, S., Gerlach, B., Dröschmeister, R. and Sudfeldt, C. 2020. Drivers of population change in common farmland birds in Germany. - Bird Conserv. Int. 30: 335–354.
Cai, T., Wu, G., Sun, L., Zhang, Y., Peng, Z., Guo, Y., ... Zhang, B. 2021. Biogeography and diversification of Old World buntings (Aves: Emberizidae): Radiation in open habitats. - J. Avian Biol.
Campetella, G., Chelli, S., Simonetti, E., Damiani, C., Bartha, S., Wellstein, C., ... Canullo, R. 2020. Plant functional traits are correlated with species persistence in the herb layer of old-growth beech forests. - Sci. Rep. 10: 19253.
Cardinale, B. J., Duffy, J. E., Gonzalez, A., Hooper, D. U., Perrings, C., Venail, P., ... Naeem, S. 2012. Biodiversity loss and its impact on humanity. - Nature 486: 59–67.
Carignan, V. and Villard, M.-A. 2002. Selecting Indicator Species to Monitor Ecological Integrity: A Review. - Environ. Monit. Assess. 78: 45–61.
Carpenter, S. R., Brock, W. A., Folke, C., van Nes, E. H. and Scheffer, M. 2015. Allowing variance may enlarge the safe operating space for exploited ecosystems. - PNAS 112: 14384–14389.
Carroll, T., Cardou, F., Dornelas, M., Thomas, C. D. and Vellend, M. 2023. Biodiversity change under adaptive community dynamics. - Global Change Biol. 29: 3525–3538.
Carson, R. 1962. Silent spring. - Houghton Mifflin Company.
Ceballos, G., Ehrlich, P. R., Barnosky, A. D., García, A., Pringle, R. M. and Palmer, T. M. 2015. Accelerated modern human–induced species losses: Entering the sixth mass extinction. - Sci. Adv. 1: e1400253.
Cebrian, J. and Lartigue, J. 2004. Patterns of herbivory and decomposition in aquatic and terrestrial ecosystems. - Ecol. Monogr. 74: 237–259.
Chase, J. M. 2000. Are there real differences among aquatic and terrestrial food webs? - Trends Ecol. Evol. 15: 408–412.
Chase, J. M., Leibold, M. A., Downing, A. L. and Shurin, J. B. 2000. The effects of productivity, herbivory, and plant species turnover in grassland food webs. - Ecology 81: 2485–2497.
Chase, J. M., Jeliazkov, A., Ladouceur, E. and Viana, D. S. 2020. Biodiversity conservation through the lens of metacommunity ecology. - Ann. N. Y. Acad. Sci. 1469: 86–104.
Chichorro, F., Juslén, A. and Cardoso, P. 2019. A review of the relation between species traits and extinction risk. - Biol. Conserv. 237: 220–229.
Christianen, M. J. A., Herman, P. M. J., Bouma, T. J., Lamers, L. P. M., van Katwijk, M. M., van der Heide, T., ... van de Koppel, J. 2014. Habitat collapse due to overgrazing threatens turtle conservation in marine protected areas. - Proc. R. Soc. B 281: 20132890.
Clark, T. J. and Luis, A. D. 2020. Nonlinear population dynamics are ubiquitous in animals. - Nat. Ecol. Evol. 4: 75–81.
Clark, A. T., Arnoldi, J.-F., Zelnik, Y. R., Barabas, G., Hodapp, D., Karakoç, C., ... Harpole, S. 2021. General statistical scaling laws for stability in ecological systems. - Ecol. Lett. 24: 1474–1486.
Clark, A. T., Mühlbauer, L. K., Hillebrand, H. and Karakoç, C. 2022. Measuring stability in ecological systems without static equilibria. - Ecosphere 13: e4328.
Clavel, J., Julliard, R. and Devictor, V. 2011. Worldwide decline of specialist species: Toward a global functional homogenization? - Front. Ecol. Environ. 9: 222–228.
Cloern, J. E. 1996. Phytoplankton bloom dynamics in coastal ecosystems: A review with some general lessons from sustained investigation of san francisco bay, california. - Rev. Geophys. 34: 127–168.
Cooper, N. and Hsing, P.-Y. 2025. Guide to Reproducible Code. - British Ecological Society.
Cowie, R. H., Bouchet, P. and Fontaine, B. 2022. The Sixth Mass Extinction: Fact, fiction or speculation? - Biol. Rev. 97: 640–663.
Craven, D., Eisenhauer, N., Pearse, W. D., Hautier, Y., Isbell, F., Roscher, C., ... Manning, P. 2018. Multiple facets of biodiversity drive the diversity–stability relationship. - Nat. Ecol. Evol. 2: 1579–1587.
Cuervo, J. J. and Møller, A. P. 2013. Temporal Variation in Population Size of European Bird Species: Effects of Latitude and Marginality of Distribution. - PLoS One 8: e77654.
Custodio, H. M., Hadjikakou, M. and Bryan, B. A. 2023. A review of socioeconomic indicators of sustainability and wellbeing building on the social foundations framework. - Ecol. Econ. 203: 107608.

Dakos, V. and Kéfi, S. 2022. Ecological resilience: What to measure and how. - Environ. Res. Lett. 17: 043003.
Dakos, V., Boulton, C. A., Buxton, J. E., Abrams, J. F., Arellano-Nava, B., Armstrong McKay, D. I., ... Kéfi, S. 2024. Tipping point detection and early warnings in climate, ecological, and human systems. - Earth Syst. Dyn. 15: 1117–1135.
Dakos, V., van Nes, E. H., D'Odorico, P. and Scheffer, M. 2012. Robustness of variance and autocorrelation as indicators of critical slowing down. - Ecology 93: 264–271.
Danet, A., Kéfi, S., Johnson, T. F. and Beckerman, A. P. 2025. Response diversity is a major driver of temporal stability in complex food webs. - Proc. R. Soc. B 292: 20250730.
Danet, A., Mouchet, M., Bonnaffé, W., Thébault, E. and Fontaine, C. 2021. Species richness and food-web structure jointly drive community biomass and its temporal stability in fish communities. - Ecol. Lett. 24: 2364–2377.
Datseris, G. 2018. DynamicalSystems.jl: A Julia software library for chaos and nonlinear dynamics. - J. Open Source Softw. 3: 598.
Davison, C. W., Rahbek, C. and Morueta-Holme, N. 2024. Changes in danish bird communities over four decades of climate and land-use change. - Oikos 2024: e10697.
de Bello, F., Lavorel, S., Hallett, L. M., Valencia, E., Garnier, E., Roscher, C., ... Lepš, J. 2021. Functional trait effects on ecosystem stability: Assembling the jigsaw puzzle. - Trends Ecol. Evol. 36: 822–836.
de Valpine, P. and Hastings, A. 2002. Fitting Population Models Incorporating Process Noise and Observation Error. - Ecol. Monogr. 72: 57–76.
DeAngelis, D. L., Mulholland, P. J., Palumbo, A. V., Steinman, A. D., Huston, M. A. and Elwood, J. W. 1989. Nutrient dynamics and food-web stability. - Annu. Rev. Ecol. Syst. 20: 71–95.
Dennis, B., Assas, L., Elaydi, S., Kwessi, E. and Livadiotis, G. 2016. Allee effects and resilience in stochastic populations. - Theor. Ecol. 9: 323–335.
Des Roches, S., Post, D. M., Turley, N. E., Bailey, J. K., Hendry, A. P., Kinnison, M. T., ... Palkovacs, E. P. 2018. The ecological importance of intraspecific variation. - Nat. Ecol. Evol. 2: 57–64.
Desrosières, A. 2003. Les qualités des quantités. - Courrier des statistiques: 51–63.
Devictor, V., Julliard, R., Clavel, J., Jiguet, F., Lee, A. and Couvet, D. 2008a. Functional biotic homogenization of bird communities in disturbed landscapes. - Global Ecol. Biogeogr. 17: 252–261.
Devictor, V., Julliard, R. and Jiguet, F. 2008b. Distribution of specialist and generalist species along spatial gradients of habitat disturbance and fragmentation. - Oikos 117: 507–514.
Di Cecco, G. J. and Hurlbert, A. H. 2022. Anthropogenic drivers of avian community turnover from local to regional scales. - Global Change Biol. 28: 770–781.
Díaz, S. and Malhi, Y. 2022. Biodiversity: Concepts, Patterns, Trends, and Perspectives. - Annu. Rev. Environ. Resour. 47: 31–63.
Dirzo, R., Young, H. S., Galetti, M., Ceballos, G., Isaac, N. J. B. and Collen, B. 2014. Defaunation in the Anthropocene. - Science 345: 401–406.
Doak, D. F., Waddle, E., Langendorf, R. E., Louthan, A. M., Isabelle Chardon, N., Dibner, R. R., ... DeMarche, M. L. 2021. A critical comparison of integral projection and matrix projection models for demographic analysis. - Ecol. Monogr. 91: e01447.
Doak, D. F., Bigger, D., Harding, E. K., Marvier, M. A., O, 'Malley. R. E. and Thomson, D. 1998. The Statistical Inevitability of Stability-Diversity Relationships in Community Ecology. - Am. Nat. 151: 264–276.
Dochtermann, N. A. and Gienger, C. M. 2012. Individual variability in life-history traits drives population size stability. - Curr. Zool. 58: 358–362.
Domínguez-García, V., Dakos, V. and Kéfi, S. 2019. Unveiling dimensions of stability in complex ecological networks. - PNAS 116: 25714–25720.
Donald, P. F., Green, R. E. and Heath, M. F. 2001. Agricultural intensification and the collapse of Europe's farmland bird populations. - Proc. R. Soc. B 268: 25–29.
Donohue, I., Petchey, O. L., Montoya, J. M., Jackson, A. L., McNally, L., Viana, M., ... Emmerson, M. C. 2013. On the dimensionality of ecological stability. - Ecol. Lett. 16: 421–429.
Donohue, I., Hillebrand, H., Montoya, J. M., Petchey, O. L., Pimm, S. L., Fowler, M. S., ... Yang, Q. 2016. Navigating the complexity of ecological stability. - Ecol. Lett. 19: 1172–1185.
Dornelas, M., Gotelli, N. J., McGill, B., Shimadzu, H., Moyes, F., Sievers, C. and Magurran, A. E. 2014. Assemblage time series reveal biodiversity change but not systematic loss. - Science 344: 296–299.
Dornelas, M., Magurran, A. E., Buckland, S. T., Chao, A., Chazdon, R. L., Colwell, R. K., ... Vellend, M. 2013. Quantifying temporal change in biodiversity: Challenges and opportunities. - Proc. R. Soc. B

280: 20121931.
Dornelas, M., Chase, J. M., Gotelli, N. J., Magurran, A. E., McGill, B. J., Antão, L. H., ... Vellend, M. 2023. Looking back on biodiversity change: Lessons for the road ahead. - Phil. Trans. R. Soc. B 378: 20220199.
Droop, M. R. 1968. Vitamin B12 and Marine Ecology. IV. The Kinetics of Uptake, Growth and Inhibition in Monochrysis Lutheri. - J. Mar. Biol. Assoc. U. K. 48: 689–733.
Droop, M. R. 1974. The nutrient status of algal cells in continuous culture. - J. Mar. Biol. Assoc. U. K.
Duchenne, F., Thébault, E., Michez, D., Elias, M., Drake, M., Persson, M., ... Fontaine, C. 2020. Phenological shifts alter the seasonal structure of pollinator assemblages in Europe. - Nat. Ecol. Evol. 4: 115–121.
Duchenne, F., Porcher, E., Mihoub, J.-B., Loïs, G. and Fontaine, C. 2022. Controversy over the decline of arthropods: A matter of temporal baseline? - Peer Community Journal
Dufresne, D. 2004. The log-normal approximation in financial and other computations. - Adv. Appl. Probab. 36: 747–773.
Dupuy, J. and Sallé, L. 2022. Atlas des oiseaux migrateurs de France. - MNHN, Biotope, LPO.
Ehrlich, E. and Gaedke, U. 2020. Coupled changes in traits and biomasses cascading through a tritrophic plankton food web. - Limnol. Oceanogr. 65: 2502–2514.
Elmhagen, B., Ludwig, G., Rushton, S. P., Helle, P. and Lindén, H. 2010. Top predators, mesopredators and their prey: Interference ecosystems along bioclimatic productivity gradients. - J. Anim. Ecol. 79: 785–794.
Elser, J. J., Bracken, M. E. S., Cleland, E. E., Gruner, D. S., Harpole, W. S., Hillebrand, H., ... Smith, J. E. 2007. Global analysis of nitrogen and phosphorus limitation of primary producers in freshwater, marine and terrestrial ecosystems. - Ecol. Lett. 10: 1135–1142.
Elton, C. S. 1927. Animal ecology. - University of Chicago Press.
Engen, S., Bakke, Ø. and Islam, A. 1998. Demographic and Environmental Stochasticity-Concepts and Definitions. - Biometrics 54: 840–846.
European Commission 2021. COMMUNICATION FROM THE COMMISSION TO THE EUROPEAN PARLIAMENT, THE COUNCIL, THE EUROPEAN ECONOMIC AND SOCIAL COMMITTEE AND THE COMMITTEE OF THE REGIONS EU Soil Strategy for 2030 Reaping the benefits of healthy soils for people, food, nature and climate.
Ezard, T. H. G., Bullock, J. M., Dalgleish, H. J., Millon, A., Pelletier, F., Ozgul, A. and Koons, D. N. 2010. Matrix models for a changeable world: The importance of transient dynamics in population management. - J. Appl. Ecol. 47: 515–523.
Fandos, G., Talluto, L., Fiedler, W., Robinson, R. A., Thorup, K. and Zurell, D. 2023. Standardised empirical dispersal kernels emphasise the pervasiveness of long-distance dispersal in european birds. - J. Anim. Ecol. 92: 158–170.
Fewster, R. M., Buckland, S. T., Siriwardena, G. M., Baillie, S. R. and Wilson, J. D. 2000. Analysis of Population Trends for Farmland Birds Using Generalized Additive Models. - Ecology 81: 1970–1984.
Finn, C., Grattarola, F. and Pincheira-Donoso, D. 2023. More losers than winners: Investigating anthropocene defaunation through the diversity of population trends. - Biol. Rev. 98: 1732–1748.
Fontaine, B., Moussy, C., Carricaburu, J. C., Dupuis, J., Corolleur, E., Schmaltz, L., ... Gaudard, C. 2020. Suivi des oiseaux communs en france 1989-2019: 30 ans de suivis participatifs. - MNHN-Cent. Écol. Sci. Conserv. LPO BirdLife Fr.-Serv. Connaiss. Minist. Transit. écol. solidaire
Forbes, E. S., Cushman, J. H., Burkepile, D. E., Young, T. P., Klope, M. and Young, H. S. 2019. Synthesizing the effects of large, wild herbivore exclusion on ecosystem function. - Funct. Ecol. 33: 1597–1610.
Frederiksen, M., Edwards, M., Richardson, A. J., Halliday, N. C. and Wanless, S. 2006. From plankton to top predators: Bottom-up control of a marine food web across four trophic levels. - J. Anim. Ecol. 75: 1259–1268.
Froidevaux, J. S. P., Le Viol, I., Barré, K., Bas, Y. and Kerbiriou, C. 2025. A modeling framework for biodiversity assessment in renewable energy development: A case study on European bats and wind turbines. - Renewable and Sustainable Energy Rev. 211: 115323.
Fuchs, J., Johnson, J. A. and Mindell, D. P. 2015. Rapid diversification of falcons (Aves: Falconidae) due to expansion of open habitats in the Late Miocene. - Mol. Phylogenet. Evol. 82: 166–182.
Fuller, E. 2015. The passenger pigeon. - Princeton University Press.
Fussmann, G. F., Ellner, S. P., Shertzer, K. W. and Hairston Jr., N. G. 2000. Crossing the Hopf Bifurcation in a Live Predator-Prey System. - Science 290: 1358–1360.
Galiana, N., Arnoldi, J.-F., Barbier, M., Acloque, A., de Mazancourt, C. and Loreau, M. 2021. Can

biomass distribution across trophic levels predict trophic cascades? - Ecol. Lett. 24: 464–476.
Gamelon, M., Gimenez, O., Baubet, E., Coulson, T., Tuljapurkar, S. and Gaillard, J.-M. 2014. Influence of Life-History Tactics on Transient Dynamics: A Comparative Analysis across Mammalian Populations. - Am. Nat. 184: 673–683.
Garcia, R. A., Cabeza, M., Rahbek, C. and Araújo, M. B. 2014. Multiple Dimensions of Climate Change and Their Implications for Biodiversity. - Science
García-Navas, V., Stervander, M. and Alström, P. 2024. Diversification history and morphological evolution of larks. - Evol. J. Linn. Soc. 3: kzae002.
Gaston, K. J., Cox, D. T. C., Canavelli, S. B., García, D., Hughes, B., Maas, B., ... Inger, R. 2018. Population abundance and ecosystem service provision: The case of birds. - Bioscience 68: 264–272.
Gaüzère, P. and Devictor, V. 2021. Mismatches between birds' spatial and temporal dynamics reflect their delayed response to global changes. - Oikos 130: 1284–1296.
Gaüzère, P., Barbaro, L., Calatayud, F., Princé, K., Devictor, V., Raison, L., ... Balent, G. 2020. Long-term effects of combined land-use and climate changes on local bird communities in mosaic agricultural landscapes. - Agric. Ecosyst. Environ. 289: 106722.
Gaüzère, P., Doulcier, G., Devictor, V. and Kéfi, S. 2019. A framework for estimating species-specific contributions to community indicators. - Ecol. Indic. 99: 74–82.
Gaüzère, P., Violle, C., Schrodt, F., Grenié, M., Santini, L., Hedde, M., ... Thuiller, W. 2025. Bridging macroecology and temporal dynamics to better attribute global change impacts on biodiversity. - Global Ecol. Biogeogr. 34: e70086.
Ghislain, M., Bonnet, T., Godeau, U., Dehorter, O., Gimenez, O. and Henry, P.-Y. 2024. Synchrony in adult survival is remarkably strong among common temperate songbirds across france. - Ecology 105: e4305.
Gómez-Llano, M. and De Lisle, S. P. 2026. Demonstrations of reproducibility are not reproducibility. - Nat. Ecol. Evol. 10: 615–616.
Gonzalez, A., Germain, R. M., Srivastava, D. S., Filotas, E., Dee, L. E., Gravel, D., ... Loreau, M. 2020. Scaling-up biodiversity-ecosystem functioning research. - Ecol. Lett. 23: 757–776.
Gould, E., Fraser, H. S., Parker, T. H., Nakagawa, S., Griffith, S. C., Vesk, P. A., ... Whelan, S. 2025. Same data, different analysts: Variation in effect sizes due to analytical decisions in ecology and evolutionary biology. - BMC Biol. 23: 35.
Gounand, I., Little, C. J., Harvey, E. and Altermatt, F. 2020. Global quantitative synthesis of ecosystem functioning across climatic zones and ecosystem types. - Global Ecol. Biogeogr. 29: 1139–1176.
Gounand, I., Mouquet, N., Canard, E., Guichard, F., Hauzy, C. and Gravel, D. 2014. The Paradox of Enrichment in Metaecosystems. - Am. Nat. 184: 752–763.
Gravel, D., Guichard, F., Loreau, M. and Mouquet, N. 2010. Source and sink dynamics in meta-ecosystems. - Ecology 91: 2172–2184.
Gregory, R. D., Eaton, M. A., Burfield, I. J., Grice, P. V., Howard, C., Klvaňová, A., ... Burns, F. 2023. Drivers of the changing abundance of European birds at two spatial scales. - Phil. Trans. R. Soc. B 378: 20220198.
Gregory, R. D., Skorpilova, J., Vorisek, P. and Butler, S. 2019. An analysis of trends, uncertainty and species selection shows contrasting trends of widespread forest and farmland birds in Europe. - Ecol. Indic. 103: 676–687.
Gregory, R. D., G. Noble, D. and Custance, J. 2004. The state of play of farmland birds: Population trends and conservation status of lowland farmland birds in the United Kingdom. - Ibis 146: 1–13.
Gregory, R. D., van Strien, A., Vorisek, P., Gmelig Meyling, A. W., Noble, D. G., Foppen, R. P. B. and Gibbons, D. W. 2005. Developing indicators for European birds. - Phil. Trans. R. Soc. B 360: 269–288.
Greyson-Gaito, C. J., Gellner, G. and McCann, K. S. 2023. Life-history speed, population disappearances and noise-induced ratchet effects. - Proc. R. Soc. B 290: 20222149.
Grimm, V. and Wissel, C. 1997. Babel, or the ecological stability discussions: An inventory and analysis of terminology and a guide for avoiding confusion. - Oecologia 109: 323–334.
Grzegorczyk, E., Caizergues, A., Eraud, C., Francesiaz, C., Le Rest, K. and Guillemain, M. 2024. Demographic and evolutionary consequences of hunting of wild birds. - Biol. Rev. 99: 1298–1313.
Grzegorczyk, E., Mihoub, J.-B., Barnier, F., Robert, A., Barnier, F. and Robert, A. 2025. Rapport technique Indice France Vivante.
Guerber, J., Loeuille, N. and Gounand, I. 2026a. Overexploitation can counteract top-down control and the paradox of enrichment in simple food chains. - Oikos 2026: e11470.

Guerber, J., Fontaine, C. and Thébault, E. 2026c. Code and data for population trends and variability within bird communities are amplified by intense land use. - Dryad Digital Repository
Guerber, J., Fontaine, C. and Thébault, E. 2026b. Population trends and variability within bird communities are amplified by intense land use. - J. Anim. Ecol. 95: 1047–1058.
Guerber, J., Genettais, D., Fontaine, C. and Thébault, E. 2026d. Population and community variability deviate from stationary expectations during transient dynamics. - bioRxiv
Harmsen, B. J. and Foster, R. J. 2014. What Are We Trying to Conserve? - BioScience 64: 170.
Hart, E. E., Haigh, A. and Ciuti, S. 2023. A scoping review of the scientific evidence base for rewilding in Europe. - Biol. Conserv. 285: 110243.
Hartig, F., Lohse, L. and Leite, M. de S. 2024. DHARMa: Residual diagnostics for hierarchical (multi-level / mixed) regression models. - CRAN
Hastings, A. 2004. Transients: The key to long-term ecological understanding? - Trends Ecol. Evol. 19: 39–45.
Hastings, A. 2016. Timescales and the management of ecological systems. - PNAS 113: 14568–14573.
Hastings, A., Abbott, K. C., Cuddington, K., Francis, T., Gellner, G., Lai, Y.-C., ... Zeeman, M. L. 2018. Transient phenomena in ecology. - Science 361: eaat6412.
Hastings, A., Abbott, K. C., Cuddington, K., Francis, T. B., Lai, Y.-C., Morozov, A., ... Zeeman, M. L. 2021. Effects of stochasticity on the length and behaviour of ecological transients. - J R. Soc. Interface 18: 20210257.
Henn, J. J., Anderson, K. E., Brigham, L. M., Bueno de Mesquita, C. P., Collins, C. G., Elmendorf, S. C., ... Spasojevic, M. J. 2024. Long-Term Alpine Plant Responses to Global Change Drivers Depend on Functional Traits. - Ecol. Lett. 27: e14518.
Hillebrand, H., Blasius, B., Borer, E. T., Chase, J. M., Downing, J. A., Eriksson, B. K., ... Ryabov, A. B. 2018a. Biodiversity change is uncoupled from species richness trends: Consequences for conservation and monitoring. - J. Appl. Ecol. 55: 169–184.
Hillebrand, H., Langenheder, S., Lebret, K., Lindström, E., Östman, Ö. and Striebel, M. 2018b. Decomposing multiple dimensions of stability in global change experiments. - Ecol. Lett. 21: 21–30.
Himes, A., Muraca, B., Anderson, C. B., Athayde, S., Beery, T., Cantú-Fernández, M., ... Zent, E. 2024. Why nature matters: A systematic review of intrinsic, instrumental, and relational values. - BioScience 74: 25–43.
Holling, C. S. 1973. Resilience and stability of ecological systems. - Annu. Rev. Ecol. Syst. 4: 1–23.
Holling, C. S. 1996. Engineering resilience versus ecological resilience. - In: Engineering within ecological constraints. The National Academies Press, Washington, DC, pp. 31.
Hooper, D. U., Chapin III, F. S., Ewel, J. J., Hector, A., Inchausti, P., Lavorel, S., ... Wardle, D. A. 2005. Effects of Biodiversity on Ecosystem Functioning: A Consensus of Current Knowledge. - Ecol. Monogr. 75: 3–35.
Hoyo, J. del, Fjeldså, J. and Burn, H. 2013. Handbook of the birds of the world. - Lynx.
Hulot, F. D. and Loreau, M. 2006. Nutrient-limited food webs with up to three trophic levels: Feasibility, stability, assembly rules, and effects of nutrient enrichment. - Theor. Popul. Biol. 69: 48–66.
Hulot, F. D., Lacroix, G., Lescher-Moutoué, F. and Loreau, M. 2000. Functional diversity governs ecosystem response to nutrient enrichment. - Nature 405: 340–344.
Hung, C.-M., Shaner, P.-J. L., Zink, R. M., Liu, W.-C., Chu, T.-C., Huang, W.-S. and Li, S.-H. 2014. Drastic population fluctuations explain the rapid extinction of the passenger pigeon. - PNAS 111: 10636–10641.
Hunter, M. D. and Price, P. W. 1992. Playing Chutes and Ladders: Heterogeneity and the Relative Roles of Bottom-Up and Top-Down Forces in Natural Communities. - Ecology 73: 724–732.
IPBES 2019a. Global assessment report on biodiversity and ecosystem services of the intergovernmental science-policy platform on biodiversity and ecosystem services.
IPBES 2019b. Summary for policymakers of the global assessment report on biodiversity and ecosystem services.
Isbell, F., Mori, A. S., Loreau, M., Reich, P. B., Tilman, D., Anderson, M. I., ... Zirbel, C. R. 2026. Predicting temporal stability and resilience from resistance and recovery. - Nature: 1–7.
IUCN 2024. The IUCN red list of threatened species. Version 2024-2.
Ives, A. R., Gross, K. and Klug, J. L. 1999. Stability and variability in competitive communities. - Science 286: 542–544.
Jaureguiberry, P., Titeux, N., Wiemers, M., Bowler, D. E., Coscieme, L., Golden, A. S., ... Purvis, A. 2022. The direct drivers of recent global anthropogenic biodiversity loss. - Sci. Adv. 8: eabm9982.
Jenkins, G. B., Beckerman, A. P., Bellard, C., Benítez-López, A., Ellison, A. M., Foote, C. G., ...

Peres-Neto, P. R. 2023. Reproducibility in ecology and evolution: Minimum standards for data and code. - Ecol. Evol. 13: e9961.
Jensen, C. X. J. and Ginzburg, L. R. 2005. Paradoxes or theoretical failures? The jury is still out. - Ecol. Modell. 188: 3–14.
Jetz, W., Thomas, G. H., Joy, J. B., Hartmann, K. and Mooers, A. O. 2012. The global diversity of birds in space and time. - Nature 491: 444–448.
Jiguet, F., Devictor, V., Julliard, R. and Couvet, D. 2012. French citizens monitoring ordinary birds provide tools for conservation and ecological sciences. - Acta Oecol. 44: 58–66.
Johnston, A., Rodewald, A. D., Strimas-Mackey, M., Auer, T., Hochachka, W. M., Stillman, A. N., ... Fink, D. 2025. North American bird declines are greatest where species are most abundant. - Science 388: 532–537.
Johnston, A., Newson, S. E., Risely, K., Musgrove, A. J., Massimino, D., Baillie, S. R. and Pearce-Higgins, J. W. 2014. Species traits explain variation in detectability of UK birds. - Bird Study 61: 340–350.
Justus, J. 2008. Complexity, Diversity, and Stability. - In: Sarkar, S. and Plutynski, A. (eds), A companion to the philosophy of biology. Blackwell, pp. 321–350.
Kallio, P. and Lehtonen, J. 1975. On the Ecocatastrophe of Birch Forests Caused by Oporinia autumnata (Bkh.) and the Problem of Reforestation. - In: Wielgolaski, F. E. (ed), Fennoscandian Tundra Ecosystems: Part 2 Animals and Systems Analysis. Ecological Studies. Springer, pp. 174–180.
Kamata, N. 2002. Outbreaks of forest defoliating insects in Japan, 1950–2000. - Bull. Entomol. Res. 92: 109–117.
Karlis, D. and Xekalaki, E. 2005. Mixed Poisson Distributions. - International Statistical Review / Revue Internationale de Statistique 73: 35–58.
Kéfi, S., Domínguez-García, V., Donohue, I., Fontaine, C., Thébault, E. and Dakos, V. 2019. Advancing our understanding of ecological stability. - Ecol. Lett. 22: 1349–1356.
Kéfi, S., Rietkerk, M., Alados, C. L., Pueyo, Y., Papanastasis, V. P., ElAich, A. and de Ruiter, P. C. 2007. Spatial vegetation patterns and imminent desertification in Mediterranean arid ecosystems. - Nature 449: 213–217.
Kéfi, S., Génin, A., Garcia-Mayor, A., Guirado, E., Cabral, J. S., Berdugo, M., ... Maestre, F. T. 2024. Self-organization as a mechanism of resilience in dryland ecosystems. - PNAS 121: e2305153121.
Kirk, K. L. 1998. Enrichment Can Stabilize Population Dynamics: Autotoxins and Density Dependence. - Ecology 79: 2456–2462.
Kittelberger, K. D., Tanner, C. J., Buxton, A. N., Prewett, A. and Şekercioğlu, Ç. H. 2024. Correlates of avian extinction timing around the world since 1500 CE. - Avian Res. 15: 100213.
Klauschies, T., Vasseur, D. A. and Gaedke, U. 2016. Trait adaptation promotes species coexistence in diverse predator and prey communities. - Ecol. Evol. 6: 4141–4159.
Knape, J., Jonzén, N. and Sköld, M. 2011. On observation distributions for state space models of population survey data. - J. Anim. Ecol. 80: 1269–1277.
Kuemmerle, T., Levers, C., Erb, K., Estel, S., Jepsen, M. R., Müller, D., ... Reenberg, A. 2016. Hotspots of land use change in Europe. - Environ. Res. Lett. 11: 064020.
Kuussaari, M., Bommarco, R., Heikkinen, R. K., Helm, A., Krauss, J., Lindborg, R., ... Steffan-Dewenter, I. 2009. Extinction debt: A challenge for biodiversity conservation. - Trends Ecol. Evol. 24: 564–571.
Lajaaiti, I., Kéfi, S., Loreau, M., Ardichvili, A. and Arnoldi, J.-F. 2025. Linking biotic interactions to species stability. - bioRxiv
Landau, W. M. 2021. The targets R package: A dynamic make-like function-oriented pipeline toolkit for reproducibility and high-performance computing. - J. Open Source Softw. 6: 2959.
Lande, R., Engen, S. and Saether, B.-E. 2003. Stochastic population dynamics in ecology and conservation. - Oxford University Press, USA.
Lavorel, S. and Garnier, E. 2002. Predicting changes in community composition and ecosystem functioning from plant traits: Revisiting the holy grail. - Funct. Ecol. 16: 545–556.
Le Monde-AFP 2026. La population d'oiseaux communs a décliné de 18 % en vingt-cinq ans en France, selon la Ligue pour la protection des oiseaux.
Le Viol, I., Jiguet, F., Brotons, L., Herrando, S., Lindström, Å., Pearce-Higgins, J. W., ... Devictor, V. 2012. More and more generalists: Two decades of changes in the European avifauna. - Biol. Lett. 8: 780–782.
Lefcheck, J. S. 2016. piecewiseSEM: Piecewise structural equation modelling in r for ecology, evolution, and systematics. - Methods Ecol. Evol. 7: 573–579.
Lehikoinen, A., Foppen, R. P. B., Heldbjerg, H., Lindström, Å., van Manen, W., Piirainen, S., ... Butchart, S. H. M. 2016. Large-scale climatic drivers of regional winter bird population trends. - Divers. Distrib.

22: 1163–1173.
Lehman, C. L. and Tilman, D. 2000. Biodiversity, stability, and productivity in competitive communities. - Am. Nat. 156: 534–552.
Leone, F. C., Nelson, L. S. and Nottingham, R. B. 1961. The Folded Normal Distribution. - Technometrics 3: 543–550.
Lepš, J., Götzenberger, L., Valencia, E. and de Bello, F. 2019. Accounting for long-term directional trends on year-to-year synchrony in species fluctuations. - Ecography 42: 1728–1741.
Levrel, H. 2007. Quels indicateurs pour la gestion de la biodiversité? - Institut français de la biodiversité.
Levrel, H., Loïs, G. and Couvet, D. 2007. Indicateurs de biodiversité pour les forêts françaises. État des lieux et perspectives. - Revue forestière française 59: 45–56.
Liang, M., Yang, Q., Chase, J. M., Isbell, F., Loreau, M., Schmid, B., ... Wang, S. 2025. Unifying spatial scaling laws of biodiversity and ecosystem stability. - Science 387: eadl2373.
Lindeman, R. L. 1942. The trophic-dynamic aspect of ecology. - Ecology 23: 399–417.
Lindenmayer, D. B., Lavery, T. and Scheele, B. C. 2022. Why We Need to Invest in Large-Scale, Long-Term Monitoring Programs in Landscape Ecology and Conservation Biology. - Curr. Landscape Ecol. Rep. 7: 137–146.
Li, Y., Zhang, S., Hobbs, R., Caiado, C., Sproson, A. D., Selby, D. and Rooney, A. D. 2019. Monte Carlo sampling for error propagation in linear regression and applications in isochron geochronology. - Sci. Bull. 64: 189–197.
Li, Z., Zhang, H., Xu, Y. and Wang, S. 2021. Composition of “fast–slow” traits drives avian community stability over north america. - Funct. Ecol. 35: 2831–2840.
Loeuille, N. and Loreau, M. 2004. Nutrient enrichment and food chains: Can evolution buffer top-down control? - Theor. Popul. Biol. 65: 285–298.
Loh, J., Green, R. E., Ricketts, T., Lamoreux, J., Jenkins, M., Kapos, V. and Randers, J. 2005. The Living Planet Index: Using species population time series to track trends in biodiversity. - Phil. Trans. R. Soc. B 360: 289–295.
Loreau, M. 1995. Consumers as maximizers of matter and energy flow in ecosystems. - Am. Nat.
Loreau, M. and de Mazancourt, C. 2008. Species synchrony and its drivers: Neutral and nonneutral community dynamics in fluctuating environments. - Am. Nat. 172: E48–E66.
Loreau, M. and de Mazancourt, C. 2013. Biodiversity and ecosystem stability: A synthesis of underlying mechanisms. - Ecol. Lett. 16: 106–115.
Loreau, M., Mouquet, N. and Holt, R. D. 2003. Meta-ecosystems: A theoretical framework for a spatial ecosystem ecology. - Ecol. Lett. 6: 673–679.
Loreau, M., Daufresne, T., Gonzalez, A., Gravel, D., Guichard, F., Leroux, S. J., ... Mouquet, N. 2013. Unifying sources and sinks in ecology and Earth sciences. - Biol. Rev. 88: 365–379.
Lotka, A. J. 1925. Elements of physical biology. - Williams & Wilkins.
Lundberg, P., Ranta, E., Ripa, J. and Kaitala, V. 2000. Population variability in space and time. - Trends Ecol. Evol. 15: 460–464.
Lu, X., Jia, Y. and Wang, Y. 2024. The effect of landscape composition, complexity, and heterogeneity on bird richness: A systematic review and meta-analysis on a global scale. - Landscape Ecol. 39: 132.
Maestre, F. T., Le Bagousse-Pinguet, Y., Delgado-Baquerizo, M., Eldridge, D. J., Saiz, H., Berdugo, M., ... Gross, N. 2022. Grazing and ecosystem service delivery in global drylands. - Science 378: 915–920.
Magurran, A. E., Baillie, S. R., Buckland, S. T., Dick, J. McP., Elston, D. A., Scott, E. M., ... Watt, A. D. 2010. Long-term datasets in biodiversity research and monitoring: Assessing change in ecological communities through time. - Trends Ecol. Evol. 25: 574–582.
Mancini, F., Cooke, R., Woodcock, B. A., Greenop, A., Johnson, A. C. and Isaac, N. J. B. 2023. Invertebrate biodiversity continues to decline in cropland. - Proc. R. Soc. B 290: 20230897.
Marrec, L., Bank, C. and Bertrand, T. 2023. Solving the stochastic dynamics of population growth. - Ecol. Evol. 13: e10295.
Martin, G., Devictor, V., Motard, E., Machon, N. and Porcher, E. 2019. Short-term climate-induced change in french plant communities. - Biol. Lett. 15: 20190280.
May, R. M. 1972. Will a large complex system be stable? - Nature 238: 413–414.
McCann, K., Cazelles, K., MacDougall, A. S., Fussmann, G. F., Bieg, C., Cristescu, M., ... Gonzalez, A. 2021. Landscape modification and nutrient-driven instability at a distance. - Ecol. Lett. 24: 398–414.
McCann, K., Hastings, A. and Huxel, G. R. 1998. Weak trophic interactions and the balance of nature. - Nature 395: 794–798.
McCauley, D. J., Gellner, G., Martinez, N. D., Williams, R. J., Sandin, S. A., Micheli, F., ... McCann, K. S. 2018. On the prevalence and dynamics of inverted trophic pyramids and otherwise top-heavy

communities. - Ecol. Lett. 21: 439–454.
McGillycuddy, M., Popovic, G., Bolker, B. M. and Warton, D. I. 2025. Parsimoniously fitting large multivariate random effects in glmmTMB. - J. Stat. Softw. 112: 1–19.
McKinney, M. L. and Lockwood, J. L. 1999. Biotic homogenization: A few winners replacing many losers in the next mass extinction. - Trends Ecol. Evol. 14: 450–453.
Menck, P. J., Heitzig, J., Marwan, N. and Kurths, J. 2013. How basin stability complements the linear-stability paradigm. - Nat. Phys. 9: 89–92.
Mentges, A., Clark, A. T., Blowes, S. A., Kunze, C., Hillebrand, H. and Chase, J. M. 2024. Accounting for effects of growth rate when measuring ecological stability in response to pulse perturbations. - Ecol. Evol. 14: e11637.
Merow, C., Dahlgren, J. P., Metcalf, C. J. E., Childs, D. Z., Evans, M. E. K., Jongejans, E., … McMahon, S. M. 2014. Advancing population ecology with integral projection models: A practical guide. - Methods Ecol. Evol. 5: 99–110.
Meyer, M., Ott, D., Götze, P., Koch, H.-J. and Scherber, C. 2019. Crop identity and memory effects on aboveground arthropods in a long-term crop rotation experiment. - Ecol. Evol. 9: 7307–7323.
Milot, E., Béchet, A. and Maris, V. 2020. The dimensions of evolutionary potential in biological conservation. - Evol. Appl. 13: 1363–1379.
Ministère de la Transition écologique 2023. ZAN : Guide synthétique.
Molenaar, E., Viechtbauer, W., van de Crommenacker, J. and Kingma, S. A. 2024. Neonicotinoids impact all aspects of bird life: A meta-analysis. - Ecol. Lett. 27: e14534.
Monnet, A.-C., Jiguet, F., Meynard, C. N., Mouillot, D., Mouquet, N., Thuiller, W. and Devictor, V. 2014. Asynchrony of taxonomic, functional and phylogenetic diversity in birds. - Global Ecol. Biogeogr. 23: 780–788.
Monnet, A.-C., Cairo, M., Deguines, N., Jiguet, F., Vimont, M., Fontaine, C. and Porcher, E. 2026. Common birds have higher abundances in croplands with lower pesticide purchases. - Proc. R. Soc. B 293: 20252370.
Morelli, F., Benedetti, Y., Møller, A. P. and Fuller, R. A. 2019. Measuring avian specialization. - Ecol. Evol. 9: 8378–8386.
Morelli, F., Pruscini, F., Santolini, R., Perna, P., Benedetti, Y. and Sisti, D. 2013. Landscape heterogeneity metrics as indicators of bird diversity: Determining the optimal spatial scales in different landscapes. - Ecol. Indic. 34: 372–379.
Morelli, F., Brlík, V., Benedetti, Y., Bussière, R., Moudrá, L., Reif, J. and Svitok, M. 2022. Detection Rate of Bird Species and What It Depends on: Tips for Field Surveys. - Front. Ecol. Evol.
Mouchet, M. A., Villéger, S., Mason, N. W. H. and Mouillot, D. 2010. Functional diversity measures: An overview of their redundancy and their ability to discriminate community assembly rules. - Funct. Ecol. 24: 867–876.
Murray, J. D. 2002. Mathematical biology. - Springer.
Nabias, J., Lorrillière, R., Dupuy, J., Couzi, L. and Barbaro, L. 2025. Improving national-scale breeding bird surveys with integrated distance sampling. - Sci. Rep. 15: 18312.
Nabias, J., Barbaro, L., Fontaine, B., Dupuy, J., Couzi, L., Vallé, C. and Lorrilliere, R. 2024. Reassessment of french breeding bird population sizes using citizen science and accounting for species detectability. - PeerJ 12: e17889.
Nåsell, I. 2003. Moment closure and the stochastic logistic model. - Theor. Popul. Biol. 63: 159–168.
Newman, T. J., Ferdy, J.-B. and Quince, C. 2004. Extinction times and moment closure in the stochastic logistic process. - Theor. Popul. Biol. 65: 115–126.
Nguyen, P. L., Pomati, F. and Rohr, R. P. 2025. Inferring coexistence likelihood in changing environments from ecological time series. - PNAS 122: e2417905122.
Nolting, B. C. and Abbott, K. C. 2016. Balls, cups, and quasi-potentials: Quantifying stability in stochastic systems. - Ecology 97: 850–864.
Northrup, J. M., Rivers, J. W., Yang, Z. and Betts, M. G. 2019. Synergistic effects of climate and land-use change influence broad-scale avian population declines. - Global Change Biol. 25: 1561–1575.
O'Sullivan, M., Smith, W. K., Sitch, S., Friedlingstein, P., Arora, V. K., Haverd, V., … Buermann, W. 2020. Climate-driven variability and trends in plant productivity over recent decades based on three global products. - Global Biogeochem. Cycles 34: e2020GB006613.
oiseaux.net. - Association écopains d'abord
Oksanen, L. and Oksanen, T. 2000. The Logic and Realism of the Hypothesis of Exploitation Ecosystems. - Am. Nat. 155: 703–723.
Oksanen, L., Fretwell, S. D., Arruda, J. and Niemela, P. 1981. Exploitation ecosystems in gradients of

primary productivity. - Am. Nat. 118: 240–261.
Olden, J. D. and Rooney, T. P. 2006. On defining and quantifying biotic homogenization. - Global Ecol. Biogeogr. 15: 113–120.
Oliver, T., Roy, D. B., Hill, J. K., Brereton, T. and Thomas, C. D. 2010. Heterogeneous landscapes promote population stability. - Ecol. Lett. 13: 473–484.
Olivier, T., Thébault, E., Elias, M., Fontaine, B. and Fontaine, C. 2020. Urbanization and agricultural intensification destabilize animal communities differently than diversity loss. - Nat. Commun. 11: 2686.
Oro, D. and Martínez-Abraín, A. 2023. Ecological non-equilibrium and biological conservation. - Biol. Conserv. 286: 110258.
Palmer, M. W. and White, P. S. 1994. On the Existence of Ecological Communities. - J. Veg. Sci. 5: 279–282.
Pausas, J. G. and Fernández-Muñoz, S. 2012. Fire regime changes in the Western Mediterranean Basin: From fuel-limited to drought-driven fire regime. - Clim. Change 110: 215–226.
Pausas, J. G. and Bond, W. J. 2020. Alternative biome states in terrestrial ecosystems. - Trends Plant Sci. 25: 250–263.
PECBMS 2025. The State of Europe's Wild Birds.
Pélissié, M., Devictor, V. and Dakos, V. 2024. A systematic approach for detecting abrupt shifts in ecological timeseries. - Biol. Conserv. 290: 110429.
Pellissier, V., Mimet, A., Fontaine, C., Svenning, J.-C. and Couvet, D. 2017. Relative importance of the land-use composition and intensity for the bird community composition in anthropogenic landscapes. - Ecol. Evol. 7: 10513–10535.
Pels, B. and Sabelis, M. W. 1999. Local dynamics, overexploitation and predator dispersal in an acarine predator-prey system. - Oikos 86: 573–583.
Pennekamp, F., Pontarp, M., Tabi, A., Altermatt, F., Alther, R., Choffat, Y., ... Petchey, O. L. 2018. Biodiversity increases and decreases ecosystem stability. - Nature 563: 109–112.
Pereira, H. M., Leadley, P. W., Proença, V., Alkemade, R., Scharlemann, J. P. W., Fernandez-Manjarrés, J. F., ... Walpole, M. 2010. Scenarios for Global Biodiversity in the 21st Century. - Science 330: 1496–1501.
Perrot, T., Princé, K., Porcher, E., Wolfram, J., Schulz, R. and Fontaine, C. 2025. Weak recovery of insectivorous bird populations after ban of neonicotinoids in France, hinting at lasting impacts. - Environ. Pollut. 385: 127132.
Pichon, B., Kéfi, S., Loeuille, N., Lajaaiti, I. and Gounand, I. 2026. Integrating ecological feedbacks across scales and levels of organization. - Ecography 2026: e07167.
Pigot, A. L., Sheard, C., Miller, E. T., Bregman, T. P., Freeman, B. G., Roll, U., ... Tobias, J. A. 2020. Macroevolutionary convergence connects morphological form to ecological function in birds. - Nat. Ecol. Evol. 4: 230–239.
Pimm, S. L. 1984. The complexity and stability of ecosystems. - Nature 307: 321–326.
Pimm, S. L. and Lawton, J. H. 1977. Number of trophic levels in ecological communities. - Nature 268: 329–331.
Pinheiro, J., Bates, D. and R Core Team 2025. Nlme: Linear and nonlinear mixed effects models. - CRAN
Polazzo, F., Hämmig, T., Petchey, O. L. and Pennekamp, F. 2025. The Imbalance of Nature: The Role of Species Environmental Responses for Community Stability. - Ecol. Lett. 28: e70224.
Polazzo, F., Limberger, R., Pennekamp, F., Ross, S. R. P.-J., Simpson, G. L. and Petchey, O. L. 2024. Measuring the response diversity of ecological communities experiencing multifarious environmental change. - Global Change Biol. 30: e17594.
Pollock, H. S., Toms, J. D., Tarwater, C. E., Benson, T. J., Karr, J. R. and Brawn, J. D. 2022. Long-term monitoring reveals widespread and severe declines of understory birds in a protected Neotropical forest. - PNAS 119: e2108731119.
Princé, K., Lorrillière, R., Barbet-Massin, M. and Jiguet, F. 2013. Predicting the fate of french bird communities under agriculture and climate change scenarios. - Environ. Sci. Policy 33: 120–132.
Princé, K., Rouveyrol, P., Pellissier, V., Touroult, J. and Jiguet, F. 2021. Long-term effectiveness of Natura 2000 network to protect biodiversity: A hint of optimism for common birds. - Biol. Conserv. 253: 108871.
R Core Team 2024. R: A language and environment for statistical computing.
Radchuk, V., Laender, F. D., Cabral, J. S., Boulangeat, I., Crawford, M., Bohn, F., ... Kramer-Schadt, S. 2019. The dimensionality of stability depends on disturbance type. - Ecol. Lett. 22: 674–684.
Rao, C. R. 1982. Diversity and dissimilarity coefficients: A unified approach. - Theor. Popul. Biol. 21:

24–43.
Rasmussen, L. V., Coolsaet, B., Martin, A., Mertz, O., Pascual, U., Corbera, E., ... Ryan, C. M. 2018. Social-ecological outcomes of agricultural intensification. - Nat. Sustain. 1: 275–282.
Reif, J., Vermouzek, Z., Voříšek, P., Romportl, D. and Morelli, F. 2022. Birds' ecological characteristics differ among habitats: An analysis based on national citizen science data. - Community Ecol. 23: 173–186.
Reif, J., Gamero, A., Hologšková, A., Aunins, A., Chodkiewicz, T., Hristov, I., ... Voříšek, P. 2024. Accelerated farmland bird population declines in european countries after their recent EU accession. - Sci. Total Environ. 946: 174281.
Richardson, K., Steffen, W., Lucht, W., Bendtsen, J., Cornell, S. E., Donges, J. F., ... Rockström, J. 2023. Earth beyond six of nine planetary boundaries. - Sci. Adv. 9: eadh2458.
Rigal, S., Devictor, V. and Dakos, V. 2020. A method for classifying and comparing non-linear trajectories of ecological variables. - Ecol. Indic. 112: 106113.
Rigal, S., Dakos, V., Alonso, H., Auniņš, A., Benkő, Z., Brotons, L., ... Devictor, V. 2023. Farmland practices are driving bird population decline across europe. - PNAS 120: e2216573120.
Rip, J. and McCann, K. 2011. Cross-ecosystem differences in stability and the principle of energy flux. - Ecol. Lett. 14: 733–740.
Ripple, W. J. and Beschta, R. L. 2012a. Trophic cascades in Yellowstone: The first 15 years after wolf reintroduction. - Biol. Conserv. 145: 205–213.
Ripple, W. J. and Beschta, R. L. 2012b. Large predators limit herbivore densities in northern forest ecosystems. - Eur. J. Wildl. Res. 58: 733–742.
Ripple, W. J., Beschta, R. L., Wolf, C., Painter, L. E. and Wirsing, A. J. 2025. The strength of the Yellowstone trophic cascade after wolf reintroduction. - Global Ecol. Conserv. 58: e03428.
Robert, A., Fontaine, C., Veron, S., Monnet, A.-C., Legrand, M., Clavel, J., ... Mouchet, M. 2017. Fixism and conservation science. - Conserv. Biol. 31: 781–788.
Rodrigues, B. 2023. Building reproducible analytical pipelines with R.
Rodrigues, A. V., Rissanen, T., Jones, M. M., Huikkonen, I.-M., Huitu, O., Korpimäki, E., ... Laine, A.-L. 2025. Cross-Taxa Analysis of Long-Term Data Reveals a Positive Biodiversity-Stability Relationship With Taxon-Specific Mechanistic Underpinning. - Ecol. Lett. 28: e70003.
Rosenberg, K. V., Dokter, A. M., Blancher, P. J., Sauer, J. R., Smith, A. C., Smith, P. A., ... Marra, P. P. 2019. Decline of the North American avifauna. - Science 366: 120–124.
Rosenzweig, M. L. 1971. Paradox of Enrichment: Destabilization of Exploitation Ecosystems in Ecological Time. - Science 171: 385–387.
Rosenzweig, M. L. 1973. Exploitation in three trophic levels. - Am. Nat. 107: 275–294.
Rosenzweig, M. L. and MacArthur, R. H. 1963. Graphical Representation and Stability Conditions of Predator-Prey Interactions. - Am. Nat. 97: 209–223.
Rößler, A. 2010. Runge–Kutta Methods for the Strong Approximation of Solutions of Stochastic Differential Equations. - SIAM J. Numer. Anal. 48: 922–952.
Roy, S. and Chattopadhyay, J. 2007. The stability of ecosystems: A brief overview of the paradox of enrichment. - J. Biosci. 32: 421–428.
Ruano-Chamorro, C., Gurney, G. G., Barnes, M. L., Gelcich, S. and Cinner, J. E. 2023. Disparities in the impacts of co-management on fishers' livelihoods. - Sustain. Sci. 18: 2723–2733.
Rueda-Cediel, P., Anderson, K. E., Regan, T. J. and Regan, H. M. 2018. Effects of uncertainty and variability on population declines and IUCN Red List classifications. - Conserv. Biol. 32: 916–925.
Rue, H., Riebler, A., Sørbye, S. H., Illian, J. B., Simpson, D. P. and Lindgren, F. K. 2017. Bayesian Computing with INLA: A Review. - Annu. Rev. Stat. Appl. 4: 395–421.
Sæther, B.-E., Grøtan, V., Engen, S., Coulson, T., Grant, P. R., Visser, M. E., ... Weimerskirch, H. 2016. Demographic routes to variability and regulation in bird populations. - Nat. Commun. 7: 12001.
Sánchez-Pinillos, M., Dakos, V. and Kéfi, S. 2024. Ecological dynamic regimes: A key concept for assessing ecological resilience. - Biol. Conserv. 289: 110409.
Sanderson, E. W., Fisher, K., Robinson, N., Sampson, D., Duncan, A. and Royte, L. 2022. The March of the human footprint. - EcoEvoRxiv
Santisteban, L., Benkman, C. W., Fetz, T. and Smith, J. W. 2012. Survival and population size of a resident bird species are declining as temperature increases. - J. Anim. Ecol. 81: 352–363.
Särkkä, S. and Solin, A. 2019. Applied stochastic differential equations. - Cambridge University Press.
Sarrazin, F. and Lecomte, J. 2016. Evolution in the Anthropocene. - Science 351: 922–923.
Sauer, J. R., Link, W. A., Fallon, J. E., Pardieck, K. L. and Ziolkowski, D. J., Jr. 2013. The North American Breeding Bird Survey 1966–2011: Summary Analysis and Species Accounts. - North American

Fauna 79: 1–32.
Saunders, M. E., Lees, A. C. and Grames, E. M. 2025. Understanding and counteracting the denial of insect biodiversity loss. - Curr. Opin. Insect Sci. 68: 101338.
Saunders, S. P., Meehan, T. D., Michel, N. L., Bateman, B. L., DeLuca, W., Deppe, J. L., ... Wilsey, C. B. 2022. Unraveling a century of global change impacts on winter bird distributions in the eastern United States. - Global Change Biol. 28: 2221–2235.
Scheffer, M. 2009. Early-warning signals for critical transitions. - Nature 461: 53–59.
Scheffer, M., Carpenter, S., Foley, J. A., Folke, C. and Walker, B. 2001. Catastrophic shifts in ecosystems. - Nature 413: 6.
Schmitz, O. J. 2008. Herbivory from Individuals to Ecosystems. - Annu. Rev. Ecol. Evol. Syst. 39: 133–152.
Schnoerr, D., Sanguinetti, G. and Grima, R. 2017. Approximation and inference methods for stochastic biochemical kinetics—a tutorial review. - J. Phys. A: Math. Theor. 50: 093001.
Sébastien, L., Lehtonen, M. and Bauler, T. 2017. Introduction. Les indicateurs participatifs tiennent-ils leurs promesses ? - Participations 18: 9–38.
Seddon, A. W. R., Macias-Fauria, M., Long, P. R., Benz, D. and Willis, K. J. 2016. Sensitivity of global terrestrial ecosystems to climate variability. - Nature 531: 229–232.
Sekercioglu, C. 2006. Ecological significance of bird populations. - In: Handbook of the birds of the world. pp. 15–51.
Şekercioğlu, Ç. H., Daily, G. C. and Ehrlich, P. R. 2004. Ecosystem consequences of bird declines. - PNAS 101: 18042–18047.
Şekercioğlu, Ç. H., Loarie, S. R., Oviedo-Brenes, F., Mendenhall, C. D., Daily, G. C. and Ehrlich, P. R. 2015. Tropical countryside riparian corridors provide critical habitat and connectivity for seed-dispersing forest birds in a fragmented landscape. - J. Ornithol. 156: 343–353.
Şekercioğlu, Ç. H., Kittelberger, K. D., Mota, F. M. M., Buxton, A. N., Orton, N., DeNiro, A., ... Neate-Clegg, M. H. C. 2025. BIRDBASE: A Global Dataset of Avian Biogeography, Conservation, Ecology and Life History Traits. - Sci. Data 12: 1558.
Selwood, K. E., McGeoch, M. A. and Mac Nally, R. 2015. The effects of climate change and land-use change on demographic rates and population viability. - Biol. Rev. 90: 837–853.
Sharp, B. R. and Whittaker, R. J. 2003. The irreversible cattle-driven transformation of a seasonally flooded Australian savanna. - J. Biogeogr. 30: 783–802.
Shipley, B. 2000. A New Inferential Test for Path Models Based on Directed Acyclic Graphs. - Struct. Equation Modell. Multidiscip. J. 7: 206–218.
Shoemaker, L. G., Sullivan, L. L., Donohue, I., Cabral, J. S., Williams, R. J., Mayfield, M. M., ... Abbott, K. C. 2020. Integrating the underlying structure of stochasticity into community ecology. - Ecology 101: e02922.
Shrubb, M. 2003. Birds, Scythes and Combines: A History of Birds and Agricultural Change. - Cambridge University Press.
Shufeldt, R. W. 1921. Published figures and plates of the extinct passenger pigeon. - Utica, N.Y. : Science Press.
Shurin, J. B., Gruner, D. S. and Hillebrand, H. 2005. All wet or dried up? Real differences between aquatic and terrestrial food webs. - Proc. R. Soc. B 273: 1–9.
Smith, S. J., Edmonds, J., Hartin, C. A., Mundra, A. and Calvin, K. 2015. Near-term acceleration in the rate of temperature change. - Nature Clim. Change 5: 333–336.
Smith, P. A., McKinnon, L., Meltofte, H., Lanctot, R. B., Fox, A. D., Leafloor, J. O., ... Smith, A. C. 2020. Status and trends of tundra birds across the circumpolar Arctic. - Ambio 49: 732–748.
Smith, A. C., D. Binley, A., Daly, L., Edwards, B. P. M., Ethier, D., Frei, B., ... Smith, P. A. 2024. Spatially explicit Bayesian hierarchical models improve estimates of avian population status and trends. - Ornithol. Appl. 126: duad056.
Smith, O. M., Kennedy, C. M., Echeverri, A., Karp, D. S., Latimer, C. E., Taylor, J. M., ... Snyder, W. E. 2022. Complex landscapes stabilize farm bird communities and their expected ecosystem services. - J. Appl. Ecol. 59: 927–941.
Soldaat, L. L., Pannekoek, J., Verweij, R. J. T., van Turnhout, C. A. M. and van Strien, A. J. 2017. A Monte Carlo method to account for sampling error in multi-species indicators. - Ecol. Indic. 81: 340–347.
Sólymos, P., Matsuoka, S. M., Stralberg, D., Barker, N. K. S. and Bayne, E. M. 2018. Phylogeny and species traits predict bird detectability. - Ecography 41: 1595–1603.
Soulé, M. E. et al. 1985. What is conservation biology? - The Science of Scarcity and Diversity. Sinauer. Sunderlands, MA, EEUU

Sousa, W. P. 1984. The Role of Disturbance in Natural Communities. - Annual Review of Ecology and Systematics 15: 353–391.
Stanton, R. L., Morrissey, C. A. and Clark, R. G. 2018. Analysis of trends and agricultural drivers of farmland bird declines in North America: A review. - Agriculture, Ecosystems & Environment 254: 244–254.
Stephens, P. A., Mason, L. R., Green, R. E., Gregory, R. D., Sauer, J. R., Alison, J., ... Willis, S. G. 2016. Consistent response of bird populations to climate change on two continents. - Science 352: 84–87.
Stoehr, J. and Robin, S. 2026. Composite likelihood inference for the Poisson log-normal model. - Stat. Comput. 36: 55.
Storchová, L. and Hořák, D. 2018. Life-history characteristics of European birds. - Global Ecol. Biogeogr. 27: 400–406.
Stott, I., Townley, S. and Hodgson, D. J. 2011. A framework for studying transient dynamics of population projection matrix models. - Ecol. Lett. 14: 959–970.
Stroud, J. T., Bush, M. R., Ladd, M. C., Nowicki, R. J., Shantz, A. A. and Sweatman, J. 2015. Is a community still a community? Reviewing definitions of key terms in community ecology. - Ecol. Evol. 5: 4757–4765.
Sugihara, G., May, R., Ye, H., Hsieh, C., Deyle, E., Fogarty, M. and Munch, S. 2012. Detecting causality in complex ecosystems. - Science 338: 496–500.
Su, H., Feng, Y., Chen, J., Chen, J., Ma, S., Fang, J. and Xie, P. 2021. Determinants of trophic cascade strength in freshwater ecosystems: A global analysis. - Ecology 102: e03370.
Tassin de Montaigu, C. and Goulson, D. 2023. Habitat quality, urbanisation & pesticides influence bird abundance and richness in gardens. - Sci. Total Environ. 870: 161916.
Taylor, L. R. 1961. Aggregation, variance and the mean. - Nature 189: 732–735.
Thépault, A., Adenot, T., Lorrilliere, R., Cuchot, P. and Henry, P.-Y. 2025. Warm or Dry Springs (Still) Boost the Reproduction of Most Temperate Songbirds. - Global Ecol. Biogeogr. 34: e70138.
Thibaut, L. M. and Connolly, S. R. 2013. Understanding diversity–stability relationships: Towards a unified model of portfolio effects. - Ecol. Lett. 16: 140–150.
Thomas, A., Thuiller, W. and Gonzalez, A. 2026. Complementary causal approaches to support biodiversity change attribution. - Nat. Rev. Biodivers. 2: 322–334.
Tiegs, S. D., Costello, D. M., Isken, M. W., Woodward, G., McIntyre, P. B., Gessner, M. O., ... Zwart, J. A. 2019. Global patterns and drivers of ecosystem functioning in rivers and riparian zones. - Sci. Adv. 5: eaav0486.
Tilman, D. 1996. Biodiversity: Population versus ecosystem stability. - Ecology 77: 350–363.
Tilman, D. 1999. The Ecological Consequences of Changes in Biodiversity: A Search for General Principles. - Ecology 80: 1455–1474.
Tilman, D. and Downing, J. A. 1994. Biodiversity and stability in grasslands. - Nature 367: 363–365.
Tilman, D., Lehman, C. L. and Bristow, C. E. 1998. Diversity-Stability Relationships: Statistical Inevitability or Ecological Consequence? - Am. Nat. 151: 277–282.
Tilman, D., Isbell, F. and Cowles, J. M. 2014. Biodiversity and ecosystem functioning. - Annu. Rev. Ecol. Evol. Syst. 45: 471–493.
Tilman, D., Reich, P. B. and Knops, J. M. H. 2006. Biodiversity and ecosystem stability in a decade-long grassland experiment. - Nature 441: 629–632.
Tilman, D., May, R. M., Lehman, C. L. and Nowak, M. A. 1994. Habitat destruction and the extinction debt. - Nature 371: 65–66.
Tobias, J. A., Sheard, C., Pigot, A. L., Devenish, A. J. M., Yang, J., Sayol, F., ... Schleuning, M. 2022. AVONET: Morphological, ecological and geographical data for all birds. - Ecol. Lett. 25: 581–597.
Traba, J. and Morales, M. B. 2019. The decline of farmland birds in Spain is strongly associated to the loss of fallowland. - Sci. Rep. 9: 9473.
Tree, I. 2018. Wilding: The Return of Nature to a British Farm. - Pan Macmillan.
Troudet, J., Grandcolas, P., Blin, A., Vignes-Lebbe, R. and Legendre, F. 2017. Taxonomic bias in biodiversity data and societal preferences. - Sci. Rep. 7: 9132.
Valencia, E., de Bello, F., Lepš, J., Galland, T., E-Vojtkó, A., Conti, L., ... Götzenberger, L. 2020a. Directional trends in species composition over time can lead to a widespread overemphasis of year-to-year asynchrony. - J. Veg. Sci. 31: 792–802.
Valencia, E., de Bello, F., Galland, T., Adler, P. B., Lepš, J., E-Vojtkó, A., ... Götzenberger, L. 2020b. Synchrony matters more than species richness in plant community stability at a global scale. - PNAS 117: 24345–24351.
Vallé, C., Le Viol, I., Kerbiriou, C., Bas, Y., Jiguet, F. and Princé, K. 2023. Farmland biodiversity benefits

from small woody features. - Biol. Conserv. 286: 110262.
Van Meerbeek, K., Jucker, T. and Svenning, J.-C. 2021. Unifying the concepts of stability and resilience in ecology. - J. Ecol. 109: 3114–3132.
van Voorn, G. A. K., Hemerik, L., Boer, M. P. and Kooi, B. W. 2007. Heteroclinic orbits indicate overexploitation in predator–prey systems with a strong allee effect. - Math. Biosci. 209: 451–469.
Vázquez, D. P., Gianoli, E., Morris, W. F. and Bozinovic, F. 2017. Ecological and evolutionary impacts of changing climatic variability. - Biol. Rev. 92: 22–42.
Vellend, M. 2017. The biodiversity conservation paradox. - Am. Sci. 105: 94–101.
Venter, O., Sanderson, E. W., Magrach, A., Allan, J. R., Beher, J., Jones, K. R., ... Watson, J. E. M. 2016. Sixteen years of change in the global terrestrial human footprint and implications for biodiversity conservation. - Nat. Commun. 7: 12558.
Vergés, A., Steinberg, P. D., Hay, M. E., Poore, A. G. B., Campbell, A. H., Ballesteros, E., ... Wilson, S. K. 2014. The tropicalization of temperate marine ecosystems: Climate-mediated changes in herbivory and community phase shifts. - Proc. R. Soc. B 281: 20140846.
Verschoor, A. M., Vos, M. and Van Der Stap, I. 2004. Inducible defences prevent strong population fluctuations in bi- and tritrophic food chains. - Ecol. Lett. 7: 1143–1148.
Vimont, M., Bartholus, L., Bas, Y., Fontaine, B., Fontaine, C., Julliard, R., ... Porcher, E. 2025. Routine production of population trends from citizen science data: insights into the dynamics of common bird and plant species in France. - Comptes Rendus. Biologies 348: 229–247.
Violle, C., Enquist, B. J., McGill, B. J., Jiang, L., Albert, C. H., Hulshof, C., ... Messier, J. 2012. The return of the variance: Intraspecific variability in community ecology. - Trends Ecol. Evol. 27: 244–252.
Volterra, V. 1928. Variations and fluctuations of the number of individuals in animal species living together. - ICES J. Mar. Sci. 3: 3–51.
Vos, M., Verschoor, A. M., Kooi, B. W., Wäckers, F. L., DeAngelis, D. L. and Mooij, W. M. 2004. Inducible defenses and trophic structure. - Ecology 85: 2783–2794.
Vuorinen, K. E. M., Oksanen, T., Oksanen, L., Vuorisalo, T. and Speed, J. D. M. 2021. Why don't all species overexploit? - Oikos 130: 1835–1848.
Wagner, D. L. 2020. Insect Declines in the Anthropocene. - Annu. Rev. Entomol. 65: 457–480.
Wang, S. and Loreau, M. 2016. Biodiversity and ecosystem stability across scales in metacommunities (F Jordan, Ed.). - Ecol. Lett. 19: 510–518.
Wang, S., Loreau, M., de Mazancourt, C., Isbell, F., Beierkuhnlein, C., Connolly, J., ... Craven, D. 2021. Biotic homogenization destabilizes ecosystem functioning by decreasing spatial asynchrony. - Ecology 102: e03332.
Wang, S., Loreau, M., Arnoldi, J.-F., Fang, J., Rahman, K. A., Tao, S. and de Mazancourt, C. 2017. An invariability-area relationship sheds new light on the spatial scaling of ecological stability. - Nat. Commun. 8: 15211.
Wang, S., Lamy, T., Hallett, L. M. and Loreau, M. 2019. Stability and synchrony across ecological hierarchies in heterogeneous metacommunities: Linking theory to data. - Ecography 42: 1200–1211.
Ware, D. M. and Thomson, R. E. 2005. Bottom-up ecosystem trophic dynamics determine fish production in the northeast pacific. - Science 308: 1280–1284.
Watts, K., Whytock, R. C., Park, K. J., Fuentes-Montemayor, E., Macgregor, N. A., Duffield, S. and McGowan, P. J. K. 2020. Ecological time lags and the journey towards conservation success. - Nat. Ecol. Evol. 4: 304–311.
Weeks, T. L., Walkden, P. A., Edwards, D. P., Lees, A. C., Pigot, A. L., Purvis, A. and Tobias, J. A. 2026. Land-use change undermines the stability of avian functional diversity. - Nature 649: 381–387.
White, T. C. R. 2005. Why Does the World Stay Green?: Nutrition and Survival of Plant-eaters. - Csiro Publishing.
White, H. J., Bailey, J. J., Bogdan, C. and Ross, S. R. P.-J. 2023. Response trait diversity and species asynchrony underlie the diversity–stability relationship in romanian bird communities. - J. Anim. Ecol. 92: 2309–2322.
Whittaker, R. J., Fernández-Palacios, J. M., Matthews, T. J., Borregaard, M. K. and Triantis, K. A. 2017. Island biogeography: Taking the long view of nature's laboratories. - Science 357: eaam8326.
Willis, K. J., Araújo, M. B., Bennett, K. D., Figueroa-Rangel, B., Froyd, C. A. and Myers, N. 2007. How can a knowledge of the past help to conserve the future? Biodiversity conservation and the relevance of long-term ecological studies. - Phil. Trans. R. Soc. B 362: 175–187.
Wilson, J. D., Evans, J., Browne, S. J. and King, J. R. 1997. Territory Distribution and Breeding Success of Skylarks Alauda arvensis on Organic and Intensive Farmland in Southern England. - J. Appl. Ecol.

34: 1462–1478.
Winkler, K., Fuchs, R., Rounsevell, M. and Herold, M. 2021. Global land use changes are four times greater than previously estimated. - Nat. Commun. 12: 2501.
Wolkovich, E. M., Cook, B. I., McLauchlan, K. K. and Davies, T. J. 2014. Temporal ecology in the anthropocene. - Ecol. Lett. 17: 1365–1379.
Wollrab, S., Diehl, S. and De Roos, A. M. 2012. Simple rules describe bottom-up and top-down control in food webs with alternative energy pathways. - Ecol. Lett. 15: 935–946.
Wu, Z., Huang, N. E., Long, S. R. and Peng, C.-K. 2007. On the trend, detrending, and variability of nonlinear and nonstationary time series. - PNAS 104: 14889–14894.
Xu, Q., Yang, X., Yan, Y., Wang, S., Loreau, M. and Jiang, L. 2021. Consistently positive effect of species diversity on ecosystem, but not population, temporal stability. - Ecol. Lett. 24: 2256–2266.
Yachi, S. and Loreau, M. 1999. Biodiversity and ecosystem productivity in a fluctuating environment: The insurance hypothesis. - PNAS 96: 1463–1468.
Yodzis, P. and Innes, S. 1992. Body Size and Consumer-Resource Dynamics. - Am. Nat. 139: 1151–1175.
Zechner, C., Ruess, J., Krenn, P., Pelet, S., Peter, M., Lygeros, J. and Koeppl, H. 2012. Moment-based inference predicts bimodality in transient gene expression. - PNAS 109: 8340–8345.
Zelnik, Y. R., Arnoldi, J.-F. and Loreau, M. 2018. The Impact of Spatial and Temporal Dimensions of Disturbances on Ecosystem Stability. - Front. Ecol. Evol.
Zhang, Y., Loreau, M., Lü, X., He, N., Zhang, G. and Han, X. 2016. Nitrogen enrichment weakens ecosystem stability through decreased species asynchrony and population stability in a temperate grassland. - Global Change Biol. 22: 1445–1455.
Zhao, L., Wang, S., Shen, R., Gong, Y., Wang, C., Hong, P. and Reuman, D. C. 2022. Biodiversity stabilizes plant communities through statistical-averaging effects rather than compensatory dynamics. - Nat. Commun. 13: 7804.
Zimov, S. A., Chuprynin, V. I., Oreshko, A. P., Chapin, F. S., Reynolds, J. F. and Chapin, M. C. 1995. Steppe-tundra transition: A herbivore-driven biome shift at the end of the pleistocene. - Am. Nat. 146: 765–794.
Zurell, D., Schifferle, K., Herrando, S., Keller, V., Lehikoinen, A., Sattler, T. and Wiedenroth, L. 2024. Range and climate niche shifts in European and North American breeding birds. - Phil. Trans. R. Soc. B 379: 20230013.
Zuur, A. F., Ieno, E. N., Walker, N. J., Saveliev, A. A. and Smith, G. M. 2009. Mixed effects models and extensions in ecology with R. - Springer.

A . Other research project

A.1 Article: “Overexploitation can counteract top-down control and the paradox of enrichment in simple food chains”

The following work (Guerber et al. 2026a) was initiated during my time as an intern at iEES Paris, with Nicolas Loeuille and Isabelle Gounand. At the end of the internship, six months before starting my PhD, the corresponding manuscript was still a preliminary draft, and we continued to work on it during the first half of my PhD time. Therefore, even though it is not directly related to the dissertation’s subject, I wish to include it as an appendix because it definitely was part of my PhD experience.

The published version as well as the Supporting information are available online at: doi.org/10.1002/oik.11470.

Abstract

Because of its high abundance or its high feeding intensity, a consumer can overexploit its resource by consuming it on a shorter timescale than resource regeneration. While this short-term overexploitation is widespread in nature, its general implications for biotic control patterns and ecosystem stability are not clear. Here we use a resource-plant-herbivore food chain model allowing for short-term overexploitation (i.e. the plant can overexploit the resource and/or the herbivore can overexploit the plant). We uncover the conditions under which either type of overexploitation occurs and show that they qualitatively change ecological patterns, mainly by suppressing top-down control when interaction strength is high. When plant productivity increases, top-down control patterns are suppressed above the level at which plants start to

overexploit resources. Similarly, when herbivory intensity increases, top-down control patterns disappear when plants become overexploited. Overexploitation also prevents enrichment-driven destabilization by capping the energy fluxes in the ecosystem. These findings connect top-down and bottom-up controls in a single framework, and highlight the role overexploitation can play in structuring and stabilizing food chains via the modulation of interaction strengths.

Keywords: Plant-herbivore interactions, overexploitation, top-down control, bottom-up control, enrichment, stability.

Introduction

Interactions between primary producers and their consumers are at the base of all natural ecosystems, playing a key role in their maintenance and functioning (Schmitz 2008, Forbes et al. 2019). Since its formulation by Elton in 1927, the concept of food chain has helped to investigate the interactions between trophic levels, highlighting mechanisms that constrain community dynamics and distribution of biomass across trophic levels (Elton 1927). In particular, characterizing the conditions where food chains are under so-called “bottom-up” or “top-down” controls is critical in understanding ecosystem functioning (Barbier and Loreau 2019, Bideault et al. 2021). Under bottom-up control (Fig. A.1a), increasing the productivity of a basal trophic level benefits the biomasses of all higher trophic levels (Lindeman 1942, Chase et al. 2000, Ware and Thomson 2005, Frederiksen et al. 2006). Under top-down control (Fig. A.1b), the productivity increase of a resource benefits not itself but its consumer, and biomass increases alternate along the food chain (Oksanen and Oksanen 2000, Elmhagen et al. 2010, Ripple and Beschta 2012b). In top-down controlled systems, consumer-resource theory also predicts that increasing the energy flow to the consumer benefits consumer biomass while decreasing resource biomass (Rip and McCann (2011); Fig. A.1c), with cascading changes across the food chain if there are more than two trophic levels (Wollrab et al. 2012). Manipulating the number of trophic levels in experimental systems shows that top-down control is associated with strong trophic cascades, with ongoing debates about their underlying drivers (Chase 2000, McCauley et al. 2018, Su et al. 2021).

When considering the possibility for control between different trophic levels, it is important to note that a variety of ecological systems exhibit situations where, at a timescale smaller than the timescale of resource regeneration, the amount of resource that the current consumer population could consume exceeds the available resource stock. We define this phenomenon as “short-term overexploitation”. Though defined on a smaller timescale, it can be maintained over longer timescales if the consumer population consistently requires more resources than what is able to regenerate and has some strategy to persist during the regeneration time. Unlike other definitions of overexploitation where the trophic interaction is unsustainable (Pels and Sabelis 1999, van Voorn et al. 2007, Vuorinen et al. 2021), here resource regeneration allows the system to be maintained in time. For example, in a deciduous forest, the biomass eaten by an abundant defoliating insect cannot exceed the leaf biomass present

at the end of spring, introducing an upper limit to the consumed biomass in a year. This consumed biomass is converted to overwintering eggs or larvae and, the next year, leaves may grow and get consumed again, with both the herbivore and the tree populations being maintained over several years (Kamata 2002). One trophic level below, seasonal algae blooms almost completely deplete the available nutrients, but can occur every year as nutrients are regenerated during periods of lower algal productivity (Cloern 1996). More generally, short-term overexploitation can happen when consumer abundance or consumption strength generates feeding requirements that cannot be met by the available resource, although longer-term resource regeneration can prevent the consumer from getting extinct.

While such situations are not ubiquitous, they are widespread in nature. High herbivore abundances occur in cases of overgrazing (Sharp and Whittaker 2003, Christianen et al. 2014) or insect outbreaks (Kallio and Lehtonen 1975, Kamata 2002). As stated by Liebig's law of the minimum, primary producers that rely on several nutrients are limited by the least available of them (Lindeman 1942, Droop 1968), further reducing its availability (Droop 1974) and shaping worldwide patterns of resource limitation (Elser et al. 2007, Browning and Moore 2023). High consumption strength can occur when several environmental drivers conjointly increase algal productivity in phytoplankton blooms, depleting the nutrients (Cloern 1996), or when large herbivores have higher metabolic needs than available vegetation stocks (Zimov et al. 1995, Pausas and Bond 2020). In many of these systems, resource regeneration allows these strong consumer abundances or strong consumption strengths to be sustained over longer timescales and depending on environmental conditions or on external perturbations, some systems can shift between overexploitation and no overexploitation (Pausas and Bond 2020).

The possibility for overexploitation is often overlooked when investigating top-down or bottom-up regulations. In classical consumer-resource dynamical models based on Lotka-Volterra (Lotka 1925, Volterra 1928) or Rosenzweig-MacArthur approaches (Rosenzweig and MacArthur 1963, Rosenzweig 1973), a higher consumer abundance always increases consumption and the limitation by the resource is either implicit (through the use of a carrying capacity) or an emergent property (through changes in resource abundance). This may lead to overshooting effects due to delays between the growths of consumers and resources, where the resource can be completely depleted, leading to the crash of the system (Rosenzweig 1971). Conversely, models based on the scaling of energy transfer between trophic levels imply bottom-up control, as the energy available to a trophic level cannot exceed the energy represented by the

biomass of the lower trophic level, which therefore conditions its existence (Lindeman 1942). However, these energy-based models mainly describe steady states and do not investigate explicit population dynamics. Others have introduced dynamical models that focus on the lower trophic levels' availability. In Droop's model, the growth rate of an algae population is determined by the intracellular concentration of its limiting nutrient (Droop 1968). With ratio-dependent functional responses (Arditi and Ginzburg 1989), consumption strength depends on both species abundances, which prevents overshooting effects and exhibits bottom-up control patterns. However, by construction, while these models do indeed present consumer limitation by their resource, they cannot reproduce top-down control patterns.

Dynamical consumer-resource models on one side and energy-based, resource-focused models on the other side have provided different insights on producer-consumer interactions, which may or may not hold when accounting for short-term overexploitation (Fig. A.1). Systems with a heavy top-down control imply that increase in a resource trophic level's biomass may only be stopped by the presence of its consumer (Oksanen et al. 1981). In such models, increasing plant productivity in a plant-herbivore system (without upper levels) increases herbivore biomass while the plant stays at the same biomass (Fig. A.1b), given the top-down control exerted by herbivores (Oksanen and Oksanen 2000). When ecosystem productivity allows the persistence of a carnivore which exerts a top-down control on the herbivore, herbivore biomass stops increasing or even decreases, thereby enabling plant abundance to grow. In contrast, in systems with strong bottom-up control (Fig. A.1a), higher basal productivity increases the biomass of all trophic levels (Frederiksen et al. 2006), while increases in consumption strength do not affect biomass stocks at lower levels. Variations in biomass with productivity of adjacent trophic levels are thus positively correlated under bottom-up control, and anti-correlated under top-down control (Fig. A.1). Reconciliation of the two paradigms is emerging in ecological theory (Barbier and Loreau 2019, Galiana et al. 2021), showing the strength of trophic interactions as a key parameter for determining bottom-up and top-down control. When interaction strength scales with consumer metabolism, the control is more top-down (Barbier and Loreau 2019). Conversely, when interaction strength scales with resource metabolism, bottom-up control dominates (Barbier and Loreau 2019). Under short-term overexploitation, consumption is limited by the availability of the resource to the consumer, which could produce patterns similar to bottom-up control patterns when interaction becomes too high, further reconciling top-down and bottom-up paradigms.

Short-term overexploitation also likely constrains the stability of ecological dynamics. As suggested by

Rosenzweig in 1971, the paradox of enrichment states that energy or resource input in simple food chains can destabilize consumer-resource interactions, inducing oscillations or even the crash of the system. Later works showed that strong interaction strength destabilizes communities (McCann et al. 1998), helping to build a generic theory that states that strong energy fluxes destabilize top-down controlled food chains (Rip and McCann 2011). In this framework, enriched top-down systems (i.e. systems with increased energy availability to higher trophic levels, either through increased nutrient input or stronger trophic interactions) exhibit higher energy fluxes and are therefore less stable. However, strong trophic interactions could also favor resource overexploitation, which could potentially affect stability while also changing the biotic control type, although this aspect is not explicitly considered in these models.

The role of possible short-term overexploitation for shaping the direction of ecological control as well as biomass patterns and dynamical regimes still needs to be investigated. We here build a simple food chain model with recycling, integrating overexploitation of resources by plants (thereafter "resource overexploitation"), of plants by herbivores (thereafter "plant overexploitation"), or both at the same time. With this model, we question how short-term overexploitation alters resource-plant-herbivore interactions by answering three main points: 1) the conditions under which coexistence and overexploitation of either type occur. We expect coexistence when both plant and herbivore productivities are sufficient relative to their mortality, with short-term overexploitation occurring when consumption becomes too high. 2) The modifications of classical patterns linking productivity and standing biomass given overexploitation. We expect that plant overexploitation can cap herbivore biomass, even in the absence of carnivores and contrary to classical dynamical consumer-resource models. However, we also expect that, without overexploitation, increasing herbivore consumption should decrease or cap plant biomass, due to top-down control. 3) The effects of short-term overexploitation on stability. We expect that while stronger interactions and enrichment decrease the stability of the system, this effect can be limited by overexploitation. Our results show that short-term overexploitation, favored by stronger interactions, puts a halt to the top-down control of the system, suppressing classically expected biomass and stability patterns.

Methods

We built a discrete-time model of a generic plant-herbivore food chain with nutrient recycling and explicit short-term overexploitation possibility for both nutrient and plant by their respective consumer. We analytically calculated steady states and analyzed how their biomass composition and stability varied with the consumption parameters: plant productivity and herbivory intensity. Varying these parameters allows us to highlight conditions leading to short-term overexploitation (thereafter "overexploitation") and the associated dynamical regimes.

Model description

We express the dynamics of the mass of a single nutrient as it is consumed and recycled through three compartments: inorganic resources R, plants P, and herbivores H. We use a discrete timescale t where a time step represents the timescale on which overexploitation may occur: when the mass of resource required by a consumer for its growth between t and $t+1$ exceeds the available mass of its resource at time t, the resource is overexploited and its current (bio)mass is consumed. Before $t+1$, the resource regenerates according to its own growth terms in the resource equation in Equation A.1, yielding a positive resource mass available at time $t+1$ which can in turn be consumed partially or totally. We assume that the total (bio-)mass of a compartment is proportional to the mass of nutrients it contains. The dynamics within the food chain are thus determined by the following system:

$$\begin{aligned} \Delta R_t &= -\delta(R_t - R_b) - f_P + \nu\left((1-e_P)f_P + (1-e_H)f_H + \mu_P P_t + \mu_H H_t\right) \\ \Delta P_t &= e_P f_P - \mu_P P_t - f_H \\ \Delta H_t &= e_H f_H - \mu_H H_t \end{aligned} \tag{A.1}$$

These equations model four phenomena:

- Basal resource dynamics as a chemostat tending towards a background resource mass R_b with a diffusion efficiency
- Feeding intensity of plants on resources f_P and of herbivores on plants f_H (see below for the detail of their expressions), with conversion efficiencies e_P and e_H.

- Metabolic losses for the plant and herbivore compartments, P and H.
- Recycling efficiency of the loss terms from the biotic compartments to the resource compartment. Nutrient mass that is not recycled is lost by the system (e.g. by leaking to surrounding ecosystems).

Feeding terms for the plant and the herbivore compartments are defined by the following functions:

$$\begin{aligned} f_P(t) &= \min(rR_tP_t, R_t) \\ f_H(t) &= \min(aP_tH_t, P_t) \end{aligned} \tag{A.2}$$

These minimum functions allow us to distinguish two regimes: (i) available resource is sufficient and feeding is a Lotka-Volterra linear term, where the consumption of the resource depends both on resource and consumer masses and (ii) available resource would not be sufficient to cover the Lotka-Volterra interaction term, so that all the resource is consumed (overexploitation). Plant and herbivore feeding are scaled using the parameters r (hereafter "plant productivity") and a (hereafter "herbivory intensity"), respectively. Note that system (2) also allows us to mathematically define the conditions under which overexploitation occurs. Indeed, given (2) and taking the example of overexploitation of plants by herbivores, it occurs whenever $aP_tH_t > P_t$, *i.e.* $aH_t > 1$, so that it is clear that overexploitation depends on two factors: high herbivore abundance (H_t) and/or high herbivory intensity (a). Similarly, overexploitation of resources by plants relies on plant abundance P_t and productivity r. While system (1) could theoretically lead to negative biomass stocks (for instance when the recycling efficiency is too low; Supporting information), we restricted our analyses to parameter values that never yielded negative biomasses during simulations.

All symbols, their definitions, and their default values are summarized in Tab. 1.

Analytical and numerical methods for the analysis of the model

Depending on functions f_P and f_H, the complete system can yield four different outcomes. Equation A.2 implies that resource and plant overexploitations occur when $P_t > 1/r$ and $H_t > 1/a$, respectively, *i.e.* when plants (respectively herbivores) are too abundant or plant productivity (resp. herbivory intensity) is too high. Based on these inequalities, four situations may occur: no overexploitation, overexploitation of resources, of plants, and overexploitation of both resources and plants. For each situation, we analytically

obtained explicit expressions for each compartment's mass at steady state (fixed points), available in the Supporting information. The expressions found for the fixed points of a given situation are restrained by the overexploitation conditions of the concerned situation, yielding validity boundaries between situations. We estimated the stability of fixed points by numerically computing the dominant eigenvalue of the Jacobian of the system around each fixed point. This allowed us to distinguish whether each fixed point corresponded to a stable equilibrium, eventually reached by damped oscillations (stable node or stable spiral), or if it was unstable (Murray 2002). We characterized the dynamics around unstable states (e.g. presence of cycles) by inspecting simulations. For each combination of parameter values, we calculated the equilibrium values for all valid fixed points using the analytical expressions. We then numerically evaluated their stability. Throughout the parameter space, we thus either could identify a single valid and stable fixed point or noticed that the system produced cycles around the only valid (but unstable) fixed point. For each combination, we report which trophic levels are above zero (Fig. A.2a), the corresponding overexploitation situation (Fig. A.2b) as well as the corresponding fixed point and stability (Fig. A.2c).

We investigated the influence of plant productivity r and herbivory intensity a on the system biomass patterns and stability by combining analytical results with simulations of system dynamics. When differentiating the analytical expression for each fixed point with respect to r (respectively to a), the sign of the derivative directly gives the sign of the variation in compartment mass under an increase of r (respectively a). We further illustrate the results from the derivatives by plotting compartment mass patterns under variations of r or a. To do so, we examined the values of R, P and H over the last third of each simulation's time steps to characterize long-term dynamics. We 1) distinguished which overexploitation situation each parameter combination corresponded to, by averaging the biomass values and comparing them to the analytical expressions for the fixed points and 2) checked the presence of oscillations (even damped), by detecting the local extrema for each compartment. Simulations were run over 500 time steps, which was sufficient to reach steady states, using the `Julia` programming language (Bezanson et al. 2012) with the help of the `DynamicalSystems.jl` package (Datseris 2018). See Supporting information for examples of simulation outputs.

To test our prediction that overexploitation should introduce an upper cap in the increase of herbivore biomass with plant productivity r, we explored the effects of varying r from close to 0 to 10 for two different

values of herbivory intensity. To test that increasing herbivory intensity a should decrease the stability of the system (Rip and McCann 2011) and favor plant overexploitation, we explored a from close to 0 to 10 for three different values of plant productivity (see Supporting information for a representation of explored parameter ranges as transects across the parameter space). Larger ranges for r and a did not lead to regimes that qualitatively differed from those presented here. Values for the other parameters were set according to Tab. A.1: δ reflected a chemostat with low exchanges per time step and ν an efficient recycling with low losses per time step. Herbivore trophic efficiency was set as $e_H = 0.55$, following Yodzis and Innes (1992). Other parameter values were set in order to maintain the two biotic compartments in the four overexploitation situations. In particular, P and r were set higher than H and a, respectively, to ensure that plant population dynamics could be maintained in the presence of herbivores. We checked that our results did not substantially change for lower recycling efficiencies (Supporting information).

In our choice of framework, biotic compartments are indirectly self-regulated by the dynamics of the recycled nutrient (DeAngelis et al. 1989, Loreau 1995). We also analyze the corresponding model without resource dynamics, introducing a plant self-regulation parameter α, and show that our main results are not sensitive to this modelling choice (Supporting information). In this simplified model, we also show that the results are robust to a change in the functional response used in f_H (Supporting information).

Results

Community composition and overexploitation patterns interact in complex ways. Sufficient plant productivity, r, and herbivory intensity, a, allow coexistence of resources, plants and herbivores (Fig. A.2a, light gray area). Further increasing r or a leads to overexploitation, with overexploitation of both resources and plants occurring at high plant productivity and high herbivory intensity (Fig. A.2b, blue area). The intersection between coexistence and overexploitation conditions yields seven different situations (Fig. A.2c). When plants are alone, they can overexploit resources only when their productivity is sufficiently high (regime B1 in Fig. A.2c). Also, note that the top-down control exerted by herbivores is not always sufficient to prevent overexploitation of resources by plants: resource, plant, both or no overexploitation are all possible when both biotic compartments are maintained. While analysis of stability shows that equilibria are stable in most of these qualitative scenarios and for much of the parameter space, limit cycles occur at low productivity and high herbivory in the regime without overexploitation (D3 in Fig. A.2c).

Including this unstable outcome therefore yields an eighth possible situation, highlighted in brown on Fig. A.2c.

Biomass patterns with increasing interaction strength

Overexploitation of a given trophic level severely limits the top-down control exerted by its consumer. This general result appears directly in the equations of compartment masses at equilibrium, where herbivore parameters a, e_H and H explicitly set plant biomass, but only when plants are not overexploited (Supporting information). Similarly, plant parameters r, e_P and P only set resource biomass when resources are not overexploited (Supporting information).

This general law translates into systematic variations in biotic control type, which we obtain directly from the signs of the derivatives of the different equilibrium masses with respect to plant productivity and herbivory intensity (Tab. A.2, see details in Supporting information). As expected, classical top-down patterns are observed when no overexploitation occurs; that is, increasing plant productivity benefits the herbivore and not the top-down regulated plant, and increasing herbivory pressure benefits the resource and reduces plant biomass (Tab. A.2a). Such an outcome is conserved in part of the food chain when the consumption of the overexploited level is not being manipulated. Increasing herbivory intensity while resources are overexploited indeed benefits herbivores and reduces plant biomass (Tab. A.2b), and increasing plant productivity while plants are overexploited benefits plants and reduces resource mass (Tab. A.2c). Interestingly, when only plants are overexploited, raising plant productivity benefits plants and herbivores (a sign of bottom-up control of herbivores by plants), and disfavors resources (a sign of top-down control of resources by plants). This situation thus allows a coexistence of top-down and bottom-up controls along the food chain (Tab. A.2c, olive color). Classical top-down variations are progressively eroded when overexploitation occurs, as highlighted by grey colors on Tab. A.2.

As intuitively expected, when increasing plant productivity, overexploitation of inorganic resources by plants introduces an upper limit to plant and herbivore biomasses, eventually suppressing top-down control of plants by herbivores (Tab. A.2b, Fig. A.3, Supporting information). This suppression of a classical pattern in ecology (Oksanen and Oksanen 2000) occurs both at high and at low herbivory intensity past a certain plant productivity (Fig. A.3). For both herbivory levels, herbivore biomass first typically increases while plant biomass stays constant or near-constant (top-down control) and inorganic

resource decreases until it becomes overexploited. Thereafter, top-down controls are eroded, and higher productivity no longer increases biomasses in the system. Note that many situations where top-down control is suppressed by overexploitation do not directly show bottom-up patterns as in Fig. A.1a, but rather situations where biomass levels are kept constant under parameter variations (grey cells of Tab. A.2). However, when only plants are overexploited, they exert both a bottom-up control on herbivores and a top-down control on resources (Tab. A.2c, Fig. A.3b).

Similarly, when increasing herbivory intensity, top-down control is eventually suppressed when the plant becomes overexploited (Tab. A.2c, Fig. A.4b and c), with herbivore biomass reaching a plateau at high herbivory. Note that when plant productivity is low, plant overexploitation does not occur because plant production cannot sustain the levels of herbivores that would lead to plant overexploitation (Fig. A.4a). In these settings, a classical top-down pattern is first observed at low herbivory (correlated positive variations of herbivore and resource associated with a decrease in plant biomass around $a = 0.2$), but as herbivory increases the herbivore biomass starts to decline. In this situation, the top-down control of plants by herbivores is so strong that it interferes with the consumption of resources by plants, leading to a decline in both plant and herbivore (Supporting information). Intermediate values of plant productivity sustain higher herbivore biomass (Fig. A.4b), that allows the overexploitation of plants by herbivores at high herbivory intensity, thus halting the herbivore decline observed on Fig. A.4a. At high plant productivity, plants and herbivores reach sufficiently high levels to impose overexploitation of first resources, then both resources and plants with increasing herbivory, without the step where the herbivore biomass is sufficient to relax resource overexploitation via top-down control but too low to impose plant overexploitation (Fig. A.4c).

Stability, interaction strength and the paradox of enrichment

As expected, both the decrease in stability with interaction strength (Rip and McCann 2011) and the paradox of enrichment (Rosenzweig 1971) are often present without overexploitation but are suppressed by overexploitation as shown by the temporal dynamics of our model.

Without overexploitation, the stability of the system decreases both with plant productivity and with herbivory intensity, because increasing any of them increases energy fluxes, which can cause the appearance of oscillations. In this regime, no fluctuations happen at low productivity and herbivory

(stable node). Increase in plant productivity or herbivory leads to damped oscillations (spiral node) and eventually to sustained cycles (brown on Fig. A.2c). Particularly, increased plant productivity r represents enhanced upward energy fluxes to plants. This enrichment is destabilizing at high herbivory intensity, but the destabilization is suppressed when plant productivity is so high that plants become overexploited by overabundant herbivores (Fig. A.3b). When herbivory intensity is low, enrichment is not destabilizing (Fig. A.3a). Moreover, cycles appear under increases in herbivory intensity in a situation where plant overexploitation does not occur (Fig. A.4a), but they are suppressed at higher plant productivity where sufficient herbivore stocks lead to plant overexploitation (Fig. A.4b).

Discussion

While many instances of overexploitation in a variety of organisms and ecosystems have been documented, their implications for biomass variations along food chains are still largely unclear. Our work shows that while classical patterns expected from top-down controls apply without short-term overexploitation, and may still happen in particular overexploitation situations, these patterns are most often suppressed, especially when overexploitation happens for both resources and plants. Moreover, the destabilization classically found when increasing productivity or herbivory is dampened by overexploitation: under overexploitation, further increasing them does not lead to oscillating dynamics. We discuss how these results relate to existing literature on biotic control and ecosystem stability.

Overexploitation suppresses top-down control

Accounting for overexploitation explicitly, we show some unexpected relationships between the masses at equilibrium for the different compartments and the strengths of trophic interactions. Overall, the overexploitation of a trophic level halts the top-down control that would be expected under an increase in this level's consumption intensity. Herbivore biomass can be capped when plants are so productive that they start overexploiting their resources (Fig. A.3a), stopping the top-down regulation of herbivores. Similarly, herbivory pressure is classically expected to limit the plant and to allow for a larger inorganic resource pool. Again, in our model, this effect is suppressed by plant overexploitation (Fig. A.4b). Interestingly, when plants are overexploited and plant productivity increases, the plant-herbivore pair is under bottom-up control and the resource-plant pair under top-down control.

Empirically, bottom-up controlled food chains have mostly been reported in terrestrial or nutrient-limited marine ecosystems while top-down controlled chains are reported to dominate in freshwater ecosystems (Shurin et al. 2002). For example, Su et al. (2021) report a majority of typical top-down trophic cascades in a meta-analysis of fish addition experiments to freshwater communities. The timescale of regeneration has already been suggested as a major driver of the difference in biotic control between freshwater and terrestrial ecosystems (Chase 2000, but see Shurin et al. 2005), with for example faster decomposition rates in freshwater systems (Cebrian and Lartigue 2004, Tiegs et al. 2019, Gounand et al. 2020). Our study relates to this argument when showing that, when resource regeneration is not sufficient (i.e. when there is overexploitation), top-down control is suppressed from the food chain.

Our model represents a generic way to connect different perspectives on consumer-resource dynamics. Classical patterns of top-down control (Rosenzweig and MacArthur 1963, Rosenzweig 1973, Oksanen and Oksanen 2000, Rip and McCann 2011) are possible but they can also be replaced by patterns of bottom-up control (as in Arditi and Ginzburg 1989). Our model therefore complements previous models expressed in continuous time. An advantage of a discrete approach to the problem is that it allows us to clearly distinguish two timescales: a short timescale based on resource regeneration on which overexploitation is assessed (Equation A.2) and a longer timescale that reflects changes in ecosystem dynamics. Continuous-time models most often use differentiable functions for feeding terms, which prevents switches between different behaviors. An exception is the Droop model (Droop 1974), where vegetation growth is based on minimum functions that allow a switch between different limiting nutrients. Such models however put emphasis on the quality of the resource (i.e. which nutrient is limiting for growth) while our approach is based on quantitative aspects (the total amount of resource available). Functional responses that saturate at high resource abundance (e.g. Holling type II or type III) limit interaction rates and could be used in our model as an alternative to the Lotka-Volterra terms. Interestingly, these functional responses often capture how consumption rates change where resources become more abundant, while our approach mostly tackles the other side of the issue (i.e. when consumers can be overabundant). For all these reasons, we argue that formulating feeding terms with the minimum of a linear functional response and the amount of resources in discrete time is a simple, sensible choice to represent the possibility for overexploitation in a generic system that may or may not display overexploitation. Moreover, our results for biomass variation patterns seem robust to changes in the functional response (Supporting

information).

More recently, the scaling of interaction strength along the food chain has been proposed as a parameter that dictates the type of biotic control (Barbier and Loreau 2019, Galiana et al. 2021). In these studies, top-down (resp. bottom-up) control is associated with situations where the interaction strength scales with consumer (resp. resource) metabolism. Interestingly, overexploitation relates to situations where the interaction is limited by the regeneration of the resource (i.e. its metabolism) and we indeed show that overexploitation halts top-down control patterns, despite not always displaying clear bottom-up patterns. Our study thus resonates with these efforts to join top-down and bottom-up paradigms, but in our discrete time framework, formulating (bio)mass changes as quantities instead of rates allows consumer abundance itself, and not only the system parameterization, to cause switches in biotic control type.

Overexploitation counteracts the paradox of enrichment

Conditions of stability of trophic systems have received a lot of attention (Rosenzweig 1971, Pimm and Lawton 1977, McCann et al. 1998, Rip and McCann 2011), as less stable systems are less resilient to external disturbances. Particularly, while high energy flows are usually supposed to help satisfy the needs of each species and to help maintain them, they may also lead to unstable (and therefore fragile) systems (Rosenzweig 1971, Rip and McCann 2011). Under overexploitation, we do not observe this paradox of enrichment while our model reproduces it when there is no overexploitation (i.e. under top-down control). A change in species productivity or consumption pressure that switches our system from no overexploitation to overexploitation can thus suppress the paradox of enrichment in a resource-consumer system where it was previously observed. This may contribute to the debate around the discrepancy between enrichment theory and empirical evidence (Jensen and Ginzburg 2005). Indeed, as reviewed by Roy and Chattopadhyay (2007), empirical studies have both documented situations where the paradox of enrichment is observed (e.g. Fussmann et al. 2000) and situations where it is not (e.g. Kirk 1998). Among theoretical models, ratio-dependent consumer functions (Arditi and Ginzburg 1989) do suppress the paradox of enrichment, but such population models are not able to reproduce it in any condition. Interestingly, our model reproduces situations where the paradox of enrichment is suppressed while still allowing widely-used prey-dependent functional responses. Moreover, since overexploitation occurs when there is a difference in timescales between resource dynamics and consumer feeding, our model

generates the testable prediction that the paradox of enrichment should be less likely to occur when the regeneration of a prey is slower than the feeding ability of its consumer.

Similarly, Rip and McCann 2011 report a destabilizing effect of the strength of trophic interactions, but they do so in the top-down controlled Lotka-Volterra and Rosenzweig models. Short-term overexploitation in our model then alleviates this effect of the consumer on its resource and shows situations where further increasing interaction strength does not decrease stability (Fig. A.4b and c). Note that the term overexploitation has also been used to describe an intense feeding that leads to unsustainable, unstable dynamics (Pels and Sabelis 1999, van Voorn et al. 2007, Vuorinen et al. 2021). In our definition, feeding leads to complete resource consumption within a time step of our model which is indeed rapid, but we focus on ecosystem dynamics at longer timescales, where resource regeneration between time steps allows stable dynamics in the long run. Overall, our results suggest that short-term overexploitation might contribute to the temporal stability of ecosystems.

Further investigations

Our model shows a simple way of suppressing top-down patterns in certain situations for a system that otherwise behaves as top-down controlled. In more complex food webs, food web structure (Abrams 1993, Wollrab et al. 2012) and functional diversity (Hulot et al. 2000, Hulot and Loreau 2006) further shape top-down and bottom-up patterns through indirect trophic interactions and trophic control heterogeneity (Hunter and Price 1992). Our approach can be extended to investigate overexploitation in these more realistic settings, for instance by introducing different overexploitation requirements between functional groups of the same trophic level with possibly different timescales of regeneration across the food web. Interestingly, our results show that even a simple food chain can display heterogeneity of biotic control across trophic levels: when plants are overexploited but still under increasing productivity (Fig. A.3b, Tab. A.2), they exert both top-down control on the resource and bottom-up control on the herbivore.

The interaction of herbivory, recycling and overexploitation patterns could also lead to the emergence of spatial patterns at all trophic levels, leading to meta-ecosystems (Loreau et al. 2003). Source and sink dynamics and nutrient exports reported in meta-ecosystems (Gravel et al. 2010, Loreau et al. 2013, Gounand et al. 2014) should have a strong impact in a spatialized equivalent of our model, because dispersing herbivores or plants may be able to escape local overexploitation of their resources (Vuorinen

et al. 2021). By modulating food availability to the herbivore, spatial processes and their metabolic cost may alter the balance between energy dissipation and acquisition, possibly changing the way energy is transferred along the food chain. Acquiring a proper understanding of the local system here was however crucial before bringing the study of overexploitation to a spatially explicit context.

Finally, we only focused on the ecological implications of overexploitation, leaving out the possibility of eco-evolutionary dynamics. Overexploitation however corresponds to strong selective pressures within trophic levels, which can act on food chains at the scale of competition between functionally distinct species (Ehrlich and Gaedke 2020) or at the scale of trait evolution within species (Klauschies et al. 2016). For instance, plants facing resource overexploitation would be expected to evolve in resource acquisition or competitive traits. Overexploitation of plants by herbivores may yield strong selection on their foraging traits or behaviors and on the defensive phenotypes of plants. Interestingly, the evolution of defenses has been shown to decrease top-down controls in food chains (Vos et al. 2004, Loeuille and Loreau 2004), yielding a dominance of bottom-up patterns. In turn, empirical works suggest that such defended or unpalatable plants largely reduce the possibility of short-term overexploitation by their consumers (Verschoor et al. 2004, White 2005).

We here suggest that overexploitation can affect our qualitative view of trophic control and stability in natural ecosystems. Because high nutrient flows (McCann et al. 2021), changes in plant productivity (O'Sullivan et al. 2020), and overgrazing (Bertness et al. 2014, Vergés et al. 2014, Archer et al. 2017, Maestre et al. 2022) are all important current changes, we hope that our study will stimulate empirical and experimental tests of the effects of short-term overexploitation to better anticipate future possible scenarios.

Figures and tables

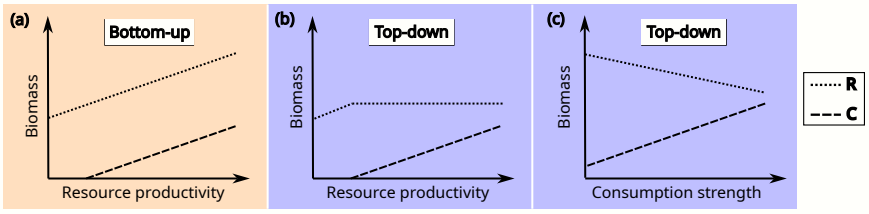

Figure A.1: Expected biomass patterns in resource-consumer systems under increase in resource productivity (a, b) or consumer consumption strength (c). Under bottom-up control (a), consumer and resource biomasses (C and R, dashed and dotted lines, respectively) are positively correlated under increasing energy availability (Ware and Thomson 2005). Under top-down control (b), productivity increases benefit only the consumer (Ripple and Beschta 2012b). (c) Top-down controlled systems are also expected to show anti-correlated biomass variations under increasing consumption strength (Rip and McCann 2011).

Table A.1: Symbols used in equations and figures. For each symbol, we provide a short description, its dimension and the default value used in most simulations. Values for R_t, P_t and H_t are used as initial conditions in numerical simulations.

Symbol	Description	Dimension	Default value
R_t	Nutrient mass in the resource compartment at time t	mass	1.1
P_t	Nutrient mass in the plant compartment at time t	mass	0.25
H_t	Nutrient mass in the herbivore compartment at time t	mass	0.1
R_b	Background resource mass	mass	1
δ	Diffusion efficiency	∅	0.05
μ_P	Plant metabolic costs (proportion of mass loss in one time step)	∅	0.25
μ_H	Herbivore metabolic costs (prop. of mass loss in one time step)	∅	0.1
ν	Recycling efficiency	∅	0.9
e_P	Plant-nutrient acquisition efficiency	∅	0.75
e_H	Herbivore-plant feeding efficiency	∅	0.55
f_P	Nutrient mass harvested from R in a time step	mass	
f_H	Nutrient mass harvested from P in a time step	mass	
r	Plant growth proportion per unit of plant mass	mass^{-1}	0.5
a	Herbivore feeding proportion (herbivory intensity) per unit of herbivore mass	mass^{-1}	0.2

Table A.2: Biomass patterns caused by increasing plant productivity or herbivory intensity at steady states where the three trophic levels coexist. Colored cells denote biotic control type: top-down (blue), bottom-up with increasing biomass levels (yellow) and bottom-up with stagnating biomass levels (grey). The olive-colored cell denotes that, when plants are overexploited, they exert both bottom-up control on the herbivore and top-down control on the nutrient. Arrow directions are based on the signs of the partial derivatives of the fixed points' analytical expressions (see Supporting information for details).

	Situation		Effect of increasing productivity	Effect of increasing herbivory
(a)	No overexploitation	R	⇘	⇗
		P	⇒	⇘
		H	⇗	⇗ (or ⇘)
(b)	Resource overexploitation	R	⇒	⇒
		P	⇒	⇘
		H	⇒	⇗
(c)	Plant overexploitation	R	⇘	⇒
		P	⇗	⇒
		H	⇗	⇒
(d)	Both overexploited	R	⇒	⇒
		P	⇒	⇒
		H	⇒	⇒

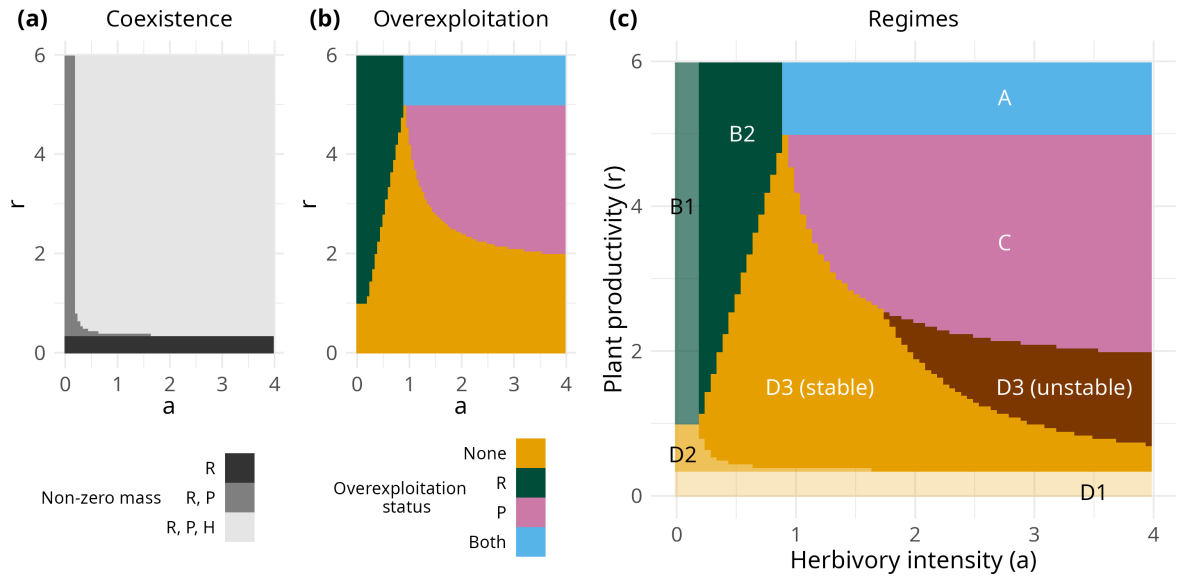

Figure A.2: Trophic levels present at steady state (a), overexploitation status at steady state (b), and parameter domains of all possible regimes (c) while varying herbivory intensity a and plant productivity, r. The analytical expressions of nutrient masses at steady states of all three trophic levels for each attractor are reported in the Supporting information. Letters in panel (c) indicate the analytical expression each domain corresponds to, with its stability in the case of the D3 regime. Parameters values other than a and r are found in Tab. A.1.

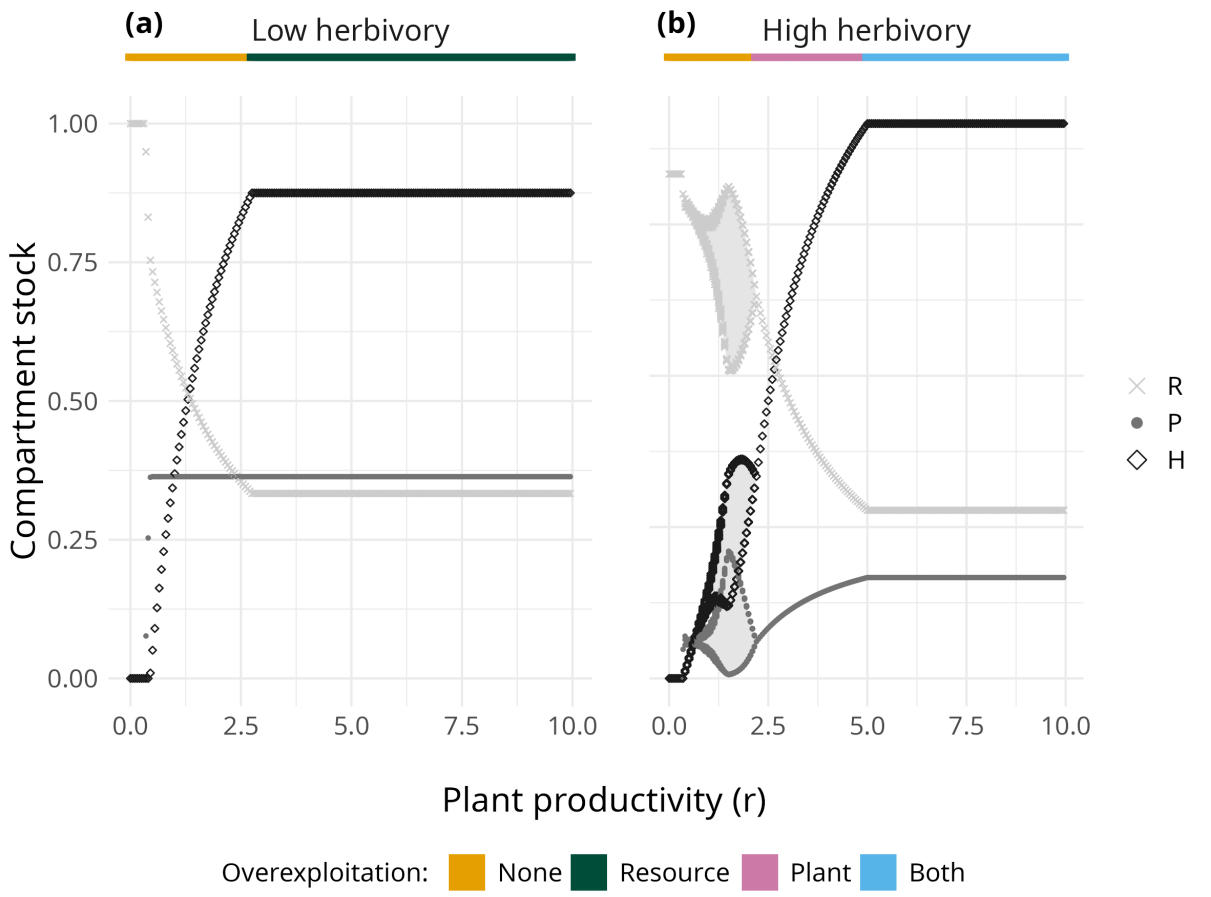

Figure A.3: Equilibrium stocks of the three trophic levels along plant productivity for (a) low and (b) high herbivory intensities. The colored bar above the plot indicates the trophic levels under overexploitation. Shaded areas in panel (b) represent the ranges of each trophic level's oscillations. a was set at 0.5 and 2.5 units for low and high herbivory, respectively. Other parameter values are found in Tab. A.1.

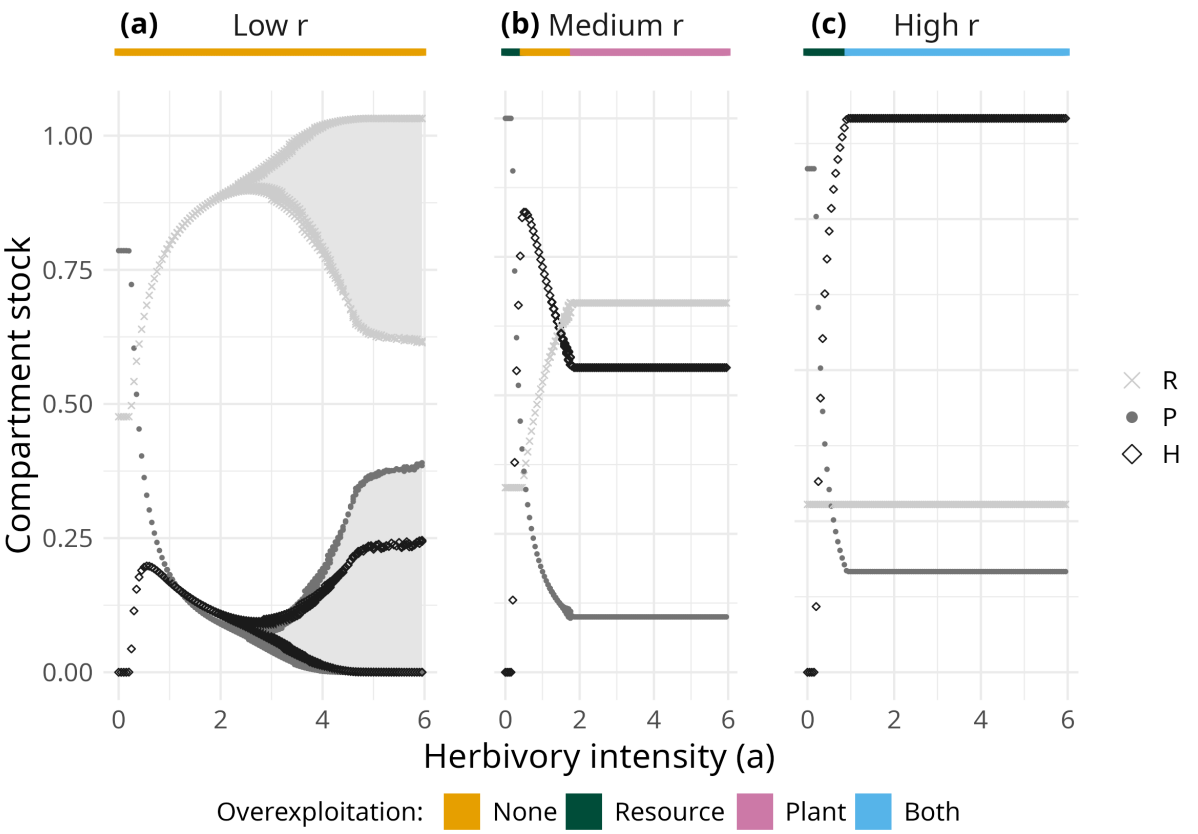

Figure A.4: Equilibrium stocks of the three trophic levels along herbivory intensity for (a) low, (b) medium, and (c) high plant productivity. The colored bar above the plot indicates the trophic levels under overexploitation. Shaded areas in panel (a) represent the ranges of each trophic level's oscillations. r was set at 0.7, 2.5 and 6 units for low, medium and high plant productivity, respectively. Other parameter values are found in Tab. A.1.